

Translational pharmacology and bioanalysis of oral taxanes

Jeroen J.M.A. Hendrikx

ISBN/EAN: 978-94-6108-605-1
© 2014 by Jeroen Hendriks. All rights reserved.
Cover Design and Layout: Jeroen Hendriks
Artwork: Bart Nijstad - www.bartnijstad.com
Printed by Gildeprint BV - www.gildeprint.nl
Standard font: Cambria, 10 pt

Translational pharmacology and bioanalysis of oral taxanes

Translatieonele farmacologie en
bioanalyse van orale taxanen
(met een samenvatting in het Nederlands)

Proefschrift

ter verkrijging van de graad van doctor aan de Universiteit Utrecht
op gezag van de rector magnificus, prof.dr. G.J. van der Zwaan,
ingevolge het besluit van het college voor promoties
in het openbaar te verdedigen op
woensdag 16 april 2014 des middags te 2.30 uur

door

Jeroen Johannes Maria Antonius Hendrixx

geboren op 19 februari 1983
te Grubbenvorst

Promotoren:

Prof.dr. J.H. Beijnen

Prof.dr. J.H.M. Schellens

Co-promotoren:

Dr. H. Rosing

Dr. A.H. Schinkel

The research described in this thesis was performed at:

The Department of Pharmacy & Pharmacology of the Slotervaart Hospital / The Netherlands Cancer Institute, Amsterdam, The Netherlands,

The Division of Molecular Oncology, The Netherlands Cancer Institute, Amsterdam, The Netherlands,

and

The Department of Clinical Pharmacology, The Netherlands Cancer Institute, Amsterdam, The Netherlands.

Publication of this thesis was financially supported by:

The Netherlands Laboratory for Anticancer Drug Formulation (NLADF)

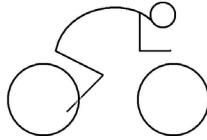
Utrecht Institute of Pharmaceutical Sciences (UIPS)

Astellas Pharma BV

Boehringer Ingelheim BV

Takeda Nederland BV

The Netherlands Cancer Institute



De veut vast op 't pedaal
En de spiere die staon strak
Elken berg haet zien verhaal
Gènnen maeter deën is vlak

Aan de kant ik lig op stoam
Onderwaeg nar mienen droom

't Podium dat kump in zicht
Oet de schaduw in 't licht

Uit "Nar Boave",
Rowwen Hèze

Table of contents

Preface	11
---------	----

Chapter 1 Bionalysis of taxanes

1.1	<i>Quantification of taxanes in biological matrices: A review of bioanalytical assays and recommendations for development of new assays.</i>	21
	Bioanalysis. <i>Accepted</i>	
1.2	<i>A sensitive combined assay for the quantification of paclitaxel, docetaxel and ritonavir in human plasma using liquid chromatography coupled with tandem mass spectrometry.</i>	55
	J Chromatogr B Analyt Technol Biomed Life Sci. 2011 ; 879 (28): 2984-90	
1.3	<i>Combined quantification of paclitaxel, docetaxel and ritonavir in human feces and urine using LC-MS/MS.</i>	71
	Biomed Chromatogr. 2014 ; 28 (2): 302-10.	
1.4	<i>Quantification of docetaxel and its metabolites in human plasma by liquid chromatography/tandem mass spectrometry.</i>	89
	Rapid Commun Mass Spectrom. 2013 ; 27 (17): 1925-34	

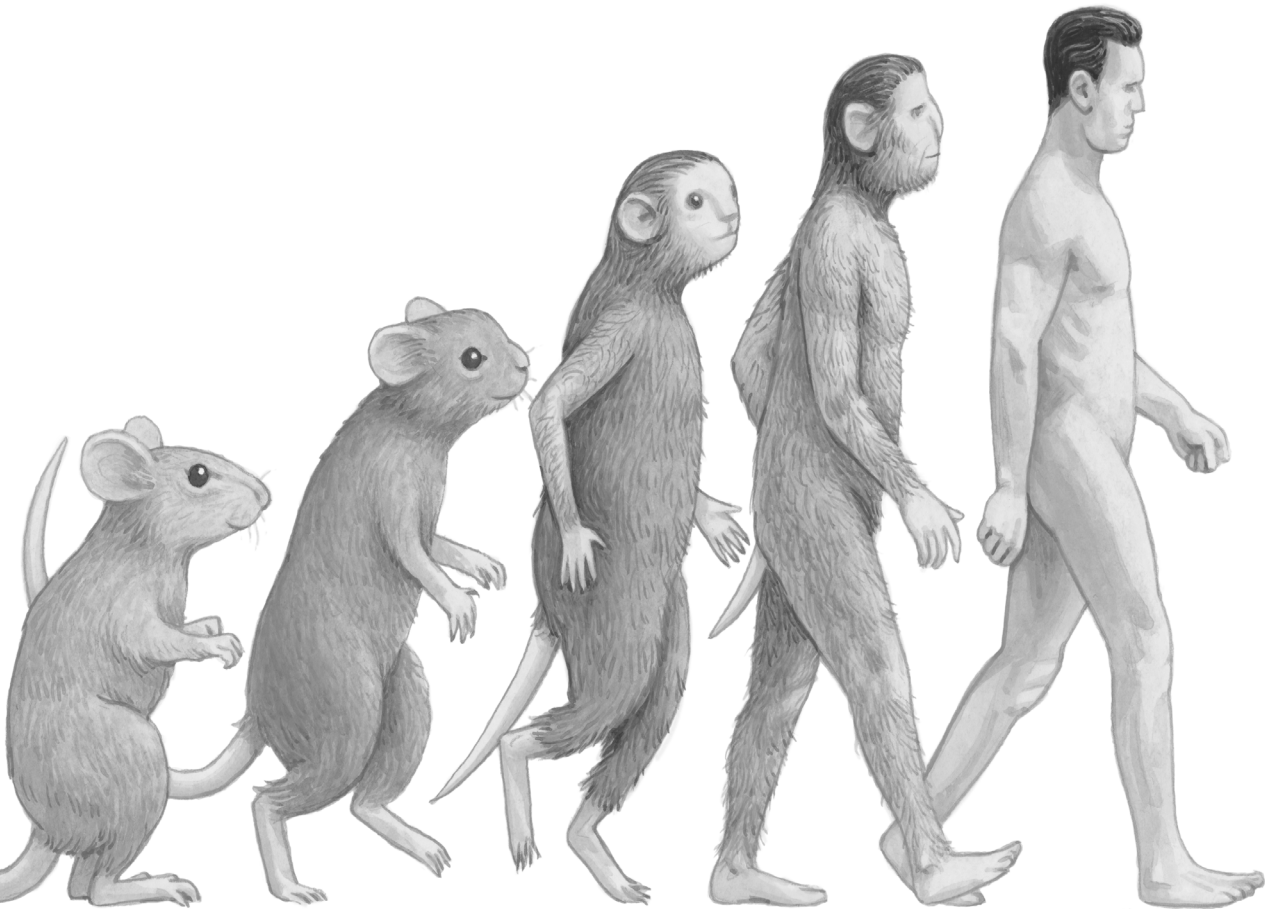
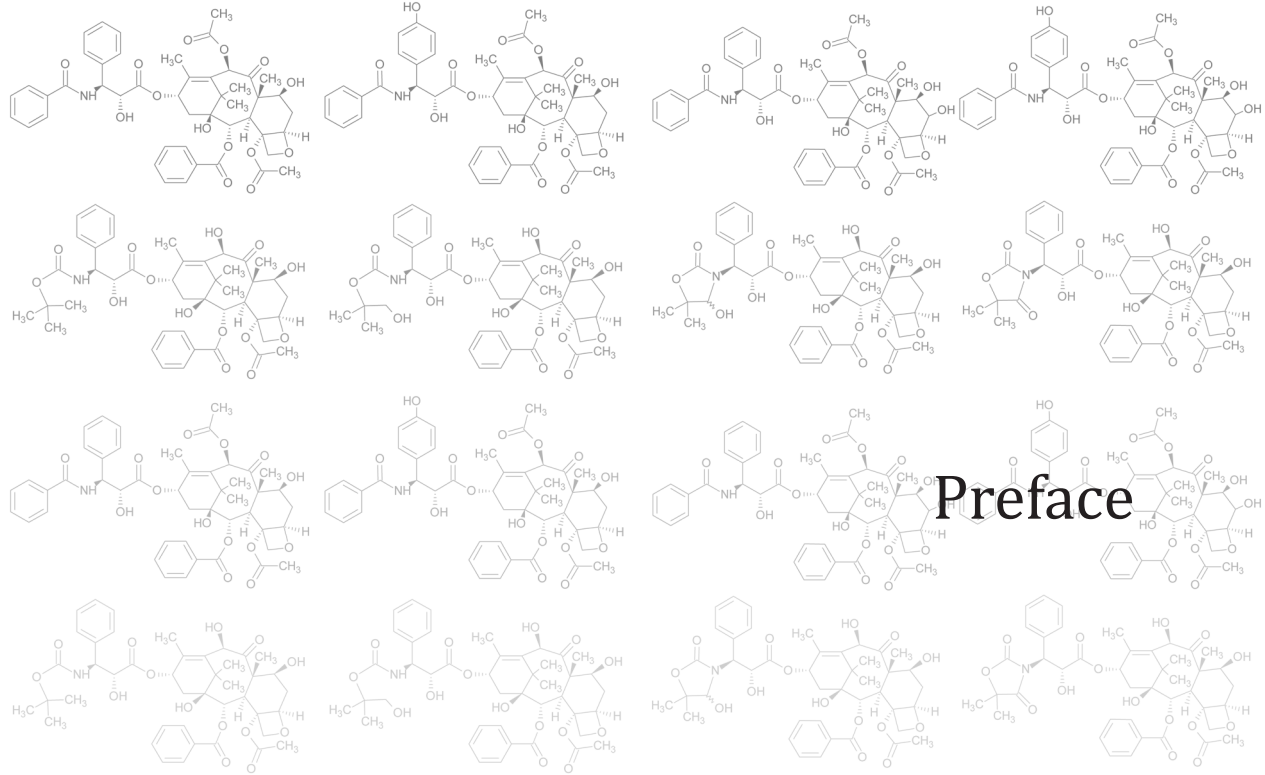
Chapter 2 Preclinical studies on taxanes

2.1	<i>Genetically modified mouse models for oral drug absorption and disposition.</i>	109
	Curr Opin Pharmacol. 2013 ; 13 (6): 853-8	
2.2	<i>P-glycoprotein and Cytochrome P450 3A act together in restricting the oral bioavailability of paclitaxel.</i>	121
	Int J Cancer. 2013 ; 132 (10): 2439-47	
2.3	<i>Oral co-administration of elacridar and ritonavir safely enhances plasma levels of oral paclitaxel and docetaxel without affecting relative brain accumulation.</i>	141
2.4	<i>Human OATP1B1, OATP1B3 and OATP1A2 mediate the in vivo uptake of docetaxel.</i>	159
2.5	<i>Ritonavir inhibits intratumoral docetaxel metabolism and enhances docetaxel anti-tumor efficacy in a mouse model for hereditary breast cancer.</i>	177

Chapter 3 Clinical studies on taxanes

3.1	<i>Relationship between systemic exposure to docetaxel and severe intestinal toxicity after oral docetaxel administration in mice and patients.</i>	201
3.2	<i>Plasma levels of docetaxel metabolites in humans after oral administration of docetaxel with and without ritonavir.</i>	223
	Conclusions and perspectives	237
	Summary	251
	Samenvatting	257
	Dankwoord	262
	Curriculum Vitae	264
	List of publications	266
	Chemical structures	268





Preface

Cancer is one of the leading causes of death worldwide, accounting for 7.6 million deaths in 2008 and an estimated 13.1 million deaths in 2030.¹ Cancer is a generic term for a number of disease subtypes affecting multiple organs with a great variety in mortality rates per subtype.¹ Despite the variety in cancer subtypes and disease progression, this complex neoplastic disease is characterized by multiple biological capabilities, often referred to as the '*Hallmarks of Cancer*'. At the beginning of this century, six hallmarks were proposed.² In the last decade, understanding of the pathways involved in cancer has rapidly improved. This resulted in the addition of more biological capabilities of tumors to the '*Hallmarks of Cancer*' concept.³ The increase in knowledge of the onset and behavior of cancer is accompanied by new therapeutic options and treatment strategies. Nowadays the focus is on targeted therapy and potential targets for new compounds, although rediscovery and improvement of old anticancer agents can also result in new strategies. An example of the latter is the development of new oral formulations of taxanes, a group of widely used anticancer agents that are currently administered intravenously (i.v.).

The first taxane discovered was paclitaxel. Paclitaxel (Taxol[®]) was isolated in the early 1970s from the bark of *Taxus brevifolia*.⁴ The semisynthetic analogue docetaxel (Taxotere[®]) was discovered a decade later and is a derivative of a taxane isolated from the needles of *Taxus baccata*.^{4,5} Paclitaxel was approved by the Food and Drug Administration (FDA) in 1992 and docetaxel approval followed in 1996. Both compounds share the baccatin core ring structure and are widely used as intravenously administered anticancer agents for several types of cancer such as non-small cell lung cancer (NSCLC), ovarian, breast, gastric, prostate and head-and-neck cancer.^{4,6} The anticancer effect of taxanes is attributed to binding of the taxanes to β -tubulin. This binding promotes polymerization of tubulin and stabilises microtubules. The stabilisation of microtubules leads to cell cycle arrest and apoptosis.⁷

The development of oral formulations of paclitaxel and docetaxel is the focus of preclinical and clinical research in our groups because oral administration has many advantages over i.v. administration.^{6,8} Oral administration is more practical and convenient for patients, since oral medication can be taken by the patient at home while i.v. administration requires hospitalisation during infusion. Oral administration in the home situation also reduces treatment cost. Moreover, oral administration enables other dosing schedules like metronomic therapy (e.g. continuous or frequent treatment with low doses of anticancer drugs), which can increase efficacy of taxane treatment and reduce adverse effects caused by high plasma concentrations of docetaxel or paclitaxel.^{9,10}

A major limitation in the concept of oral administration of taxanes is the low oral availability of paclitaxel and docetaxel.^{6,8} Paclitaxel and docetaxel have poor aqueous solubility and upon oral administration, intestinal uptake can be seriously hampered by drug efflux through P-glycoprotein (P-gp/MDR1/ABCB1) and by drug metabolism via Cytochrome P450 (CYP) 3A.¹¹⁻¹⁶

P-gp is a member of the ATP-binding cassette (ABC) efflux transporter family and is expressed in multiple tissues like intestine, liver, and kidney, but also at the blood-brain barrier.¹⁷ P-gp-mediated transport limits drug absorption across intestinal cells and brain penetration across the blood-brain barrier. In enterocytes, P-gp pumps back absorbed taxanes into the intestinal lumen, while at the blood-brain barrier, taxanes are pumped back into the systemic circulation. In liver and kidney, P-gp increases drug excretion by active efflux transport into the bile and urine.¹⁸

CYP3A is a member of the CYP superfamily and CYP enzymes are responsible for most phase-I drug metabolism.¹⁹ CYP enzymes are mainly expressed in the liver, but some CYP members are also expressed in enterocytes. CYP3A is the most abundant CYP enzyme in liver and intestine, representing 40% and 80% of the total CYP enzymes expressed in each tissue, respectively.²⁰ Docetaxel is primarily metabolized by enzymes of the CYP3A subfamily, while paclitaxel is metabolized by both CYP3A4 and CYP2C8.⁵ In contrast to CYP3A, CYP2C8 is only expressed in liver cells.²⁰

Several studies by our group have shown that the oral bioavailability of paclitaxel and docetaxel in humans can be enhanced by combining the taxanes with inhibitors of P-gp and/or CYP3A.²¹⁻²⁶ The CYP3A4 inhibitor ritonavir (Norvir[®]) was selected to boost oral bioavailability during further development of oral formulations of the taxanes.

Ritonavir was originally developed as antiretroviral therapy in HIV-infected patients. The drug was licensed as one of the first protease inhibitors and 400-600 mg of the drug was administered twice daily.²⁷ Although ritonavir treatment was successful in HIV-infected patients, it was poorly tolerated due to severe side effects (e.g. gastrointestinal symptoms) of the drug and use of full-dose ritonavir is no longer recommended.^{27;28} However, sub-therapeutic daily doses of 100-400 mg ritonavir are used to increase oral absorption of other protease inhibitors.²⁸ This boosting effect of ritonavir is caused by CYP3A4 inhibition and near-maximal CYP3A blockade is observed at these low doses.²⁷ Side effects of ritonavir were more tolerable at sub-therapeutic doses and ritonavir-boosted protease inhibitors are currently used in first and second-line regimens for HIV-infected patients.^{27;28}

The aim of this thesis was to obtain mechanistic insights in the boosting effect of ritonavir on orally administered taxanes and to support clinical development of oral formulations of paclitaxel and docetaxel.

During drug development in preclinical and clinical setting, distribution, metabolism and excretion of drugs are studied. Reliable and sensitive bioanalytical assays for quantification are prerequisites to support these trials. Over time, multiple assays have been developed and described to quantify taxanes and in **Chapter 1.1** we present a comprehensive overview of these assays. Moreover, we bring forward recommendations for the development of new bioanalytical assays for the quantification of taxanes. In **Chapter 1.2** and **Chapter 1.3** we describe the development of bioanalytical assays for simultaneous quantification of paclitaxel, docetaxel and ritonavir in human plasma, feces and urine. In **Chapter 1.4** development and validation of a bioanalytical assay for the quantification of docetaxel and its metabolites is described.

Intestinal absorption is an essential step in the therapeutic use of most orally administered drugs and often mediated by enterocyte transmembrane transporters. In **Chapter 2.1** we discuss several of these drug transport systems and knockout mouse models to study them. The oral plasma AUC (area under the plasma concentration-time curve, which is a measure of the systemic exposure upon oral administration) of paclitaxel and docetaxel can be strongly enhanced in humans by co-administration of the potent CYP3A4 inhibitor ritonavir.²⁴⁻²⁶ For docetaxel, this is explained by the fact that docetaxel is extensively metabolized by CYP3A.⁴ However, the impact of drug-metabolizing enzymes on the oral bioavailability of paclitaxel is not yet fully elucidated. In **Chapter 2.2** we present the roles of CYP3A4 and P-gp in restricting oral bioavailability of paclitaxel. The impact of oral co-administration of paclitaxel and docetaxel with the CYP3A4 inhibitor ritonavir and the P-gp inhibitor elacridar on plasma exposure and brain penetration of the taxanes is presented in **Chapter 2.3**. Not only P-gp, but also other drug transporters can be involved in distribution of taxanes.^{29;30} The role of the uptake transporters Organic Anion Transporting Polypeptide (OATP/SLCO) 1B1, 1B3 and 1A2 is discussed in **Chapter 2.4**.

In the last decade, possible anticancer effects of ritonavir are described. Based on the inhibitory effect on endothelial cell invasion, ritonavir might inhibit angiogenesis.³¹ In vivo, anti-tumor effects of ritonavir are described for mouse models of Kaposi sarcoma³², lymphoma³³, head and neck carcinoma³⁴ and breast cancer.³⁵ Therefore, co-administration of taxanes with ritonavir potentially increases anti-tumor efficacy. In **Chapter 2.5** we discuss tumor growth after co-administration of intravenous docetaxel and oral ritonavir in a mouse model for hereditary breast cancer.

A switch from intravenous to oral administration of taxanes potentially results in altered toxicity profiles. Oral administration of chemotherapeutic agents results in high concentrations of the drugs in the intestinal lumen. In the lumen, the drugs can have a direct damaging effect on the epithelium of the intestine. This is observed after irinotecan administration.^{36;37} Otherwise, intestinal damage could be an effect of mitotic arrest of intestinal crypt cells caused by exposure to chemotherapeutic agents in the systemic circulation. Mitotic arrest of the deep crypt cells results in impaired renewal of the intestinal epithelium and thereby a loss of epithelial function. This is observed after administration of 5-fluorouracil.³⁸ In **Chapter 3.1** we discuss severe intestinal toxicity after oral docetaxel administration in mice and patients.

Not only toxicity, but also metabolism might change when formulations for intravenous administration are switched to oral formulations. Orally applied taxanes are subject to a first-pass effect and are co-administered with the CYP3A4 inhibitor ritonavir. This raises the question if metabolite plasma concentrations in humans are altered – or if even other metabolites are formed- after oral co-administration of taxanes and ritonavir. We address this question in **Chapter 3.2**, where we present a screening for docetaxel metabolites after oral co-administration of docetaxel and ritonavir to human patients.

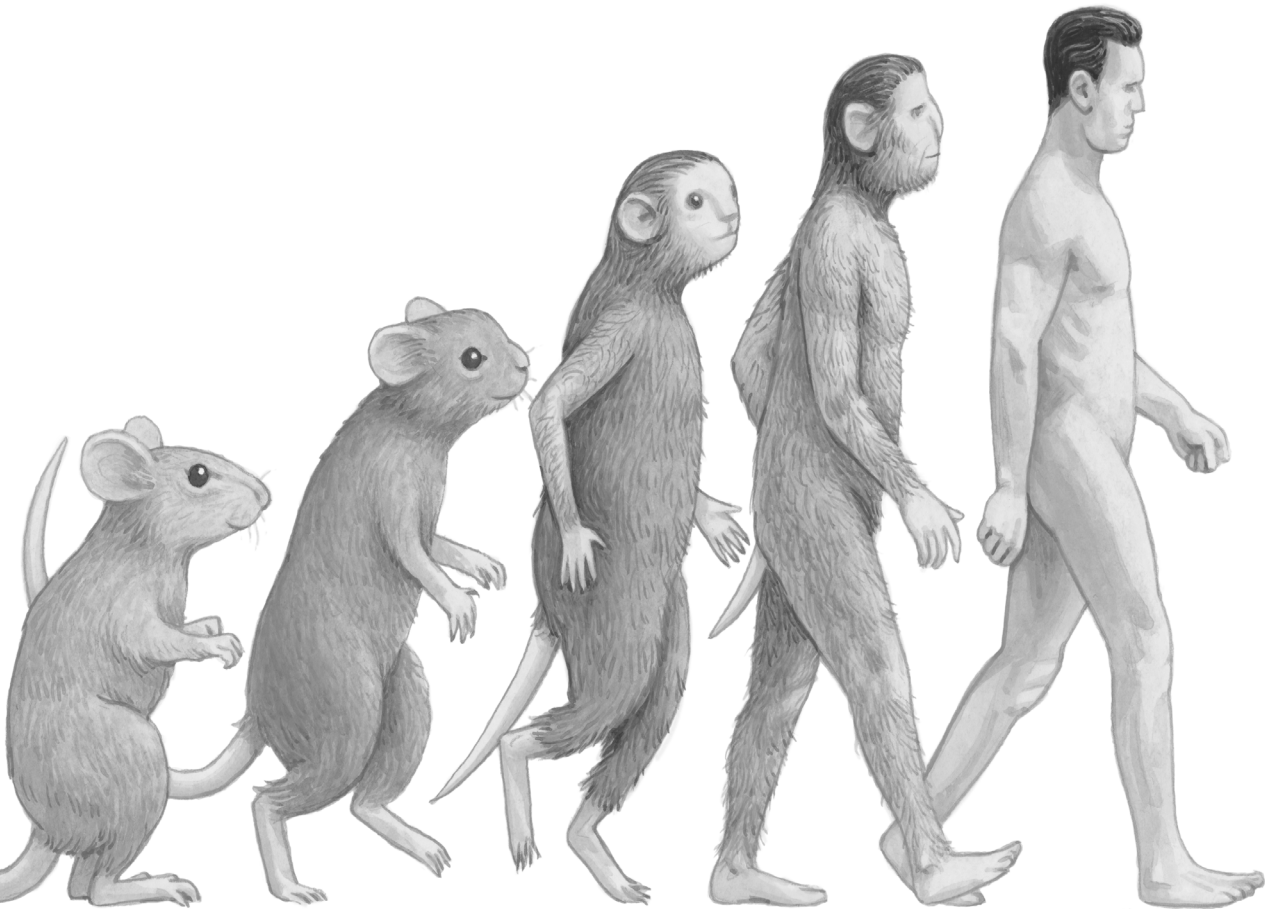
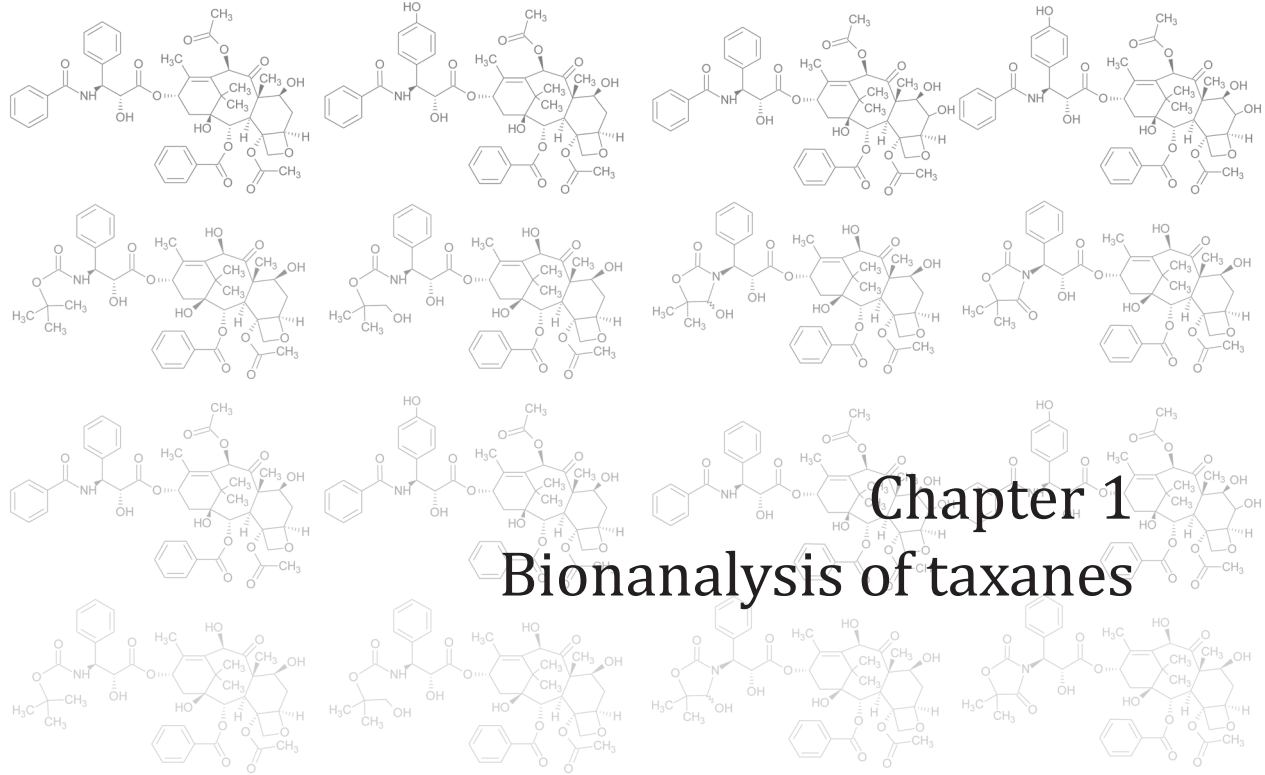
Finally, in a general discussion the results of all studies are discussed and put into perspective.

References

1. International Agency for Research on Cancer; Globocan 2008. <http://globocan.iarc.fr/>. visited 18-10-2013.
2. Hanahan D, Weinberg RA. The hallmarks of cancer. *Cell*. **2000**; 100 (1): 57-70.
3. Hanahan D, Weinberg RA. Hallmarks of cancer: the next generation. *Cell*. **2011**; 144 (5): 646-74.
4. Gligorov J, Lotz JP. Preclinical pharmacology of the taxanes: implications of the differences. *Oncologist*. **2004**; 9 Suppl 2): 3-8.
5. Vaishampayan U, Parchment RE, Jasti BR, Hussain M. Taxanes: an overview of the pharmacokinetics and pharmacodynamics. *Urology* **1999**; 54 (6A Suppl): 22-9.
6. Koolen SL, Beijnen JH, Schellens JHM. Intravenous-to-oral switch in anticancer chemotherapy: a focus on docetaxel and paclitaxel. *Clin.Pharmacol.Ther*. **2010**; 87 (1): 126-9.
7. Yue QX, Liu X, Guo DA. Microtubule-binding natural products for cancer therapy. *Planta Med*. **2010**; 76 (11): 1037-43.
8. Schellens JHM, Malingre MM, Kruijtzter CM, Bardelmeijer HA, van Tellingen O, Schinkel AH, Beijnen JH. Modulation of oral bioavailability of anticancer drugs: from mouse to man. *Eur.J.Pharm.Sci*. **2000**; 12 (2): 103-10.
9. Wu H, Xin Y, Zhao J, Sun D, Li W, Hu Y, Wang S. Metronomic docetaxel chemotherapy inhibits angiogenesis and tumor growth in a gastric cancer model. *Cancer Chemother.Pharmacol*. **2011**; 68 (4): 879-87.
10. Jiang H, Tao W, Zhang M, Pan S, Kanwar JR, Sun X. Low-dose metronomic paclitaxel chemotherapy suppresses breast tumors and metastases in mice. *Cancer Invest*. **2010**; 28 (1): 74-84.
11. Bardelmeijer HA, Ouwehand M, Beijnen JH, Schellens JH, van Tellingen O. Efficacy of novel P-glycoprotein inhibitors to increase the oral uptake of paclitaxel in mice. *Invest New Drugs*. **2004**; 22 (3): 219-29.
12. Meerum Terwogt JM, Beijnen JH, ten Bokkel Huinink WW, Rosing H, Schellens JH. Co-administration of cyclosporin enables oral therapy with paclitaxel. *Lancet*. **1998**; 352 (9124): 285.
13. Sparreboom A, van Asperen J, Mayer U, Schinkel AH, Smit JW, Meijer DK, Borst P, Nuijten WJ, Beijnen JH, van Tellingen O. Limited oral bioavailability and active epithelial excretion of paclitaxel (Taxol) caused by P-glycoprotein in the intestine. *Proc.Natl.Acad.Sci.U.S.A.* **1997**; 94 (5): 2031-5.
14. van Asperen J, van Tellingen O, Sparreboom A, Schinkel AH, Borst P, Nuijten WJ, Beijnen JH. Enhanced oral bioavailability of paclitaxel in mice treated with the P-glycoprotein blocker SDZ PSC 833. *Br.J.Cancer*. **1997**; 76 (9): 1181-3.
15. van Asperen J, van Tellingen O, van der Valk MA, Rozenhart M, Beijnen JH. Enhanced oral absorption and decreased elimination of paclitaxel in mice cotreated with cyclosporin A. *Clin.Cancer Res*. **1998**; 4 (10): 2293-7.
16. van Waterschoot RA, Lagas JS, Wagenaar E, van der Kruijssen CM, van Herwaarden AE, Song JY, Rooswinkel RW, van Tellingen O, Rosing H, Beijnen JH, Schinkel AH. Absence of both cytochrome P450 3A and P-glycoprotein dramatically increases docetaxel oral bioavailability and risk of intestinal toxicity. *Cancer Res*. **2009**; 69 (23): 8996-9002.
17. Gottesman MM, Ambudkar SV. Overview: ABC transporters and human disease. *J.Bioenerg.Biomembr*. **2001**; 33 (6): 453-8.
18. Glaeser H, Fromm MF. Animal models and intestinal drug transport. *Expert.Opin.Drug Metab Toxicol*. **2008**; 4 (4): 347-61.
19. Thelen K, Dressman JB. Cytochrome P450-mediated metabolism in the human gut wall. *J.Pharm.Pharmacol*. **2009**; 61 (5): 541-58.
20. Paine MF, Hart HL, Ludington SS, Haining RL, Rettie AE, Zeldin DC. The human intestinal cytochrome P450 "pie". *Drug Metab Dispos*. **2006**; 34 (5): 880-6.
21. Kruijtzter CM, Schellens JH, Mezger J, Scheulen ME, Keilholz U, Beijnen JH, Rosing H, Mathot RA, Marcus S, van TH, Baas P. Phase II and pharmacologic study of weekly oral paclitaxel plus cyclosporine in patients with advanced non-small-cell lung cancer. *J.Clin.Oncol*. **2002**; 20 (23): 4508-16.
22. Malingre MM, Beijnen JH, Rosing H, Koopman FJ, Jewell RC, Paul EM, ten Bokkel Huinink WW, Schellens JH. Co-administration of GF120918 significantly increases the systemic exposure to oral paclitaxel in cancer patients. *Br.J.Cancer*. **2001**; 84 (1): 42-7.
23. Malingre MM, Richel DJ, Beijnen JH, Rosing H, Koopman FJ, ten Bokkel Huinink WW, Schot ME, Schellens JH. Co-administration of cyclosporine strongly enhances the oral bioavailability of docetaxel. *J.Clin.Oncol*. **2001**; 19 (4): 1160-6.
24. Moes J, Koolen S, Huitema A, Schellens J, Beijnen J, Nuijten B. Development of an oral solid dispersion formulation for use in low-dose metronomic chemotherapy of paclitaxel. *Eur.J.Pharm.Biopharm*. **2013**; 83 (1): 87-94.
25. Moes JJ, Koolen SL, Huitema AD, Schellens JH, Beijnen JH, Nuijten B. Pharmaceutical development and preliminary clinical testing of an oral solid dispersion formulation of docetaxel (ModraDoc001). *Int.J.Pharm*. **2011**; 420 (2): 244-50.
26. Oostendorp RL, Huitema A, Rosing H, Jansen RS, Ter Heine R, Keessen M, Beijnen JH, Schellens JHM. Co-administration of ritonavir strongly enhances the apparent oral bioavailability of docetaxel in patients with solid tumors. *Clin.Cancer Res*. **2009**; 15 (12): 4228-33.
27. Josephson F. Drug-drug interactions in the treatment of HIV infection: focus on pharmacokinetic enhancement through

- CYP3A inhibition. *J.Intern.Med.* **2010**; 268 (6): 530-9.
28. Hull MW, Montaner JS. Ritonavir-boosted protease inhibitors in HIV therapy. *Ann.Med.* **2011**; 43 (5): 375-88.
 29. Lagas JS, Vlaming ML, van Tellingen O, Wagenaar E, Jansen RS, Rosing H, Beijnen JH, Schinkel AH. Multidrug resistance protein 2 is an important determinant of paclitaxel pharmacokinetics. *Clin.Cancer Res.* **2006**; 12 (20 Pt 1): 6125-32.
 30. van Waterschoot RA, Lagas JS, Wagenaar E, Rosing H, Beijnen JH, Schinkel AH. Individual and combined roles of CYP3A, p-glycoprotein (MDR1/ABCB1) and MRP2 (ABCC2) in the pharmacokinetics of docetaxel. *Int.J.Cancer* **2010**; 127 (12): 2954-64.
 31. Sgadari C, Monini P, Barillari G, Ensoli B. Use of HIV protease inhibitors to block Kaposi's sarcoma and tumour growth. *Lancet Oncol.* **2003**; 4 (9): 537-47.
 32. Pati S, Pelser CB, Dufraigne J, Bryant JL, Reitz MS, Jr, Weichold FF. Antitumorigenic effects of HIV protease inhibitor ritonavir: inhibition of Kaposi sarcoma. *Blood.* **2002**; 99 (10): 3771-9.
 33. Gaedicke S, Firat-Geier E, Constantiniu O, Lucchiari-Hartz M, Freudenberg M, Galanos C, Niedermann G. Antitumor effect of the human immunodeficiency virus protease inhibitor ritonavir: induction of tumor-cell apoptosis associated with perturbation of proteasomal proteolysis. *Cancer Res.* **2002**; 62 (23): 6901-8.
 34. Maggiorella L, Wen B, Frascogna V, Opolon P, Bourhis J, Deutsch E. Combined radiation sensitizing and anti-angiogenic effects of ionizing radiation and the protease inhibitor ritonavir in a head and neck carcinoma model. *Anticancer Res.* **2005**; 25 (6B): 4357-62.
 35. Srirangam A, Milani M, Mitra R, Guo Z, Rodriguez M, Kathuria H, Fukuda S, Rizzardi A, Schmechel S, Skalnik DG, Pelus LM, Potter DA. The human immunodeficiency virus protease inhibitor ritonavir inhibits lung cancer cells, in part, by inhibition of survivin. *J.Thorac.Oncol.* **2011**; 6 (4): 661-70.
 36. Ikuno N, Soda H, Watanabe M, Oka M. Irinotecan (CPT-11) and characteristic mucosal changes in the mouse ileum and cecum. *J.Natl.Cancer Inst.* **1995**; 87 (24): 1876-83.
 37. Sandmeier D, Chaubert P, Bouzourene H. Irinotecan-induced colitis. *Int.J.Surg.Pathol.* **2005**; 13 (2): 215-8.
 38. Inomata A, Horii I, Suzuki K. 5-Fluorouracil-induced intestinal toxicity: what determines the severity of damage to murine intestinal crypt epithelia? *Toxicol.Lett.* **2002**; 133 (2-3): 231-40.





Quantification of taxanes in biological matrices: A review of bioanalytical assays and recommendations for development of new assays.

Jeroen J.M.A. Hendrikx
Hilde Rosing
Alfred H. Schinkel
Jan H.M. Schellens
Jos H. Beijnen

Bioanalysis.
Accepted

Abstract

Since the isolation of paclitaxel and its approval for the treatment of breast cancer, various taxanes and taxane formulations have been developed. To date, almost 100 bioanalytical assays have been published and method development and optimization is often extensively discussed by the authors. This review presents an overview of assays published between January 1970 and September 2013 that described method development and validation of assays used to quantify taxanes in biological matrices such as plasma, urine, faeces and tissue samples. For liquid chromatography assays, sample pre-treatment, chromatographic separation and assay performance are compared. Since this review discusses the limitations of previously developed liquid chromatography assays and gives recommendations for future assay development, it can be used as a reference for future development of liquid chromatography assays for the quantification of taxanes in various biological matrices to support preclinical and clinical studies.

Introduction

Paclitaxel (Taxol[®]) and docetaxel (Taxotere[®]), both taxanes (Figure 1), are widely used as intravenously administered anticancer agents for several types of cancer.^{1,2} Paclitaxel is originally derived from the bark of *Taxus brevifolia*, whereas docetaxel is a semisynthetic derivative of a taxane isolated from the needles of *Taxus baccata*.³ Paclitaxel was isolated in the early 1970s and docetaxel was found a decade later.⁴ Paclitaxel was approved by the Food and Drug Administration (FDA) in 1992 and docetaxel approval followed in 1996. An albumin-bound formulation of paclitaxel (Abraxane[®]) was approved in 2005 for breast cancer treatment and in 2010, cabazitaxel (Jevtana[®]) was licensed for treatment of prostate cancer. More taxane analogues and taxane formulations are being reported in literature.^{5,6} The anti-cancer effect of taxanes is attributed to binding of the taxanes to β -tubulin. This binding promotes polymerization of tubulin and stabilises microtubules. The stabilisation of microtubules leads to cell cycle arrest and apoptosis.⁷

Absorption, distribution, metabolism and excretion of drugs are studied during drug development in preclinical and clinical settings. Reliable and sensitive bioanalytical assays for quantification of taxanes in plasma, urine, faeces and tissue samples are prerequisites to support these trials. Over time, multiple assays have been developed and described to quantify taxanes in these matrices. These include methods such as tubulin-based biochemical assays, immunoassays and chromatography-based assays. The last encompasses micellar electrokinetic chromatography (MEKC) or liquid chromatography (LC) platforms coupled with ultraviolet (UV) or mass spectrometry (MS) detection.

This review aims to present a comprehensive overview of publications that describe bioanalytical assays that have been developed to quantify taxanes in biological matrices. Since LC-UV and LC-MS/MS assays are mostly used for quantification of taxanes, we focus on the performance of various sample preparation procedures and separation and detection techniques used for these assays. Moreover, we bring forward recommendations for the development of new bioanalytical LC assays for the quantification of taxanes. Chemical structures of the taxanes included in this review are presented in Figure 1.

PubMed was searched and publications were selected that describe method development and validation of assays used to quantify taxanes in biological matrices originating from humans or animals. The keyword *assay* was combined with keywords *taxane; paclitaxel; docetaxel; cabazitaxel; felotaxel; azidotaxol; larotaxel; ortotaxel; BMS-184476; BMS-18879; SHR11000; SB-T-1214; SB-T-12854; DJ 927; IDN5109 or TPI-287*. Results were limited to publications in English and published between January 1970 and September 2013. Cited references were considered and included when inclusion criteria were met.

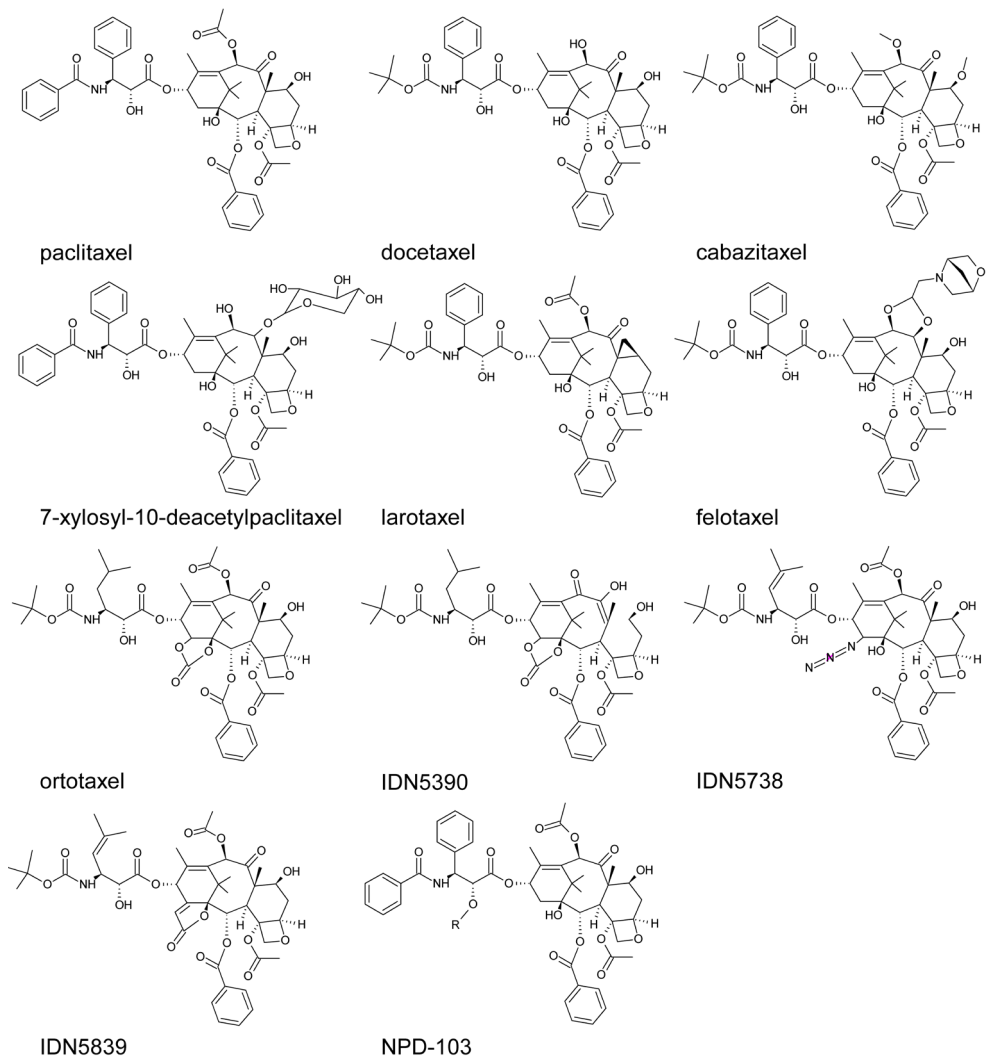


Figure 1. Structures of taxanes. The structure of NPD-103 is not further specified.¹⁰⁴

Target concentration ranges for the quantification of taxanes

The development and validation of a bioanalytical assay is never an isolated objective. The call for a new bioanalytical assay is based on the need of quantifying drug concentrations in samples derived from preclinical or clinical studies or in samples for therapeutic drug monitoring (TDM). The target concentration range is therefore based on the expected drug concentrations in the samples.

In patients, total plasma concentrations at the end of a 3h infusion of a dose of 135-225 mg/m² paclitaxel ranged from ~850 to 8500 ng/mL. At 24 hours after infusion, plasma concentrations ranged from 8 to 110 ng/mL and from 0.8 to 8 ng/mL at 72 hours after infusion.^{8,9} Plasma concentrations in samples taken during the first 24 hours after intravenous administration of 20-80 mg/m² paclitaxel as a 1 hour infusion ranged from 30 to 2000 ng/mL, depending on the time of sampling.¹⁰ Plasma concentrations of 40 mg/m² docetaxel administered as an 1 hour infusion ranged from 10 to 2000 ng/mL during the first 24 hours.¹¹ Intravenous administration of 25 mg/m² cabazitaxel over 1 hour resulted in plasma concentrations from 1 to 1000 ng/mL during the first 24 hours after administration.¹² Maximal plasma concentrations of these taxanes in animal models are often 1 to 10-fold higher than concentrations in human plasma.¹³⁻¹⁵ Based on these pharmacokinetic data of the taxanes that are approved by the FDA, in general, one should aim for a lower limit of quantification (LLOQ) of at least 1 ng/mL during development of assays to support (pre)clinical trials.

For TDM, the need for sensitive assays is usually less urgent. Most important is accurate quantification of plasma concentrations that are important for clinical decisions. Recently, Gerritsen et al.¹⁶ reviewed the level of evidence for therapeutic drug monitoring of taxanes. For docetaxel, the relation between plasma exposure and the risk for neutropenia is not clear yet. This makes TDM for docetaxel, and thus the need for bioanalytical assays for this purpose, currently not that important. However, for paclitaxel, a relation between hemotological toxicity and plasma exposure is observed. The longer the period that plasma concentrations are over 43 ng/mL, the higher the risk for severe neutropenia.¹⁷ Therefore, for bioanalytical assays to support TDM of paclitaxel an LLOQ of 30-40 ng/mL is sufficient, although Gerritsen et al. conclude that there is no strong case for standard implantation of TDM for paclitaxel.¹⁶

Techniques used for the quantification of taxanes

In this section, we briefly discuss the techniques used for the quantification of taxanes in biological matrices. LC assays coupled with UV or MS/MS detection are mostly reported. Therefore we will focus on these techniques in later sections of this review, where we discuss sample pre-treatment, chromatographic separation and performance in more detail.

High Performance Liquid Chromatography coupled Ultra Violet detection (HPLC-UV)

HPLC-UV is a commonly used technique for quantification of drugs and is also widely applied for quantification of taxanes in biological matrices (Supplemental table 1). Up to now, most HPLC-UV assays have been developed for quantification of paclitaxel¹⁸⁻³⁸, but also assays for quantification of docetaxel³⁹⁻⁴⁴ and incidentally other taxanes such as larotaxel, felotaxel and ortotaxel are described⁴⁵⁻⁴⁸. Not only assays for single taxane quantification are developed using HPLC-UV, but also assays for combined quantification of docetaxel, paclitaxel and other drugs⁴⁹⁻⁵¹ and assays for quantification of parent drugs and metabolites⁵²⁻⁵⁴. Most assays quantify taxanes in human or rodent plasma, although some assays have been designed for quantification of taxanes in serum^{18;19;37}, tissue^{22;54}, urine^{21;26;28;29;41;48;54} or faeces⁵⁴.

The calibration range of the taxanes is linear up to concentrations of 20000 ng/mL, although for paclitaxel, even a calibration range of 25 ng/ml to 10 mg/mL is reported. A limitation of UV detection is the sample volume needed, since volumes of 0.5-1 mL are often required to increase the LLOQ. The most sensitive assay for quantification of paclitaxel in human plasma has an LLOQ of 3 ng/mL using 500 μ L of sample.³³ A lower sample volume is used for analysis of rat plasma samples. Using only 100 μ L of sample, concentrations down to 10 ng/mL can be measured.^{22;23;35} The most sensitive HPLC-UV assays for quantification of docetaxel have an LLOQ of 5 ng/mL using 900 or 1000 μ L of sample^{39;41;43}, while felotaxel is quantified above 5 ng/mL using 100 μ L of sample⁴⁸. Since other taxanes share the absorption maximum at 227 nm with paclitaxel and docetaxel, it is likely that sensitivity of UV is in the same range for other taxanes. Therefore, HPLC-UV can be used when an LLOQ of 3-10 ng/mL is sufficient and sample volumes up to 1000 μ L can be collected.

Liquid Chromatography coupled tandem mass spectrometry (LC-MS/MS)

Liquid chromatography coupled tandem mass spectrometry (LC-MS/MS) is a highly selective and sensitive method, often used for quantification of taxanes in biological matrices (Supplemental table 2-6). Bioanalytical assays for quantification of paclitaxel⁵⁵⁻⁶⁹ (Supplemental table 2), paclitaxel and its metabolites⁷⁰⁻⁷⁴ (supplemental table 3), or paclitaxel and other drugs (including docetaxel)⁷⁵⁻⁸¹ (supplemental table 5) by LC-MS/MS are widely described, while for quantification of docetaxel⁸²⁻⁸⁹, docetaxel and its metabolites^{90;91} (Supplemental table 4), or docetaxel and other drugs⁹²⁻⁹⁴ (Supplemental table 5), fewer assays are published. A limited number of LC-MS/MS assays is developed for quantification of the second generation taxanes cabazitaxel^{95;96}, felotaxel^{97;98} and larotaxel⁹⁹ and other taxane analogues¹⁰⁰⁻¹⁰⁴ (Supplemental table 6). Usually tandem quadrupole mass spectrometry is performed, but assays using mass spectrometry with a single quadrupole have also been developed for quantification of paclitaxel and docetaxel.^{58;80} Like HPLC-UV assays, most LC-MS/MS assays are applied for quantification of taxanes in human or rodent plasma, although assays for taxanes in dog plasma^{70;98;99;102} and human or rodent serum^{62;88}, tissue^{58;59;64;66;97;103}, ultrafiltrate⁷⁸, urine and faeces^{81;97}, oral fluids⁷⁷ and even post mortem samples⁷⁵ are also described.

Using mass spectrometry as detection technique, sensitivity of the developed assays is drastically increased compared to UV detection. HPLC-UV assays have a quantification limit of 3-10 ng/mL using sample volumes up to 1000 μ L (see previous section), while LC-MS/MS assays with a quantification limit of 0.1-0.25 ng/mL for paclitaxel^{59;61;64-66;70;72;75;77} and docetaxel^{80;82;85;91;96}, with sample volumes of just 10-200 μ L are reported. Use of Ultra Performance Liquid Chromatography (UPLC) instead of HPLC can increase resolution and sensitivity of LC-MS/MS assays¹⁰⁵, but although UPLC-MS/MS assays are described for taxane quantification^{67;89;99;104}, so far, the use of UPLC did not result in a lower LLOQ. In assays using mass spectrometry for detection, calibration plots are mostly linear over a large concentration range (3-4 decades), reducing the need for sample dilution prior to sample pre-treatment to a minimum.

Micellar electrokinetic chromatography (MEKC)

Micellar electrokinetic chromatography (MEKC) is a separation method in which micelles act as a pseudostationary phase in a solution. Compared to HPLC, MEKC has a higher separation power and is less sensitive to endogenous compounds in the matrix. MEKC is usually coupled to a UV detector for signal detection. Since MEKC in general requires a smaller sample volume, sensitivity is usually low compared to HPLC-UV.¹⁰⁶ MEKC is used for quantification of paclitaxel in human plasma, serum and urine (Supplemental table 7).¹⁰⁷⁻¹⁰⁹ Recovery is reported to be >70% and the LLOQ is 50-280 ng/mL using 200-1000 μ L of sample. Both liquid-liquid extraction¹⁰⁷ and solid-phase extraction¹⁰⁸ are described as pre-treatment for plasma samples containing paclitaxel, although Rodríguez et al.¹⁰⁹ showed that sample pre-treatment is not necessary to quantify paclitaxel in urine samples. Hempel et al.¹⁰⁷ observed that a sodium dodecyl sulphate (SDS) concentration of 100 mmol/L resulted in good separation of paclitaxel and endogenous compounds, while 50 mmol/L did not result in good separation. Rodríguez et al.¹⁰⁸ further optimized the SDS concentration to 60 mmol/L. Although MEKC has a higher separation power and is less sensitive to endogenous interference than HPLC-UV, sensitivity for quantification of taxanes is lower. Moreover, plasma samples still require sample pre-treatment and run time is similar compared to HPLC-UV. Since HPLC-UV systems are available in most laboratories, HPLC-UV is favoured over MEKC.

Immunoassays

The development of enzyme-linked immunoassays^{110;111} and a fluoroimmunoassay¹¹² for quantification of paclitaxel in biological samples have been described (Supplemental table 7). These immunoassays utilize binding of paclitaxel to antibodies for quantification of paclitaxel. The limits of quantification are below 0.5 ng/mL, which is much lower than for HPLC-UV. However, not only the parent compound might bind to the antibodies, but also structure analogues. Cross-reactivity to these structure analogues (like metabolites) is common and results in decreased accuracy of the calculated concentrations. Since LC-MS/MS has similar sensitivity and improved selectivity, there is no obvious advantage of immunoassays over LC-MS/MS for quantification. Based on the number of developed and reported immunoassays and LC-MS/MS assays, nowadays LC-MS/MS remains the cornerstone for quantification of taxanes when high sensitivity is required.

Tubulin-based biochemical assays

Tubulin-based biochemical assays have been published for quantification of paclitaxel in human serum¹¹³ and plasma¹¹⁴ and make use of its mechanism of action for quantification (Supplemental table 7). Hamel et al.¹¹³ measured hydrolysis of labelled guanosine triphosphate (GTP) to labelled guanosine diphosphate (GDP). This hydrolysis is stimulated by paclitaxel and associated with tubulin polymerisation. GDP formation was measured since it is paclitaxel concentration dependent and a linear relation between GDP formation and paclitaxel concentration was found in a concentration range of 256 to 2562 ng paclitaxel/mL. Morais et al.¹¹⁴ developed an assay based on the binding of paclitaxel to tubulin. Competitive binding to tubulin of rhodamine-labelled paclitaxel and paclitaxel resulted in a change in fluorescence polarisation. Change in polarisation response was linear in a concentration range of 25.6 to 299 ng/mL paclitaxel. Like for immunoassays, cross-reactivity to structure analogues (e.g. metabolites) can not be excluded in tubulin based biochemical assays. Sample pre-treatment is minimal, but sensitivity of tubulin-based biochemical assays is limited compared to HPLC-UV and LC-MS.

Sample pre-treatment for liquid chromatography (LC) assays.

Liquid chromatography (LC) is usually coupled to UV or MS/MS detection. A major drawback of HPLC-UV assays for quantification of taxanes is the detection at 227 nm. At this relatively low wavelength, potential interferences of endogenous compounds can be expected. For LC-MS assays, clean samples for injection are also preferred to reduce matrix effects, although stable labelled isotope internal standards are capable to compensate for these matrix effects. In the following sections, protein precipitation, liquid-liquid extraction and solid phase extraction in LC taxane analysis are discussed as sample pre-treatment procedures to concentrate and clean up bioanalytical samples.

Protein precipitation

Protein precipitation is not favoured as sample pre-treatment for HPLC-UV assays due to potential interferences of endogenous compounds. Since spectral interferences originating from endogenous compounds are less likely in mass spectrometry due to increased specificity, protein precipitation is more frequently used in LC-MS/MS assays.

For protein precipitation, a solvent must increase protein-protein interactions, which results in protein aggregation and precipitation. Moreover, the solvent must result in a high, reproducible recovery of the analytes of interest. The sample pre-treatment recovery is usually tested by comparison of the response of the analyte in a processed sample with the response of the analyte in a neat solution.¹¹⁵ For MS assays, the sample pre-treatment recovery is usually determined by comparing the response of the analyte in a processed sample to the analyte response in a sample spiked to a processed blank sample. In this way, a correction is made for potential matrix effects. Currently six validated LC assays utilize protein precipitation as sample pre-treatment. Three of them are HPLC-UV assays that have been developed for paclitaxel quantification.^{23,25,38}

Acetonitrile was used as precipitation solvent and extraction recoveries were between 75 and 100%. Marangon et al.¹⁰¹ quantified taxane analogues IDN5738 and IDN5839 by LC-MS/MS and used protein precipitation with 0.1% formic acid in acetonitrile (v/v) as sample pre-treatment. Extraction recoveries were over 90%. Protein precipitation was also used as sample pre-treatment for LC-MS/MS assays to quantify docetaxel. Hou et al.⁸⁴ used methanol:acetonitrile (1:1, v/v) as precipitation solvent, while Yamaguchi et al.⁸⁷ used only acetonitrile. Extraction recoveries of docetaxel were above 77%. Often the volume of the extraction solvent is 2 to 4 times the volume of the sample, although Kumar et al.²³ used a 8-fold higher volume of solvent.

Protein precipitation is a fast sample pre-treatment procedure with high recovery. However, high background signals or endogenous interferences can hamper sensitive quantification. Endogenous compounds in the sample can also cause ion suppression during ionisation in MS/MS assays and the robustness of the LC method can be negatively affected due to covalent binding of proteins to the analytical column. This may lead to an increase of the backpressure of the analytical column and decrease of the number of plates (selectivity).

Liquid-liquid extraction

Although liquid-liquid extraction is more time consuming compared to protein precipitation or on-line solid phase extraction, at the moment, using this sample pre-treatment procedure, the lowest LLOQs can be obtained in taxanes assays.^{48;70;75;96}

The first step of liquid-liquid extraction is selection of the extraction solvent. Zhang et al.⁷⁴ compared recovery of paclitaxel and its metabolites after liquid-liquid extraction. It was observed that a mixture of chloroform and ether (1:1, v/v) resulted in the most efficient extraction (64-84%), compared to ether, chloroform, ethyl acetate and methylene chloride. Lee et al.²⁴ observed low recoveries (<40%) of paclitaxel after liquid-liquid extraction using methylene chloride, chloroform and hexane, while extraction using diethyl ether or tertiary-butylmethylether resulted in better recovery (93 to 99%). Rizzo et al.²⁹ also reported that recovery for paclitaxel after liquid-liquid extraction was complete using tertiary-butylmethylether instead of chloroform or ethyl acetate. Martin et al.²⁸ varied the pH during extraction of paclitaxel with diethyl ether and observed the best recovery at pH 5, although the tested pH-range and recoveries were not specified. Ciccolini et al.⁴⁰ showed that extraction of docetaxel with diethyl ether resulted in a better recovery (average 95%) than extraction with chloroform, ethyl acetate or butyl methyl ether. Felotaxel extraction was tested using diethyl ether, ethyl acetate, cyclohexane, dichloromethane or n-butanol as extraction solvents by Yan et al.⁴⁸ and using diethyl ether, ethyl acetate, cyclohexane, methylene chloride and n-butanol by Hu et al.⁹⁸. In both cases, ethyl acetate was selected as solvent since this resulted in reproducible recovery (80.5-89.3% and 70-77%, respectively). Moreover, ethyl acetate reduced interferences in the UV chromatogram.⁴⁸ Liu et al.⁹⁹ reported larotaxel recovery after liquid-liquid extraction with ether, ethyl acetate and tertiary-butylmethylether. A recovery of 80-88% was observed with ether or tertiary-butylmethylether as extraction solvent, although matrix effects in the LC-MS/MS assays were reduced with tertiary-butylmethylether compared to ether.

From these results it can be concluded that diethyl-ether or tertiary-butylmethylether are the best extraction solvents for liquid-liquid extraction of taxanes. However, the volume of extraction solvent that is used for extraction of the analyte of interest is highly variable. Volumes in the range of 3 to 20 times the volume of the sample are reported. Usually a volume of 1-3 mL extraction solvent is used, independent of the matrix or sample volume.

Surprisingly, Martin et al.²⁸ reported that pH 5 during extraction with diethyl ether increases the recovery of paclitaxel, while Lee et al.²⁴ report a recovery of 93 to 99% using the same solvent without adjusting pH. Since paclitaxel is not charged at physiological pH and estimated logarithmic acid dissociation constants (pKa's) of 10.4 and -1 are reported¹¹⁶, a decrease from pH~7 to pH 5 should theoretically not affect the charging of the molecule and thereby not affect the extraction efficiency of paclitaxel.

Based on the discussed results, we advise to start with liquid-liquid extraction with tertiary-butylmethylether during method development of taxane assays, to obtain high recoveries and to minimize endogenous interferences. Moreover, matrix effects in taxane MS assays are reduced by tertiary-butylmethylether.

Solid phase extraction

Although solid phase extraction is used in multiple developed assays, optimisation of solid phase extraction is less discussed than optimisation of liquid-liquid extraction. Reported extraction recovery of paclitaxel, docetaxel and metabolites of both taxanes after solid phase extraction is usually 75-99%^{33;35;36;41;45;50;52;53}. Rosing et al.⁵³ showed it is best to use end-capped cyano columns for solid-phase extraction of docetaxel to increase recovery and that loading flow should be optimised during assay development. A similar extraction procedure is described by Garg et al.⁴¹ and reported recoveries are 99% by Garg et al. and ~85% by Rosing et al.

Not only recovery, but also the selectivity to reduce interferences and background signals is an important parameter during the selection of a sample pre-treatment procedure. Suno et al. observed that vacuum drying of the extraction cartridge decreased background signals during analysis.³³ Another option is to wash extraction columns with methanol:water (1:1, v/v) after loading the column with the sample and prior to analyte elution.⁴⁴ Guo et al.⁵⁸ report that solid phase extraction of paclitaxel using C₁₈ extraction columns resulted in a high background signal and therefore they preferred C₂ extraction columns with less background interferences. However, in an assay for docetaxel, solid-phase extraction using C₁₈ Uptisphere® columns completely removed interferences.³⁹

Solid phase extraction cannot always completely remove interferences. For instance, Rouini et al. observed late eluting peaks after off-line solid phase extraction and therefore combined solid phase extraction with on-line solid phase extraction to reduce these interferences.⁴³ Although off-line solid phase extraction is an expensive and labour-intensive pre-treatment procedure, on-line solid phase extraction by column switching can reduce handling time. The principle of on-line solid phase extraction by column switching is based on the combination of a pre-column and an analytical column.¹¹⁷

The pre-column is used for a clean up step during analysis. An unprocessed sample is injected into the system and led onto the pre-column. Protein molecules pass the column rapidly, while the analyte of interest is adsorbed to the pre-column. This can be based on hydrophilic/hydrophobic, ion-exchange or size exclusion.¹¹⁷ The next step is a switch of solvent, after which the analyte is flushed from the pre-column and directed to an analytical column for chromatographic separation or directly transferred to the MS/MS for detection. On-line solid-phase extraction with direct injection of plasma to quantify a taxane was first described by Mader et al.²⁷. A C_4 -ADS column was used for sample clean-up and paclitaxel was quantified using an UV detector. The overall runtime was 25 minutes per sample, although a wash step of 5 minutes was used after injection of each sample for reconditioning of the pre-column. Grozav et al.⁸³ were the first to report on-line solid-phase extraction coupled with MS/MS detection for quantification of docetaxel and Yamaguchi et al.⁷³ described on-line solid-phase extraction coupled with MS/MS for the quantification of paclitaxel and its metabolites. An important limitation of on-line solid phase extraction is carry-over from the extraction cartridge. The carry-over effect can be reduced by a washing step prior to the injection of a sample⁸³ or by (automated) use of disposable cartridges¹¹⁸. The first procedure will increase the runtime, while the second procedure increases costs per analysis.¹¹⁹

In general, C_{18} columns provide a good recovery and minimal interferences. If recovery is limited, we advise to use end-capped cyano columns since the recovery of taxanes using these columns is high (85-100%). To further reduce background signals, one should optimize the washing solvent. On-line solid phase extraction by column switching can reduce sample handling time compared to off-line solid phase extraction without affecting sample clean-up. Therefore on-line solid phase extraction is a better option than offline solid-phase extraction when high sample throughput is required. However, carry-over effect may occur and should be determined during the validation of the procedures.

Selection of sample pre-treatment procedure

As described above, protein precipitation, liquid-liquid extraction and solid phase extraction have previously been used as sample pre-treatment procedure in taxane assays. When new assays are developed, often one procedure will be selected and optimised. In a few publications different sample pretreatment procedures were compared. Ardiet et al.³⁹ tested liquid-liquid extraction with ethyl acetate, dichloromethane or chloro-1-butane and compared liquid-liquid extraction with solid-phase extraction using C_{18} Uptisphere® columns for docetaxel quantification. After liquid-liquid extraction, interferences were still observed but when solid-phase extraction was applied, interferences were reduced. Lopez et al.⁴⁹ tested solid-phase extraction and liquid-liquid extraction as sample pre-treatment for paclitaxel and docetaxel quantification, but selected liquid-liquid extraction with ethyl acetate and n-butyl chloride for docetaxel and paclitaxel, respectively. Both Ardiet et al.³⁹ and Lopez et al.⁴⁹ preferred the selected extraction procedure because of reduced interferences. Since both selected another extraction procedure, the data indicate that no extraction procedure is clearly preferred.

Using protein precipitation, sample clean up is reduced, but since it is less likely that endogenous compounds interfere with MS detection than with UV detection, protein precipitation is a fast alternative as sample pre-treatment when MS detection is used. Especially when less sensitivity is required (e.g. quantification above 5 to 10 ng/mL), protein precipitation is a good alternative for liquid-liquid extraction or solid phase extraction.

At the moment, liquid-liquid extraction seems to be in favour as pre-treatment procedure in reported assays for sensitive quantification of taxanes. Extraction with tertiary-butylmethylether is advised, since it combines high recovery with an adequate reduction of spectral interferences and matrix effects, leading to robust bioanalytical assays. If high sample throughput is required, automated protein precipitation or on-line solid phase extraction are advised.

Chromatographic separation in liquid chromatography (LC) assays.

Selection of the stationary and mobile phases

Reversed-phase C_8 or C_{18} silica-bounded columns are used in LC assays for quantification of taxanes, although incidentally an alkyl amide silica bounded column¹⁰³ or a C_{12} silica bounded column⁷¹ is applied. The mobile phase usually consists of at least 50% (v/v) organic solvent to elute the analytes from the column. Both acetonitrile and methanol are applied as organic solvents. Since the reconstitution solvent often mimics the mobile phase, an additional benefit of using non-aqueous solvents is the improvement of stability of taxanes. In aqueous solutions, the stability of paclitaxel and related compounds is hampered by epimerisation, as extensively described in a series of publications by Tian and Stella.¹²⁰⁻¹²² A reconstitution solvent containing at least 50% of organic solvent (compatible with the mobile phase, preventing solvent effects), thus might increase stability of taxanes in reconstituted samples. Additives in the mobile phase are commonly used, although they do not always result in better peak shape or reduced background signal.³¹ In all developed assays, the mobile phase is optimized to reduce endogenous interferences, increase selectivity, and improve peak shape.

In HPLC-UV assays, absorbance of ultraviolet light by taxanes is usually measured at a wavelength of 227 nm. At this wavelength, there is a maximum in the UV absorbance due to the presence of the baccatin III ring structure, which is the bone structure of taxanes.¹²³ However, detection at 227 nm is not specific and unknown endogenous compounds are reported showing retention at C_{18} columns and absorbance at this wavelength.³⁵ Moreover, pharmaceutical additives can show absorbance at this wavelength and interfere with the assay. Cremophor EL[®] (polyoxyethylated castor oil), a commonly used additive in paclitaxel formulations (Taxol[®]), has an absorption maximum at 230 nm.²⁴ Polysorbate 80, the pharmaceutical additive in docetaxel formulations, has an absorption maximum at 234 nm.¹²⁴ Therefore, optimisation of the composition of the mobile phase is required for UV detection to separate taxanes from both endogenous interferences and additives in drug formulations containing

Cremophor EL and polysorbate 80. In mass spectrometry, mass to charge ratios (m/z) are selected. The molecular masses of ~ 2500 and 1310 g/mol of Cremophor EL and polysorbate 80, respectively, make chromatographic separation from taxanes not required, although it is reported that these pharmaceutical additives can cause ion suppression of docetaxel and paclitaxel.^{60;77} However, a labelled analogue of the analyte of interest as internal standard can compensate for the ion suppressive effects of the pharmaceutical additives and potential endogenous interferences.

Ionisation in liquid chromatographic mass spectrometry assays

Electrospray ionisation (ESI)

Ionisation by ESI in the positive mode is the most used ionisation technique for LC-MS/MS quantification of taxanes, although ESI in the negative ion mode is described for quantification of IDN 5390, IDN5738 and IDN5839.^{101;102} During development of multiple assays, response for ESI in positive and negative mode is compared. For docetaxel^{83;89;93}, felotaxel⁹⁷, paclitaxel^{65;66} and 7-xylosyl-10-deactetylpaclitaxel¹⁰⁰ it appears that ionisation in the positive mode results in an optimal analytical responses. Negative ion mode resulted in higher responses of IDN 5390 and ortotaxel.¹⁰² In general, all neutral substances are able to form positive ions during positive ionisation, while negative ionisation requires acidic groups or mobile phase additives.¹²⁵ Since taxanes are not charged at physiological pH and have a higher number of hydrogen acceptor counts than hydrogen donor counts¹¹⁶, it is not surprising that ionisation in the positive mode results in the best sensitivity.

Other ionization techniques

In some assays, ionisation techniques other than ESI are used for ionisation of paclitaxel. APCI is used by Mortier et al.⁶⁰ and Schellen et al.⁶² and sonic spray ionisation (SSI) in the positive mode is reported by Green et al.⁷¹. Mortier et al.¹²⁶ and Green et al.⁷¹ compared the effect of the ionisation technique on the response of paclitaxel. Mortier observed the best response using ESI, while Green reported that SSI resulted in a higher signal to noise. Both Green and Mortier confirmed that APCI for ionisation of paclitaxel resulted in low sensitivity. Since ESI is the more common technique, this is most likely usually preferred over SSI.

Additives in the mobile phase to improve ionization efficiency in MS/MS detection.

The composition of the mobile phase can influence ionisation of the analyte of interest. Guitton et al.⁹⁰ report that docetaxel response is decreased when the composition of the mobile phase is increased from 50 to 95% acetonitrile. Also the pH of the mobile phase can influence the response. Although almost all LC-MS/MS assays use a neutral or acid mobile phase, it is reported that an alkaline mobile phase can increase docetaxel, paclitaxel and cabazitaxel response.^{64;76;85;96} The increased response at alkaline pH is also reported for other compounds.¹²⁷ In general, acidic analytes have a better ionisation

response during electrospray ionization (ESI) when an alkaline mobile phase is used, while basic analytes have a better response when the mobile phase is acidic.¹²⁸ This is attributed to the charge that is already present at the analyte during droplet formation. However, this is not the only effect that a change in pH might have. Ionisation response is also determined by the disposition of an analyte in the droplets that are formed by ESI.¹²⁸ Paclitaxel, docetaxel and cabazitaxel are not charged at physiological pH.¹¹⁶ Moreover, the pKa of these drugs are around 11 (basic groups) and below 0 (acidic groups). This indicates that varying the pH in the range 3-11 (a common range used for a mobile phase) most likely does not change the charge of the compound. Therefore the charge at the analyte that is already present during droplet formation does not change. However, the change in pH might result in changed chemical characteristics of the mobile phase or the analytes (e.g. protonation or changed surface-activity) and therefore change the disposition of the analyte in the droplet as we previously proposed.¹²⁹ This speculative change in disposition could explain the increase in response of taxanes at alkaline pH.

Another way to increase detection sensitivity of analytes and improve ionization efficiency for ESI and atmospheric pressure chemical ionization (APCI), is the use of additives in the mobile phase.¹³⁰ It is reported that addition of acids like formic acid^{86,97} and acetic acid⁸⁴ increases the response of taxanes. Responses are usually increased by additives that limit formation of adducts like sodium adducts, although substantial adduct formation of docetaxel is reported despite addition of 0.1% (v/v) formic acid to the mobile phase.⁹³ This might be related to the additive used, since docetaxel response was higher after addition of acetic acid than after addition of formic acid.⁹⁰ Addition of acetic acid to the mobile phase had a more pronounced impact on decreased formation of sodium adducts of paclitaxel compared to addition of formic acid or trifluoroacetic acid.⁷⁰ Larotaxel response was higher using ammonium acetate as additive compared with formic acid and acetic acid.⁹⁹ Stokvis et al.⁶⁴ reported that ammonium-containing additives (ammonium acetate, ammonium hydroxide and ammonium formate) in the mobile phase resulted in an increased paclitaxel response compared to acetic acid, formic acid or no additive in the mobile phase. It is proposed that proton transfer from the positive ammonium ion to the neutral paclitaxel molecule increases paclitaxel response. The proton transfer could be explained by ion-molecule reactions or collision induced dissociation.⁷²

Although additives in the mobile phase are mostly used to limit adduct formation, sometimes they are deliberately added to the mobile phase to form adducts during ionisation. The response of these adducts can be higher than the response of the protonated parent ion ($[M+H]^+$). In taxane assays, sodium adducts ($[M+Na]^+$) were sometimes selected for quantification^{61,65-67,74;94;104}, although response of $[M+Na]^+$ is not always higher than response of $[M+H]^+$.⁷⁸ Not only sodium, but also ammonium¹⁰³ or carboxyl adducts^{101;102} can be used for quantification. Formation of salt adducts can also be increased by adding salts to the samples during pre-treatment and thereby result in specific formation of this adduct during ionisation.⁶¹ Addition of primary amines to the sample and detection of the adducts ($[M+\text{primary amine}+H]^+$) also increased the sensitivity and reduced formation of other adducts. Primary amines with a longer chain length (e.g. octylamine and dodecylamine) resulted in the highest sensitivity.^{56;126}

A major disadvantage of the use of uncommon additives as primary amines for adduct formation is possible contamination of the mass spectrometer. This might affect adduct formation in other assays that run on the same device.

Quantification of taxanes in biological matrices other than plasma using liquid chromatography (LC) assays.

Although most LC assays have been developed for quantification of taxanes in plasma or serum, some are also developed for quantification of taxanes in other matrices. For evaluation of tissue distribution and *in vivo* excretion, multiple assays in tissue samples and faeces or urine have been published.^{21;22;26;28;29;38;41;48;54;58;59;64;66;81;97;103} Also LC-MS/MS assays in less routinely studied matrices can be found in the literature. Paclitaxel and derivatives are quantified in post mortem samples⁷⁵, docetaxel and paclitaxel in oral fluids⁷⁷ and paclitaxel in dried blood spots⁶¹.

Handling and storage of matrices other than plasma often results in matrix-specific limitations. Previously, we showed that dilution of faeces and urine samples can result in a biased quantification of docetaxel and paclitaxel.⁸¹ Storage of homogenized faeces samples at -20 °C resulted in overestimation of the analyte concentrations (up to 33% of the nominal concentration) when stored samples are thawed and diluted. Apparently, thawing a homogenized sample after storage results in non-uniform distribution of the analytes in the sample. Since faeces samples were homogenized with water, it is hypothesized that during storage, the lipophilic drugs might bind to fecal components and this could result in non-uniform distribution. Dilution of homogenized faeces samples prior to storage resulted in unbiased quantification.

Dilution of urine samples can result in underestimation of the analyte concentration when low sample volumes of urine are used for dilution. This can be explained by adsorption of the analytes to the container wall. Therefore, for urine and homogenized faeces samples, it is advised to take aliquots and make dilutions for quantification prior to storage.⁸¹ Huizing et al.²¹ also observed biased quantification after storage of urine samples. It was reported that recovery of paclitaxel in urine was less than 70% after storage for 2 weeks at -20 °C. Recovery of paclitaxel in the urine sample was increased when 5% (v/v) Cremophor:ethanol (1:1, v/v) was added and this resulted in prolonged stability at -20 °C up to 17 months.

For LC assays with UV detection, chromatographic separation of endogenous peaks and peaks of the analyte of interest is often sufficient for accurate quantification, even when calibration standards in plasma are used to quantify taxanes in faeces, urine or tissue samples.^{22;41;54}

However, in LC assays with MS/MS detection, matrix effects can seriously hamper quantification of taxanes. Matrix effects like ion suppression or ion enhancement can be caused by endogenous compounds¹³¹ and ionisation can be different in samples originating from different matrices. Ding et al.⁹⁷ showed that the response of felotaxel was different in plasma, tissue samples, faeces and urine samples. The response of felotaxel in plasma samples was 90.6-97.2% of the response in neat methanol samples.

In urine and faeces samples, the response was 80.6-88.1% and 76.4-80.1%, respectively. In tissue samples, a different response was observed for the various types of tissue. For instance, response in liver samples was 76.9-81.1%, whereas response in tumour tissue was 90.6-97.3%. These differences in matrix effects hamper the quantification of taxanes in these matrices using calibration standards in one type of matrix, such as plasma. Therefore it is pivotal to determine any matrix effect during MS method development. Examples of well-designed procedures to determine matrix effects are previously reported.^{132;133} The use of calibration standards in the same matrix or the use of calibration standards that at least mimic the matrix effect of the samples are essential.

At the moment, one assay has been developed for quantification of taxanes using dried blood spots (DBS).⁶¹ Nageswara Rao et al. used only 10 μ L of rat whole blood to make DBS and quantified paclitaxel concentrations down to 0.2 ng/mL. This method proves the applicability of DBS sampling. Using a highly sensitive LC-MS/MS assay, the sample volume can be decreased to 10 μ L and an adequate LLOQ of 0.2 ng/mL can still be obtained.

DBS sampling has several advantages over sampling by venous puncture.¹³⁴ DBS sampling is easier to perform and requires less blood volume. Samples can be taken by the patient and stored for a long time at room temperature, which makes sampling at home feasible. After sampling, DBS can be shipped at ambient temperatures. This results in a cost-effective process. Moreover, during DBS sampling, pathogens are deactivated, resulting in a decreased risk of infection.

However, validation parameters of assays for quantification of analytes using DBS can be different from assays for quantification in plasma samples. For instance, stability on DBS is influenced by other factors such as paper type, high temperature and humidity.¹³⁵ Thereby, concentrations in DBS are not always similar to plasma concentrations since whole blood is spotted. For some analytes, one should correct for haematocrit and compound-specific plasma protein binding before DBS concentrations can be compared to plasma concentrations.¹³⁶ It is advised to include a clinical cross validation between plasma and DBS sampling during the validation of the DBS assay to compare measured concentrations.

Recommendations for development of liquid chromatography (LC) assays.

Liquid chromatography (LC) assays coupled with UV detection

In general, sensitivity of HPLC-UV assays is sufficient for quantification of taxanes in samples derived from (pre)clinical studies. Due to the low absorption maximum of the baccatin III structure at 227 nm, interferences from endogenous compounds, co-medication or additives in the drug formulation are likely to occur. By using selective sample pre-treatment procedures and LC methods, accurate HPLC-UV assays can be obtained. Based on previously developed assays, liquid-liquid extraction using tertiary-butylmethylether or solid-phase extraction using end-capped cyano columns is advised.

Reversed-phase C_8 or C_{18} columns are suitable in combination with a mobile phase containing at least 50% (v/v) of organic solvent. The mobile phase composition should be optimized for chromatographic separation of taxanes, endogenous interferences and additives in the drug formulation.

Liquid chromatography (LC) assays coupled with MS/MS detection

LC coupled to MS/MS can be implemented for sensitive and selective quantification of taxanes. Sampling can even be simplified using DBS. Due to the selectivity of mass spectrometry, sample pre-treatment can be limited. Although in general, liquid-liquid extraction is less expensive compared to off-line solid-phase extraction, on-line solid-phase extraction can save time and thereby increase sample throughput.¹¹⁹ Since interfering signals are increased after protein precipitation, liquid-liquid extraction with tertiary-butylmethylether or on-line solid-phase extraction is advised when high sensitivity is needed. Reversed phase C_8 or C_{18} columns are suitable in combination with a mobile phase containing at least 50% of organic phase and volatile components. To reduce adduct formation, addition of additives is advised. Since ammonium-containing additives and an alkaline pH can increase the response of taxanes, ammonium hydroxide is advised as additive to the mobile phase. ESI in the positive ion mode as ionisation technique results in high sensitivity, although SSI can serve as an alternative. Matrix effects should be evaluated during development of the assay, especially when taxanes are quantified in various matrices. In such cases, the use of stable labelled isotopes as internal standards is advised. If stable labelled isotopes are not available, structure analogues can serve as internal standards. As demonstrated by Mortier et al.⁶⁰, these structure analogues can correct for matrix effect when co-eluting with the analyte of interest. Since similar retention times of the internal standard and the analyte of interest are essential, this might require extra optimisation of the chromatographic system (e.g. the composition of the mobile phase).⁶⁰

Conclusion

A wide diversity of assays for quantification of taxanes has been developed, including tubulin-based biochemical assays, immunoassays and chromatography-based assays. The last encompasses MEKC or LC platforms coupled with UV or MS detection. HPLC-UV and LC-MS/MS are most frequently used and usually fulfil requirements in terms of selectivity and sensitivity. Although each taxane analogue has its own chemical properties, there seems to be an overlap in behaviour of taxanes during sample pre-treatment and the influence of mobile phase composition and interference on quantification in developed HPLC-UV and LC-MS/MS assays. For routine analysis, both HPLC-UV and LC-MS/MS can be used for quantification of taxanes. HPLC-UV systems are low in costs compared to LC-MS/MS and are available in most laboratories. LC-MS/MS provides more sensitivity and selectivity compared to HPLC-UV. Due to the high sensitivity of LC-MS assays, the sample volume can be reduced and analyses in DBS and quantification after micro sampling are feasible. Furthermore, LC-MS/MS is suitable to support studies when a low dose of taxanes is administered (e.g. microdosing or metronomic dosing) or when metabolites are quantified, which are present in low

concentrations in the biomatrix. The increased selectivity of LC-MS/MS requires less sample pre-treatment and can reduce run time since less chromatographic separation is required. This can increase sample throughput. Therefore, when sensitivity or high sample throughput is required, LC-MS/MS is the best choice for quantification of taxanes.

Future perspective

Two decades after the approval of paclitaxel by the FDA, there is still clinical interest in taxanes. New taxanes analogous will be tested in the near future. Therefore, new taxane assays will be developed and validated to support preclinical and clinical trials necessary for approval of drugs for daily clinical practice. Other matrices besides plasma will become of interest. To obtain absorption and excretion data of newly developed drugs, quantification of taxanes in urine and faeces is required. Moreover, taxane quantification in other matrices like tumour and tissue samples can improve the understanding of taxane efficacy and resistance to taxanes. Furthermore, new oral formulations of taxanes are under development (e.g. capsules with solid dispersion systems^{137,138} and nanoparticle formulations¹³⁹⁻¹⁴⁴). These oral formulations can be used for other dosing schedules like metronomic dosing. Multiple subsequent administrations of a lower, oral dose instead of i.v. administration once every week or every three weeks, will result in lower plasma concentrations of taxanes and therefore more sensitive assays for quantification are required. Sensitive assays are also needed when a sub-pharmacologic dose of a drug is administered (microdosing) as a predictive tool for assessment of pharmacokinetics, drug-drug interactions and influence of polymorphism. Co-administration of taxanes with other chemotherapeutics and supportive treatment regimens is common practice. This makes combined quantification in one sample attractive and therefore, it is likely that for this purpose new assays will be developed to improve support of clinical trials or daily practice.

For newly developed assays, sensitivity and fast sample throughput will be combined. Consequently, the focus will be on mass spectrometry, since this results in higher sensitivity and selectivity than UV absorption. Extraction with tertiary-butylmethylether is advised. The best sensitivity (lowest LLOQ levels) is obtained after liquid-liquid extraction since it combines high recovery with an adequate reduction of spectral interferences and matrix effects. This sample pre-treatment method, however, is more labour- and time-intensive than on-line solid phase extraction. However, automated off-line liquid-liquid extraction most likely can compete with on-line solid phase extraction at these points. The increased sensitivity puts liquid-liquid extraction in favour, although on-line solid phase extraction will become a good alternative since new mass spectrometers with improved sensitivity are available.

References

- Gligorov J, Lotz JP. Preclinical pharmacology of the taxanes: implications of the differences. *Oncologist*. **2004**; 9 Suppl 2): 3-8.
- Koolen SL, Beijnen JH, Schellens JHM. Intravenous-to-oral switch in anticancer chemotherapy: a focus on docetaxel and paclitaxel. *Clin.Pharmacol.Ther*. **2010**; 87 (1): 126-9.
- Vaishampayan U, Parchment RE, Jasti BR, Hussain M. Taxanes: an overview of the pharmacokinetics and pharmacodynamics. *Urology* **1999**; 54 (6A Suppl): 22-9.
- Gligorov J, Lotz JP. Preclinical pharmacology of the taxanes: implications of the differences. *Oncologist*. **2004**; 9 Suppl 2): 3-8.
- Fauzee NJ. Taxanes: promising anti-cancer drugs. *Asian Pac.J.Cancer Prev*. **2011**; 12 (4): 837-51.
- Yared JA, Tkaczuk KH. Update on taxane development: new analogs and new formulations. *Drug Des Devel.Ther*. **2012**; 6): 371-84.
- Yue QX, Liu X, Guo DA. Microtubule-binding natural products for cancer therapy. *Planta Med*. **2010**; 76 (11): 1037-43.
- Henningsson A, Sparreboom A, Sandstrom M, Freijs A, Larsson R, Bergh J, Nygren P, Karlsson MO. Population pharmacokinetic modelling of unbound and total plasma concentrations of paclitaxel in cancer patients. *Eur.J.Cancer*. **2003**; 39 (8): 1105-14.
- Henningsson A, Karlsson MO, Vigano L, Gianni L, Verweij J, Sparreboom A. Mechanism-based pharmacokinetic model for paclitaxel. *J.Clin.Oncol*. **2001**; 19 (20): 4065-73.
- Tan AR, Dowlati A, Jones SF, Infante JR, Nishioka J, Fang L, Hodge JP, Gainer SD, Arumugham T, Suttle AB, Dar MM, Lager JJ, Burris HA, III. Phase I study of pazopanib in combination with weekly paclitaxel in patients with advanced solid tumors. *Oncologist*. **2010**; 15 (12): 1253-61.
- Slaviero KA, Clarke SJ, McLachlan AJ, Blair EY, Rivory LP. Population pharmacokinetics of weekly docetaxel in patients with advanced cancer. *Br.J.Clin.Pharmacol*. **2004**; 57 (1): 44-53.
- Ferron GM, Dai Y, Semiond D. Population pharmacokinetics of cabazitaxel in patients with advanced solid tumors. *Cancer Chemother.Pharmacol*. **2013**; 71 (3): 681-92.
- Vrignaud P, Semiond D, Lejeune P, Bouchard H, Calvet L, Combeau C, Riou JF, Commercon A, Lavelle F, Bissery MC. Preclinical antitumor activity of cabazitaxel, a semisynthetic taxane active in taxane-resistant tumors. *Clin.Cancer Res*. **2013**; 19 (11): 2973-83.
- Semiond D, Sidhu SS, Bissery MC, Vrignaud P. Can taxanes provide benefit in patients with CNS tumors and in pediatric patients with tumors? An update on the preclinical development of cabazitaxel. *Cancer Chemother.Pharmacol*. **2013**; 72 (3): 515-28.
- Sparreboom A, van Tellingen O, Nooijen WJ, Beijnen JH. Preclinical pharmacokinetics of paclitaxel and docetaxel. *Anticancer Drugs*. **1998**; 9 (1): 1-17.
- Gerritsen-van Schieveen P, Royer B. Level of evidence for therapeutic drug monitoring of taxanes. *Fundam.Clin.Pharmacol*. **2011**; 25 (4): 414-24.
- Joerger M, Huitema AD, Richel DJ, Dittrich C, Pavlidis N, Briasoulis E, Vermorken JB, Stocchi E, Martoni A, Sorio R, Sleeboom HP, Izquierdo MA, Jodrell DI, Calvert H, Boddy AV, Hollema H, Fety R, Van der Vijgh WJ, Hempel G, Chatelut E, Karlsson M, Wilkins J, Tranchand B, Schrijvers AH, Twelves C, Beijnen JH, Schellens JH. Population pharmacokinetics and pharmacodynamics of paclitaxel and carboplatin in ovarian cancer patients: a study by the European organization for research and treatment of cancer-pharmacology and molecular mechanisms group and new drug development group. *Clin.Cancer Res*. **2007**; 13 (21): 6410-8.
- Andreeva M, Niedmann PD, Binder L, Armstrong VW, Meden H, Binder M, Oellerich M. A simple and reliable reverse-phase high-performance liquid chromatographic procedure for determination of paclitaxel (taxol) in human serum. *Ther.Drug Monit*. **1997**; 19 (3): 327-32.
- Coudore F, Authier N, Guillaume D, Beal A, Duroux E, Fialip J. High-performance liquid chromatographic determination of paclitaxel in rat serum: application to a toxicokinetic study. *J.Chromatogr.B Biomed.Sci.Appl*. **1999**; 721 (2): 317-20.
- el-Yazigi A, Yusuf A. Expedient liquid chromatographic assay for paclitaxel in plasma after its administration to cancer patients. *Ther.Drug Monit*. **1995**; 17 (5): 511-5.
- Huizing MT, Rosing H, Koopman F, Keung AC, Pinedo HM, Beijnen JH. High-performance liquid chromatographic procedures for the quantitative determination of paclitaxel (Taxol) in human urine. *J.Chromatogr.B Biomed.Appl*. **1995**; 664 (2): 373-82.
- Kim SC, Yu J, Lee JW, Park ES, Chi SC. Sensitive HPLC method for quantitation of paclitaxel (Genexol) in biological samples with application to preclinical pharmacokinetics and biodistribution. *J.Pharm.Biomed.Anal*. **2005**; 39 (1-2): 170-6.
- Kumar SV, Srinath S, Saha RN. A simple and rapid 3D view method for selective and sensitive determination of paclitaxel in micro volume rat plasma by LC-diode array UV and its application to a pharmacokinetic study. *J.Chromatogr.Sci*. **2012**; 50 (3): 259-70.

24. Lee SH, Yoo SD, Lee KH. Rapid and sensitive determination of paclitaxel in mouse plasma by high-performance liquid chromatography. *J.Chromatogr.B Biomed.Sci.Appl.* **1999**; 724 (2): 357-63.
25. Leslie J, Kujawa JM, Eddington N, Egorin M, Eiseman J. Stability problems with taxol in mouse plasma during analysis by liquid chromatography. *J.Pharm.Biomed.Anal.* **1993**; 11 (11-12): 1349-52.
26. Longnecker SM, Donehower RC, Cates AE, Chen TL, Brundrett RB, Grochow LB, Ettinger DS, Colvin M. High-performance liquid chromatographic assay for taxol in human plasma and urine and pharmacokinetics in a phase I trial. *Cancer Treat. Rep.* **1987**; 71 (1): 53-9.
27. Mader RM, Rizovski B, Steger GG. On-line solid-phase extraction and determination of paclitaxel in human plasma. *J.Chromatogr.B Analyt.Technol.Biomed.Life Sci.* **2002**; 769 (2): 357-61.
28. Martin N, Catalin J, Blachon MF, Durand A. Assay of paclitaxel (Taxol) in plasma and urine by high-performance liquid chromatography. *J.Chromatogr.B Biomed.Sci.Appl.* **1998**; 709 (2): 281-8.
29. Rizzo J, Riley C, von Hoff D, Kuhn J, Phillips J, Brown T. Analysis of anticancer drugs in biological fluids: determination of taxol with application to clinical pharmacokinetics. *J.Pharm.Biomed.Anal.* **1990**; 8 (2): 159-64.
30. Sharma A, Conway WD, Straubinger RM. Reversed-phase high-performance liquid chromatographic determination of taxol in mouse plasma. *J.Chromatogr.B Biomed.Appl.* **1994**; 655 (2): 315-9.
31. Song D, Au JL. Isocratic high-performance liquid chromatographic assay of taxol in biological fluids and tissues using automated column switching. *J.Chromatogr.B Biomed.Appl.* **1995**; 663 (2): 337-44.
32. Sparreboom A, de BP, Nooter K, Loos WJ, Stoter G, Verweij J. Determination of paclitaxel in human plasma using single solvent extraction prior to isocratic reversed-phase high-performance liquid chromatography with ultraviolet detection. *J.Chromatogr.B Biomed.Sci.Appl.* **1998**; 705 (1): 159-64.
33. Suno M, Ono T, Iida S, Umetsu N, Ohtaki K, Yamada T, Awaya T, Satomi M, Tasaki Y, Shimizu K, Matsubara K. Improved high-performance liquid chromatographic detection of paclitaxel in patient's plasma using solid-phase extraction, and semi-micro-bore C18 separation and UV detection. *J.Chromatogr.B Analyt.Technol.Biomed.Life Sci.* **2007**; 860 (1): 141-4.
34. Supko JG, Nair RV, Seiden MV, Lu H. Adaptation of solid phase extraction to an automated column switching method for online sample cleanup as the basis of a facile and sensitive high-performance liquid chromatographic assay for paclitaxel in human plasma. *J.Pharm.Biomed.Anal.* **1999**; 21 (5): 1025-36.
35. Wang LZ, Ho PC, Lee HS, Vaddi HK, Chan YW, Yung CS. Quantitation of paclitaxel in micro-sample rat plasma by a sensitive reversed-phase HPLC assay. *J.Pharm.Biomed.Anal.* **2003**; 31 (2): 283-9.
36. Willey TA, Bekos EJ, Gaver RC, Duncan GF, Tay LK, Beijnen JH, Farmen RH. High-performance liquid chromatographic procedure for the quantitative determination of paclitaxel (Taxol) in human plasma. *J.Chromatogr.* **1993**; 621 (2): 231-8.
37. Yonemoto H, Ogino S, Nakashima MN, Wada M, Nakashima K. Determination of paclitaxel in human and rat blood samples after administration of low dose paclitaxel by HPLC-UV detection. *Biomed.Chromatogr.* **2007**; 21 (3): 310-7.
38. Wei Y, Xue Z, Ye Y, Wang P, Huang Y, Zhao L. Pharmacokinetic and tissue distribution of paclitaxel in rabbits assayed by LC-UV after intravenous administration of its novel liposomal formulation. *Biomed.Chromatogr.* **2013**; DOI10.1002/bmc.3005.
39. Ardiet CJ, Tranchand B, Zanetta S, Guillot A, Bernard E, Peguy M, Rebattu P, Droz JP. A sensitive docetaxel assay in plasma by solid-phase extraction and high performance liquid chromatography-UV detection: validation and suitability in phase I clinical trial pharmacokinetics. *Invest New Drugs.* **1999**; 17 (4): 325-33.
40. Ciccolini J, Catalin J, Blachon MF, Durand A. Rapid high-performance liquid chromatographic determination of docetaxel (Taxotere) in plasma using liquid-liquid extraction. *J.Chromatogr.B Biomed.Sci.Appl.* **2001**; 759 (2): 299-306.
41. Garg MB, Ackland SP. Simple and sensitive high-performance liquid chromatography method for the determination of docetaxel in human plasma or urine. *J.Chromatogr.B Biomed.Sci.Appl.* **2000**; 748 (2): 383-8.
42. Loos WJ, Verweij J, Nooter K, Stoter G, Sparreboom A. Sensitive determination of docetaxel in human plasma by liquid-liquid extraction and reversed-phase high-performance liquid chromatography. *J.Chromatogr.B Biomed.Sci.Appl.* **1997**; 693 (2): 437-41.
43. Rouini MR, Lotfolahi A, Stewart DJ, Molepo JM, Shirazi FH, Vergniol JC, Tomiak E, Delorme F, Vernillet L, Giguere M, Goel R. A rapid reversed phase high performance liquid chromatographic method for the determination of docetaxel (Taxotere) in human plasma using a column switching technique. *J.Pharm.Biomed.Anal.* **1998**; 17 (8): 1243-7.
44. Vergniol JC, Bruno R, Montay G, Frydman A. Determination of Taxotere in human plasma by a semi-automated high-performance liquid chromatographic method. *J.Chromatogr.* **1992**; 582 (1-2): 273-8.
45. Colombo T, Frapolli R, Bombardelli E, Morazzoni P, Riva A, D'Incalci M, Zucchetti M. High-performance liquid chromatographic assay for the determination of the novel taxane derivative IDN5109 in mouse plasma. *J.Chromatogr.B Biomed.Sci.Appl.* **1999**; 736 (1-2): 135-41.
46. Ma H, You J, Liu Y. Cloud-point extraction combined with HPLC for determination of larotaxel in rat plasma: a pharmacokinetic study of liposome formulation. *J.Sep.Sci.* **2012**; 35 (12): 1539-46.
47. Zaffaroni M, Frapolli R, Colombo T, Fruscio R, Bombardelli E, Morazzoni P, Riva A, D'Incalci M, Zucchetti M. High-performance liquid chromatographic assay for the determination of the novel C-Seco-taxane derivative (IDN 5390) in

- mouse plasma. *J.Chromatogr.B Analyt.Technol.Biomed.Life Sci.* **2002**; 780 (1): 93-8.
48. Yan L, Yanyan J, Minchun C, Jing Y, Ying S, Chengtao L, Jie G, Caiyang L, Zhenxing Z, Aidong W, Yi D. High-Performance Liquid Chromatographic Analysis of Felotaxel, a Novel Anti-Cancer Drug, in Rat Plasma and in Human Plasma and Urine. *J.Chromatogr.Sci.* **2013**; 51 (3): 292-6.
49. Lopez L.Z., Pastor A.A., Beitia JMA, Velilla J.A., Deiro J.G. Determination of docetaxel and Paclitaxel in human plasma by high-performance liquid chromatography: validation and application to clinical pharmacokinetic studies. *Ther.Drug Monit.* **2006**; 28 (2): 199-205.
50. Andersen A, Warren DJ, Brunsvig PF, Aamdal S, Kristensen GB, Olsen H. High sensitivity assays for docetaxel and paclitaxel in plasma using solid-phase extraction and high-performance liquid chromatography with UV detection. *BMC. Clin.Pharmacol.* **2006**; 6:2): 2.
51. Bermingham S, O'Connor R, Regan F, McMahon GP. Simultaneous determination of anthracyclines and taxanes in human serum using online sample extraction coupled to high performance liquid chromatography with UV detection. *J.Sep.Sci.* **2010**; 33 (11): 1571-9.
52. Huizing MT, Sparreboom A, Rosing H, van Tellingen O, Pinedo HM, Beijnen JH. Quantification of paclitaxel metabolites in human plasma by high-performance liquid chromatography. *J.Chromatogr.B Biomed.Appl.* **1995**; 674 (2): 261-8.
53. Rosing H, Lustig V, Koopman FP, ten Bokkel Huinink WW, Beijnen JH. Bio-analysis of docetaxel and hydroxylated metabolites in human plasma by high-performance liquid chromatography and automated solid-phase extraction. *J.Chromatogr.B Biomed.Sci.Appl.* **1997**; 696 (1): 89-98.
54. Sparreboom A, van Tellingen O, Nooijen WJ, Beijnen JH. Determination of paclitaxel and metabolites in mouse plasma, tissues, urine and faeces by semi-automated reversed-phase high-performance liquid chromatography. *J.Chromatogr.B Biomed.Appl.* **1995**; 664 (2): 383-91.
55. Basileo G, Breda M, Fonte G, Pisano R, James CA. Quantitative determination of paclitaxel in human plasma using semi-automated liquid-liquid extraction in conjunction with liquid chromatography/tandem mass spectrometry. *J.Pharm. Biomed.Anal.* **2003**; 32 (4-5): 591-600.
56. Gao S, Zhang ZP, Edinboro LE, Ngoka LC, Karnes HT. The effect of alkylamine additives on the sensitivity of detection for paclitaxel and docetaxel and analysis in plasma of paclitaxel by liquid chromatography-tandem mass spectrometry. *Biomed.Chromatogr.* **2006**; 20 (8): 683-95.
57. Gardner ER, Liao CT, Chu ZE, Figg WD, Sparreboom A. Determination of paclitaxel in human plasma following the administration of Genaxol or Genetaxyl by liquid chromatography/tandem mass spectrometry. *Rapid Commun.Mass Spectrom.* **2006**; 20 (14): 2170-4.
58. Guo P, Ma J, Li S, Gallo JM. Determination of paclitaxel in mouse plasma and brain tissue by liquid chromatography-mass spectrometry. *J.Chromatogr.B Analyt.Technol.Biomed.Life Sci.* **2003**; 798 (1): 79-86.
59. Guo W, Johnson JL, Khan S, Ahmad A, Ahmad I. Paclitaxel quantification in mouse plasma and tissues containing liposome-entrapped paclitaxel by liquid chromatography-tandem mass spectrometry: application to a pharmacokinetics study. *Anal.Biochem.* **2005**; 336 (2): 213-20.
60. Mortier KA, Verstraete AG, Zhang GF, Lambert WE. Enhanced method performance due to a shorter chromatographic run-time in a liquid chromatography-tandem mass spectrometry assay for paclitaxel. *J.Chromatogr.A.* **2004**; 1041 (1-2): 235-8.
61. Nageswara Rao R, Satyanarayana Raju S, Mastan Vali R, Sarma VU, Girija Sankar G. LC-ESI-MS/MS determination of paclitaxel on dried blood spots. *Biomed.Chromatogr.* **2012**; 26 (5): 616-21.
62. Schellen A, Ooms B, van Gils M, Halmingh O, van der Vlis E, van de Lagemaat D, Verheij E. High throughput on-line solid phase extraction/tandem mass spectrometric determination of paclitaxel in human serum. *Rapid Commun.Mass Spectrom.* **2000**; 14 (4): 230-3.
63. Sottani C, Minoia C, D'Incalci M, Paganini M, Zucchetti M. High-performance liquid chromatography tandem mass spectrometry procedure with automated solid phase extraction sample preparation for the quantitative determination of paclitaxel (Taxol) in human plasma. *Rapid Commun.Mass Spectrom.* **1998**; 12 (5): 251-5.
64. Stokvis E, Ouweland M, Nan LG, Kemper EM, van Tellingen O, Rosing H, Beijnen JH. A simple and sensitive assay for the quantitative analysis of paclitaxel in human and mouse plasma and brain tumor tissue using coupled liquid chromatography and tandem mass spectrometry. *J.Mass Spectrom.* **2004**; 39 (12): 1506-12.
65. Tong X, Zhou J, Tan Y. Determination of paclitaxel in rat plasma by LC-MS-MS. *J.Chromatogr.Sci.* **2006**; 44 (5): 266-1.
66. Tong X, Zhou J, Tan Y. Liquid chromatography/tandem triple-quadrupole mass spectrometry for determination of paclitaxel in rat tissues. *Rapid Commun.Mass Spectrom.* **2006**; 20 (12): 1905-12.
67. Zhang SQ, Chen GH. Determination of Paclitaxel in Human Plasma by UPLC-MS-MS. *J.Chromatogr.Sci.* **2008**; 46 (3): 220-4.
68. Zhang SQ, Song YN, He XH, Zhong BH, Zhang ZQ. Liquid chromatography-tandem mass spectrometry for the determination of paclitaxel in rat plasma after intravenous administration of poly(L-glutamic acid)-alanine-paclitaxel conjugate. *J.Pharm.Biomed.Anal.* **2010**; 51 (5): 1169-74.
69. Gardner ER, Dahut W, Figg WD. Quantitative determination of total and unbound paclitaxel in human plasma following

- Abraxane treatment. *J.Chromatogr.B Analyt.Technol.Biomed.Life Sci.* **2008**; 862 (1-2): 213-8.
70. Alexander MS, Kiser MM, Culley T, Kern JR, Dolan JW, McChesney JD, Zygmunt J, Bannister SJ. Measurement of paclitaxel in biological matrices: high-throughput liquid chromatographic-tandem mass spectrometric quantification of paclitaxel and metabolites in human and dog plasma. *J.Chromatogr.B Analyt.Technol.Biomed.Life Sci.* **2003**; 785 (2): 253-61.
71. Green H, Vretenbrant K, Norlander B, Peterson C. Measurement of paclitaxel and its metabolites in human plasma using liquid chromatography/ion trap mass spectrometry with a sonic spray ionization interface. *Rapid Commun.Mass Spectrom.* **2006**; 20 (14): 2183-9.
72. Vainchtein LD, Thijssen B, Stokvis E, Rosing H, Schellens JH, Beijnen JH. A simple and sensitive assay for the quantitative analysis of paclitaxel and metabolites in human plasma using liquid chromatography/tandem mass spectrometry. *Biomed.Chromatogr.* **2006**; 20 (1): 139-48.
73. Yamaguchi H, Fujikawa A, Ito H, Tanaka N, Furugen A, Miyamori K, Takahashi N, Ogura J, Kobayashi M, Yamada T, Mano N, Iseki K. Quantitative determination of paclitaxel and its metabolites, 6 α -hydroxypaclitaxel and p-3'-hydroxypaclitaxel, in human plasma using column-switching liquid chromatography/tandem mass spectrometry. *Biomed.Chromatogr.* **2013**; 27 (4): 539-44.
74. Zhang W, Dutschman GE, Li X, Cheng YC. Quantitation of paclitaxel and its two major metabolites using a liquid chromatography-electrospray ionization tandem mass spectrometry. *J.Chromatogr.B Analyt.Technol.Biomed.Life Sci.* **2011**; 879 (22): 2018-22.
75. Grobosch T, Schwarze B, Stoecklein D, Binscheck T. Fatal poisoning with *Taxus baccata*: quantification of paclitaxel (taxol A), 10-deacetyltaxol, baccatin III, 10-deacetylbaccatin III, cephalomannine (taxol B), and 3,5-dimethoxyphenol in body fluids by liquid chromatography-tandem mass spectrometry. *J.Anal.Toxicol.* **2012**; 36 (1): 36-43.
76. Hendriks JJ, Hillebrand MJ, Thijssen B, Rosing H, Schinkel AH, Schellens JH, Beijnen JH. A sensitive combined assay for the quantification of paclitaxel, docetaxel and ritonavir in human plasma using liquid chromatography coupled with tandem mass spectrometry. *J.Chromatogr.B Analyt.Technol.Biomed.Life Sci.* **2011**; 879 (28): 2984-90.
77. Mortier KA, Renard V, Verstraete AG, Van GA, Van BS, Lambert WE. Development and validation of a liquid chromatography-tandem mass spectrometry assay for the quantification of docetaxel and paclitaxel in human plasma and oral fluid. *Anal.Chem.* **2005**; 77 (14): 4677-83.
78. Mortier KA, Lambert WE. Determination of unbound docetaxel and paclitaxel in plasma by ultrafiltration and liquid chromatography-tandem mass spectrometry. *J.Chromatogr.A.* **2006**; 1108 (2): 195-201.
79. Paek IB, Ji HY, Kim MS, Lee GS, Lee HS. Simultaneous determination of paclitaxel and a new P-glycoprotein inhibitor HM-30181 in rat plasma by liquid chromatography with tandem mass spectrometry. *J.Sep.Sci.* **2006**; 29 (5): 628-34.
80. Parise RA, Ramanathan RK, Zamboni WC, Egorin MJ. Sensitive liquid chromatography-mass spectrometry assay for quantitation of docetaxel and paclitaxel in human plasma. *J.Chromatogr.B Analyt.Technol.Biomed.Life Sci.* **2003**; 783 (1): 231-6.
81. Hendriks JJ, Rosing H, Schinkel AH, Schellens JH, Beijnen JH. Combined quantification of paclitaxel, docetaxel and ritonavir in human feces and urine using LC-MS/MS. *Biomed.Chromatogr.* **2013**; DOI 10.1002/bmc3021.
82. Corona G, Elia C, Casetta B, Frustaci S, Toffoli G. High-throughput plasma docetaxel quantification by liquid chromatography-tandem mass spectrometry. *Clin.Chim.Acta.* **2011**; 412 (3-4): 358-64.
83. Grozav AG, Hutson TE, Zhou X, Bukowski RM, Ganapathi R, Xu Y. Rapid analysis of docetaxel in human plasma by tandem mass spectrometry with on-line sample extraction. *J.Pharm.Biomed.Anal.* **2004**; 36 (1): 125-31.
84. Hou W, Watters JW, McLeod HL. Simple and rapid docetaxel assay in plasma by protein precipitation and high-performance liquid chromatography-tandem mass spectrometry. *J.Chromatogr.B Analyt.Technol.Biomed.Life Sci.* **2004**; 804 (2): 263-7.
85. Kuppens IE, van Maanen MJ, Rosing H, Schellens JH, Beijnen JH. Quantitative analysis of docetaxel in human plasma using liquid chromatography coupled with tandem mass spectrometry. *Biomed.Chromatogr.* **2005**; 19 (5): 355-61.
86. Wang LZ, Goh BC, Grigg ME, Lee SC, Khoo YM, Lee HS. A rapid and sensitive liquid chromatography/tandem mass spectrometry method for determination of docetaxel in human plasma. *Rapid Commun.Mass Spectrom.* **2003**; 17 (14): 1548-52.
87. Yamaguchi H, Fujikawa A, Ito H, Tanaka N, Furugen A, Miyamori K, Takahashi N, Ogura J, Kobayashi M, Yamada T, Mano N, Iseki K. A rapid and sensitive LC/ESI-MS/MS method for quantitative analysis of docetaxel in human plasma and its application to a pharmacokinetic study. *J.Chromatogr.B Analyt.Technol.Biomed.Life Sci.* **2012**; 893-894): 157-61.
88. Marzinke MA, Breaud AR, Clarke W. The development and clinical validation of a turbulent-flow liquid chromatography-tandem mass spectrometric method for the rapid quantitation of docetaxel in serum. *Clin.Chim.Acta.* **2013**; 417): 12-8.
89. Du P, Li N, Wang H, Yang S, Song Y, Han X, Shi Y. Development and validation of a rapid and sensitive UPLC-MS/MS method for determination of total docetaxel from a lipid microsphere formulation in human plasma. *J.Chromatogr.B Analyt.Technol.Biomed.Life Sci.* **2013**; 926): 101-7.
90. Guittou J, Cohen S, Tranchand B, Vignal B, Droz JP, Guillaumont M, Manchon M, Freyer G. Quantification of docetaxel and its main metabolites in human plasma by liquid chromatography/tandem mass spectrometry. *Rapid Commun.Mass Spectrom.* **2005**; 19 (17): 2419-26.

91. Hendriks JJ, Dubbelman AC, Rosing H, Schinkel AH, Schellens JH, Beijnen JH. Quantification of docetaxel and its metabolites in human plasma by liquid chromatography/tandem mass spectrometry. *Rapid Commun.Mass Spectrom.* **2013**; 27 (17): 1925-34.
92. Baker SD, Zhao M, He P, Carducci MA, Verweij J, Sparreboom A. Simultaneous analysis of docetaxel and the formulation vehicle polysorbate 80 in human plasma by liquid chromatography/tandem mass spectrometry. *Anal.Biochem.* **2004**; 324 (2): 276-84.
93. Huang Q, Wang GJ, Sun JG, Hu XL, Lu YH, Zhang Q. Simultaneous determination of docetaxel and ketoconazole in rat plasma by liquid chromatography/electrospray ionization tandem mass spectrometry. *Rapid Commun.Mass Spectrom.* **2007**; 21 (6): 1009-18.
94. Navarrete A, Martinez-Alcazar MP, Duran I, Calvo E, Valenzuela B, Barbas C, Garcia A. Simultaneous online SPE-HPLC-MS/MS analysis of docetaxel, temsirolimus and sirolimus in whole blood and human plasma. *J.Chromatogr.B Analyt. Technol.Biomed.Life Sci.* **2013**; 921-922): 35-42.
95. de Bruijn P, de Graan AJ, Nieuweboer A, Mathijssen RH, Lam MH, de Wit R, Wiemer EA, Loos WJ. Quantification of cabazitaxel in human plasma by liquid chromatography/triple-quadrupole mass spectrometry: a practical solution for non-specific binding. *J.Pharm.Biomed.Anal.* **2012**; 59): 117-22.
96. Kort A, Hillebrand MJ, Cirkel GA, Voest EE, Schinkel AH, Rosing H, Schellens JH, Beijnen JH. Quantification of cabazitaxel, its metabolite docetaxel and the determination of the demethylated metabolites RPR112698 and RPR123142 as docetaxel equivalents in human plasma by liquid chromatography-tandem mass spectrometry. *J.Chromatogr.B Analyt. Technol.Biomed.Life Sci.* **2013**; 925): 117-23.
97. Ding Y, Lu C, Yang J, Jin X, Yang L, Wang C, Ma Z, Zhu Y, Ding L, Jia Y, Wen A. Application of a liquid chromatography-tandem mass spectrometry (LC-MS/MS) method to the pharmacokinetics, tissue distribution and excretion studies of felotaxel (SHR110008) in tumor-bearing mice. *J.Chromatogr.B Analyt. Technol.Biomed.Life Sci.* **2012**; 887-888): 61-6.
98. Hu X, Sun J, Wang G, Zhu X, Hao G, Gu Y, Pruijn FB. LC-MS-MS study of the pharmacokinetics of a 9- β -dihydroxy-9,10-o-acetal derivative of docetaxel in rats and beagle dogs. *Chromatographia* **2008**; 67 (11/12): 883-92.
99. Liu Z, Zhang B, Liu Z, Li S, Li G, Geng L, Zhao X, Bi K, Tang X, Chen X. Development of a UPLC-ESI-MS/MS method for the determination of larotaxel in beagle dog plasma: application to the pharmacokinetic study. *Anal.Bioanal.Chem.* **2012**; 403 (1): 323-30.
100. Jiang SG, Zu YG, Zhang L, Fu YJ, Zhang Y, Wang Z, Hua X, Wang JT. Determination of a hydrophilic paclitaxel derivative, 7-xylosyl-10-deacetylpaclitaxel in rat plasma by LC-MS/MS. *Biomed.Chromatogr.* **2009**; 23 (5): 472-9.
101. Marangon E, Falcioni C, Manzotti C, Fontana G, D'Incalci M, Zucchetti M. Development and validation of a LC-MS/MS method for the determination of the novel oral 1,14 substituted taxane derivatives, IDN 5738 and IDN 5839, in mouse plasma and its application to the pharmacokinetic study. *J.Chromatogr.B Analyt. Technol.Biomed.Life Sci.* **2009**; 877 (32): 4147-53.
102. Song L, Prey JD, Xue J, Kanter P, Manzotti C, Bombardelli E, Morazzoni P, Pendyala L. Pharmacokinetic measurements of IDN 5390 using electrospray ionization tandem mass spectrometry: structure characterization and quantification in dog plasma. *Rapid Commun.Mass Spectrom.* **2005**; 19 (24): 3617-25.
103. Sottani C, Colombo T, Zucchetti M, Fruscio R, D'Incalci M, Minoia C. High-performance liquid chromatography/tandem mass spectrometry for the quantitative analysis of a novel taxane derivative (BAY59-8862) in biological samples and characterisation of its metabolic profile in rat bile samples. *Rapid Commun.Mass Spectrom.* **2001**; 15 (19): 1807-16.
104. Zhang SQ, Chen GH. Determination of a novel paclitaxel derivative (NPD-103) in human plasma by ultra-performance liquid chromatography-tandem mass spectrometry. *Biomed.Chromatogr.* **2009**; 23 (5): 510-5.
105. Yu K, Little D, Plumb R, Smith B. High-throughput quantification for a drug mixture in rat plasma-a comparison of Ultra Performance liquid chromatography/tandem mass spectrometry with high-performance liquid chromatography/tandem mass spectrometry. *Rapid Commun.Mass Spectrom.* **2006**; 20 (4): 544-52.
106. Thormann W, Lienhard S, Wernly P. Strategies for the monitoring of drugs in body fluids by micellar electrokinetic capillary chromatography. *J.Chromatogr.* **1993**; 636 (1): 137-48.
107. Hempel G, Lehmkuhl D, Krumpelmann S, Blaschke G, Boos J. Determination of paclitaxel in biological fluids by micellar electrokinetic chromatography. *J.Chromatogr.A.* **1996**; 745 (1-2): 173-9.
108. Rodriguez J, Contento AM, Castaneda G, Munoz L, Berciano MA. Determination of morphine, codeine, and paclitaxel in human serum and plasma by micellar electrokinetic chromatography. *J.Sep.Sci.* **2012**; 35 (17): 2297-306.
109. Rodriguez J, Castaneda G, Contento AM, Munoz L. Direct and fast determination of paclitaxel, morphine and codeine in urine by micellar electrokinetic chromatography. *J.Chromatogr.A.* **2012**; 1231): 66-72.
110. Grothaus PG, Raybould TJ, Bignami GS, Lazo CB, Byrnes JB. An enzyme immunoassay for the determination of taxol and taxanes in *Taxus* sp. tissues and human plasma. *J.Immunol.Methods.* **1993**; 158 (1): 5-15.
111. Svojanovsky SR, Egodage KL, Wu J, Slavik M, Wilson GS. High sensitivity ELISA determination of taxol in various human biological fluids. *J.Pharm.Biomed.Anal.* **1999**; 20 (3): 549-55.
112. Sheikh SH, Abela BA, Mulchandani A. Development of a fluorescence immunoassay for measurement of paclitaxel in human plasma. *Anal.Biochem.* **2000**; 283 (1): 33-8.

113. Hamel E, Lin CM, Johns DG. Tubulin-dependent biochemical assay for the antineoplastic agent taxol and application to measurement of the drug in serum. *Cancer Treat.Rep.* **1982**; 66 (6): 1381-6.
114. Morais S, O'Malley S, Chen W, Mulchandani A. A tubulin-based fluorescent polarization assay for paclitaxel. *Anal. Biochem.* **2003**; 321 (1): 44-9.
115. Tiwari G, Tiwari R. Bioanalytical method validation: An updated review. *Pharm.Methods.* **2010**; 1 (1): 25-38.
116. Knox C, Law V, Jewison T, Liu P, Ly S, Frolkis A, Pon A, Banco K, Mak C, Neveu V, Djoumbou Y, Eisner R, Guo AC, Wishart DS. DrugBank 3.0: a comprehensive resource for 'omics' research on drugs. *Nucleic Acids Res.* **2011**; 39): D1035-D1041.
117. Kole PL, Venkatesh G, Kotecha J, Sheshala R. Recent advances in sample preparation techniques for effective bioanalytical methods. *Biomed.Chromatogr.* **2011**; 25 (1-2): 199-217.
118. Xu RN, Fan L, Rieser MJ, El Shourbagy TA. Recent advances in high-throughput quantitative bioanalysis by LC-MS/MS. *J.Pharm.Biomed.Anal.* **2007**; 44 (2): 342-55.
119. Chang MS, Ji Q, Zhang J, El-Shourbagy TA. Historical Review of Sample Preparation for Chromatographic Bioanalysis: Pros and Cons. *Drug Development Research* **2012**; 68): 107-33.
120. Tian J, Stella VJ. Degradation of paclitaxel and related compounds in aqueous solutions III: Degradation under acidic pH conditions and overall kinetics. *J.Pharm.Sci.* **2010**; 99 (3): 1288-98.
121. Tian J, Stella VJ. Degradation of paclitaxel and related compounds in aqueous solutions II: Nonpimerization degradation under neutral to basic pH conditions. *J.Pharm.Sci.* **2008**; 97 (8): 3100-8.
122. Tian J, Stella VJ. Degradation of paclitaxel and related compounds in aqueous solutions I: epimerization. *J.Pharm.Sci.* **2008**; 97 (3): 1224-35.
123. Mroczek T, Glowniak K. Solid-phase extraction and simplified high-performance liquid chromatographic determination of 10-deacetylbaccatin III and related taxoids in yew species. *J.Pharm.Biomed.Anal.* **2001**; 26 (1): 89-102.
124. Wuelfing WP, Kosuda K, Templeton AC, Harman A, Mowery MD, Reed RA. Polysorbate 80 UV/vis spectral and chromatographic characteristics--defining boundary conditions for use of the surfactant in dissolution analysis. *J.Pharm.Biomed.Anal.* **2006**; 41 (3): 774-82.
125. de Hoffmann, E. and Stroobant, V. (2007) Ion sources, Mass Spectrometry; Principles and Applications 3rd Edition, John Wiley & Sons Ltd, West Sussex, England, 25.
126. Mortier KA, Zhang GF, van Peteghem CH, Lambert WE. Adduct formation in quantitative bioanalysis: effect of ionization conditions on paclitaxel. *J.Am.Soc.Mass Spectrom.* **2004**; 15 (4): 585-92.
127. Rainville PD, Smith NW, Cowan D, Plumb RS. Comprehensive investigation of the influence of acidic, basic, and organic mobile phase compositions on bioanalytical assay sensitivity in positive ESI mode LC/MS/MS. *J.Pharm.Biomed.Anal.* **2012**; 59): 138-50.
128. Cech NB, Enke CG. Practical implications of some recent studies in electrospray ionization fundamentals. *Mass Spectrom. Rev.* **2001**; 20 (6): 362-87.
129. Hendriks JJ, Hillebrand MJ, Thijssen B, Rosing H, Schinkel AH, Schellens JH, Beijnen JH. A sensitive combined assay for the quantification of paclitaxel, docetaxel and ritonavir in human plasma using liquid chromatography coupled with tandem mass spectrometry. *J.Chromatogr.B Analyt.Technol.Biomed.Life Sci.* **2011**; 879 (28): 2984-90.
130. Gao S, Zhang ZP, Karnes HT. Sensitivity enhancement in liquid chromatography/atmospheric pressure ionization mass spectrometry using derivatization and mobile phase additives. *J.Chromatogr.B Analyt.Technol.Biomed.Life Sci.* **2005**; 825 (2): 98-110.
131. Antignac JP, Wash F, Monteau HD, Brabander FA. The ion suppression phenomenon in liquid chromatography-mass spectrometry and its consequences in the field of residue analysis. *Anal Chim Acta* **2005**; 529 (1-2): 129-36.
132. Bonfiglio R, King RC, Olah TV, Merkle K. The effects of sample preparation methods on the variability of the electrospray ionization response for model drug compounds. *Rapid Commun.Mass Spectrom.* **1999**; 13 (12): 1175-85.
133. Matuszewski BK, Constanzer ML, Chavez-Eng CM. Matrix effect in quantitative LC/MS/MS analyses of biological fluids: a method for determination of finasteride in human plasma at picogram per milliliter concentrations. *Anal.Chem.* **1998**; 70 (5): 882-9.
134. Deglon J, Thomas A, Mangin P, Staub C. Direct analysis of dried blood spots coupled with mass spectrometry: concepts and biomedical applications. *Anal.Bioanal.Chem.* **2012**; 402 (8): 2485-98.
135. Demirev PA. Dried blood spots: analysis and applications. *Anal.Chem.* **2013**; 85 (2): 779-89.
136. Kromdijk W, Mulder JW, Rosing H, Smit PM, Beijnen JH, Huitema AD. Use of dried blood spots for the determination of plasma concentrations of nevirapine and efavirenz. *J.Antimicrob.Chemother.* **2012**; 67 (5): 1211-6.
137. Moes JJ, Koolen SL, Huitema AD, Schellens JH, Beijnen JH, Nuijen B. Pharmaceutical development and preliminary clinical testing of an oral solid dispersion formulation of docetaxel (ModraDoc001). *Int.J.Pharm.* **2011**; 420 (2): 244-50.
138. Moes J, Koolen S, Huitema A, Schellens J, Beijnen J, Nuijen B. Development of an oral solid dispersion formulation for use in low-dose metronomic chemotherapy of paclitaxel. *Eur.J.Pharm.Biopharm.* **2013**; 83 (1): 87-94.
139. Li Y, Bi Y, Xi Y, Li L. Enhancement on oral absorption of paclitaxel by multifunctional pluronic micelles. *J.Drug Target.* **2013**; 21 (2): 188-99.

140. Zeng N, Gao X, Hu Q, Song Q, Xia H, Liu Z, Gu G, Jiang M, Pang Z, Chen H, Chen J, Fang L. Lipid-based liquid crystalline nanoparticles as oral drug delivery vehicles for poorly water-soluble drugs: cellular interaction and in vivo absorption. *Int.J.Nanomedicine*. **2012**; 7:3703-18. doi: 10.2147/IJN.S32599. Epub; %2012 Jul 13.): 3703-18.
141. Baek JS, So JW, Shin SC, Cho CW. Solid lipid nanoparticles of paclitaxel strengthened by hydroxypropyl-beta-cyclodextrin as an oral delivery system. *Int.J.Mol.Med*. **2012**; 30 (4): 953-9.
142. Jain S, Kumar D, Swarnakar NK, Thanki K. Polyelectrolyte stabilized multilayered liposomes for oral delivery of paclitaxel. *Biomaterials*. **2012**; 33 (28): 6758-68.
143. Yoncheva K, Calleja P, Agueros M, Petrov P, Miladinova I, Tsvetanov C, Irache JM. Stabilized micelles as delivery vehicles for paclitaxel. *Int.J.Pharm*. **2012**; 436 (1-2): 258-64.
144. Nassar T, Attili-Qadri S, Harush-Frenkel O, Farber S, Lecht S, Lazarovici P, Benita S. High plasma levels and effective lymphatic uptake of docetaxel in an orally available nanotransporter formulation. *Cancer Res*. **2011**; 71 (8): 3018-28.

Supplemental table 1. Overview of bioanalytical HPLC-UV assays for quantification of taxanes.

Analyte(s)	Matrix	Pre-treatment	Sample volume (µl)	Wavelength (nm)	Runtime (min)	LLOQ (ng/mL)	ULOQ (ng/mL)	Ref
paclitaxel	human serum	LLE	400	227	13	10	10,000	6
paclitaxel	rat serum	LLE	250	230	15	180	1,430	7
paclitaxel	human plasma	LLE	1000	227		10	1,600	8
paclitaxel	urine	SPE or LLE	500	227	45	10 (SPE) 250 (LLE)	50,000 (SPE) 10,000 (LLE)	9
paclitaxel	mouse plasma, tissue and tumour	LLE	100	227	31	10	20,000	10
paclitaxel	rat plasma	PP	100	233	10	10	1,500	11
paclitaxel	mouse plasma	LLE	100	227	10	10	500,000	12
paclitaxel	mouse plasma	PP	100	227	18	500	170,000	13
paclitaxel	human plasma and urine	LLE	800	227	33	50	20,000	14
paclitaxel	human plasma	online SPE	100	229	30 (extraction included)	42.7	8,540	15
paclitaxel	human plasma and urine	LLE	50-1000	227	10	25 (plasma) 40 (urine)	1,000	16
paclitaxel	human plasma and urine	LLE/SPE	1000	227	6	80.8	8,080	17
paclitaxel	mouse plasma	LLE	50-500	227	20	128	8,540	18
paclitaxel	human plasma	LLE/online SPE	200-1000	229	23 (extraction included)	10	10,000	19
paclitaxel	human plasma	LLE	1000	230	30	10	500	20
paclitaxel	human plasma	SPE	500	230	30	3	1,200	21
paclitaxel	human plasma	LLE/online SPE	1000	227	20	5	500	22
paclitaxel	rat plasma	SPE	100	227	30	10	1,000	23
paclitaxel	human plasma	SPE	500	227	15	10	1,000	24
paclitaxel	human and rat plasma, human serum	LLE	100	230	30	150	15,000	25
paclitaxel	rabbit plasma and tissue	PP	500	227	15	25 (plasma and heart) 125 (other tissues)	10,000,000 (plasma and heart) 200,000,000 (other tissues)	26

Abbreviations: LLOQ: Lower limit of quantification; ULOQ: Upper limit of quantification; PP: protein precipitation; LLE: Liquid-liquid extraction; SPE: Solid-phase extraction; CPE: Cloud point extraction; Ref: Reference.

Supplemental table 1. Overview of bioanalytical HPLC-UV assays for quantification of taxanes (continued).

Analyte(s)	Matrix	Pre-treatment	Sample volume (µl)	Wavelength (nm)	Runtime (min)	LLOQ (ng/mL)	ULOQ (ng/mL)	Ref
paclitaxel and metabolites	human plasma	SPE	1000	227		10	500	40
paclitaxel and metabolites	mouse plasma, tissue, urine and faeces	LLE/SPE	200 (plasma/ faeces) 200-1000 (tissue) 1000 (urine)	227	30	25 (plasma) 25-100 (tissue) 125 (faeces) 25 (urine)	10000 (paclitaxel) 500 (metabolites)	42
docetaxel and paclitaxel	human plasma	SPE	2000 (docetaxel) 4000 (paclitaxel)	227	15	0.81 (docetaxel) 1.02 (paclitaxel)	808 (docetaxel) 854 (paclitaxel)	38
docetaxel, paclitaxel and anthracyclines	human serum	online SPE	100	234	23 (extraction included)	500	25000	39
docetaxel and paclitaxel	human plasma	LLE	1000	225 (docetaxel) 230 (paclitaxel)		15	3000	37
docetaxel	human plasma	SPE	1000	230	30	5	500	27
docetaxel	human plasma	LLE	1000	227	20	25	1000	28
docetaxel	human plasma and urine	SPE	600-1000 (plasma)	227	13	5	1000	29
docetaxel	human plasma	LLE	1000	230	30	10	20000	30
docetaxel	human plasma	SPE/ online SPE	900	227	9 (online extraction included)	5	2000	31
docetaxel	human plasma	Semi automatic SPE	500-1000	225	20	10	2500	32
docetaxel and metabolites	human plasma	SPE	1000	227	22	10	1000 (docetaxel) 500 (metabolites)	41
IDN 5109	mouse plasma	SPE	400	227	30	100	10000	33
larotaxel	rat plasma	CPE	100	230	8	50	10000	34
IDN 5390	mouse plasma	SPE	400	227	15	50	5000	35
felotaxel	rat plasma, human plasma and urine	LLE	100	275	11	5	1000	36

Abbreviations: LLOQ: Lower limit of quantification; ULOQ: Upper limit of quantification; PP: protein precipitation; LLE: Liquid-liquid extraction; SPE: Solid-phase extraction; CPE: Cloud point extraction; Ref: Reference.

Supplemental table 2. Overview of bioanalytical LC-MS assays for quantification of paclitaxel

Analyte(s)	Mass or mass transition	Matrix	Pre-treatment	Sample volume (µl)	Internal standard	Runtime (min)	LLOQ (ng/mL)	ULOQ (ng/mL)	Ref
paclitaxel	854>286	human plasma	Semi automatic LLE	100	structure analogue	6	1	1000	46
paclitaxel	984>130	human plasma	LLE	200	docetaxel	4	1	1000	47
paclitaxel	854>569	human plasma	LLE	100	D ₅ -paclitaxel	8	2	2500	48
paclitaxel	854	mouse plasma and brain	SPE	50 (plasma) 200 (brain)	cephalothalminine	8	36 (plasma) 54 ng/g (brain tissue)	9900 (plasma) 1960 ng/g (brain)	49
paclitaxel	854>286	mouse plasma and tissue	LLE	100	docetaxel	3.5	0.2 (plasma) 0.5 ng/g (tissue)	500 (plasma) 1000 ng/g (tissue)	50
paclitaxel	854>105	human plasma	LLE	500	docetaxel	2 (Method A) 0.8 (Method B)	10	10000	51
paclitaxel	876>569	rat whole blood	Dried blood spots	10	docetaxel	7	0.2	20	52
paclitaxel	912>525	human serum	online SPE	100	docetaxel	2.5 (extraction included)	1	1000	53
paclitaxel	854>286	human plasma	PP/ automatic SPE	500	2'-methylpaclitaxel	8	5	500	54
paclitaxel	854>509	human and mouse plasma, brain tumour	LLE	200 (human plasma) 25 (mouse plasma) 0.2 g (tumour)	¹³ C ₆ -paclitaxel	9	0.25 (human plasma) 5 ng/g (brain tumour) 1 (mouse plasma)	1000 (plasma) 5000 ng/g (tumour)	55
paclitaxel	876>308	rat plasma	LLE	100	docetaxel	6	0.2	1000	56
paclitaxel	876>308	rat tissue	LLE	500	docetaxel	6	0.2-0.5 (low range) 10-50 (high range)	10-50 (low range) 200-2000 (high range)	57
paclitaxel	876>308	human plasma	LLE	200	¹³ C ₆ -paclitaxel	2	102.1	20420	58
paclitaxel	854>286	rat plasma	LLE	100	docetaxel	5	0.5	5000	59
total and unbound paclitaxel	854>569	human plasma	PP/SPE	100	D ₅ -paclitaxel	4	10	2500	60

Abbreviations: LLOQ: Lower limit of quantification; ULOQ: Upper limit of quantification; PP: protein precipitation; LLE: Liquid-liquid extraction; SPE: Solid-phase extraction Ref: Reference.

Supplemental table 3. Overview of bioanalytical LC-MS assays for quantification of paclitaxel and its metabolites

Analyte(s)	Mass transition	Matrix	Pre-treatment	Sample volume (µl)	Internal standard	Runtime (min)	LLOQ (ng/mL)	ULOQ (ng/mL)	Ref
paclitaxel and metabolites	854>509 (paclitaxel)	human and dog plasma	LLE	400	¹³ C ₆ -paclitaxel	5	0.1	100	61
	870>525 (6α-OH-paclitaxel)								
	870>509 (p-3'-OH-paclitaxel)								
	870>509 (p-3'-OH-paclitaxel)								
paclitaxel and metabolites	854>569+551 (paclitaxel)	human plasma	SPE	500	docetaxel	9	0.5	7500 (paclitaxel) 750 (6α-OH-paclitaxel) 400 (p-3'-OH-paclitaxel)	62
	870>585+567 (6α-OH-paclitaxel)								
	870>569+551 (p-3'-OH-paclitaxel)								
paclitaxel and metabolites	854>509 (paclitaxel)	human plasma	LLE	200	¹³ C ₆ -paclitaxel	9	0.25	1000 (paclitaxel) 100 (metabolites)	63
	870>525 (6α-OH-paclitaxel)								
	870>509 (p-3'-OH-paclitaxel)								
paclitaxel and metabolites	854>286 (paclitaxel)	human plasma	online SPE	90	docetaxel	30 (extraction included)	5 (paclitaxel) 0.87 (metabolites)	5000 (paclitaxel) 870 (6α-OH-paclitaxel) 435 (p-3'-OH-paclitaxel)	64
	870>286 (6α-OH-paclitaxel)								
	870>302 (p-3'-OH-paclitaxel)								
paclitaxel and metabolites	876>308 (paclitaxel)	human plasma	LLE	100	docetaxel		0.5	500	65
	892>607 (6α-OH-paclitaxel)								
	892>324 (p-3'-OH-paclitaxel)								

Abbreviations: LLOQ: Lower limit of quantification; ULOQ: Upper limit of quantification; LLE: Liquid-liquid extraction; SPE: Solid-phase extraction; Ref: Reference.

Supplemental table 4. Overview of bioanalytical LC-MS assays for quantification of docetaxel and its metabolites

Analyte(s)	Mass transition	Matrix	Pre-treatment	Sample volume (µl)	Internal standard	Runtime (min)	LLOQ (ng/mL)	ULOQ (ng/mL)	Ref
docetaxel	808>527	human plasma	PP/ automatic SPE	100	paclitaxel	3	0.15	1500	73
docetaxel	830>304	human plasma	online SPE	20	paclitaxel	7 (extraction included)	1	3000	74
docetaxel	808>527	mouse plasma	PP	40	paclitaxel	10	20.2	2020	75
docetaxel	808>527	human plasma	LLE	200	paclitaxel	7.5	0.25	1000	76
docetaxel	808>527	human plasma	LLE	50	paclitaxel	3	5	1000	77
docetaxel	808>527	human plasma	PP	50	paclitaxel	5	5	5000	78
docetaxel	808>226	human serum	PP/TFC	Not reported	D ₉ -docetaxel	6 (extraction included)	8	2000	79
docetaxel	808>527	human plasma	LLE	200	paclitaxel	2.5	2	5000	80
docetaxel and metabolites	808>527+509 (docetaxel) 822>527+509 (M1) 824>298 (M2) 822>527+509 (M3) 820>527+327 (M4)	human plasma	LLE	100	paclitaxel	10	0.5	1000	81
docetaxel and metabolites	808>527 (docetaxel) 839>527 (M1/M3) 824>298 (M2) 817>527 (M4)	human plasma	LLE	200	D9-docetaxel	9	0.25	500	82

Abbreviations: LLOQ: Lower limit of quantification; ULOQ: Upper limit of quantification; PP: protein precipitation; LLE: Liquid-liquid extraction; SPE: Solid-phase extraction; TFC: turbulent-flow liquid chromatography; Ref: Reference.

Supplemental table 5. Overview of bioanalytical LC-MS assays for quantification of paclitaxel and docetaxel combination assays

Analyte(s)	Mass or mass transition	Matrix	Pre-treatment	Sample volume (µl)	Internal standard	Runtime (min)	LLOQ (ng/mL)	ULOQ (ng/mL)	Ref
unbound docetaxel and paclitaxel	Not specified	human plasma (ultrafiltrate)	LLE	2000	cephalomannine	11	0.4	100	69
paclitaxel and 5 other taxane derivatives	854.2>405/286 (paclitaxel)	postmortal samples	LLE	100	D ₃ -trimipramine	15	0.1	100	66
paclitaxel and HM-30181	854>286	rat plasma	LLE	50	docetaxel	7	2	500	70
docetaxel, paclitaxel, ritonavir	808>527 (docetaxel) 854>509 (paclitaxel)	human plasma	LLE	200	¹³ C ₆ -paclitaxel D ₃ -docetaxel	9	0.5	500	67
docetaxel, paclitaxel, ritonavir	808>527 (docetaxel) 854>509 (paclitaxel)	human faeces and urine	LLE	200	¹³ C ₆ -paclitaxel D ₃ -docetaxel	9	0.5	500	72
docetaxel, paclitaxel and metabolites	808>527+226 (docetaxel) 854>569+509 (paclitaxel) 870>525+286 (6α-OH-paclitaxel) 870>509+302 (p-3'-OH-paclitaxel)	human plasma and oral fluid	LLE	250 (plasma)	cephalomannine	11	2 (plasma) 0.125 (oral fluid)	1000 (plasma) 62.5 (oral fluid)	68
docetaxel and paclitaxel	808 (docetaxel) 854 (paclitaxel)	human plasma	SPE	1000	paclitaxel and docetaxel	7	0.24 (docetaxel) 8.5 (paclitaxel)	808 (docetaxel) 854 (paclitaxel)	71
docetaxel and polysorbate 80	808>527	human plasma	LLE	1000	paclitaxel	7	0.4	80.8	83
docetaxel and ketoconazol	830>549	rat plasma	LLE	90	paclitaxel	9	2	500	84
docetaxel, temsirolimus and sirolimus	830>599	Human plasma and whole blood	PP/Online SPE	450	paclitaxel	10 (extraction included)	10	200	85

Abbreviations: LLOQ: Lower limit of quantification; ULOQ: Upper limit of quantification; PP: protein precipitation; LLE: Liquid-liquid extraction; SPE: Solid-phase extraction; Ref: Reference.

Supplemental table 6. Overview of bioanalytical LC-MS assays for quantification of other taxanes

Analyte(s)	Mass transition	Matrix	Pre-treatment	Sample volume (µl)	Internal standard	Runtime (min)	LLOQ (ng/mL)	ULOQ (ng/mL)	Ref
7-xylosyl-10-deacetylpaclitaxel	944>286	rat plasma	LLE	50	docetaxel	8	2	1000	91
BAV59-8862	889>772	mouse plasma and liver	PP/automatic SPE (plasma) LLE (liver)	200 (plasma) 1000 (liver)	IDN 5127	12	50	5000	94
cabazitaxel	836>555	human plasma	LLE	100	D ₆ -cabazitaxel	5	1 (low range) 40 (high range)	100 (low range) 4000 (high range)	86
cabazitaxel and its metabolites docetaxel, RPR112698 and RPR123142	837>556 (cabazitaxel) 808>527 (docetaxel) 822>541 (RPR112698 and RPR123142)	Human plasma	LLE	200	2:7-bisacetyltaxol (cabazitaxel, RPR112698 and RPR123142) D ₃ -docetaxel (docetaxel)	12	1 (cabazitaxel) 0.1 (docetaxel)	150 (cabazitaxel) 15 (docetaxel)	87
felotaxel	933>142	Mouse plasma, urine, faeces and tissue	LLE	100	diazepam	5	1 (plasma/brain) 10 (urine/faeces/tissue)	10000	88
felotaxel	933>142	rat and dog plasma	LLE	50-100 (rat) 200 (dog)	ketoconazol	4	5 and 200 (rat) 2 (dog)	500 and 10000 (rat) 500 (dog)	89
larotaxel	832>551	dog plasma	LLE	400	docetaxel	3	2.5	5000	90
NPD-103	1002>434	human plasma	LLE	200	¹³ C ₆ -paclitaxel	3	100	20000	95
IDN5738 and IDN5839	915>260 (IDN5738) 912>623 (IDN5839)	mouse plasma	PP	100	IDN 5127	20	2.5	1500 (IDN5738) 5000 (IDN5839)	92
IDN 5390	832>664	dog plasma	SPE	500	paclitaxel	>8	5	1000	93

RPR112698 and RPR123142 expressed as ng docetaxel equivalents/mL

Abbreviations: LLOQ: Lower limit of quantification; ULOQ: Upper limit of quantification; PP: protein precipitation; LLE: Liquid-liquid extraction; SPE: Solid-phase extraction; Ref: Reference.

Supplemental table 7. Overview of bionalytical assays other than HPLC-UV and LC-MS for quantification of taxanes

Assay type	Analyte(s)	Matrix	Sample volume (µl)	Runtime (min)	LLOQ (ng/mL)	ULOQ (ng/mL)	Ref
MEKC	paclitaxel	human plasma and urine	500 (plasma) 200 (urine)	15	50 (plasma) 125 (urine)	5000	106
MEKC	paclitaxel, morphine, codeine	human serum and plasma	1000	25	280 (serum) 250 (plasma)	50000 (serum) 50000 (plasma)	107
MEKC	paclitaxel, morphine, codeine	human urine	500	15	100	10000	108
enzyme linked immunoassay	paclitaxel	human serum	50		0.3	20	109
fluoroimmunoassay	paclitaxel	human plasma	10	4	5.85	400	111
enzyme linked immunoassay	paclitaxel	human plasma, ultrafiltrate and saliva	Not reported	10	0.05 (saliva) 0.002 (plasma ultrafiltrate) 0.35 (plasma)	100	110
tubulin-based biochemical assay	paclitaxel	human plasma	180	10	25.6	299	113
tubulin-based biochemical assay	paclitaxel	human serum	500	Not reported	256	2562	112

Abbreviations: MEKC: Micellar electrokinetic chromatography; LLOQ: Lower limit of quantification; ULOQ: Upper limit of quantification; Ref: Reference.

A sensitive combined assay for
the quantification of paclitaxel,
docetaxel and ritonavir in
human plasma using liquid
chromatography coupled with
tandem mass spectrometry.

Jeroen J.M.A. Hendriks
Michel J.X. Hillebrand
Bas Thijssen
Hilde Rosing
Alfred H. Schinkel
Jan H.M. Schellens
Jos H. Beijnen

J Chromatogr B Analyt Technol Biomed Life Sci.
2011; 879 (28): 2984-90

Abstract

A combined assay for the determination of paclitaxel, docetaxel and ritonavir in human plasma is described. The drugs were extracted from 200 μ L human plasma using liquid-liquid extraction with tertiar-butylmethylether, followed by high performance liquid chromatography analysis using 10 mM ammonium hydroxide pH 10: methanol (3:7, v/v) as mobile phase. Chromatographic separation was obtained using a Zorbax Extend C₁₈ column. Labelled analogues of the analytes are used as internal standards. For detection, positive ionization electrospray tandem mass spectrometry was used. Method development including optimisation of the mass transitions and response, mobile phase optimisation and column selection are discussed. The method was validated according to FDA guidelines and the principles of Good Laboratory Practice (GLP). The validated range was 0.5-500 ng/mL for paclitaxel and docetaxel and 2-2,000 ng/mL for ritonavir. For quantification, quadratic calibration curves were used ($r^2 > 0.99$). The total runtime of the method is 9 minutes and the assay combines analytes with differences in ionisation and desired concentration range. Inter-assay accuracy and precision were tested at four concentration levels and were within $\pm 10\%$ and less than 10%, respectively, for all analytes. Carry-over was less than 6% and endogenous interferences or interferences between analytes and internal standards were less than 20% of the response at the lower limit of quantification level. The matrix factor and recovery were determined at low, mid and high concentration levels. The matrix factor was around 1 for all analytes and total recovery between 77.5 and 104%. Stability was investigated in stock solutions, human plasma, dry extracts, final extracts and during 3 freeze/thaw cycles. The described method was successfully applied in clinical studies with oral administration of docetaxel or paclitaxel in combination with ritonavir.

Introduction

Docetaxel (Taxotere®) and paclitaxel (Taxol®) are both taxanes and share the baccatin ring structure (Figure 1).¹ Paclitaxel was isolated in the early 70s from *Taxus brevifolia* and docetaxel, a semi-synthetic derivative of a taxane from *Taxus baccata* was found a decade later.² Both taxanes are widely used as intravenously administered anticancer agents but oral formulations with paclitaxel and docetaxel are currently under investigation in both *in vitro* and *in vivo* studies.³ The taxanes are subject to a complex detoxification mechanism involving both ABC drug transporters and drug metabolizing enzymes, which results in a low bioavailability after oral administration.⁴ *In vivo*, both P-glycoprotein (PgP) and Multidrug resistance-associated protein (MRP) 2 are involved in paclitaxel and docetaxel pharmacokinetics by decreasing exposure to the taxanes.^{5;6} Thereby, MRP7 reduces *in vivo* tissue sensitivity to paclitaxel.⁷ Paclitaxel is metabolized by Cytochrome P450 (CYP) 2C8 and CYP3A4, while docetaxel is primarily metabolized by the CYP3A subfamily.¹ Due to the involvement of the transporters and CYP enzymes, the oral bioavailability of the taxanes is limited and several studies have assessed enhancers in combination with oral formulations to increase the bioavailability.³ One of the currently applied boosting agents is the CYP3A inhibitor ritonavir (Norvir®) (Figure 1). Low doses of ritonavir are also widely used as booster to increase the bioavailability of protease inhibitors in HIV therapy.⁸ Previously, several methods for the (combined) quantification of taxanes in human plasma are described⁹⁻²⁰ and separate methods for the quantification of ritonavir mostly in combination with other antiretroviral drugs.²¹⁻²⁵

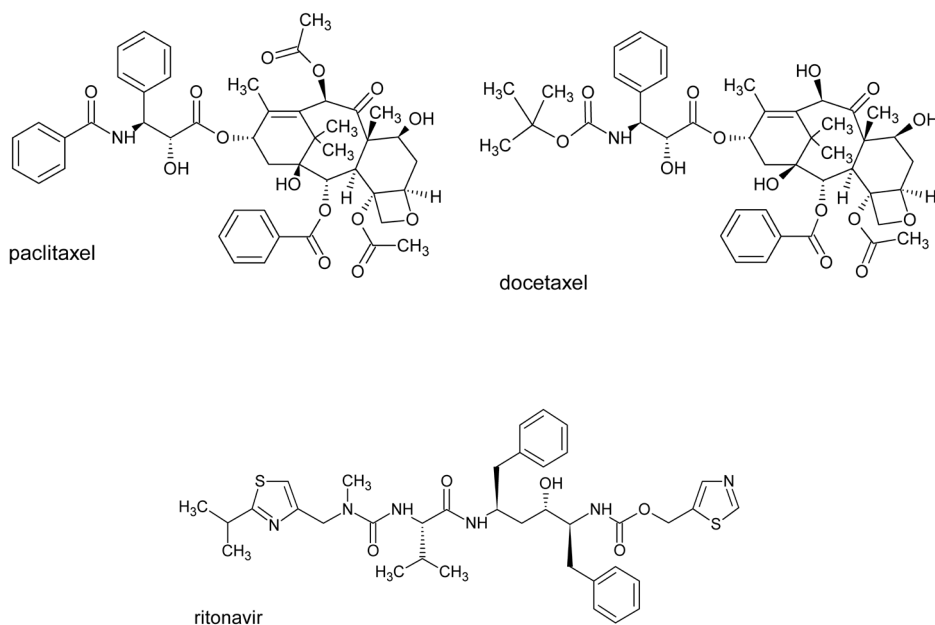


Figure 1. Structures of paclitaxel, docetaxel and ritonavir.

To support further studies with ritonavir-boosted oral taxanes, we developed and validated a sensitive and fast liquid chromatography-/tandem mass spectrometry (LC-MS/MS) method for the simultaneous detection of docetaxel, paclitaxel and ritonavir. We aimed for a lower limit of quantification of 0.5 and 2 ng/ml for the taxanes and ritonavir, respectively. According to previous pharmacokinetic profiling^{14;26-28}, these limits provide sufficient sensitivity to support clinical studies.

Material and Methods

Chemicals

Paclitaxel and docetaxel were purchased from Sequoia Research Products (Oxford, UK). Ritonavir, ¹³C₃-labelled ritonavir and D₉-labelled docetaxel were purchased from Toronto Research Chemicals (North York, ON, Canada). ¹³C₆-labelled paclitaxel was kindly provided by Pharmacia Corporation (Nerviano, Italy). Methanol (HPLC grade) was obtained from Biosolve Ltd (Amsterdam, the Netherlands), tert-butylmethylether (tert.-butylmethylether/ TBME, Analytical grade) and water for chromatography (LiChrosolv) were obtained from Merck (Darmstadt, Germany). Drug free lithium-heparinized human plasma was obtained from Bioreclamation LLC (New York, NY, USA).

Mass spectrometric and chromatographic conditions

The chromatographic conditions were based on previously developed assays for quantification of docetaxel and paclitaxel.^{14;29} An API 4000 triple quadrupole MS with electrospray ionisation (ESI) (AB Sciex, Foster City, CA, USA) was coupled to an Agilent 1100 liquid chromatographic system (Agilent Technologies, Palo Alto, CA, USA). The Agilent 1100 system consisted of a binary pump, an autosampler, a mobile phase degasser and a column oven. The mobile phase consisted of methanol:10 mM ammonium hydroxide in water (70:30, v/v) at a flow of 0.3 mL/min. Chromatographic separation was obtained using a Zorbax Extend C₁₈ column (150 mm x 2.1 mm I.D., particle size 5 µm; Agilent Technologies) protected with an inline filter (0.5 µm). The column oven was set at 35 °C, while the autosampler was thermostatted at 4 °C. A sample volume of 25 µL was injected and the injection needle was washed for 3 s with methanol after each injection. Mass transitions were optimized for each compound in positive ion mode. Ion specific parameters were optimized for each analyte separately. An overview of the mass transitions and MS/MS settings is listed in Table 1. The total run time was 9 min. A switching valve was used to direct the eluent during the first 3 min of the run to waste. For quantification, the multiple reactions monitoring (MRM) chromatograms were acquired with Analyst software version 1.5 (AB Sciex).

Preparation of stock and working solutions

Two stock solutions of each analyte from independent weightings were prepared in methanol at a concentration of 1 mg/mL. The stock solutions of the three analytes were diluted to combined working solutions with methanol. One set of working solutions was used for the preparation of calibration standards, while the other set was used

Table 1. MS/MS parameters and mass transitions of the analytes.

Parameter	Setting					
Entrance Potential	10.0 V					
Ionspray Voltage	5500 V					
Collision gas	5.0 psi					
Curtain gas	20.0 psi					
Ionsource gas 1	60.0 psi					
Ion source gas 2	50.0 psi					
Temperature	400 °C					
	PAC	DOC	RTV	IS PAC	IS DOC	IS RTV
Declustering Potential (V)	60	56	81	60	56	81
Collision Energy (V)	23	15	93	23	15	39
Collision Cell Exit Potential (V)	16	14	18	16	14	18
ScanTime (sec)	0.2	0.2	0.2	0.2	0.2	0.2
Precursor ion (m/z)	854	808	721	860	817	726
Product ion (m/z)	509	527	196	515	527	296
Typical R.T (minutes)	3.8	4.4	6.9	3.8	4.3	6.8

Abbreviations: PAC: paclitaxel; DOC: docetaxel; RTV: ritonavir; IS PAC: $^{13}\text{C}_6$ -labelled paclitaxel; IS DOC: D_9 -labelled docetaxel; IS RTV: $^{13}\text{C}_3$ -labelled ritonavir.

for the preparation of quality control (QC) samples. For the internal standards $^{13}\text{C}_3$ -ritonavir, D_9 -docetaxel and $^{13}\text{C}_6$ -paclitaxel stock solutions of respectively 0.5, 1.0 and 0.1 mg/mL were prepared in methanol. The three internal standards were diluted to one combined internal standard working solution of 500, 40 and 200 ng/mL ($^{13}\text{C}_3$ -ritonavir, D_9 -docetaxel and $^{13}\text{C}_6$ -paclitaxel, respectively). All solutions were stored at $-20\text{ }^\circ\text{C}$.

Preparation of Calibration standards and Quality Controls

Calibrations standards (CAL) were prepared by diluting a fixed amount of working solution containing each analyte in blank human plasma. The CALs contained the analytes in a range of 0.5 to 500 ng/mL (paclitaxel/docetaxel) and 2 to 2,000 ng/mL (ritonavir). In a similar way, QC samples at three concentrations were prepared from another set of working solutions. The QCs contained the taxanes in concentrations of 1.5, 100 and 400 ng/mL and ritonavir in concentrations of 6, 400 and 1,600 ng/mL. For validation purpose, additional QCs were made at lower limit of quantification (LLOQ) level (0.5/2 ng/mL; taxanes/ritonavir) and higher than the upper limit of quantification (ULOQ; 2,000/8,000 ng/mL; taxanes/ritonavir). Samples were transferred to 2.0 mL polypropylene tubes (Eppendorf, Merck) in aliquots of 200 μL and stored at $-20\text{ }^\circ\text{C}$.

Sample preparation

To 200 μL sample, 20 μL internal standard working solution was added and the sample was vortex-mixed for 10 s. Blank samples were spiked with 20 μL of methanol instead of internal standard working solution. After mixing, 1.0 mL of tertiar-butylmethylether

was added and again, the sample was mixed for 10 s. Samples were successively shaken automatically for 10 min at 1,250 rpm (L46, Labinco, Breda, The Netherlands) and centrifuged for 5 min at 23,000 *g* (5403 Eppendorf, Netheler Hinz GmbH, Hamburg, Germany). The aqueous layer was frozen in a bath of ethanol and dry ice and the organic layer was transferred into a clean 1.5 mL tube. The sample was dried under a gentle stream of nitrogen at 40 °C. The residue was reconstituted in methanol: water (1:1, v/v), vortex-mixed for 10 s and centrifuged for 3 min at 23,000 *g*. The supernatant was transferred to a glass autosampler vial with insert and 25 µL was injected onto the LC-MS/MS system.

Validation

For the assay, a full validation program was executed, including calibration model, accuracy, precision, carry-over, dilution test, specificity and selectivity, matrix effect, recovery and stability. Stability of each analyte separately during 3 freeze/thaw cycles^{14;30;31} has been previously determined at our institute, so only long-term stability in human plasma and stability of the dried extract, the processed sample stability and re-injection reproducibility were executed. Long-term stability was tested for each analyte separately, while all other stability testing was executed with all analytes combined. The validation was executed according to the FDA guidelines³² on bioanalytical method validation and to the guidelines of the 3rd AAPS/FDA bioanalytical workshop.³³ The validation was performed in compliance with the OECD principles of Good Laboratory Practice (GLP).³⁴

Results and discussion

Mass spectrometric and chromatographic conditions

Mass transition

The molecular ions ($[M+H]^+$) of paclitaxel, docetaxel and ritonavir observed at m/z 854, 808 and 721, respectively, were used as precursor ions to generate product ion spectra. The most abundant product ions of paclitaxel and docetaxel were optimized for Multiple Reactions Monitoring (MRM) (Table 1). For ritonavir the product ion at m/z 196, and not the most abundant product ion at m/z 296, was optimized for MRM since back-calculated calibration concentrations at the transition 721 to 196 provided the lowest total bias across the range. For the internal standard $^{13}C_3$ -ritonavir, the isotope ion at m/z 726 was selected as precursor ion, instead of the protonated molecular ion at m/z 724, as the molecular isotopic ions of ritonavir monitored at m/z 724 and 725 interfered with the molecular isotopic ions of $^{13}C_3$ -ritonavir at these mass transitions. At mass transition m/z 726, ritonavir showed no isotope ions, while $^{13}C_3$ -ritonavir showed isotope ions at an intensity which was 2-fold lower compared to the intensity at m/z 724. To increase the sensitivity for the detection of $^{13}C_3$ -ritonavir, the most abundant product ion at m/z 296 was selected instead of the same product ion as used for ritonavir to obtain a maximum response. For D_9 -docetaxel and $^{13}C_6$ -paclitaxel the molecular ions observed at m/z 860 and 817, respectively, were used as precursor ions and the most abundant product ions were used for MRM (Table 1).

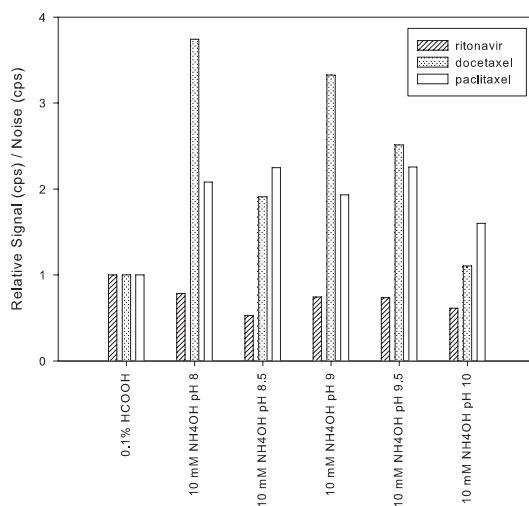


Figure 2. Relative signal-to-noise ratios of ritonavir, docetaxel and paclitaxel after flow injection analysis. During the experiments no column was used and the mobile phase contained 70% (v/v) methanol.

Acid versus alkaline mobile phase

During development of the method, 0.1% formic acid (pH 2.7) and 10 mM ammonium hydroxide (pH 8-10) were tested as aqueous phases of the eluent. Docetaxel and paclitaxel responses increased 1.1- to 3.7-fold when alkaline mobile phases were applied, while the response of ritonavir decreased (see Figure 2). For these tests, a small volume (2 μ L) was injected from a solution containing all analytes at a concentration of 5,000 ng/mL (taxanes) or 20,000 ng/mL (ritonavir). Compared to 10 mM ammonium hydroxide pH 9.5, a mobile phase of pH 10 showed a slightly higher response of docetaxel, but also a higher background signal. Both observations resulted in a lower signal-to-noise ratio for 10 mM ammonium hydroxide pH 10. It was observed that the background signal of alkaline mobile phases was reduced when a column was used. Due to the reduction in noise by using a column, a mobile phase of pH 10 resulted in the highest signal-to-noise ratio and the best performance at LLOQ concentration level. Therefore 10 mM ammonium hydroxide pH 10 was selected as aqueous phase. It is known that the disposition of the analytes in the formed droplets has an effect on the ESI response as described in detail by Check and Enke.³⁵ It is hypothesized that by changing the mobile phase from acid to alkaline, the disposition of the analytes in the droplets formed by ESI is changed resulting in an increase of the docetaxel and paclitaxel responses. The change of disposition could be the result of changed chemical characteristics of the mobile phase or the analytes due to pH changes (e.g. protonation or changed surface-activity) or adduct forming of the analyte with ammonium. The results of the experiments with different pH types suggest that the increase in response is due to a change in pH and not due to the presence of ammonium ions. Although the mechanism is not clear yet, the increase in the response of docetaxel by changing the pH of the mobile phase with ammonium hydroxide is supported by observations from other research groups.^{12-14;17;19}

Column selection

During development of the method, several columns were tested. Chromatography of a Zorbax Extend C₁₈ column (150 mm x 2.1 mm I.D., particle size 5 µm; Agilent Technologies), a Kinetex C₁₈ column (150 mm x 2.1 mm I.D., particle size 2.6 µm; Phenomenex), an Xbridge C₁₈ column (50 mm x 2.1 mm I.D., particle size 5 µm; Waters) and a Gemini C₁₈ 110A column (150 mm x 2.0 mm I.D., particle size 5.0 µm; Phenomenex) were compared at a flow rate of 0.2 mL/min. All other mass spectrometric and chromatographic conditions were as described above, except for the Kinetex column. For the Kinetex column the mobile phase consisted of 80% methanol instead of 70% and the column oven was set at 60 °C. This was necessary to reduce the pressure in the system. The Zorbax Extend column was considered superior to the other columns in terms of accuracy, precision and carry-over for all analytes and mainly for docetaxel. Injection of spiked docetaxel samples on the Kinetex column resulted in an increase of background signal at *m/z* 808 at the retention time of docetaxel. The signal remained constant over three subsequent injections of water: methanol (1:1, v/v) and this is probably due to a memory effect of the Kinetex column. This effect was observed during multiple runs and not seen with any of the other tested columns. The chromatographic conditions of the Zorbax Extend column were further optimized resulting in a flow rate of 0.3 mL/min. To reduce the run time, a mobile phase containing 75% (v/v) methanol was tested but under these conditions an endogenous interference shifted towards the docetaxel peak. Finally, a Zorbax Extend Column was selected and a mobile phase containing 70% (v/v) methanol was used. The flow rate was set at 0.3 mL/min and the column oven was set at 35 °C.

Optimization of ritonavir response

The combination of the taxanes paclitaxel and docetaxel in one assay with ritonavir was challenging as not only the desired concentration range of ritonavir was 4-fold higher, but also because ritonavir is a better responder compared to the taxanes. Consequently obtaining sensitivity of docetaxel and paclitaxel at LLOQ level resulted in saturation of the response of ritonavir at the ULOQ concentration level. For paclitaxel and docetaxel the most abundant product ions were selected for quantification. To prevent saturation of the detector, not the most abundant product ion at *m/z* 296 was selected for ritonavir but an apparently suboptimal product ion at *m/z* 196. The response of this transition was almost 30 times lower compared to the transition 721 to 296, however, saturation of the signal response was still observed. To reduce the amount of product ions, the collision energy was changed from 86 to 93 V. The combination of the selected mass transition and the apparently non-optimal collision energy resulted in the most accurate and precise quantification of ritonavir, despite the differences in ionisation and target concentration ranges between ritonavir and the taxanes.

Sample pre-treatment

Sample pre-treatment as described previously by our group for the quantification of docetaxel¹⁴ and paclitaxel³¹ was followed. Liquid-liquid extraction (LLE) was compared with protein precipitation. Relative recovery of both pre-treatment procedures was comparable, however using LLE, cleaner plasma extracts were obtained. Furthermore sample concentration was favourable to decrease the LLOQ. During development the

following solvents for reconstitution were tested: methanol-water (1:1, v/v), methanol-water (7:3, v/v), acetonitrile-water (1:1, v/v) or 10 mM ammonium hydroxide pH 5-acetonitrile. Methanol-water (1:1, v/v) was selected as reconstitution solvent since peak shapes improved and the lowest noise levels in the MRM chromatograms were observed. A reduction in noise levels was not expected since analytes are eluting far from time zero. Probably less matrix ions are dissolved during the reconstitution in methanol-water (1:1, v/v) resulting in improved noise levels compared to the other tested solvents.

Validation of the method

Calibration model

CALs (8) with duplicate points at each concentration in the range 0.5 to 500 ng/mL (paclitaxel and docetaxel) and 2 to 2,000 ng/mL (ritonavir) were prepared in control lithium heparinized human plasma and analyzed in three independent analytical runs. Calibration curves were fitted by quadratic regression of the peak area ratio with the internal standard versus the concentration with $1/x^2$ (the reciprocal of the squared concentration) as the weighting factor. At high concentration levels of the analytes, the calibration curves were not linear, resulting in a higher total bias in the upper ranges of the calibration curves when linear regression was applied instead of quadratic regression. Although both quadratic and linear regression met the criteria³², quadratic regression was used to minimize the bias across the range of 0.5 to 500 ng/mL for the taxanes and 2 to 2,000 ng/mL for ritonavir. Reduction of the calibration ranges was not desirable because this would result in an excessive number of re-analysis of study samples after dilution in control matrix. When calibration data was fitted by quadratic regression, correlation coefficients (r^2) of 0.9989 or better were obtained for all analytes. For every calibration curve the calibration concentrations were back-calculated from the response ratios. The deviations of the nominal concentrations should be within $\pm 15\%$. At the LLOQ level a deviation of $\pm 20\%$ was permitted. For paclitaxel at all calibration standard concentration levels, the deviations of measured concentrations from nominal concentration were between -1.9 and 3.9% with coefficient of variation (CV) values of less than 12.5%. For the calibration standards of docetaxel, the deviations of measured concentrations from nominal concentration were between -1.9 and 1.7% with CV values of less than 4.3% and for ritonavir the deviations of measured concentrations were between -1.8 and 2.4% with CV values of less than 4.1%. Typical MRM chromatograms of blank plasma and the analytes at LLOQ-level are presented in Figure 3.

Accuracy and precision

QC samples were prepared in control lithium heparinized human plasma and five replicates of each level were analyzed in three independent analytical runs. The accuracy was determined in percentage difference between the mean concentration and the nominal concentration. The CV was used to report the precisions. The intra- and inter-assay accuracies and precisions should be within $\pm 20\%$ and less than 20%, respectively, for the LLOQ concentration and within $\pm 15\%$ and less than 15%, respectively, for other concentrations. Assay performance data of paclitaxel, docetaxel and ritonavir are in Table 2. For all the analytes, all intra- and inter-assay accuracies and precisions fulfilled the required criteria.^{32;33}

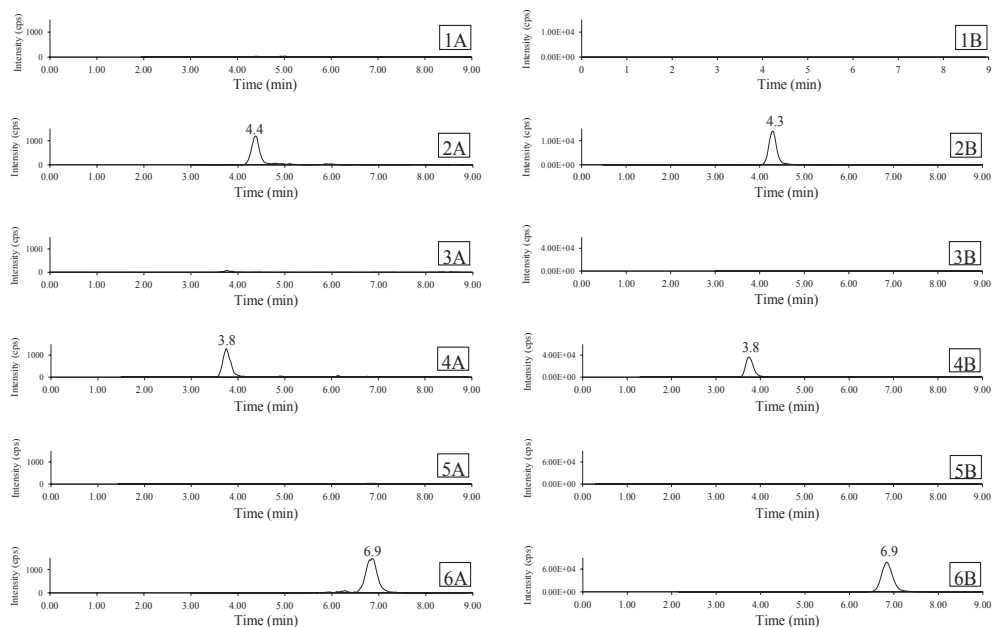


Figure 3. Typical MRM chromatograms of the analytes in a blank plasma sample and at LLOQ level (0.5 ng/mL and 2 ng/mL for the taxanes and ritonavir, respectively). Panels show the response in a blank plasma sample and in a calibration sample at LLOQ level at the transition of docetaxel (1A and 2A, respectively), D₉-labeled docetaxel (1B and 2B), paclitaxel (3A and 4A), ¹³C₆-labeled paclitaxel (3B and 4B), ritonavir (5A and 6A) and ¹³C₃-labeled ritonavir (5B and 6B).

Table 2. Assay performance for paclitaxel, docetaxel and ritonavir.

Compound	Nominal conc. (ng/mL)	Mean measured conc. (ng/mL)	Inter-assay bias (%)	Inter-assay precision (%)	No. of replicates
Paclitaxel	0.504	0.459	-8.8	3.8	15
	1.51	1.45	-4.1	2.7	15
	101	92.6	-8.3	1.9	15
	403	383	-4.9	1.4	15
Docetaxel	0.5	0.459	-8.2	7	15
	1.5	1.45	-3.2	6.8	15
	100	95.9	-4.1	5.2	15
	400	398	-0.5	5.3	15
Ritonavir	1.98	1.91	-3.5	2.9	15
	5.94	5.96	0.4	1.7	15
	396	387	-2.2	1.3	15
	1580	1570	-0.8	0.9	15

Abbreviation: conc.: concentration.

Carry-over

Carry-over was tested by injecting two processed blank matrix samples subsequently after injection of an ULOQ sample in three independent runs. The response in the first blank matrix at the retention time of the analytes or internal standards should be less than 20% of the mean response of a LLOQ sample for the analytes and less than 5% of the mean response for the IS. The response in the first blank matrix at the retention time of the analytes was less than 6% of the mean response at the LLOQ for all analytes. At the retention times of the internal standards no response was observed. Therefore, the carry-over test was found to be acceptable.

Dilution test

To assess the reliability of the method at concentration levels above the ULOQ (500/2,000 ng/mL; taxanes/ritonavir), an intra-assay accuracy and precision test was executed. A sample at a concentration level above the ULOQ was diluted 2 (800 to 400 ng/mL; taxanes), 5 (800 to 160 ng/mL; taxanes), 10 (2,000 to 200 ng/mL; taxanes) and 100 times (2,000 to 200 and subsequently 200 to 20 ng/mL; taxanes) with human blank plasma. All samples also contained ritonavir in 4 times higher concentrations compared to paclitaxel and docetaxel. Diluted samples were processed in 5-fold and analyzed. Accuracy and precision were determined as described for QC samples and should be within $\pm 15\%$ and less than 15%, respectively. For all dilution factors, accuracies and precisions fulfilled these acceptance criteria.^{32,33}

Specificity and selectivity

From 6 different batches of control human heparinized plasma, blank (without the internal standards) and spiked samples (with paclitaxel, docetaxel, ritonavir and the internal standards) at the LLOQ concentration level were prepared. The samples were prepared to determine whether endogenous compounds interfere at the mass transitions chosen for the analytes and internal standards. Samples were processed according to the described procedures and analyzed. Interferences co-eluting with the analytes or internal standards should not exceed 20% of the peak area of the analytes at LLOQ or 5% of the internal standard areas. Deviations of the nominal concentrations should be within $\pm 20\%$. MRM chromatograms of the double blanks did not show peaks that co-eluted with one of the analytes with areas exceeding 11% of the area at LLOQ level or peaks that co-eluted with the internal standards with areas that exceeded 0.3% of the internal standard area. Deviations from the nominal concentrations at the LLOQ level of the analytes in all batches were between -12.6 and 5.8%.

To assess cross-analyte/internal standard interferences, samples containing only one of the analytes at ULOQ level or one of the internal standards in control human heparinized plasma were processed and analyzed. Interferences were less than 20% of the peak area of the analytes at the LLOQ or 5% of the internal standard areas. During cross-analyte interference tests, the interferences at the retention times of paclitaxel, docetaxel and ritonavir were less than 5.1, 18.5 and 7.1% of the area of their LLOQ standards, respectively. Interference at the retention times of $^{13}\text{C}_6$ -paclitaxel, D_9 -docetaxel and $^{13}\text{C}_3$ -ritonavir were less than 0.3, 1.4 and 5% of their area, respectively. Therefore the cross analyte/internal standard interferences were considered acceptable for all analytes and internal standards.

Matrix factor and Recovery

The matrix factor was determined by comparing the signals of the analytes in processed QC samples at low, mid and high concentration levels to the signals of the same concentration levels in methanol: water (1:1, v/v). Responses were corrected for the internal standard area. The variability in matrix factor, as measured by the coefficient of variation should be less than 15%³³. The matrix factor for paclitaxel, determined as the area ratio with and without matrix ions present, was between 0.992 and 1.02 for all concentration levels, with CV values less than 1.8%. For docetaxel, the matrix factor was between 0.933 and 0.99, with CV values less than 4.7%, when one outlier at low concentration was rejected. For ritonavir, the matrix factor was between 1.00 and 1.02, with CV values less than 1.9%. Overall, the results (matrix factor around 1) indicate that the stable-isotopically labelled internal standards of all analytes are most effective minimizing the influence of matrix effects.

The overall recovery was calculated by comparing the absolute areas in a processed QC sample to the areas measured in an unprocessed sample. The overall recovery was determined for all analytes at 3 concentration levels. The total recoveries for paclitaxel, docetaxel and ritonavir were between 77.5 and 104% with CV values of less than 15%. It was observed, that recovery increased with the concentration level. An underestimation of the total recovery at low concentration was caused by disproportional high areas of the analytes in the samples in absence of matrix ions. However, the total recovery was constant, precise and reproducible.

Stability

Stock solutions in methanol are stable for at least 12, 21 and 36 months for paclitaxel, docetaxel and ritonavir, respectively, when stored at nominally -20 °C. All analytes are stable in human plasma at ambient temperature for at least 24 h and at least 19 months (paclitaxel), 31 months (docetaxel) or 36 months (ritonavir) at nominally -20 °C and after three freeze/thaw cycles. The stability in dry extract and final extract samples containing all analytes was evaluated at nominally 2-8 °C at low and high level. The analytes were considered stable in the matrix when 85-115% of the initial measured concentration was found. Stability was demonstrated for at least 8 days at 2-8 °C under both conditions. The re-injection reproducibility was evaluated in processed samples of human plasma containing all analytes after storage at nominally 2-8 °C for 9 days. The bias was within $\pm 15\%$ of the nominal concentration for all the analytes. Therefore it is concluded that the samples can be re-injected within 9 days when kept at nominally 2-8 °C.

Application of the method

The validated assay is currently in use to support clinical studies. In these studies patients receive either paclitaxel or docetaxel in combination with ritonavir. In Figure 4 concentration-time curves are presented of two patients receiving taxanes in combination with ritonavir, both orally administered. One patient received paclitaxel and ritonavir in doses of 100 mg and 200 mg, respectively. The other patient also received 200 mg ritonavir, co-administered with 60 mg docetaxel. Maximal plasma

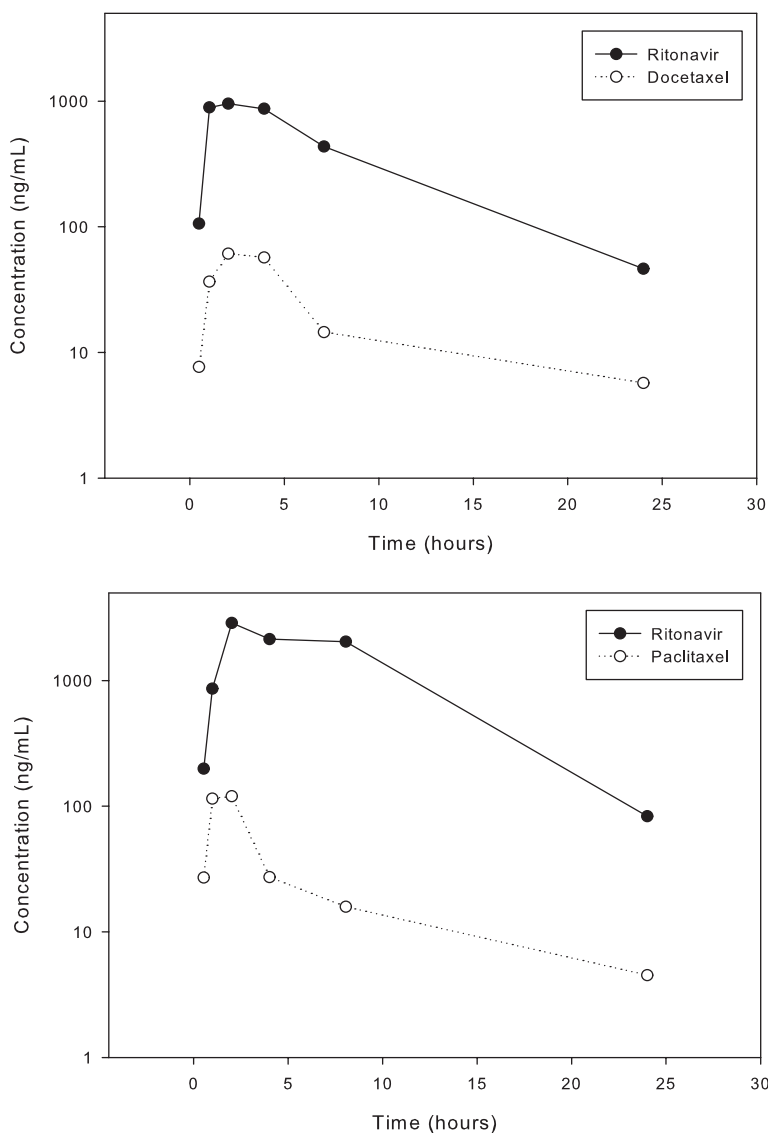


Figure 4. Concentration-time curves after oral co-administration of 200 mg ritonavir with 60 mg docetaxel (A) or 200 mg ritonavir with 100 mg paclitaxel (B).

concentrations of oral paclitaxel and docetaxel were 120 and 61 ng/mL, respectively. The maximal plasma concentrations of ritonavir were 956 and 2,879 ng/mL. The variation in plasma concentrations of ritonavir is observed in modelling of population pharmacokinetics after administration of 100 mg ritonavir bi-daily.³⁶ Phase I and II studies are currently ongoing to further investigate the oral co-administration of taxanes and ritonavir.

Conclusion

The development and validation of a combined assay for the quantification of paclitaxel, docetaxel and ritonavir in human plasma is described. The validated range for the taxanes was 0.5-500 ng/mL and for ritonavir was 2-2,000 ng/mL using 200 μ L plasma aliquots. The assay was validated according to FDA guidelines and has been successfully applied in clinical studies. During development we showed that using an alkaline mobile phase instead of an acid mobile phase the sensitivity for docetaxel and paclitaxel can be increased. Moreover, we demonstrated that each of the applied drugs in this single assay could be quantified successfully, although the individual chemical properties, concentration ranges and ionisation responses are diverse.

References

1. Vaishampayan U, Parchment RE, Jasti BR, Hussain M. Taxanes: an overview of the pharmacokinetics and pharmacodynamics. *Urology*. **1999**; 54 (6A Suppl): 22-9.
2. Gligorov J, Lotz JP. Preclinical pharmacology of the taxanes: implications of the differences. *Oncologist*. **2004**; 9 Suppl 2): 3-8.
3. Koolen SL, Beijnen JH, Schellens JHM. Intravenous-to-oral switch in anticancer chemotherapy: a focus on docetaxel and paclitaxel. *Clin.Pharmacol.Ther*. **2010**; 87 (1): 126-9.
4. Schellens JHM, Malingre MM, Kruijtzter CM, Bardelmeijer HA, van Tellingen O, Schinkel AH, Beijnen JH. Modulation of oral bioavailability of anticancer drugs: from mouse to man. *Eur.J.Pharm.Sci*. **2000**; 12 (2): 103-10.
5. Lagas JS, Vlaming ML, van Tellingen O, Wagenaar E, Jansen RS, Rosing H, Beijnen JH, Schinkel AH. Multidrug resistance protein 2 is an important determinant of paclitaxel pharmacokinetics. *Clin.Cancer Res*. **2006**; 12 (20 Pt 1): 6125-32.
6. van Waterschoot RA, Lagas JS, Wagenaar E, Rosing H, Beijnen JH, Schinkel AH. Individual and combined roles of CYP3A, P-glycoprotein (MDR1/ABCB1) and MRP2 (ABCC2) in the pharmacokinetics of docetaxel. *Int.J.Cancer*. **2010**; 127 (12): 2959-64.
7. Hopper-Borge EA, Churchill T, Paulose C, Nicolas E, Jacobs JD, Ngo O, Kuang Y, Grinberg A, Westphal H, Chen ZS, Klein-Szanto AJ, Belinsky MG, Kruh GD. Contribution of Abcc10 (Mrp7) to in vivo paclitaxel resistance as assessed in Abcc10(-/-) mice. *Cancer Res*. **2011**; 71 (10): 3649-57.
8. Cooper CL, van Heeswijk RP, Gallicano K, Cameron DW. A review of low-dose ritonavir in protease inhibitor combination therapy. *Clin.Infect.Dis*. **2003**; 36 (12): 1585-92.
9. Alexander MS, Kiser MM, Culley T, Kern JR, Dolan JW, McChesney JD, Zygmunt J, Bannister SJ. Measurement of paclitaxel in biological matrices: high-throughput liquid chromatographic-tandem mass spectrometric quantification of paclitaxel and metabolites in human and dog plasma. *J.Chromatogr.B Analyt.Technol.Biomed.Life Sci*. **2003**; 785 (2): 253-61.
10. Gardner ER, Dahut W, Figg WD. Quantitative determination of total and unbound paclitaxel in human plasma following Abraxane treatment. *J.Chromatogr.B Analyt.Technol.Biomed.Life Sci*. **2008**; 862 (1-2): 213-8.
11. Green H, Vretenbrant K, Norlander B, Peterson C. Measurement of paclitaxel and its metabolites in human plasma using liquid chromatography/ion trap mass spectrometry with a sonic spray ionization interface. *Rapid Commun.Mass Spectrom*. **2006**; 20 (14): 2183-9.
12. Grozav AG, Hutson TE, Zhou X, Bukowski RM, Ganapathi R, Xu Y. Rapid analysis of docetaxel in human plasma by tandem mass spectrometry with on-line sample extraction. *J.Pharm.Biomed.Anal*. **2004**; 36 (1): 125-31.
13. Guitton J, Cohen S, Tranchand B, Vignal B, Droz JP, Guillaumont M, Manchon M, Freyer G. Quantification of docetaxel and its main metabolites in human plasma by liquid chromatography/tandem mass spectrometry. *Rapid Commun.Mass Spectrom*. **2005**; 19 (17): 2419-26.
14. Kuppens IE, van Maanen MJ, Rosing H, Schellens JHM, Beijnen JH. Quantitative analysis of docetaxel in human plasma using liquid chromatography coupled with tandem mass spectrometry. *Biomed.Chromatogr*. **2005**; 19 (5): 355-61.
15. Mortier KA, Renard V, Verstraete AG, Van Gussem A, Van Belle S, Lambert WE. Development and validation of a liquid chromatography-tandem mass spectrometry assay for the quantification of docetaxel and paclitaxel in human plasma and oral fluid. *Anal.Chem*. **2005**; 77 (14): 4677-83.
16. Mortier KA, Lambert WE. Determination of unbound docetaxel and paclitaxel in plasma by ultrafiltration and liquid chromatography-tandem mass spectrometry. *J.Chromatogr.A*. **2006**; 1108 (2): 195-201.
17. Parise RA, Ramanathan RK, Zamboni WC, Egorin MJ. Sensitive liquid chromatography-mass spectrometry assay for quantitation of docetaxel and paclitaxel in human plasma. *J.Chromatogr.B Analyt.Technol.Biomed.Life Sci*. **2003**; 783 (1):

- 231-6.
18. Sottani C, Minoia C, D'Incalci M, Paganini M, Zucchetti M. High-performance liquid chromatography tandem mass spectrometry procedure with automated solid phase extraction sample preparation for the quantitative determination of paclitaxel (Taxol) in human plasma. *Rapid Commun.Mass Spectrom.* **1998**; 12 (5): 251-5.
 19. Wang LZ, Goh BC, Grigg ME, Lee SC, Khoo YM, Lee HS. A rapid and sensitive liquid chromatography/tandem mass spectrometry method for determination of docetaxel in human plasma. *Rapid Commun.Mass Spectrom.* **2003**; 17 (14): 1548-52.
 20. Zhang W, Dutschman GE, Li X, Cheng YC. Quantitation of paclitaxel and its two major metabolites using a liquid chromatography-electrospray ionization tandem mass spectrometry. *J.Chromatogr.B Analyt.Technol.Biomed.Life Sci.* **2011**; 879 (22): 2018-22.
 21. Estrela RC, Ribeiro FS, Seixas BV, Suarez-Kurtz G. Determination of lopinavir and ritonavir in blood plasma, seminal plasma, saliva and plasma ultra-filtrate by liquid chromatography/tandem mass spectrometry detection. *Rapid Commun.Mass Spectrom.* **2008**; 22 (5): 657-64.
 22. Martin J, Deslandes G, Dailly E, Renaud C, Reliquet V, Raffi F, Jolliet P. A liquid chromatography-tandem mass spectrometry assay for quantification of nevirapine, indinavir, atazanavir, amprenavir, saquinavir, ritonavir, lopinavir, efavirenz, tipranavir, darunavir and maraviroc in the plasma of patients infected with HIV. *J.Chromatogr.B Analyt.Technol.Biomed.Life Sci.* **2009**; 877 (27): 3072-82.
 23. Quaranta S, Woloch C, Paccou A, Giocanti M, Solas C, Lacarelle B. Validation of an electrospray ionization LC-MS/MS method for quantitative analysis of raltegravir, etravirine, and 9 other antiretroviral agents in human plasma samples. *Ther.Drug Monit.* **2009**; 31 (6): 695-702.
 24. Rezk NL, White NR, Jennings SH, Kashuba AD. A novel LC-ESI-MS method for the simultaneous determination of etravirine, darunavir and ritonavir in human blood plasma. *Talanta.* **2009**; 79 (5): 1372-8.
 25. Ter Heine R, Alderden-Los CG, Rosing H, Hillebrand MJ, van Gorp EC, Huitema AD, Beijnen JH. Fast and simultaneous determination of darunavir and eleven other antiretroviral drugs for therapeutic drug monitoring: method development and validation for the determination of all currently approved HIV protease inhibitors and non-nucleoside reverse transcriptase inhibitors in human plasma by liquid chromatography coupled with electrospray ionization tandem mass spectrometry. *Rapid Commun.Mass Spectrom.* **2007**; 21 (15): 2505-14.
 26. Oostendorp RL, Huitema A, Rosing H, Jansen RS, Ter Heine R, Keessen M, Beijnen JH, Schellens JHM. Coadministration of ritonavir strongly enhances the apparent oral bioavailability of docetaxel in patients with solid tumors. *Clin.Cancer Res.* **2009**; 15 (12): 4228-33.
 27. van Waterschoot RA, Lagas JS, Wagenaar E, Rosing H, Beijnen JH, Schinkel AH. Individual and combined roles of CYP3A, p-glycoprotein (MDR1/ABCB1) and MRP2 (ABCC2) in the pharmacokinetics of docetaxel. *Int.J.Cancer.* **2010**; 127 (12): 2954-64.
 28. Veltkamp SA, Rosing H, Huitema AD, Fetell MR, Nol A, Beijnen JH, Schellens JHM. Novel paclitaxel formulations for oral application: a phase I pharmacokinetic study in patients with solid tumours. *Cancer Chemother.Pharmacol.* **2007**; 60 (5): 635-42.
 29. Vainchtein LD, Thijssen B, Stokvis E, Rosing H, Schellens JHM, Beijnen JH. A simple and sensitive assay for the quantitative analysis of paclitaxel and metabolites in human plasma using liquid chromatography/tandem mass spectrometry. *Biomed.Chromatogr.* **2006**; 20 (1): 139-48.
 30. Hoetelmans RM, van Essenberg M, Profijt M, Meenhorst PL, Mulder JW, Beijnen JH. High-performance liquid chromatographic determination of ritonavir in human plasma, cerebrospinal fluid and saliva. *J.Chromatogr.B Biomed.Sci.Appl.* **1998**; 705 (1): 119-26.
 31. Stokvis E, Ouweland M, Nan LG, Kemper EM, van Tellingen O, Rosing H, Beijnen JH. A simple and sensitive assay for the quantitative analysis of paclitaxel in human and mouse plasma and brain tumor tissue using coupled liquid chromatography and tandem mass spectrometry. *J.Mass Spectrom.* **2004**; 39 (12): 1506-12.
 32. U.S. Food and Drug Administration, Center for Drug Evaluation and Research, Guidance for Industry Bioanalytical Method Validation, 2001. <http://www.fda.gov/downloads/Drugs/GuidanceComplianceRegulatoryInformation/Guidances/UCM070107.pdf>. Visited 18-2-2011.
 33. Viswanathan CT, Bansal S, Booth B, DeStefano AJ, Rose MJ, Sailstad J, Shah VP, Skelly JP, Swann PG, Weiner R. Quantitative bioanalytical methods validation and implementation: best practices for chromatographic and ligand binding assays. *Pharm.Res.* **2007**; 24 (10): 1962-73.
 34. OECD, Principles of Good Laboratory practice, 1998. [http://www.oecd.org/officialdocuments/displaydocumentpdf?cote=env/mc/chem\(98\)17&doclanguage=en](http://www.oecd.org/officialdocuments/displaydocumentpdf?cote=env/mc/chem(98)17&doclanguage=en). Visited 18-2-2011.
 35. Cech NB, Enke CG. Practical implications of some recent studies in electrospray ionization fundamentals. *Mass Spectrom.Rev.* **2001**; 20 (6): 362-87.
 36. Molto J, Barbanoj MJ, Miranda C, Blanco A, Santos JR, Negro E, Costa J, Domingo P, Clotet B, Valle M. Simultaneous population pharmacokinetic model for lopinavir and ritonavir in HIV-infected adults. *Clin.Pharmacokinet.* **2008**; 47 (10): 681-92.

Combined quantification of paclitaxel, docetaxel and ritonavir in human feces and urine using LC-MS/MS.

Jeroen J.M.A. Hendrikx
Hilde Rosing
Alfred H. Schinkel
Jan H.M. Schellens
Jos H. Beijnen

Biomed Chromatogr.
2014; 28 (2): 302-10

Abstract

A combined assay for the determination of paclitaxel, docetaxel and ritonavir in human feces and urine is described. The drugs were extracted from 200 μ L urine or 50 mg feces followed by high performance liquid chromatography analysis coupled with positive ionization electrospray tandem mass spectrometry.

The validation program included calibration model, accuracy and precision, carry-over, dilution test, specificity and selectivity, matrix effect, recovery and stability. Acceptance criteria were according to US Food and Drug Administration guidelines on bioanalytical method validation. The validated range was 0.5-500 ng/mL for paclitaxel and docetaxel and 2-2,000 ng/mL for ritonavir in urine and 2-2,000 ng/mg for paclitaxel and docetaxel and 8-8,000 ng/mg for ritonavir in feces. Inter-assay accuracy and precision were tested for all analytes at four concentration levels and were within 8.5% and less than 10.2%, respectively in both matrices. Recovery at three concentration levels was between 77 and 94% in feces samples and between 69 and 85% in urine samples. Method development, including feces homogenization and spiking blank urine samples, are discussed.

We demonstrated that each of the applied drugs could be quantified successfully in urine and feces using the described assay. The method was successfully applied for quantification of the analytes in feces and urine samples of patients.

Introduction

Paclitaxel (Taxol®) and docetaxel (Taxotere®), both taxanes, are widely used as intravenously administered anticancer agents for several types of cancer. Paclitaxel (Figure 1) is derived from the bark of *Taxus brevifolia*, whereas docetaxel is a semisynthetic derivative of a taxane isolated from the needles of *Taxus baccata*.¹ Ritonavir is a protease inhibitor, which is used at a low dose for boosting other protease inhibitors in HIV therapy.² Oral formulations of both paclitaxel and docetaxel are currently under investigation^{3,4}, wherein boosting the availability of the taxanes with a low dose of ritonavir results in clinically relevant exposure after oral administration of the taxanes.⁵⁻⁷ To further investigate this combination, assays for quantification of paclitaxel, docetaxel and ritonavir in biological matrices are needed to support clinical pharmacologic studies with these agents.

Several methods have been described for the quantification of taxanes⁸⁻¹⁹ and ritonavir²⁰⁻²⁴ in human plasma. Recently, we developed and validated an LC-MS/MS assay for simultaneous quantification of paclitaxel, docetaxel and ritonavir in human plasma.²⁵ However, for quantification of taxanes and ritonavir in other biological matrices, few methods have been described. Assays for paclitaxel in urine²⁶⁻²⁸ have most often been reported; however, none of these methods includes MS/MS detection. For docetaxel, an HPLC-UV assay has also been described for quantification in urine²⁹, while for quantification of ritonavir in urine no methods have been reported. In feces, quantification of paclitaxel has only been described for murine samples.³⁰ Quantification

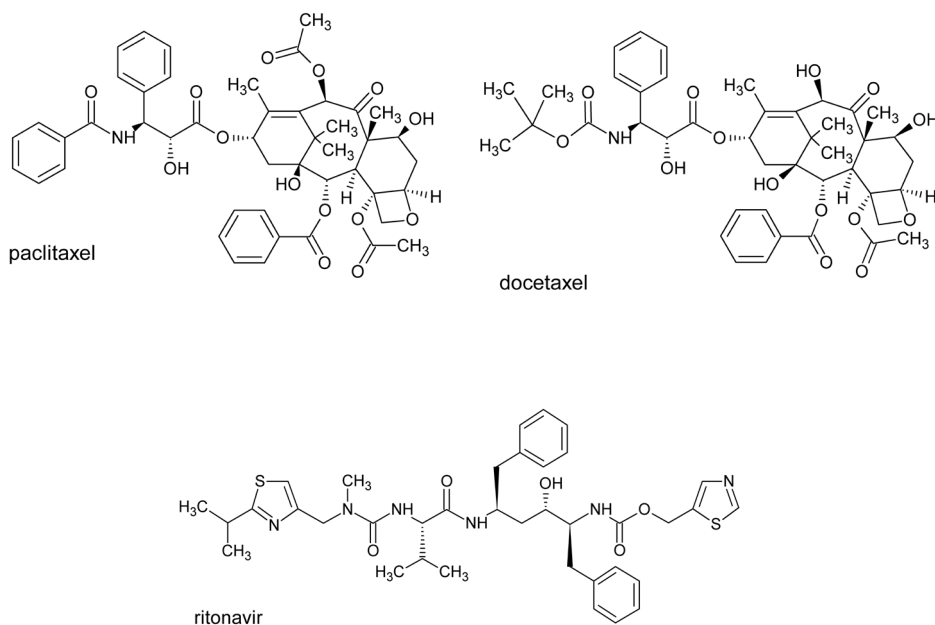


Figure 1. Structures of paclitaxel, docetaxel and ritonavir.

of docetaxel and ritonavir in feces has not been described as far as we know, although measurement of radioactivity of labeled compounds has been reported.^{31,32}

To support clinical studies, investigating the boosting effect of ritonavir on oral bioavailability of taxanes, we developed a sensitive and fast LC-MS/MS method for simultaneous detection of paclitaxel, docetaxel and ritonavir in urine and feces without loss of sensitivity or increase in run time. Quantification of the analytes in human feces gives important information that can be used to further optimize oral docetaxel and paclitaxel formulations. Thereby, the possibility to quantify paclitaxel, docetaxel and ritonavir in feces and urine can be used for the support of absorption and excretion studies to further characterize pharmacokinetic behavior of the presented analytes. Here, the development and validation of this LC-MS/MS method is described.

Material and Methods

Chemicals

Paclitaxel and docetaxel were purchased from Sequoia Research Products (Oxford, UK). Ritonavir, ¹³C₃-labelled ritonavir and D₉-labelled docetaxel were purchased from Toronto Research Chemicals (North York, ON, Canada). ¹³C₆-labelled paclitaxel was kindly provided by Pharmacia Corporation (Nerviano, Italy). Methanol (HPLC grade) was obtained from Biosolve Ltd (Amsterdam, the Netherlands), tertiary-butylmethylether (tert.-butylmethylether/ TBME, Analytical grade) and water for chromatography (LiChrosolv) were obtained from Merck (Darmstadt, Germany).

Mass spectrometric and chromatographic conditions

An API 4000 triple quadrupole MS with positive electrospray ionization (ESI; AB Sciex, Foster City, CA, USA) was coupled to an Agilent 1100 liquid chromatographic system (Agilent Technologies, Palo Alto, CA, USA). Methanol-10 mM ammonium hydroxide in water (70:30, v/v) was used as mobile phase at a flow of 0.3 mL/min. Chromatographic separation was obtained using a Zorbax Extend C₁₈ column (150 x 2.1 mm I.D., particle size 5 μm; Agilent Technologies) protected with an inline filter (0.5 μm). The column oven was set at 35 °C, while the autosampler was kept at 4 °C. A sample volume of 25 μL was injected and the injection needle was washed for 3 s with methanol after each injection. The total run time was 9 min. A switching valve was used to direct the eluent during the first 3 min of the run to waste. The multiple reaction monitoring (MRM) transitions monitored were *m/z* 854→509, 808→527 and 721→196 for paclitaxel, docetaxel and ritonavir, respectively. We previously observed that using the transition 721→196 for ritonavir instead of the transition 721→296 provided the lowest total bias across the calibration range.²⁵ ¹³C-Labelled isotopes were used as internal standards for paclitaxel and ritonavir and a D₉-labeled isotope was used as internal standard for docetaxel. Monitored MRM transitions were *m/z* 860→515, 726→296 and 817→527 respectively. For the internal standard ¹³C₃-ritonavir, the isotope ion at *m/z* 726 was selected as precursor ion to decrease interference of molecular isotopic ions of ritonavir at the mass transition *m/z* 724 of the labeled isotope.²⁵ Data were collected and processed using Analyst software version 1.5 (AB Sciex).

Preparation of stock and working solutions

Two stock solutions of each analyte from independent weighings were prepared in methanol at a concentration of 1 mg/mL. The stock solutions of the three analytes were diluted to combined working solutions with methanol. One set of working solutions was used for the preparation of calibration standards, while the other set was used for the preparation of quality control (QC) samples. For the internal standards $^{13}\text{C}_3$ -ritonavir, D_9 -docetaxel and $^{13}\text{C}_6$ -paclitaxel stock solutions of respectively 0.5, 1.0 and 0.1 mg/mL were prepared in methanol. The three internal standards were diluted to one combined internal standard working solution containing 500, 40 and 200 ng/mL of $^{13}\text{C}_3$ -ritonavir, D_9 -docetaxel and $^{13}\text{C}_6$ -paclitaxel, respectively. All solutions were stored at $-20\text{ }^\circ\text{C}$.

Preparation of Calibration standards and Quality Controls

Blank human feces was homogenized in water (1:3, m/v) using a Ultra-Turrax homogenizer (IKA, Stauen Germany). Calibrations standards were prepared by diluting a fixed amount of working solution containing each analyte in blank urine and in blank human feces homogenate. The calibration standards contained the analytes in concentrations of 0.5; 1; 5; 10; 50; 100; 250 and 500 ng/mL (paclitaxel/docetaxel) and 2; 4; 20; 40; 200; 400; 1,000 and 2,000 ng/mL (ritonavir) in urine and 2; 4; 20; 40; 200; 1,000 and 2,000 ng/g (paclitaxel/docetaxel) and 8; 16; 80; 160; 800; 4,000 and 8,000 ng/g (ritonavir) in feces. In a similar way, QC samples were prepared from another set of working solutions. The QCs in urine contained the taxanes in concentrations of 0.5; 1.5; 100 and 400 ng/mL and ritonavir in concentrations of 2; 6; 400 and 1,600 ng/mL. In feces, concentrations of the taxanes were 2; 6; 400 and 1,600 ng/g and concentrations of ritonavir 8; 24; 1,600 and 6,400 ng/g. Samples were stored at $-20\text{ }^\circ\text{C}$ in 2.0 mL polypropylene tubes (Eppendorf, Merck) in aliquots of 200 μL .

Sample pre-treatment

To a 200 μL sample, 20 μL internal standard working solution was added and the sample was vortex-mixed for 10 s. Blank samples were spiked with 20 μL of methanol instead of internal standard working solution. After mixing, 1.0 mL of tertiary-butylmethylether was added and the sample was mixed again for 10 s. Samples were successively shaken automatically for 10 min at 1,250 rpm (L46, Labinco, Breda, The Netherlands) and centrifuged for 5 min at 23,000 g (5403 Eppendorf, Netheler Hinz GmbH, Hamburg, Germany). The aqueous layer was frozen in a bath of ethanol and dry ice and the organic layer was transferred into a clean 1.5 mL tube. The sample was dried under a gentle stream of nitrogen at $40\text{ }^\circ\text{C}$. The residue was reconstituted in 100 μL methanol-water (1:1, v/v), vortex-mixed for 10 s and centrifuged for 3 min at 23,000 g . The supernatant was transferred to a glass autosampler vial with insert and 25 μL was injected onto the LC-MS/MS system.

Validation

For both human urine and human feces, a full validation program was executed according to the US Food and Drug Administration guidelines³³ on bioanalytical method validation and to the guidelines of the third American Association of Pharmaceutical

Scientists (AAPS/FDA)/US Food and Drug Administration bioanalytical workshop.³⁴ The validation program included calibration model, accuracy and precision, carry-over, dilution test, specificity and selectivity, matrix effect, recovery and stability. Stability testing included freeze (-20° C)/thaw stability in the biomatrix, short term stability at ambient temperature, long-term stability at -20° C, stability of the processed sample (dried extract and final extract) and re-injection stability. Stability in methanol for stock and working solutions was previously tested.²⁵

Clinical samples

At our institute, phase I studies are currently ongoing to investigate the oral co-administration of taxanes and ritonavir. In these studies, oral paclitaxel or docetaxel is co-administered with ritonavir.^{6,35} The Medical Ethics Committee of the Netherlands Cancer Institute approved collection of feces and urine samples from a limited number of patients in these studies. Written informed consent for additional collection of feces and urine was obtained from all patients prior to sample collection.

Samples were collected and stored at -20° C. Within 24 hours after collection, samples arrived at the laboratory. After arrival, feces was homogenized in water (1:3, m/v) as described in section 2.4. Feces homogenates and urine were diluted 10- and 100-fold and 200 µL aliquots were stored at -20° C together with aliquots of 200 µL undiluted feces homogenate and urine. At the day of analysis, samples were thawed and processed prior to quantification.

Results and discussion

Method Development

Column selection

Previously, we showed that an alkaline mobile phase results in increased signal-to-noise ratios compared with an acid mobile phase.²⁵ According to specifications of the manufacturer, the selected Zorbax Extend C₁₈ column can be used up to pH 11.5. Since carry-over and noise at the retention time of the analytes were minimum for this column, it was selected for further development of the assay.

Sample pre-treatment

Since the body excretes most of its waste via feces or urine, these matrices contain potential interfering compounds. To obtain a clean sample for injection, liquid-liquid extraction or solid phase extraction is preferable over protein precipitation, although in general, liquid-liquid extraction is less expensive compared to solid-phase extraction.³⁶ To reduce costs and since we have most experience with liquid-liquid extraction, we selected this extraction procedure as sample pre-treatment method to clean up the feces and urine samples. Recovery after liquid-liquid extraction was tested during validation (Section Matrix factor and recovery) and were >76% and >69% in feces and urine, respectively.

Spiking feces homogenate

Quantitative analysis in feces is hard to perform since spiked samples do not always mimic patient samples. Dilution prior to homogenization of the feces sample reduces this problem.³⁷ Therefore, during method development we diluted and homogenized blank feces samples prior to spiking the sample with the analytes. It was noticed that quantification of the analytes in feces homogenate sample was influenced by storage at -20°C. After storage for one day at -20°C in a volume of 5 mL and subsequent thawing, re-homogenization and taking 200 µL aliquots, analytes concentrations increased up to 33%, compared with the nominal concentrations with a precision <7.7%. Interestingly, taking 200 µL aliquots prior to storage for one day at -20°C did not result in increased analyte concentrations. Apparently, thawing a homogenized sample after storage at -20°C results in nonuniform distribution of the analytes in the sample. Since feces samples were homogenated with water, this might be related to the lipophilicity of the analytes. It is hypothesized that during storage, the lipophilic drugs might bind to fecal components to avoid the aqueous environment and this could result in nonuniform distribution. During validation of the assay, feces homogenate samples were spiked and stored in aliquots of 200 µL. Spiked samples above the upper limit of quantification (ULOQ) were diluted before storage and 200 µL aliquots were taken subsequently. Before analysis, these aliquots were thawed.

These results indicate that quantification of docetaxel, paclitaxel, ritonavir -and maybe also other drugs- in feces samples of patients might be biased when homogenized samples are stored in large portions and when aliquots for quantification are taken after storage. Therefore, we advise taking aliquots for quantification immediately after homogenization of samples, prior to storage. After storage, sample pre-treatment should be performed in the same tubes as used for storage.

Spiking urine samples

We observed that quantification of the analytes in urine samples after spiking of these compounds in a small volume resulted in underestimation of the concentration. During method development, urine QC samples were prepared by spiking the analytes in a volume of 1.0 mL of control human urine with 20 µL working solution. Spiked samples were mixed and an aliquot of 200 µL was taken and processed. Calculated concentrations of all analytes decreased to 60-80% of the nominal concentration, while precision was less than 6%. The accuracy was increased to 80-90% of the nominal concentration when 5.0 mL of control human urine was spiked and an aliquot of 200 µL was taken and processed. However, the best results were obtained when a total volume of 200 µL of blank human urine was spiked and processed in the same tube. This resulted in deviations within +/- 15% of the nominal concentration.

As paclitaxel, docetaxel and ritonavir all have a low solubility in aqueous solutions, it is hypothesized that the analytes stick to the wall of the tubes resulting in underestimation of the spiked samples. When samples were spiked as 200 µL urine aliquots and are processed in the same tube, the total spiked amount of the analytes was recovered. After mixing the spiked sample with tertiary-butylmethylether, the analytes detached from the wall of the tube and dissolved in the organic solvent. Based on these findings, urine samples were spiked and stored in aliquots of 200 µL. Spiked samples above the

ULOQ were diluted in one step to a total volume of 200 μL in a 2 mL tube and stored at $-20\text{ }^{\circ}\text{C}$ before processing. This procedure resulted in an unbiased quantification of the analytes.

When large volumes ($>5.0\text{ mL}$) of urine are spiked, accurate quantification can be performed. Urine samples taken during clinical studies are usually large, therefore a 200 μL aliquot out of these samples will not result in biased quantification. However, when portions of 5.0 mL or less are stored, no homogenous sample can be taken, resulting in underestimation of the analyte concentration. Therefore, it is advised to take 200 μL aliquots for quantification immediately after receipt of the total urine portions. After storage, sample pre-treatment should be performed in the same tubes as used for storage. These observations indicate that adsorption to the container wall takes place when analytes are spiked to urine, as long as the contact area is high in comparison to the total volume.

Validation of the method

Calibration model

Calibration standards in the range 0.5 to 500 ng/mL (paclitaxel and docetaxel) and 2 to 2,000 ng/mL (ritonavir) were prepared urine. In feces, calibration standards in the range 2 to 2,000 ng/g (paclitaxel and docetaxel) and 8 to 8,000 ng/g (ritonavir) were prepared. All calibration standards (8) with duplicate points at each concentration were analyzed in three independent analytical runs. Calibration curves per matrix were fitted by quadratic regression of the peak area ratio with the internal standard versus the concentration with $1/x^2$ (the reciprocal of the squared concentration) as the weighting factor. The calibration model was evaluated by means of the back-calculated concentrations of the calibration standards: these values should be within $\pm 15\%$ of the actual concentration, except for the lower limit of quantification (LLOQ) where it should be within $\pm 20\%$ of the actual concentration.³³ At least four out of six nonzero standards (including at least one calibration standard at the LLOQ and ULOQ) should meet these criteria. When calibration data was fitted by quadratic regression, correlation coefficients (r^2) of 0.9961 or better were obtained for all analytes in both matrices. For all analytes, the deviations of measured concentrations of the included calibration standards in feces from nominal concentration were between -9.1 and 8.7% with coefficient of variation (CV) values of less than 9.5% . In urine, the deviations of measured concentrations from nominal concentration were between -4.2 and 4.2% with CV values of less than 8.1% for all analytes. For all analytes, the calibration data fulfilled the required criteria. Typical MRM chromatograms of blank samples and the analytes at LLOQ-level in human feces are presented in Figure 2. Chromatograms of these samples in urine were similar.

Accuracy and precision

Accuracy and precision were investigated at four different concentration levels and five replicates of each level in three independent analytical runs. The accuracy was determined as percentage difference between the mean concentration and the nominal concentration. The %CV was used to report the precisions. The intra- and inter-assay accuracies and precisions should be within $\pm 20\%$ and less than 20% , respectively, for

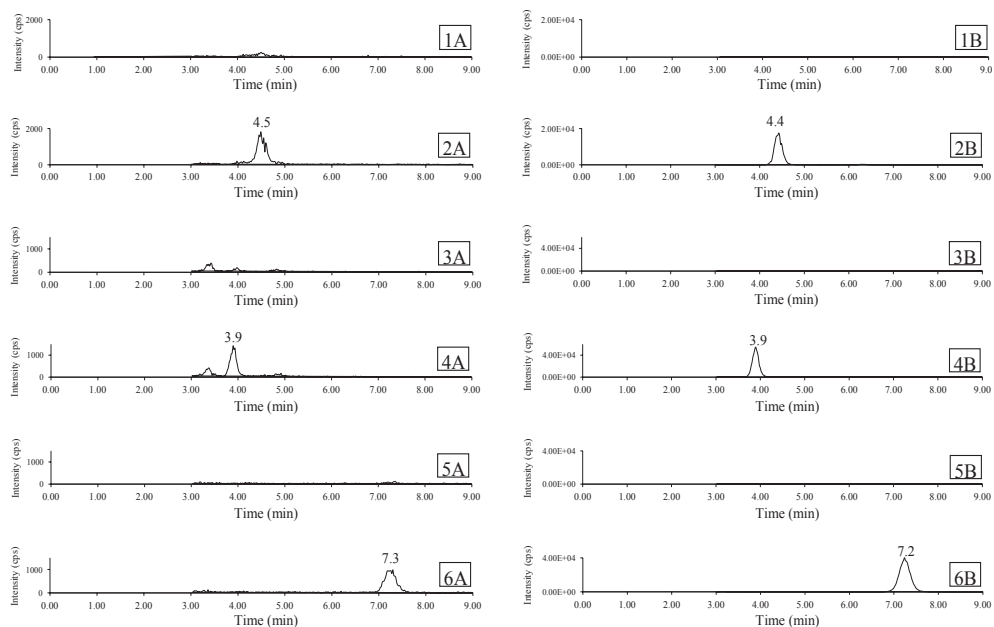


Figure 2. Typical MRM chromatograms of the analytes in a blank feces sample and at LLOQ level (2 ng/g and 8 ng/g for the taxanes and ritonavir, respectively). Panels show the response in a blank feces sample and in a calibration sample at LLOQ level at the transition of docetaxel (1A and 2A, respectively), D₉-labeled docetaxel (1B and 2B), paclitaxel (3A and 4A), ¹³C₆-labeled paclitaxel (3B and 4B), ritonavir (5A and 6A) and ¹³C₃-labeled ritonavir (5B and 6B).

the LLOQ concentration and within $\pm 15\%$ and less than 15%, respectively, for other concentrations. In feces, intra-assay accuracy at each concentration level was within $\pm 10.4\%$, $\pm 12.1\%$ and $\pm 8.3\%$ for paclitaxel, docetaxel and ritonavir, respectively in all runs. Intra-assay precisions were less than 11.5%, 7.5% and 5.2%, respectively. In urine, intra-assay accuracy and precision were in a similar range. Inter-assay performance data of paclitaxel, docetaxel and ritonavir are presented in Table 1. For all the analytes, all intra- and inter-assay accuracies and precisions fulfilled the required criteria.^{33;34}

Carry-over

In three independent runs, two processed blank matrix samples were injected subsequently after injection of an ULOQ sample. The response in the first blank matrix at the retention time of the analytes or internal standards should be less than 20% of the mean response of a LLOQ sample for the analytes and less than 5% of the mean response for the internal standards. In both matrices, the response in the first blank matrix was less than these criteria (Table 2). Therefore, the carry-over test was found to be acceptable.

Dilution test

To assess the reliability of the method at concentration levels above the ULOQ (500/2,000 ng/mL; taxanes/ritonavir in urine and 2,000/8,000 ng/g; taxanes/ritonavir in feces), an intra-assay accuracy and precision test was executed. A sample at a concentration level 4-fold higher than ULOQ was diluted 2, 10 and 100 times with

blank matrix. All urine samples were diluted to a total volume of 200 μL and processed in the same tube. Feces homogenate samples were diluted to a total volume of 1 mL and 200 μL was processed. Samples were diluted and processed in 5-fold. Accuracy and precision were determined as described for QC samples and should be within $\pm 15\%$ and less than 15%, respectively.^{33;34} For all dilution factors in both matrices, accuracies and precisions fulfilled these acceptance criteria.

Specificity and selectivity

Specificity and selectivity were assessed using 6 different batches of control human feces and urine. Blank (without the internal standards) and spiked samples (with paclitaxel, docetaxel, ritonavir and the internal standards) at the LLOQ concentration

Table 1. Assay performance for paclitaxel, docetaxel and ritonavir in feces and urine.

Matrix	Compound	Nominal conc.	Mean measured conc.	Inter-assay bias (%)	Inter-assay precision (%)
Feces	Paclitaxel	2.06	2.12	3.1	8.4
		6.16	6.12	-0.5	4.1
		412	420	2.0	4.0
		1650	1740	5.6	5.7
	Docetaxel	1.97	1.93	-1.9	6.1
		5.92	5.84	-1.4	5.9
		394	398	1.0	4.4
		1580	1640	3.9	7.3
	Ritonavir	7.88	7.76	-1.5	2.9
		23.6	23.4	-1.0	3.0
		1580	1620	2.7	3.9
		6280	6580	4.8	4.9
Urine	Paclitaxel	0.514	0.491	-4.4	4.8
		1.54	1.51	-2.1	5.9
		103	102	-0.6	4.5
		412	428	3.9	6.2
	Docetaxel	0.492	0.450	-8.5	9.0
		1.48	1.39	-0.4	7.3
		98.4	98.3	-0.1	7.6
		394	402	2.1	10.2
	Ritonavir	1.97	1.88	-4.8	7.7
		5.90	5.84	-1.1	8.3
		394	390	-1.0	5.9
		1570	1559	-0.7	8.0

Abbreviation: conc.: concentration.

Values based on 15 replicates. Concentrations in feces are in ng/g and concentrations in urine are in ng/mL.

Table 2. Validated parameters for paclitaxel, docetaxel and ritonavir in feces and urine. Accuracy and precision values are tabulated in Table 1.

Parameter	Feces			Urine		
	Paclitaxel	Docetaxel	Ritonavir	Paclitaxel	Docetaxel	Ritonavir
Calibration Model	Quadratic weighted $1/x^2$			Quadratic weighted $1/x^2$		
Calibration range	2-2,000 ng/g	2-2,000 ng/g	8-8,000 ng/g	0.5-500 ng/mL	0.5-500 ng/mL	2-2,000 ng/mL
Validated dilution factors	2, 10 and 100 times			2, 10 and 100 times		
Signal to noise ratio at LLOQ level	≥5 for all analytes			≥5 for all analytes		
Carry over in first blank (calculated against LLOQ)	≤ 12.4%	≤ 19.5%	≤ 13.0%	≤ 13.2%	≤ 16.4%	≤ 18.0%
Specificity and Selectivity						
Endogenous interferences (n=6 batches) (calculated against LLOQ)	≤ 8.6%	≤ 14.1% ¹⁾	≤ 5.4%	≤ 2.4%	≤ 4.5%	≤ 4.5%
Cross analyte/IS interferences (calculated against LLOQ)	≤ 13.9%	≤ 12.3%	≤ 6.8%	≤ 3.7%	≤ 5.9%	≤ 13.5%
Matrix factor (n=3)						
QC low level	0.93	0.87	0.90	0.94	0.92	0.89
QC mid level	1.01	1.02	0.96	0.95	0.99	0.86
QC high level	1.00	1.00	0.92	0.95	0.91	0.83
Extraction recovery (n=3)						
QC low level	82.7%	82.5%	88.9%	69.4%	79.3%	74.9%
QC mid level	84.0%	87.3%	94.0%	78.0%	83.2%	81.0%
QC high level	93.0%	87.5%	76.0%	78.0%	83.4%	85.0%
Stability						
Freeze/thaw stability	At least 3 (-20°C/ambient temperature) cycles			At least 3 (-20°C/ambient temperature) cycles		
Long-term stability in matrix	At least 1 months at -20°C			At least 1 month at -20°C		
Short-term stability in matrix	At least 18 hours at ambient temperature			At most 17 hours at ambient temperature		
Dried extract stability	At least 7 days at 2-8°C			At least 9 days at 2-8°C		
Processed sample stability	At least 7 days at 2-8°C			At least 9 days at 2-8°C		
Re-injection stability	At least 7 days at 2-8°C			At least 7 days at 2-8°C		

Abbreviation: LLOQ: Lower Limit Of Quantification; QC: QC: quality control.

¹⁾ Endogenous interference in one batch was 27.8%, but accuracy at LLOQ level in that specific batch was 6.1%; see also section *Specificity and selectivity*.

level were prepared. The samples were prepared to determine whether endogenous compounds interfere at the retention time and at the mass transitions chosen for the analytes and internal standards. Samples were processed according to the described procedures and analyzed. Interferences co-eluting with the analytes or internal standards should not exceed 20% of the peak area of the analytes at LLOQ or 5% of the internal standard areas. Deviations of the nominal concentrations should be within $\pm 20\%$. In urine, no endogenous interferences exceeding 4.5% of the area of the analytes at LLOQ level were observed (Table 2). No endogenous peaks co-eluting with the internal standards were observed. Therefore the validation test in urine was accepted for all analytes.

In feces, interferences at the retention time of the analytes were less than 14.1% of the area of the analytes and less than 0.9% of the area of the internal standards at LLOQ level. In one batch of feces, an endogenous interference of 27.8% at the transition of docetaxel was observed. As the deviation of the nominal concentration of docetaxel at LLOQ level in that specific batch was 6.1%, the validation test in feces was accepted not only for paclitaxel and ritonavir, but also for docetaxel.

Cross-analyte/internal standard interferences were assessed by analyzing samples containing only one of the analytes at ULOQ level or one of the internal standards in control matrix and by monitoring all transitions. Interferences in processed samples should be less than 20% of the peak area of the analytes at the LLOQ or 5% of the internal standard areas. During cross-analyte interference tests, the interferences of the internal standards at the retention times of paclitaxel, docetaxel and ritonavir in feces and urine samples were less than 15.0% of the area of their LLOQ standards (Table 2). Interferences of the analytes at the retention times of $^{13}\text{C}_6$ -paclitaxel and D_9 -docetaxel were less than 5% of their area in feces and urine samples. Interference of ritonavir at the retention time of $^{13}\text{C}_3$ -ritonavir was 3.5% in urine and 6.2% in feces. Although the interference of ritonavir at ULOQ level in feces at the retention time of $^{13}\text{C}_3$ -ritonavir was not below 5%, it was reproducible in multiple samples ($n=4$). The interference of ritonavir at the retention time of its labeled internal standard could theoretically result in increased internal standard area and thereby result in decreased analyte/internal standard area ratios. However, the mean area of $^{13}\text{C}_3$ -ritonavir in feces samples containing ritonavir and $^{13}\text{C}_3$ -ritonavir was -9.3% compared with the area of a sample containing only $^{13}\text{C}_3$ -ritonavir at the same concentration level. It was concluded that the interference at the retention time of the internal standard of ritonavir did not affect the quantification of ritonavir and therefore it was considered acceptable. Overall, the cross analyte/internal standard interferences were considered acceptable for all analytes and internal standards in both matrices.

Matrix factor and Recovery

The signals of the analytes in processed QC samples at low, mid and high concentration levels were compared to the signals of the same concentration levels in methanol-water (1:1, v/v) for determination of the matrix factors. Responses were corrected for the internal standard area. The variability in matrix factor, as measured by the CV should be less than 15%. The matrix factor in feces, determined as the area ratio with and without matrix ions present, was between 0.87 and 1.02 for all analytes at all concentration

levels, with %CV values less than 10% (see table 2). In urine, the matrix factor was between 0.83 and 0.99 with %CV values less than 9.4%. Overall, the results (matrix factor around 1) indicate that the stable-isotopically labeled internal standards of all analytes are most effective minimizing the influence of matrix effects.

The recovery after liquid-liquid extraction was calculated by comparing the absolute areas in a processed QC sample to the areas measured after spiking a blank processed sample after liquid-liquid extraction. The recovery was determined for all analytes at three concentration levels. Recoveries in feces were between 76 and 94% and between 69 and 85% in urine (Table 2).

Stability

Stock solutions in methanol are stable for at least 12, 21 and 36 months for paclitaxel, docetaxel and ritonavir, respectively, when stored at nominally -20 °C.²⁵ Stability of the analytes in feces homogenate and urine was evaluated at low and high level after storage at ambient temperature and at -20° C and during three freeze/thaw cycles. Stability at low and high level was also evaluated in the dried extract and the processed sample after storage at 2-8 °C. Re-injection stability of a set of calibration standards and QC samples at low, mid and high level was evaluated after storage at 2-8 °C for 7 days. The analytes were considered stable in the matrix when 85-115% of the initial measured concentration was found.

It was observed that all analytes were stable in feces homogenate and urine during three freeze/thaw cycles and when kept for 17 h at ambient temperature (Table 2). At nominally -20 °C, all analytes were stable in urine and feces homogenate after storage up to 1 month. Dried extract and processed samples of urine were stable after storage at nominally 2-8 °C for 9 days. Samples of feces homogenate were stable after storage at nominally 2-8 °C for 7 days. After re-injection of processed samples after storage at nominally 2-8 °C for 7 days, the bias was within $\pm 15\%$ of the nominal concentration for all the analytes in both urine and feces homogenate. Therefore it is concluded that the samples can be re-injected within 7 days when kept at nominally 2-8 °C.

Application of the method

The validated assay is currently in use to support clinical studies. In these studies patients receive either paclitaxel or docetaxel in combination with ritonavir. In Figure 3 the excretion of docetaxel, paclitaxel and ritonavir via feces and urine is shown.

Docetaxel excretion was quantified in samples of two patients. One patient received orally 60 mg docetaxel and 200 mg ritonavir and urine was collected during the first 24 h after administration. The second patient received orally 40 mg docetaxel and 200 mg ritonavir and feces was collected during the first 24 h after administration. A pre-dose urine or feces sample was collected prior to administration. Almost 50% of the docetaxel dose and 11% of the ritonavir dose was recovered as parent drug in feces. In urine, recovery of the parent drugs was much lower. The high recovery of docetaxel during the first 8 h is probably caused by incomplete absorption of docetaxel in the gastrointestinal tract.

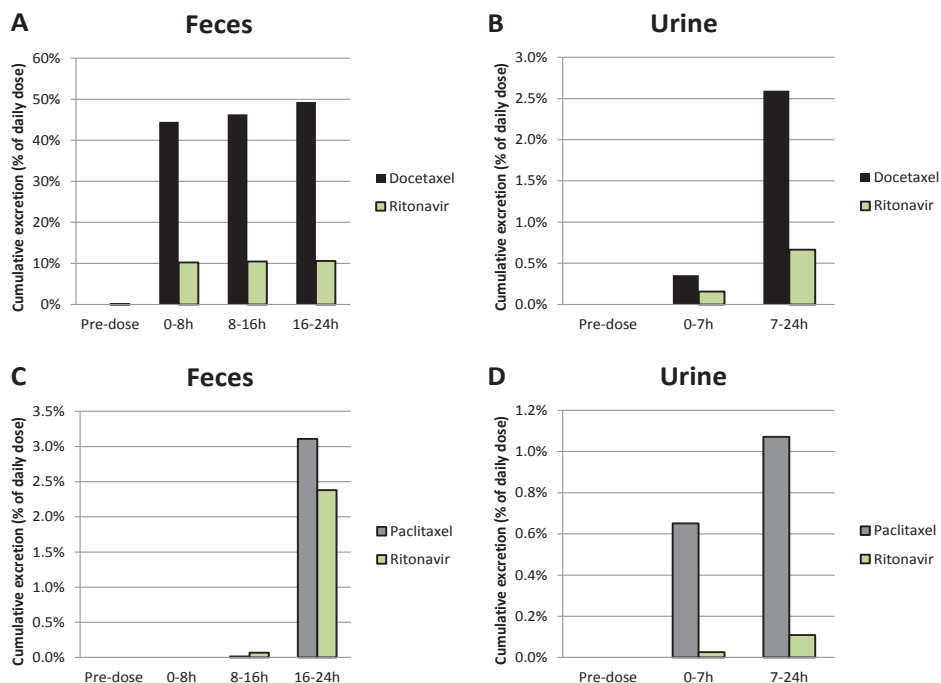


Figure 3. Cumulative excretion as percentage of daily dose of docetaxel and ritonavir in feces (A) after single oral co-administration of 40 mg docetaxel combined with 200 mg ritonavir to a patient, cumulative excretion in urine (B) after single oral co-administration of 60 mg docetaxel combined with 200 mg ritonavir to a patient, and cumulative excretion in feces (C) and urine (D) after oral bi-daily co-administration of 20 mg paclitaxel combined with 100 mg ritonavir to a patient.

Paclitaxel excretion was quantified in samples of one patient. To this patient, 20 mg paclitaxel and 100 mg ritonavir were coadministered orally twice daily. Urine and feces were collected during the first 24 hours after the first administration. The second administration was seven hours after the first administration. Prior to the first administration, pre-dose samples were collected. Paclitaxel recovery in feces was 3.1% of the daily administered dose during the first 24 h after administration. In the same period, 1.1% of the daily administered dose of paclitaxel was recovered in urine.

This is the first time that excretion of docetaxel and paclitaxel after oral administration has been described. Since we collected feces during the first 24 h we showed that at least 50% of the docetaxel dose and over 95% of the paclitaxel dose is absorbed in the intestinal lumen. This information can be used to further optimize oral docetaxel and paclitaxel formulations. The absorption of ritonavir (over 89% of the administered dose) is in line with previously reported -almost complete- absorption after oral administration of 600 mg ^{14}C -labeled ritonavir.³¹

Conclusion

The development and validation of a combined assay for the quantification of paclitaxel, docetaxel and ritonavir in feces and urine is described. In urine, the validated range for the taxanes was 0.5-500 ng/mL and for ritonavir was 2-2,000 ng/mL using 200 μ L urine and in feces the validated range for the taxanes was 2-2,000 ng/g and for ritonavir was 8-8,000 ng/g using 50 mg feces. The assay was validated according to US Food and Drug Administration guidelines and has been successfully applied in clinical studies. During development, it was observed that one should be careful when storing feces homogenate samples and when diluting urine samples for the quantification of drugs that are poorly soluble in water. Despite feces and urine being difficult matrices, we demonstrated that each of the applied drugs in this assay could be quantified successfully in these matrices. This assay can be used to test absorption and excretion of orally administered taxane and ritonavir formulations. This assay is the first reported assay for quantification of each of the unlabeled analytes in human feces. Other assays are reported for quantification of docetaxel²⁹ or paclitaxel in urine^{26,27,38}, but the presented assay has a shorter runtime and a 10-fold lower LLOQ than the previously reported assays.

References

1. Vaishampayan U, Parchment RE, Jasti BR, Hussain M. Taxanes: an overview of the pharmacokinetics and pharmacodynamics. *Urology* **1999**; 54 (6A Suppl): 22-9.
2. Hull MW, Montaner JS. Ritonavir-boosted protease inhibitors in HIV therapy. *Ann.Med.* **2011**; 43 (5): 375-88.
3. Koolen SL, Beijnen JH, Schellens JHM. Intravenous-to-oral switch in anticancer chemotherapy: a focus on docetaxel and paclitaxel. *Clin.Pharmacol.Ther.* **2010**; 87 (1): 126-9.
4. Malingre MM, Beijnen JH, Schellens JH. Oral delivery of taxanes. *Invest New Drugs* **2001**; 19 (2): 155-62.
5. Koolen SL, Oostendorp RL, Beijnen JH, Schellens JHM, Huitema AD. Population pharmacokinetics of intravenously and orally administered docetaxel with or without co-administration of ritonavir in patients with advanced cancer. *Br.J.Clin. Pharmacol.* **2010**; 69 (5): 465-74.
6. Koolen, S. L. Intravenous-to-oral switch in anticancer chemotherapy. Focus on taxanes and gemcitabine. [Dissertation]. 105-115. 16-2-2011. Utrecht University. 16-2-2011.
7. Oostendorp RL, Huitema A, Rosing H, Jansen RS, Ter Heine R, Keessen M, Beijnen JH, Schellens JHM. Coadministration of ritonavir strongly enhances the apparent oral bioavailability of docetaxel in patients with solid tumors. *Clin.Cancer Res.* **2009**; 15 (12): 4228-33.
8. Alexander MS, Kiser MM, Culley T, Kern JR, Dolan JW, McChesney JD, Zygmunt J, Bannister SJ. Measurement of paclitaxel in biological matrices: high-throughput liquid chromatographic-tandem mass spectrometric quantification of paclitaxel and metabolites in human and dog plasma. *J.Chromatogr.B Analyt. Technol.Biomed.Life Sci.* **2003**; 785 (2): 253-61.
9. Gardner ER, Dahut W, Figg WD. Quantitative determination of total and unbound paclitaxel in human plasma following Abraxane treatment. *J.Chromatogr.B Analyt. Technol.Biomed.Life Sci.* **2008**; 862 (1-2): 213-8.
10. Green H, Vretenbrant K, Norlander B, Peterson C. Measurement of paclitaxel and its metabolites in human plasma using liquid chromatography/ion trap mass spectrometry with a sonic spray ionization interface. *Rapid Commun.Mass Spectrom.* **2006**; 20 (14): 2183-9.
11. Grozav AG, Hutson TE, Zhou X, Bukowski RM, Ganapathi R, Xu Y. Rapid analysis of docetaxel in human plasma by tandem mass spectrometry with on-line sample extraction. *J.Pharm.Biomed.Anal.* **2004**; 36 (1): 125-31.
12. Guitton J, Cohen S, Tranchand B, Vignal B, Droz JP, Guillaumont M, Manchon M, Freyer G. Quantification of docetaxel and its main metabolites in human plasma by liquid chromatography/tandem mass spectrometry. *Rapid Commun.Mass Spectrom.* **2005**; 19 (17): 2419-26.
13. Kuppens IE, van Maanen MJ, Rosing H, Schellens JHM, Beijnen JH. Quantitative analysis of docetaxel in human plasma using liquid chromatography coupled with tandem mass spectrometry. *Biomed.Chromatogr.* **2005**; 19 (5): 355-61.
14. Mortier KA, Renard V, Verstraete AG, Van Gussem A, Van Belle S, Lambert WE. Development and validation of a liquid chromatography-tandem mass spectrometry assay for the quantification of docetaxel and paclitaxel in human plasma and oral fluid. *Anal.Chem.* **2005**; 77 (14): 4677-83.

15. Mortier KA, Lambert WE. Determination of unbound docetaxel and paclitaxel in plasma by ultrafiltration and liquid chromatography-tandem mass spectrometry. *J.Chromatogr.A* **2006**; 1108 (2): 195-201.
16. Parise RA, Ramanathan RK, Zamboni WC, Egorin MJ. Sensitive liquid chromatography-mass spectrometry assay for quantitation of docetaxel and paclitaxel in human plasma. *J.Chromatogr.B Analyt.Technol.Biomed.Life Sci.* **2003**; 783 (1): 231-6.
17. Sottani C, Minoia C, D'Incalci M, Paganini M, Zucchetti M. High-performance liquid chromatography tandem mass spectrometry procedure with automated solid phase extraction sample preparation for the quantitative determination of paclitaxel (Taxol) in human plasma. *Rapid Commun.Mass Spectrom.* **1998**; 12 (5): 251-5.
18. Wang LZ, Goh BC, Grigg ME, Lee SC, Khoo YM, Lee HS. A rapid and sensitive liquid chromatography/tandem mass spectrometry method for determination of docetaxel in human plasma. *Rapid Commun.Mass Spectrom.* **2003**; 17 (14): 1548-52.
19. Zhang W, Dutschman GE, Li X, Cheng YC. Quantitation of paclitaxel and its two major metabolites using a liquid chromatography-electrospray ionization tandem mass spectrometry. *J.Chromatogr.B Analyt.Technol.Biomed.Life Sci.* **2011**; 879 (22): 2018-22.
20. Estrela RC, Ribeiro FS, Seixas BV, Suarez-Kurtz G. Determination of lopinavir and ritonavir in blood plasma, seminal plasma, saliva and plasma ultra-filtrate by liquid chromatography/tandem mass spectrometry detection. *Rapid Commun.Mass Spectrom.* **2008**; 22 (5): 657-64.
21. Martin J, Deslandes G, Dailly E, Renaud C, Reliquet V, Raffi F, Jolliet P. A liquid chromatography-tandem mass spectrometry assay for quantification of nevirapine, indinavir, atazanavir, amprenavir, saquinavir, ritonavir, lopinavir, efavirenz, tipranavir, darunavir and maraviroc in the plasma of patients infected with HIV. *J.Chromatogr.B Analyt.Technol.Biomed.Life Sci.* **2009**; 877 (27): 3072-82.
22. Quaranta S, Woloch C, Paccou A, Giocanti M, Solas C, Lacarelle B. Validation of an electrospray ionization LC-MS/MS method for quantitative analysis of raltegravir, etravirine, and 9 other antiretroviral agents in human plasma samples. *Ther.Drug Monit.* **2009**; 31 (6): 695-702.
23. Rezk NL, White NR, Jennings SH, Kashuba AD. A novel LC-ESI-MS method for the simultaneous determination of etravirine, darunavir and ritonavir in human blood plasma. *Talanta.* **2009**; 79 (5): 1372-8.
24. Ter Heine R, Alderden-Los CG, Rosing H, Hillebrand MJ, van Gorp EC, Huitema AD, Beijnen JH. Fast and simultaneous determination of darunavir and eleven other antiretroviral drugs for therapeutic drug monitoring: method development and validation for the determination of all currently approved HIV protease inhibitors and non-nucleoside reverse transcriptase inhibitors in human plasma by liquid chromatography coupled with electrospray ionization tandem mass spectrometry. *Rapid Commun.Mass Spectrom.* **2007**; 21 (15): 2505-14.
25. Hendriks JJ, Hillebrand MJ, Thijssen B, Rosing H, Schinkel AH, Schellens JH, Beijnen JH. A sensitive combined assay for the quantification of paclitaxel, docetaxel and ritonavir in human plasma using liquid chromatography coupled with tandem mass spectrometry. *J.Chromatogr.B Analyt.Technol.Biomed.Life Sci.* **2011**; 879 (28): 2984-90.
26. Huizang MT, Rosing H, Koopman F, Keung AC, Pinedo HM, Beijnen JH. High-performance liquid chromatographic procedures for the quantitative determination of paclitaxel (Taxol) in human urine. *J.Chromatogr.B Biomed.Appl.* **1995**; 664 (2): 373-82.
27. Martin N, Catalin J, Blachon MF, Durand A. Assay of paclitaxel (Taxol) in plasma and urine by high-performance liquid chromatography. *J.Chromatogr.B Biomed.Sci.Appl.* **1998**; 709 (2): 281-8.
28. Rodriguez J, Castaneda G, Contento AM, Munoz L. Direct and fast determination of paclitaxel, morphine and codeine in urine by micellar electrokinetic chromatography. *J.Chromatogr.A.* **2012**; 1231:66-72. Epub;2012 Feb 8): 66-72.
29. Garg MB, Ackland SP. Simple and sensitive high-performance liquid chromatography method for the determination of docetaxel in human plasma or urine. *J.Chromatogr.B Biomed.Sci.Appl.* **2000**; 748 (2): 383-8.
30. Sparreboom A, van Tellingen O, Nooijen WJ, Beijnen JH. Determination of paclitaxel and metabolites in mouse plasma, tissues, urine and faeces by semi-automated reversed-phase high-performance liquid chromatography. *J.Chromatogr.B Biomed.Appl.* **1995**; 664 (2): 383-91.
31. Denissen JF, Grabowski BA, Johnson MK, Buko AM, Kempf DJ, Thomas SB, Surber BW. Metabolism and disposition of the HIV-1 protease inhibitor ritonavir (ABT-538) in rats, dogs, and humans. *Drug Metab Dispos.* **1997**; 25 (4): 489-501.
32. Engels FK, Buijs D, Loos WJ, Verweij J, Bakker WH, Krenning EP. Quantification of [3H]docetaxel in feces and urine: development and validation of a combustion method. *Anticancer Drugs.* **2006**; 17 (1): 63-7.
33. U.S.Food and Drug Administration. Center for Drug Evaluation and Research, Guidance for Industry Bioanalytical Method Validation, 2001. <http://www.fda.gov/downloads/Drugs/GuidanceComplianceRegulatoryInformation/Guidances/UCM070107.pdf>. Visited 18-2-2011.
34. Viswanathan CT, Bansal S, Booth B, DeStefano AJ, Rose MJ, Sailstad J, Shah VP, Skelly JP, Swann PG, Weiner R. Quantitative bioanalytical methods validation and implementation: best practices for chromatographic and ligand binding assays. *Pharm.Res.* **2007**; 24 (10): 1962-73.
35. Marchetti S, Stuurman FE, Koolen SL, Moes JJ, Hendriks JJ, Thijssen B, Huitema AD, Nuijen B, Rosing H, Keessen M, Voest EE, Mergui-Roelvink M, Beijnen JH, Schellens JH. Phase I study of weekly oral docetaxel (ModraDoc001) plus ritonavir

- in patients with advanced solid tumors. *ASCO Meeting Abstracts* **2012**; 30 (15_suppl): 2550.
36. Chang MS, Ji Q, Zhang J, El-Shourbagy TA. Historical Review of Sample Preparation for Chromatographic Bioanalysis: Pros and Cons. *Drug Development Research* **2012**; 68): 107-33.
 37. Dubbelman AC, Rosing H, Schellens JH, Beijnen JH. Bioanalytical aspects of clinical mass balance studies in oncology. *Bioanalysis*. **2011**; 3 (23): 2637-55.
 38. Longnecker SM, Donehower RC, Cates AE, Chen TL, Brundrett RB, Grochow LB, Ettinger DS, Colvin M. High-performance liquid chromatographic assay for taxol in human plasma and urine and pharmacokinetics in a phase I trial. *Cancer Treat.Rep.* **1987**; 71 (1): 53-9.

Quantification of docetaxel and its metabolites in human plasma by liquid chromatography/tandem mass spectrometry.

Jeroen J.M.A. Hendriks
Anne-Charlotte Dubbelman
Hilde Rosing
Alfred H. Schinkel
Jan H.M. Schellens
Jos H. Beijnen

Rapid Commun Mass Spectrom.
2013; 27 (17): 1925-34

Abstract

Rationale: During drug development accurate quantification of metabolites in biological samples using mass spectrometry is often hampered by the lack of metabolites of chemically pure quality. However, quantification of metabolites can be useful for assessment and interpretation of (pre)clinical data. We now describe an approach to quantify docetaxel metabolites in human plasma by LC-MS/MS using docetaxel calibration standards.

Methods: Metabolites (M1/M3, M2 and M4) were generated using microsomal incubations. Retention times of docetaxel and its metabolites were assessed using an LC-UV assay and peak identification was performed by LC-MSⁿ. Samples containing isolated metabolites from human faeces were quantified by LC-UV and used as references for spiking human plasma samples. LC-MS/MS was applied to sensitively quantify docetaxel and its metabolites in human plasma using docetaxel calibration standards in a range of 0.25-500 ng/mL.

Results: Because ionisation of docetaxel and its metabolites differed, correction factors were established to quantify the metabolites using docetaxel calibration samples. During method validation, accuracy and precision of the metabolites were within $\pm 7.7\%$ and $\leq 17.6\%$, respectively, and within $\pm 14.3\%$ and $\leq 10.1\%$, respectively, for docetaxel. Metabolites were found to be unstable in human plasma at ambient temperature. After storage up to 1 year at $-20\text{ }^{\circ}\text{C}$, recovered metabolite concentrations were within $\pm 25\%$.

Conclusions: Development and validation of an LC-MS/MS assay for the quantification of docetaxel and its metabolites M1/M3, M2 and M4 using docetaxel calibration standards is described. The same approach may be used for quantification of metabolites of other drugs by LC-MS/MS when chemically pure reference substances are unavailable.

Introduction

Docetaxel (Taxotere®) is a semi-synthetic taxane, originating from the *Taxus baccata* and is currently used as anticancer agent in several types of cancer, including lung, breast, gastric and prostate cancer.¹ In humans, docetaxel is metabolised by CYP3A enzymes into four metabolites.^{2,3} The affinity of docetaxel for CYP3A4 is higher than for CYP3A5, but the maximal transformation rate is comparable.³ The first step in docetaxel metabolism is hydroxylation of the synthetic isobutoxy side chain into metabolite M2 (Figure 1). Oxidation of M2 leads to the formation of an unstable aldehyde intermediate metabolite, which is immediately cyclized into the stereoisomers M1 and M3.^{2,3} Further oxidation of M1 and M3 results in the formation of M4.² M2 exhibits some cytotoxicity, however its cytotoxic effects are much lower compared to docetaxel. The other metabolites show no relevant cytotoxic activity.⁴

Today, docetaxel metabolites are usually quantified by liquid chromatography coupled with ultraviolet absorption detection (LC-UV).^{2,3;5-7} LC-UV is a straight forward and routine technique for metabolite quantification and the parent drug can be used for quantification if the chromophore offers sufficient selectivity and is not altered by metabolic reactions.⁸ However, the high sensitivity and selectivity of liquid chromatography coupled with tandem mass spectrometry (LC-MS/MS) are frequently required, since metabolite plasma concentrations are in general lower as compared to plasma concentrations of the parent drug. A limitation of metabolite quantification using LC-MS/MS, is that development of assays requires the use of chemically pure reference standards, while during drug development, metabolites of chemically pure quality are usually commercially not -or hardly- available and often expensive. To our knowledge, only one LC-MS/MS assay for the quantification of docetaxel and its metabolites using chemically pure reference standards has been described.⁹ To date, multiple approaches have been described to determine metabolite concentrations using

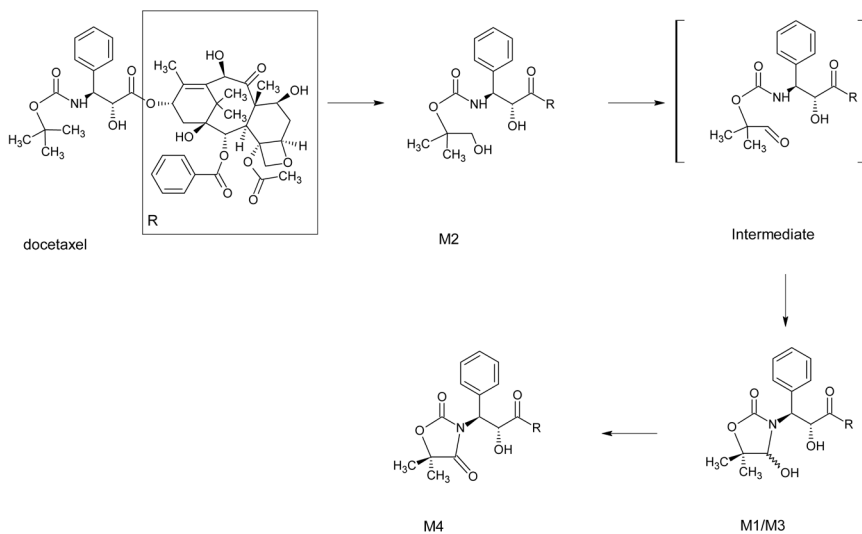


Figure 1. Structures of docetaxel and metabolites.

MS without the use of reference standards.¹⁰⁻¹³ These methods are used to compare the area under the plasma concentration-time curve (AUC) of the metabolite with the AUC of the parent compound and are not used for exact quantification of the metabolites. As FDA guidelines for safety testing of drug metabolites recommend further testing of the metabolites in case of metabolite quantities of >10% compared to the AUC of the parent drug¹⁴, the less abundant metabolites do not require quantification. A major drawback of LC-MS/MS for quantification in the approach in the FDA guidelines is the possibility of different ionisation patterns for the parent drug and its metabolites. This may result in under- or overestimation of the AUC of a metabolite. Apart from that, sometimes accurate quantification of the metabolites is highly desirable, e.g., in the case of active metabolites, which may influence pharmaceutical activity as well as toxicity even at low amounts. Additionally, metabolite formation is often used as parameter in cytochrome P450 interaction screening. Assessment of metabolite formation, and (semi)quantification of the metabolite concentration is then essential. Quantification of metabolites is pivotal in the comparison of preclinical and clinical data and can help to explain interspecies differences or improve extrapolation of preclinical data to the clinical setting. And lastly, metabolite quantification can also become important in specific populations such as patients with hepatic impairment. To be able to support these studies, we aimed to establish a method for quantification of docetaxel metabolites by LC-MS/MS by using docetaxel calibration standards, thus avoiding the need to purchase expensive reference substances of the metabolites.

Experimental

Chemicals

Docetaxel was purchased from Sequoia Research Products (Oxford, UK), D₃-labelled docetaxel was purchased from Toronto Research Chemicals (North York, ON, Canada). Pooled human liver microsomes and NADPH regeneration system were obtained from BD Biosciences (Erembodegem, Belgium). Methanol and acetonitrile (both HPLC grade) were purchased from Biosolve Ltd (Amsterdam, the Netherlands), tertiary-butylmethylether (tert.-butylmethylether/ TBME, Analytical grade), 25% ammonium hydroxide (v/v, Analytical grade), potassium dihydrophosphate, dipotassium hydrophosphate and water for chromatography (LiChrosolv) were obtained from Merck (Darmstadt, Germany). Drug free lithium-heparinised human plasma was obtained from Bioreclamation Inc (Hicksville, NY, USA).

Synopsis of assay development and validation

Development of the assay was started by the generation of docetaxel metabolites. Docetaxel was incubated with human liver microsomes to generate docetaxel metabolites. After incubation, sample pre-treatment was started and retention times of docetaxel and its metabolites were determined using an LC-UV assay. Subsequently, peaks in the incubation samples were identified using LC-MSⁿ. Metabolite formation in the incubation samples was optimised during peak identification to enlarge metabolite yield. For development of an LC-MS/MS assay, previously isolated metabolites from human faeces were used⁴, although metabolites could also be isolated from microsomal

incubations. Metabolite concentrations in the isolated samples were quantified using docetaxel calibration standards analysed with a LC-UV assay. Subsequently, the isolated samples were used for spiking of quality control (QC) samples. Since molar absorption of docetaxel and its metabolites is similar at 227 nm, docetaxel calibration curves can be used for metabolite quantification.⁵ Molar concentrations of docetaxel and its metabolites were compared and back-calculated to ng/mL taking into account differences in molar mass. After sample pre-treatment, these spiked samples were used for LC-MS/MS development and validation.

Microsomal incubation

Microsomal incubations were performed with human liver microsomes to generate metabolites. A 150 μ L sample containing 10 μ M docetaxel, 2 mg/mL microsomal proteins, 100 mM phosphate buffer pH = 7.4 and water was preincubated for 5 min at 37 °C. After preincubation, 50 μ L of a NADPH regeneration system was added and the samples were incubated for 4 h at 37 °C (Thermomixer Comfort, Eppendorf Netheler Hinz GmbH, Hamburg, Germany), while being automatically shaken at 1,000 rpm. After incubation the samples were placed on ice and the enzymatic reaction was stopped by adding 100 μ L ice-cold acetonitrile. An aliquot of 200 μ L supernatant was collected.

Isolation of the metabolites

We used previously isolated metabolites⁴ from human faeces for validation of the LC-MS/MS method, but metabolites can also be isolated from microsome incubations. To isolate docetaxel metabolites from microsome incubations, an aliquot of the supernatant should be injected on the described LC-UV assay (see below) and eluate fractions containing the metabolites can be collected. In this chromatographic system, M1 and M2 are not separated. The M1/M2 containing fraction should be re-injected on the described LC-MS/MS assay (see below) and separate fractions containing M1 and M2 can be collected.

Sample pre-treatment

To 200 μ L sample, 1.0 mL of TBME was added and the sample was mixed for 10 s. For LC-MS/MS quantification, as internal standard, 25 μ L of a 200 ng/mL D₃-labelled docetaxel solution was added prior to TBME. Samples were successively shaken automatically for 10 min at 1,250 rpm (L46, Labinco, Breda, The Netherlands) and centrifuged for 5 min at 23,000 g (5403 Eppendorf, Netheler Hinz GmbH, Hamburg, Germany). The aqueous layer was frozen in a bath of ethanol and dry ice and the organic layer was decanted into a clean 1.5 mL tube. The sample was dried under a gentle stream of nitrogen at 40 °C. The residue was reconstituted in 100 mM ammonium acetate (pH 5)/acetonitrile (1:1, v/v), vortex-mixed for 10 s and centrifuged for 3 min at 23,000 g. The supernatant was transferred to a glass autosampler vial with insert.

LC-UV for identification and quantification

The chromatographic conditions were based on a previously developed assay by our group for quantification of docetaxel and metabolites.⁵ A UV detector (UV1000, Thermo

Fischer Scientific, Waltham, MA, USA) was coupled to a HP1100 liquid chromatographic system (Agilent Technologies, Palo Alto, CA, USA). The HP1100 system consisted of a binary pump, an autosampler, a mobile phase degasser and a column oven. The mobile phase consisted of 20 mM ammonium acetate in water pH 5-acetonitrile (40:60, v/v) at a flow rate of 0.3 mL/min. Chromatographic separation was obtained using a SymmetryShield RP8 column (150 x 2.1 mm I.D., particle size 3.5 μ m; Waters Corp., Milford, MA, USA). The column oven was set at 30 °C. A sample volume of 25 μ L was injected and the injection needle was washed during 3 s with methanol after each injection. The UV signal was measured at a wavelength of 227 nm. The total runtime was 18 min. A set of calibration samples containing docetaxel (150-100,000 ng/mL) in 20 mM ammonium acetate in water (pH 5)/acetonitrile (40:60, v/v) was used to quantify docetaxel and metabolites in incubation samples and metabolite fractions. Calibration curves were fitted by linear regression of the peak area versus the concentration with $1/x^2$ (the reciprocal of the squared concentration) as the weighting factor. Data acquisition and processing were carried out using Chromeleon version 6.5 SP5 (Dionex, Sunnyvale, CA, USA).

LC-MSⁿ for identification

An LTQ XL mass spectrometer (Thermo Fischer Scientific, Waltham, MA, USA) was coupled to an Accela pump and autosampler (Thermo Fischer Scientific). Chromatographic conditions were identical to the LC-UV method. An injection volume of 20 μ L was used and the total run time was 17 min. Microsomal incubation samples were measured and UV and MS spectra were recorded after chromatographic separation. The UV signal was measured at a wavelength of 227 nm and MS spectra at m/z 200-1100 were obtained. Ion Trap Mass Spectrometry (MSⁿ) spectra were used for identification of docetaxel and metabolite peaks. Data acquisition and processing were carried out using LC Quan version 2.5.6 (Thermo Fisher Scientific).

LC-MS/MS for quantification and validation

An API3000 triple quadrupole with electrospray ionisation (ESI) (AB Sciex, Foster City, CA, USA) was coupled to a binary pump, an autosampler, a mobile phase degasser and a column oven, all part of an HP1100 system (Agilent Technologies, Palo Alto, CA, USA). Chromatographic separation was obtained using a Zorbax Extend C₁₈ column (150 x 2.1mm I.D., particle size 5 μ m, Agilent Technologies). The column oven was set at 30 °C. A sample volume of 25 μ L was injected and the injection needle was washed during 3 s with methanol after each injection. A gradient of 10 mM ammonium hydroxide in water and methanol was used at a flow rate of 0.2 mL/min. At the start the mobile phase consisted of 50% (v/v) methanol. After 0.2 min, 70% (v/v) methanol was used for 6.8 min, after which the methanol was reset to 50% (v/v) for 2 min. A switching valve was used to direct the eluent during the first 1.5 min of the run to waste. Mass transitions and MS/MS settings were optimised for docetaxel in positive ion mode. An overview of the mass transitions and MS/MS settings is listed in Table 1. For quantification, the multiple reaction monitoring (MRM) chromatograms were acquired with Analyst software version 1.5 (AB Sciex). Docetaxel calibration curves were fitted by linear regression of the peak area ratio with the internal standard versus the concentration

Table 1. MS/MS parameters and mass transitions of the analytes.

Parameter	Setting				
Entrance Potential	10.0 V				
Ionspray Voltage	5500 V				
Nebulizer gas	9.0 psi				
Curtain gas	9.0 psi				
Collision gas	3.0 psi				
Temperature	250°C				
Declustering Potential	66 V				
Collision Cell Exit Potential	20 V				
Focussing Potential	330 V				
	DOC	M1/M3	M2	M4	IS DOC
Collision Energy (V)	15	20	15	25	15
ScanTime (s)	0.2	0.2	0.2	0.2	0.2
Precursor ion (m/z)	808	839	824	837	817
Product ion (m/z)	527	527	298	527	527
Typical RT (min)	7.2	4.4	4.7	5.5	7.0

Abbreviations: DOC: docetaxel; M1/M3: docetaxel metabolites M1/M3; M2: docetaxel metabolite M2; M4: docetaxel metabolite M4; IS DOC: D₉-labelled docetaxel; RT: retention time.

with $1/x^2$ (the reciprocal of the squared concentration) as the weighting factor. Metabolite concentrations were calculated in ng/mL using docetaxel calibration curves and established correction factors.

Preparation of stock and working solutions

For docetaxel, two stock solutions from independent weighings were prepared in methanol at a concentration of 1 mg/mL. The stock solutions were diluted to working solutions with methanol. One set of working solutions was used for the preparation of calibration standards, while the other set was used for the preparation of QC samples. For the internal standard D₉-docetaxel a stock solution of 1.0 mg/mL was prepared in methanol. The stock solution of the internal standard was further diluted to obtain a working solution of 200 ng/mL. Previously isolated metabolites from human faeces⁴ were used. Fractions containing one of the metabolites were diluted with methanol to obtain working solutions that contained one metabolite. All solutions were stored at -20 °C.

Preparation of calibration standards and QC samples

Calibrations standards (CAL) of docetaxel were prepared by diluting a fixed amount of docetaxel working solution in blank human plasma. The CALs contained 0.25–500 ng/mL docetaxel. In a similar way, QC samples at three concentrations were prepared from another set of working solutions. The QC samples contained docetaxel concentrations of 0.75, 25 and 375 ng/mL. Samples were transferred to 2.0 mL polypropylene tubes

(Eppendorf, Merck) in aliquots of 200 μL and stored at $-20\text{ }^{\circ}\text{C}$. For QC samples of the metabolites, metabolite concentrations in the working solutions were quantified by HPLC-UV. Working solutions containing the metabolites were diluted 100, 500 and 1000 times with blank human plasma. Diluted samples contained only one of the metabolites per sample. The metabolite concentrations in the diluted samples were 0.89/1.56/1.24/1.61 (M1/M2/M3/M4), 1.78/3.12/2.48/3.21 and 8.88/15.6/12.4/16.1 ng/mL, respectively.

Validation program

For the LC-MS/MS assay, a partial validation program for docetaxel was executed, including calibration model and accuracy and precision. Stability of docetaxel in human plasma and processed samples, recovery and matrix effects were previously determined at our institute.^{15;16} Docetaxel metabolites were quantified using the docetaxel calibration curve. A correction factor was calculated to quantify docetaxel metabolites at a docetaxel calibration curve by quantifying the spiked samples with the HPLC-UV and HPLC-MS/MS assays. The validation program for the metabolites included robustness of the correction factor, accuracy and precision and stability. Stability was established for each metabolite separately during 1-3 freeze/thaw cycles and in human plasma. The validation and acceptance criteria were based on the FDA guidelines¹⁷ on bioanalytical method validation and on the guidelines of the 3rd AAPS/FDA bioanalytical workshop^{17;18} unless otherwise specified.

Proof of concept

The concept of quantification of structural analogues like metabolites using a calibration curve of the parent drug and applying a correction factor was tested using paclitaxel as test compound. Paclitaxel is a taxane that shares the baccatin ring structure with docetaxel. Paclitaxel was quantified in human plasma samples by a validated LC-MS/MS method¹⁵ using paclitaxel calibration curves and by using docetaxel calibration curves and a correction factor. The correction factor was calculated as described for the docetaxel metabolites using QC samples containing paclitaxel at three concentration levels. The calculated paclitaxel concentrations in the human plasma samples of the two methods were compared using weighted Deming regression analyses. The software package Analyse-it[®] (Method Evaluation edition version 2.30, Analyse-it Software Ltd, Leeds, United Kingdom) was used for regression analyses. Moreover, paclitaxel concentrations as quantified by the validated assay were used as nominal concentration and compared with paclitaxel concentrations as quantified using docetaxel calibration curves. Acceptation criteria for this test were based on the guideline on bioanalytical method validation of the EMA¹⁹: the difference in concentration should be within $\pm 20\%$ of their mean for at least 67% of the samples.

Results

Optimisation of metabolite formation

Human pooled liver microsomes were used to obtain docetaxel metabolites. To increase the metabolite yield, multiple incubation times were tested. An excess of docetaxel was used; thus incubation time and protein concentrations determined rate of metabolite formation. Protein concentrations were fixed at 2 mg/mL and samples were incubated for 2, 4 and 6 h. Metabolite yield increased with time, however, after 4 h metabolite yield was 300-1000 nM. Since this was sufficient for development of the assay, a 4 h incubation period was maintained during assay development.

Method development

UV-detection

Method development was started with the development of the LC-UV assay as described in the *Experimental* section. Calibration samples of docetaxel in water (pH 5)/acetonitrile (40:60, v/v) were prepared to determine linearity and sensitivity of the assay. The assay was linear in the range of 0.05 to 100 µg/mL for docetaxel in reconstitution solvent (see section Sample pre-treatment). Microsome samples were used to verify the retention times of docetaxel and its metabolites. A sample incubated without NADPH was used as a control for metabolite formation, as docetaxel metabolism by CYP enzymes is NADPH-dependent.³ In microsome samples, docetaxel eluted at a retention time (RT) of 14.8 min and metabolite peaks were observed at 5.5, 6.6 and 11.9 min (Figure 2). For identification of metabolite peaks in the LC-UV

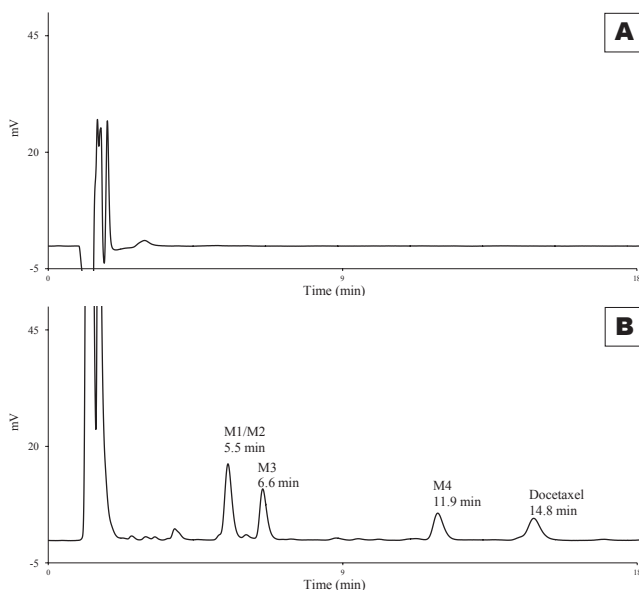


Figure 2. Typical UV chromatograms recorded at 227 nm of blank solvent (methanol-water, 1:1, v/v, panel A) and analytes spiked to solvent (1420; 1120; 1420; 1830; 1230 ng/mL for docetaxel, M1, M2, M3 and M4, respectively, panel B).

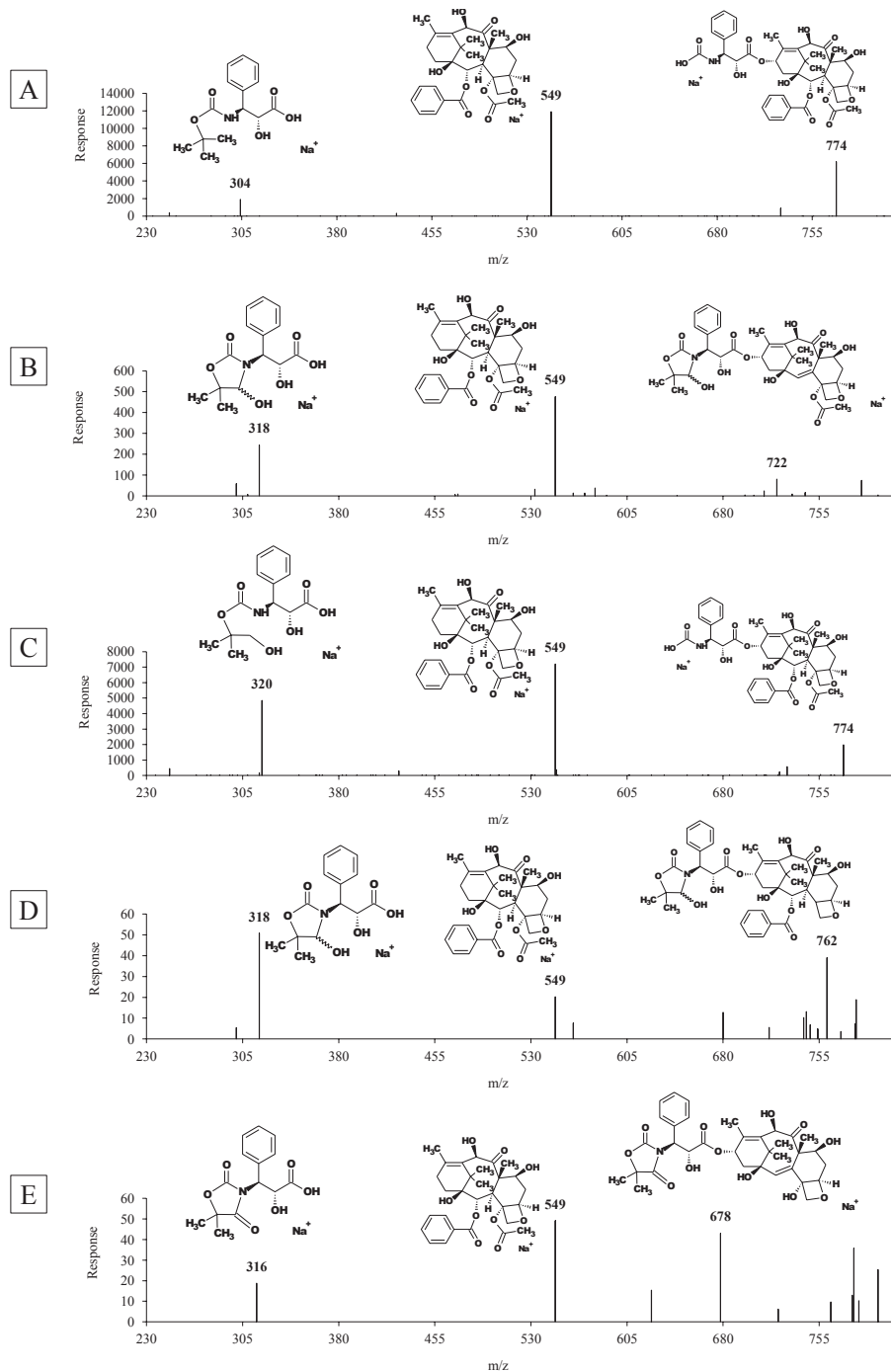


Figure 3. Fragmentation of sodium adducts of docetaxel (panel A), M1 (panel B), M2 (panel C), M3 (panel D) and M4 (panel E) using an LTQ XL mass spectrometer. Proposed structures of the main fragmentation products are included.

assay the assay was transferred to LC-MSⁿ. The MS spectrum showed no ions at the m/z $[M+H]^+$ of the analytes, however ions at m/z $[M+Na]^+$ were observed. Fragmentation of the precursor ions also resulted in sodium adducts of docetaxel-related fragments. M1 and M3 were observed at m/z 844 ($[M+Na]^+$), M2 was observed at m/z 842 ($[M+Na]^+$) and M4 was observed at m/z 840 ($[M+Na]^+$). Fragmentation of the sodium adducts and proposed structures of the main fragments are presented in Figure 3. The fragmentation pattern confirmed identity of the metabolites of docetaxel in the samples and enabled identification of the observed peaks with LC-UV. M1 and M2 were not separated and eluted after 5.5 min. M3 and M4 eluted after 6.6 and 11.9 min, respectively.

MS/MS-detection

As previously described, docetaxel response is increased when an alkaline mobile phase is used.¹⁵ Therefore, to increase sensitivity for LC-MS/MS detection a gradient of 10 mM ammonium hydroxide in water and methanol was used. Since the product specification of the SymmetryShield RP8 column discourages a mobile phase pH >8, a Zorbax Extend C₁₈ column was used. Flow and composition of the mobile phase were optimized for chromatographic separation. Metabolite M1 and M3 were not separated, however separation of metabolite M1 and M2 was considered more interesting for our research than separation of the stereoisomers M1 and M3. Thereby, the increased sensitivity for docetaxel and its metabolites was also assessed as more important (Figure 4). During LC-MS/MS optimization, ions at the m/z $[M+H]^+$ and $[M+NH_4]^+$ were observed in the mass spectrum and the most abundant ion for each compound was selected as precursor ion (Table 1).

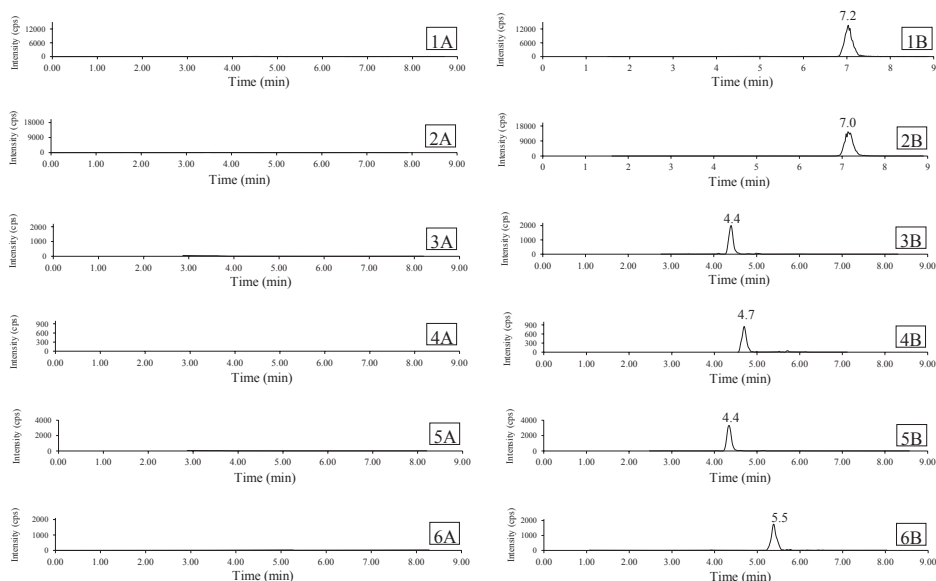


Figure 4. Typical MRM chromatograms of the analytes in a blank plasma sample and at QC mid level (25; 1.78; 3.12; 2.48; 3.21 ng/mL for docetaxel, M1, M2, M3 and M4, respectively). Panels show the response in a blank plasma sample and in a QC sample at mid level at the transition of docetaxel (1A and 1B, respectively), D₉-labeled docetaxel (2A and 2B), M1 (3A and 3B), M2 (4A and 4B), M3 (5A and 5B) and M4 (6A and 6B). QC samples were spiked separately with docetaxel or one of the metabolites.

Method validation

Calibration model

CALs (9) with duplicate points at each concentration in the range 0.25 to 500 ng/mL docetaxel were prepared in control lithium heparinized human plasma and analysed in three independent analytical runs. Calibration curves were fitted by linear regression of the peak area ratio with the internal standard versus the concentration with $1/x^2$ (the reciprocal of the squared concentration) as the weighting factor. When calibration data was fitted by linear regression, correlation coefficients (r^2) of 0.9955 or better were obtained for docetaxel. For every calibration curve the calibration concentrations of docetaxel were back-calculated from the response ratios. At all tested concentration levels we accepted a deviation of $\pm 15\%$ and at the lower limit of quantification (LLOQ) level a deviation of $\pm 20\%$. At the lowest calibration level (0.25 ng/mL) the deviation of the measured concentration from nominal concentration was 2.1%, with a coefficient of variation (CV) value of 12.4%. At all other calibration standard concentration levels the deviations of measured concentrations from nominal concentration were between -6.9 and 8.1% with CV values of less than 11.1%.

Table 2. Assay performance for docetaxel and its metabolites.

Compound	Nominal conc. (ng/mL)	Inter-assay bias (%)	Inter-assay precision (%)	No. of replicates
Docetaxel	0.699	10.4	10.1	15
	23.3	14.3	3.8	15
	373	2.3	5.9	15
M1	0.888	-2.9	16.6	15
	1.78	-0.6	12.9	15
	8.88	-7.5	12.0	15
M2	1.56	-3.5	17.6	15
	3.12	0.8	11.1	15
	15.6	7.7	10.4	15
M3	1.24	-2.7	12.1	15
	2.48	1.4	12.3	15
	12.4	3.3	13.2	15
M4	1.61	0.1	12.0	15
	3.21	-0.7	13.7	15
	16.1	6.4	14.1	15

Abbreviations: conc.: concentration; M1: docetaxel metabolite M1; M2: docetaxel metabolite M2; M3: docetaxel metabolite M3; M4: docetaxel metabolite M4. Metabolites were quantified using docetaxel calibration standards and samples contained the metabolites separately. Inter-assay bias and precision of the metabolites were calculated after correction of the metabolite concentration for differences in ionisation compared to docetaxel.

Accuracy and precision

QC samples were prepared in control lithium heparinised human plasma and five replicates of each level were analysed in three independent analytical runs. The accuracy was determined by percentage difference between the mean concentration and the nominal concentration. The CV was used to report the precisions. The intra- and inter-assay accuracies and precisions were accepted if $\pm 15\%$ and less than 15%, respectively, for docetaxel and within $\pm 20\%$ and less than 20% for docetaxel metabolites, respectively. Since we used docetaxel calibration standards to quantify docetaxel metabolites we accepted higher accuracy and precision limits for docetaxel metabolites than for docetaxel itself. Assay performance data of docetaxel and its metabolites are given in Table 2. A correction factor was determined and used for quantification of the metabolites using the docetaxel calibration line. For each run, correction factors for each metabolite at three concentrations levels were calculated. The nominal concentrations as quantified by HPLC-UV were divided by the mean calculated concentration as docetaxel equivalent. For example, the mean calculated concentration of M2 at the high concentration level in the first run was 5.69 ng docetaxel equivalent/mL. Since the nominal concentration of M2 was 15.6 ng/mL, the calculated correction factor was 2.74 (15.6/5.69). The overall correction factor for a metabolite was calculated as the mean of all calculated correction factors for that metabolite. The overall established correction factors for M1, M2, M3 and M4 were 0.73, 2.59, 0.46 and 0.92, respectively, with CV values <12.6%.

Stability of the metabolites

Stability of the metabolites after multiple freeze/thaw cycles was evaluated by comparing stored samples at two concentration levels with freshly prepared samples. The metabolites were considered stable in the plasma when 80-120% of the initial measured concentration was found. Docetaxel metabolite concentrations decreased after multiple freeze/thaw cycles, however stability of metabolites M1, M2 and M3 after 3 freeze/thaw cycles was considered acceptable as after 3 freeze/thaw cycles minimally 80% of the initial concentration was measured. Metabolite M4 was stable after 2 freeze/thaw cycles, while after 3 freeze/thaw cycles, ~65% of initial concentration was measured. The CV was <20% for all the measured samples. Stability of the metabolites in human plasma was tested at ambient temperature and at 37 °C for 3 days at two concentration levels and compared to freshly prepared samples. After storage at ambient temperature for 3 days, measured metabolite concentrations were decreased with 73, 56, 35 and 73% for M1, M2, M3 and M4, respectively. After storage at 37 °C, even lower concentrations of the metabolites were observed. Although the metabolites were found to be unstable at ambient temperature or higher, degradation of the metabolites did not result in formation of one of the other known metabolites. Incurred sample reproducibility of docetaxel and its metabolites was evaluated after storage at -20 °C of plasma samples of patients who received docetaxel. After 1 year of storage, the samples were re-analysed and the measured concentrations were compared to the initial measured concentrations. The mean bias in the re-analysed samples was -13, -25 and -22% for the metabolites M1/M3, M2 and M4, respectively. Metabolites M1/M3 could be measured in 47 samples, while M2 and M4 could be measured in 14 and 10 samples, respectively.

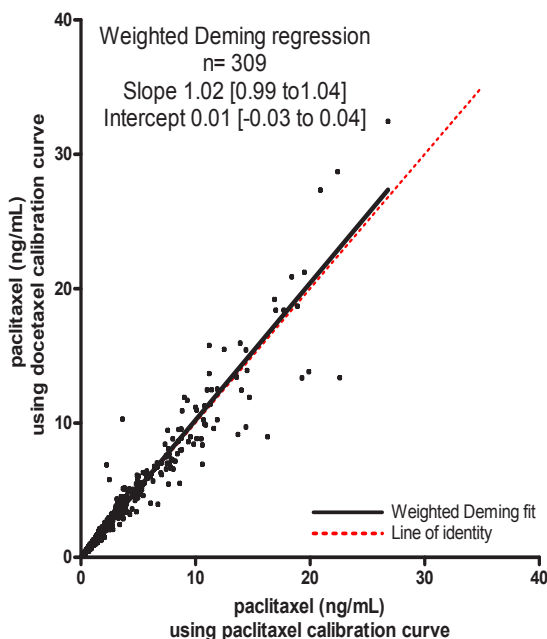


Figure 5. Compared results of paclitaxel concentrations in human plasma samples calculated using a paclitaxel calibration curve (x-axis) vs concentrations calculated using a docetaxel calibration curve and a correction factor (y-axis). The solid line represents the line calculated by weighted Deming regression and the dotted line the line of identity. Between brackets is the 95% confidence interval of the slope and intercept.

Proof of concept

Paclitaxel was quantified in 309 human plasma samples by a validated LC-MS/MS method¹⁵ using paclitaxel calibration curves and by using docetaxel calibration curves and a correction factor. Weighted Deming regression showed that the intercept and slope were not significantly different from 0 and 1, respectively, within the 95% level of significance (Figure 5). This indicates that both assays are comparable. Paclitaxel concentrations as quantified by using docetaxel calibration curves were within $\pm 20\%$ of the mean concentration in 76.4% of the samples. These results indicate that the concept of quantifying metabolites using a calibration curve of the parent drug combined with a correction factor can be used for quantification without the need of certified reference standard of these metabolites.

Discussion

We describe an approach to quantify docetaxel metabolites by LC-MS/MS using docetaxel calibration samples. To obtain the metabolites, we incubated docetaxel with human liver microsomes and used metabolites isolated from human faeces. Without having chemically pure reference substances of the metabolites, it is hard to validate a bioanalytical assay using triple quadrupole mass-spectrometric detection, however with head-to-head comparison of both UV and MS/MS detection we showed that our

method was accurate and precise in quantifying docetaxel metabolites using docetaxel calibration standards. The concept of this approach was proved using human plasma samples containing paclitaxel. The described approach may be used in general to quantify metabolites of other agents by LC-MS/MS using parent drug calibration standards.

The validation of this assay was based on the criteria in the FDA guidelines¹⁷, although broader acceptance criteria were set for the metabolites. For a full validation according to FDA guidelines, it is necessary to use reference standards of the metabolites. In the described assay, metabolites are not quantified using reference standards, but using the parent compound. Additionally, amounts of docetaxel metabolites in human plasma are low.^{9;20} However, even low amounts might yield useful information. Quantification based on reference standards of the parent compound and quantification of low levels might cause increased variability in the quantification of the metabolites. On the other hand, reporting plasma concentrations with increased uncertainty is more useful for population pharmacokinetic analysis than censoring by reporting no concentrations.²¹ We expanded the acceptance criteria for accuracy and precision of the metabolites to $\pm 20\%$ and less than 20%, respectively, for this assay for the quantification of docetaxel metabolite concentrations.

Vishwanathan et al¹³ previously reported that when similar UV spectra are observed for a parent compound and its metabolites UV responses are also similar. Rosing et al⁵ reported that for docetaxel and its metabolites molar absorption at 227 nm is similar, thus for quantification of docetaxel metabolites by UV absorption a docetaxel calibration curve can be used. However, switching from UV to MS detection can result in significant differences in response between parent compound and metabolites. It is known that ionisation of analytes using ESI-MS is influenced by multiple factors like polarity, analyte surface activity and pKa.²² Therefore, it is likely that there are major differences in ionisation between the parent compound and its metabolites. We compared quantification by UV and MS detection and observed clear differences in response of docetaxel and its metabolites. The observed differences were equal over multiple concentration levels and three independent runs, as reflected by the calculated correction factors. Therefore, it is possible to quantify the metabolites using docetaxel calibration lines, despite differences in ionisation. For method-transfer, it is advised to establish correction factors during a site-validation program to ensure exact quantification of the metabolites since performance of hardware might differ between sites.

Since M1 and M3 are not separated and correction factors differ (0.73 vs 0.46, respectively), quantification of the metabolites M1 and M3 in clinical samples can only be performed semi-quantitatively. An estimation of M1 plus M3 (M1/M3) concentrations can be made using the correction factor of M3 (0.46), since this metabolite is more abundant compared to M1.⁹ This will result in an underestimation of the concentration of M1/M3 by maximally 37% if only M1 is present in the sample. However, it is unlikely that *in-vivo* only one of the two stereoisomers is formed. If metabolite concentrations of M1 and M3 are equal the underestimation will be around 22%.

During stability testing, we observed that docetaxel metabolites are unstable in human plasma when exposed to higher temperatures. During storage at -20 °C for up to 1 year, 13-25% of the original metabolite concentration is lost. Interestingly, degradation products are other than the known metabolites M1/M3, M2 and M4. Our data indicate that storage of samples for quantification of docetaxel metabolites is limited and high temperatures during sample pre-treatment should be avoided.

Application of the method

The described assay was used for quantification of docetaxel metabolites in human plasma of two patients after intravenous administration of a fixed dose of 20 mg docetaxel (Taxotere®, Sanofi Aventis, France) over a 30 min infusion. Prior to docetaxel infusion, the patients received an oral 100 mg ritonavir capsule (Norvir®, Abbott, Illinois, USA). Blood samples were drawn at baseline, end of infusion and at multiple time points during the first 48 h after infusion. Docetaxel plasma concentrations at the end of infusion were 552 and 251 ng/mL in patient 1 and 2, respectively. The AUC extrapolated to infinity was 526 ng/mL*h in patient 1 and 624 ng/mL*h in patient 2. Maximal metabolite concentrations were observed within 1 h after the end of infusion and were undetectable after 4 h after the end of infusion. Metabolites M1/M3 were most abundant in the patients with maximal plasma concentrations of 1.37 and 1.51 ng/mL in patient 1 and 2, respectively. Metabolite M2 was observed at maximal plasma concentrations of 0.939 and 0.858 ng/mL, while M4 could hardly be detected and reached maximal plasma concentrations of 0.422 and 0.229 ng/mL in patients 1 and 2, respectively.

Conclusion

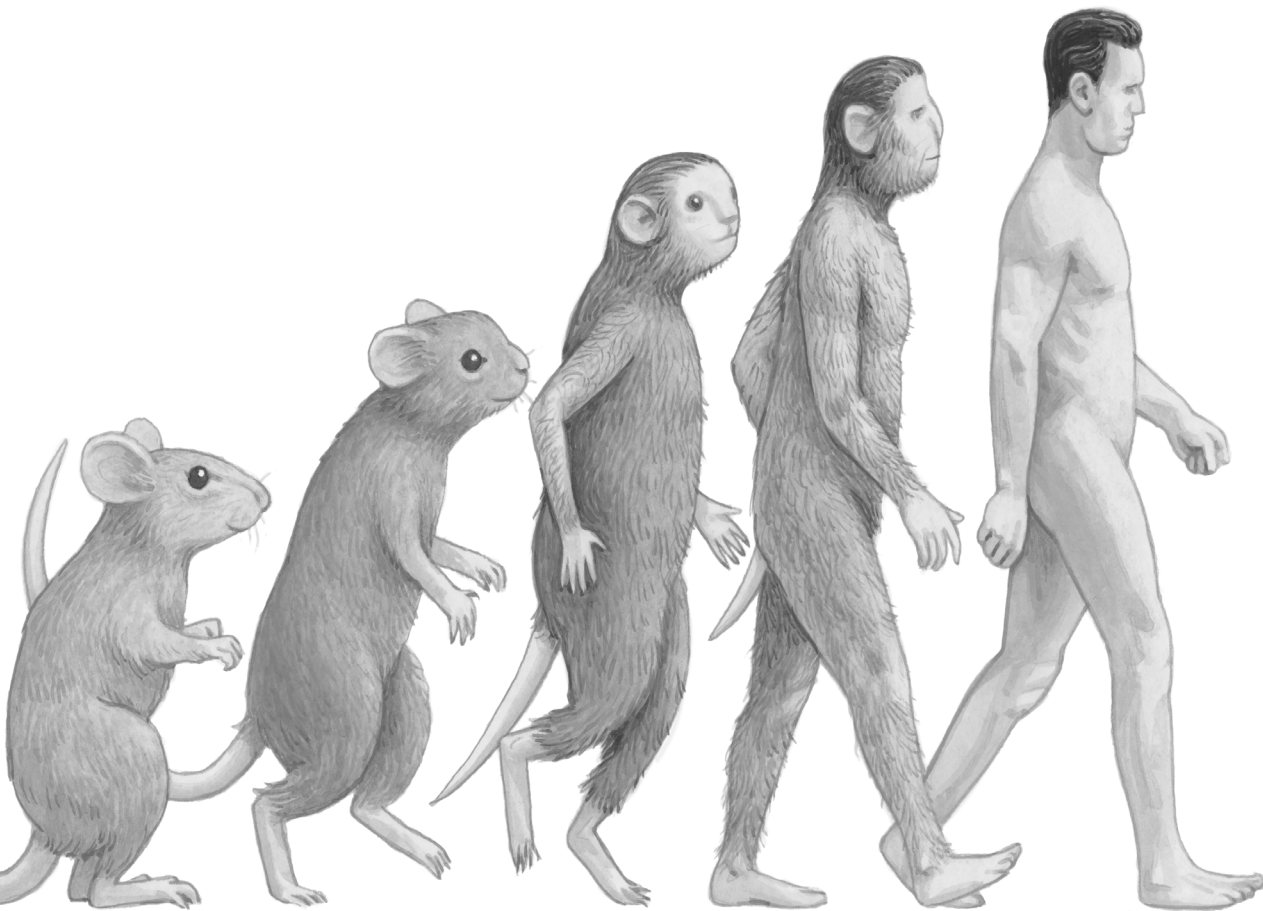
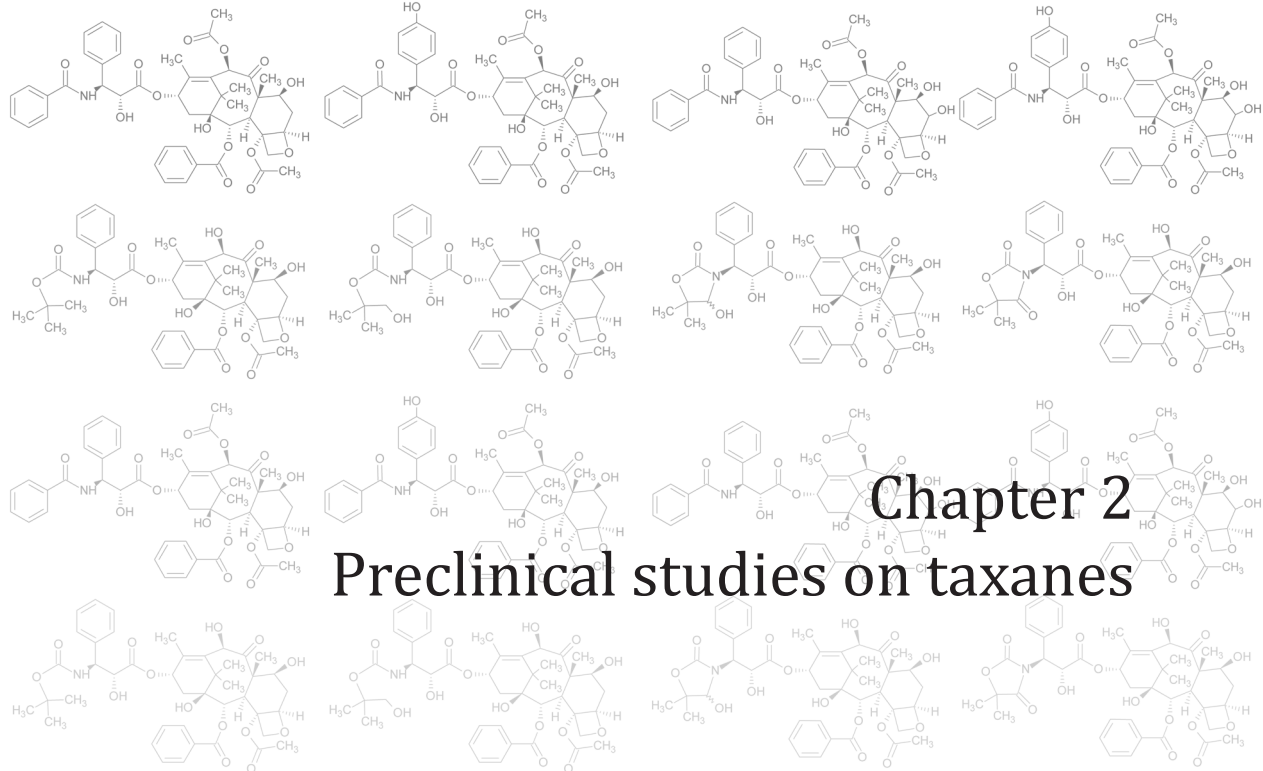
The development and validation of an LC-MS/MS assay for the quantification of docetaxel and its metabolites in human plasma is described. The validated range for docetaxel was 0.25-500 ng/mL using 200 µL plasma aliquots. This assay was used for quantification of docetaxel metabolites in human plasma without chemically pure reference standards of the metabolites and using docetaxel calibrations standards.

References

1. Gligorov J, Lotz JP. Preclinical pharmacology of the taxanes: implications of the differences *Oncologist*. **2004**; 9 (Suppl 2): 3-8.
2. Marre F, Sanderink GJ, de Sousa G, Gaillard C, Martinet M, Rahmani R. Hepatic biotransformation of docetaxel (Taxotere) in vitro: involvement of the CYP3A subfamily in humans. *Cancer Res*. **1996**; 56 (6): 1296-302.
3. Shou M, Martinet M, Korzekwa KR, Krausz KW, Gonzalez FJ, Gelboin HV. Role of human cytochrome P450 3A4 and 3A5 in the metabolism of taxotere and its derivatives: enzyme specificity, interindividual distribution and metabolic contribution in human liver. *Pharmacogenetics*. **1998**; 8 (5): 391-401.
4. Sparreboom A, van Tellingen O, Scherrenburg EJ, Boesen JJ, Huizing MT, Nooijen WJ, Versluis C, Beijnen JH. Isolation, purification and biological activity of major docetaxel metabolites from human feces. *Drug Metab Dispos*. **1996**; 24 (6): 655-8.
5. Rosing H, Lustig V, Koopman FP, ten Bokkel Huinink WW, Beijnen JH. Bio-analysis of docetaxel and hydroxylated metabolites in human plasma by high-performance liquid chromatography and automated solid-phase extraction. *J.Chromatogr.B Biomed.Sci.Appl*. **1997**; 696 (1): 89-98.
6. Vaclavikova R, Soucek P, Svobodova L, Anzenbacher P, Simek P, Guengerich FP, Gut I. Different in vitro metabolism of

- paclitaxel and docetaxel in humans, rats, pigs, and minipigs. *Drug Metab Dispos.* **2004**; 32 (6): 666-74.
7. van Tellingen O, Beijnen JH, Verweij J, Scherrenburg EJ, Nooijen WJ, Sparreboom A. Rapid esterase-sensitive breakdown of polysorbate 80 and its impact on the plasma pharmacokinetics of docetaxel and metabolites in mice. *Clin.Cancer Res.* **1999**; 5 (10): 2918-24.
 8. Leclercq L, Cuyckens F, Mannens GS, de VR, Timmerman P, Evans DC. Which human metabolites have we MIST? Retrospective analysis, practical aspects, and perspectives for metabolite identification and quantification in pharmaceutical development. *Chem.Res.Toxicol.* **2009**; 22 (2): 280-93.
 9. Guitton J, Cohen S, Tranchand B, Vignal B, Droz JP, Guillaumont M, Manchon M, Freyer G. Quantification of docetaxel and its main metabolites in human plasma by liquid chromatography/tandem mass spectrometry. *Rapid Commun.Mass Spectrom.* **2005**; 19 (17): 2419-26.
 10. Ma S, Li Z, Lee KJ, Chowdhury SK. Determination of exposure multiples of human metabolites for MIST assessment in preclinical safety species without using reference standards or radiolabeled compounds. *Chem.Res.Toxicol.* **2010**; 23 (12): 1871-3.
 11. Holcapek M, Kolarova L, Nobilis M. High-performance liquid chromatography-tandem mass spectrometry in the identification and determination of phase I and phase II drug metabolites. *Anal.Bioanal.Chem.* **2008**; 391 (1): 59-78.
 12. Gao H, Obach RS. Addressing MIST (Metabolites in Safety Testing): bioanalytical approaches to address metabolite exposures in humans and animals. *Curr.Drug Metab.* **2011**; 12 (6): 578-86.
 13. Vishwanathan K, Babalola K, Wang J, Espina R, Yu L, Adedoyin A, Talaat R, Mutlib A, Scatina J. Obtaining exposures of metabolites in preclinical species through plasma pooling and quantitative NMR: addressing metabolites in safety testing (MIST) guidance without using radiolabeled compounds and chemically synthesized metabolite standards. *Chem.Res.Toxicol.* **2009**; 22 (2): 311-22.
 14. U.S. Food and Drug Administration, Center for Drug Evaluation and Research, Guidance for industry: Safety Testing of Drug Metabolites, 2008. <http://www.fda.gov/downloads/Drugs/GuidanceComplianceRegulatoryInformation/Guidances/ucm079266.pdf>. Visited 3-9-2012.
 15. Hendriks JJ, Hillebrand MJ, Thijssen B, Rosing H, Schinkel AH, Schellens JH, Beijnen JH. A sensitive combined assay for the quantification of paclitaxel, docetaxel and ritonavir in human plasma using liquid chromatography coupled with tandem mass spectrometry. *J.Chromatogr.B Analyt.Technol.Biomed.Life Sci.* **2011**; 879 (28): 2984-90.
 16. Kuppens IE, van Maanen MJ, Rosing H, Schellens JHM, Beijnen JH. Quantitative analysis of docetaxel in human plasma using liquid chromatography coupled with tandem mass spectrometry. *Biomed.Chromatogr.* **2005**; 19 (5): 355-61.
 17. U.S. Food and Drug Administration, Center for Drug Evaluation and Research, Guidance for Industry Bioanalytical Method Validation, 2001. <http://www.fda.gov/downloads/Drugs/GuidanceComplianceRegulatoryInformation/Guidances/UCM070107.pdf>. Visited 18-2-2011.
 18. Viswanathan CT, Bansal S, Booth B, DeStefano AJ, Rose MJ, Sailstad J, Shah VP, Skelly JP, Swann PG, Weiner R. Quantitative bioanalytical methods validation and implementation: best practices for chromatographic and ligand binding assays. *Pharm.Res.* **2007**; 24 (10): 1962-73.
 19. Fast MD, Kelly M, Viswanathan CT, O'Shaughnessy J, King SP, Chaudhary A, Weiner R, DeStefano AJ, Tang D. Workshop Report and Follow-Up—AAPS Workshop on Current Topics in GLP Bioanalysis: Assay Reproducibility for Incurred Samples—Implications of Crystal City Recommendations. *The AAPS Journal* **2013**; 11 (2): 238-41.
 20. Rosing H, Lustig V, van Warmerdam LJ, Huizing MT, ten Bokkel Huinink WW, Schellens JH, Rodenhuis S, Bult A, Beijnen JH. Pharmacokinetics and metabolism of docetaxel administered as a 1-h intravenous infusion. *Cancer Chemother. Pharmacol.* **2000**; 45 (3): 213-8.
 21. Keizer, R. J. Pharmacometrics in early clinical drug development [Dissertation]. 217-238. 22-9-2010. Utrecht University.
 22. Cech NB, Enke CG. Practical implications of some recent studies in electrospray ionization fundamentals. *Mass Spectrom. Rev.* **2001**; 20 (6): 362-87.





Genetically modified mouse models for oral drug absorption and disposition.

Jeroen J.M.A. Hendrikx*
Seng Chuan Tang*
Jos H. Beijnen
Alfred H. Schinkel

* Both authors contributed equally

Curr Opin Pharmacol.
2013; 13 (6): 853-8

Abstract

Intestinal absorption is an essential step in the therapeutic use of most orally administered drugs and often mediated by enterocyte transmembrane transporters. Here we discuss several of these drug transport systems and knockout mouse models to study them. These studies showed that Multidrug resistance-associated protein 2 (Mrp2) can limit intestinal drug absorption. Organic cation transporter n1 (Ocn1) and Ocn2 might also facilitate intestinal drug absorption, although direct in vivo evidence is lacking. On the other hand, intestinal uptake of drugs is facilitated by the Equilibrative nucleoside transporter 1 (Ent1), Mrp3 and possibly Mrp4. No significant role in intestinal absorption for Oct1 and Oct2 or for Organic anion-transporting polypeptides (Oatp) 1a and 1b was found so far.

The problem of intestinal drug absorption

Intestinal absorption is an essential factor in the therapeutic use of virtually all orally administered drugs. Given its importance, it is surprising how little is clearly established about the transmembrane transport processes involved. Almost every oral drug that needs to act systemically has to pass at least two membranes: the apical and basolateral membranes of the enterocytes (Figure 1). Only very small, hydrophilic drugs can pass the tight junction barrier between the enterocytes. All others need to cross the enterocyte. Whereas some drugs may be lipophilic and small enough to pass the enterocyte membranes by passive diffusion at sufficient rates to be therapeutically relevant, this is unlikely to be the case for the great majority of drugs. Most will be too big, too polar or even charged, or have a combination of these properties. Only mediated transport, usually by various types of transmembrane transporters, will allow these molecules to pass the apical and the basolateral membranes of the enterocytes and thus to enter the bloodstream at sufficient rates. Surprisingly, for only very few drugs is it exactly clear what transporters are involved.

We here discuss several enterocyte transmembrane transport systems that may play a role in enhancement or reduction of the intestinal absorption of drugs. As we limit ourselves to transporters studied in knockout mouse models, this review is not exhaustive. Also, in view of other recent reviews, not much attention is given here to the roles of the Abcb1 (P-glycoprotein; Mdr1a/b) and Abcg2 (Bcrp) drug efflux transporters, or the PepT1 (Slc15a1) peptide and Lat1 (Slc7a5), Lat2 (Slc7a5), and Tat1 (Slc16a10) amino acid transporters.

Equilibrative nucleoside transporter 1 (Ent1)

The equilibrative nucleoside transporter 1 (Ent1; Slc29a1) belongs to the nucleoside transporter family (Slc29). It can transport endogenous nucleosides bidirectionally across plasma membranes, probably by a facilitated diffusion mechanism dependent on the transmembrane electrochemical gradient of the substrate.¹ In the human intestinal tract, ENT1 is concentrated predominantly in the lateral membrane of crypt cells, but it is also found in the lateral and apical membranes of more superficial enterocytes.² Ent1 mRNA is broadly expressed in tissues of the mouse, including the intestine. This intestinal expression suggests a possible role of Ent1 in the intestinal absorption of drugs (Figure 1).

Ent1^{-/-} mice were used to study *in vivo* drug disposition roles of Ent1, but data on the role of Ent1 in oral drug absorption are limited to the polar hepatitis C antiviral drug ribavirin.³ After oral administration, plasma concentrations of ³H-labeled ribavirin and its primary metabolites were up to 3.7-fold decreased in *Ent1*^{-/-} mice compared to wild-type mice. Interestingly, plasma concentrations after intravenous administration in both strains were comparable, suggesting that the intestinal absorption of ribavirin (and metabolites) is facilitated by Ent1, whereas its systemic clearance is not affected.

Probably Ent1, as a bidirectional equilibrative transporter primarily present in basolateral membranes, is necessary for efficient egress of ribavirin (and metabolites) from the enterocytes into blood. The preceding uptake of ribavirin from the intestinal

lumen is likely mediated by the concentrative nucleoside transporters Cnt2 and/or Cnt3 (not shown), which may also provide part of the driving force of the overall intestinal uptake. However, Ent1 can apparently be a rate-limiting step in this overall uptake process.³ This interpretation was further supported by intestinal perfusion studies in *Ent1*^{-/-} mice.⁴ Extrapolating from these data, Ent1 may also be involved in the oral absorption of other nucleoside-like drugs.

Organic cation transporters (Oct) 1 and 2 (Slc22a1 and a2)

The organic cation transporters Oct1 and 2 are thought to be passive diffusion transporters for a diverse range of organic cations. Transport direction of substrates is thus dependent on their electrochemical gradient across the membrane. Contradictory evidence in the literature suggests that Oct1 is located either at the apical or at the basolateral membrane of enterocytes, while Oct2 is located at the basolateral membrane of polarized cells.^{5,6} mRNA of these transporters is strongly expressed in various tissues among which the small intestine (Figure 1), especially for Oct1.⁶ Studies in *Oct1*^{-/-} mice demonstrated that small intestinal Oct1 can facilitate the direct intestinal excretion of the cation tetraethylammonium from blood to the intestinal lumen after i.v. administration, but oral drug uptake studies (requiring transport in the other direction) have not been done with these mice.⁷ As Oct1 might mediate both (basolateral) influx, and (apical) efflux of tetraethylammonium in enterocytes, the intestinal excretion data in the *Oct1*^{-/-} mice do not exclude either an apical or basolateral localization of Oct1.

The commonly prescribed antidiabetic drug metformin is a substrate of Oct1 and Oct2 and its pharmacokinetic behavior may be influenced by these transporters. Both Oct1 and Oct2 mRNA are expressed in the small intestine (Figure 1), and after oral administration plasma concentrations of metformin were substantially increased in *Oct1;Oct2*^{-/-} versus wild-type mice. However, the oral bioavailability ($AUC_{\text{oral}}/AUC_{\text{i.v.}}$) was not changed.⁸ In *Oct1;Oct2*^{-/-} mice, $AUC_{0-\text{inf}}$ was increased 4.5-fold compared to wild-type, whereas the systemic clearance was decreased 4.5-fold, presumably by decreases in both renal and hepatic clearance. Thus, the increased metformin plasma concentrations were due to decreased systemic clearance in *Oct1;Oct2*^{-/-} mice rather than due to changes in intestinal absorption after oral administration. These results do not support a significant role of Oct1/2 in the intestinal absorption rate of metformin, although we cannot exclude that more direct studies might still reveal some contribution.

Organic cation transporters Octn1 and Octn2 (Slc22a4 and a5)

In contrast to Oct1 and Oct2, Octn1 and Octn2 are usually located at the apical membrane of epithelial cells (Figure 1) and mRNA is strongly expressed in the kidney. mRNA expression is also observed in various tissues such as liver, muscles and brain. In the small intestine of rodents, both Octn1 and Octn2 are substantially expressed in the apical membrane of enterocytes.^{6,9} Both transport the zwitterion L-carnitine and a variety of other organic cations and zwitterions including several drugs. Depending on the circumstances and substrate, they can translocate substrates in both directions. Transport can be Na⁺-dependent, but does not have to be, and it may involve H⁺/cation exchange. The data suggest a substantial flexibility in the modes of transport mediated

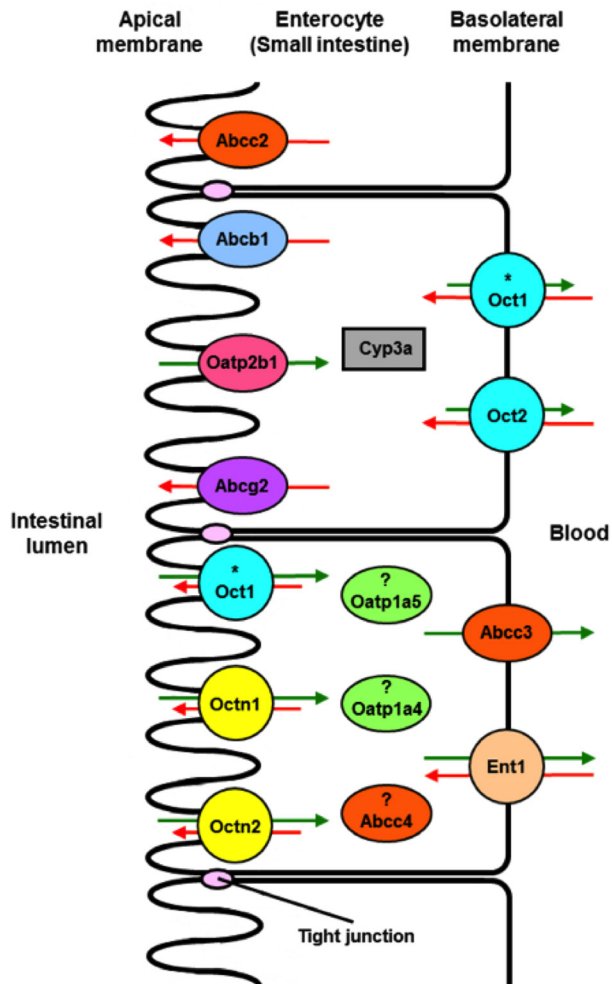


Figure 1. Schematic diagram illustrating the intestinal transporters and metabolizing enzyme discussed in this review. Efflux and/or influx transporters are localized at the apical or basolateral membrane of enterocytes in mouse small intestine. Transporters in the same color indicate that the transporters are from the same group. (?) indicates mRNA expression of mouse protein was detected in the small intestine, but its protein localization has not been unequivocally established yet. (*) indicates that there have been contradictory reports concerning the apical or basolateral localization of Oct1 in enterocytes, although current evidence for an apical localization seems stronger. Ovals indicate transporters with mostly single-directional transport, while circles indicate transporters with bidirectional transport. Green arrows indicate net absorptive direction of transport and red arrows indicate net excretory direction of transport. Long arrows indicate preferential transport and short arrows indicate less preferential transport directions by transporters that can mediate bidirectional transport. Protein and gene names: Ent1 (*Slc29a1*), equilibrative nucleoside transporter 1; Oct1/Oct2 (*Slc22a1/Slc22a2*), organic cation transporters 1 and 2; Octn1/Octn2 (*Slc22a4/Slc22a5*), organic cation/carnitine transporters 1 and 2; P-gp (*Abcb1a/1b*), P-glycoprotein; Bcrp (*Abcg2*), breast cancer resistance protein; Cyp3a (*Cyp3a*), cytochrome P450 3A; Mrp2 (*Abcc2*), multidrug resistance-associated protein 2; Mrp3 (*Abcc3*), multidrug resistance-associated protein 3; Mrp4 (*Abcc4*), multidrug resistance-associated protein 4; Oatp1a4/Oatp1a5 (*Slco1a4/Slco1a5*), organic anion-transporting polypeptides 1a4 and 1a5. Oatp2b1 (*Slco2b1*), organic anion-transporting polypeptide 2b1.

by these transporters, and they have been implicated both in uptake and secretory processes.⁶ Renal L-carnitine reabsorption is an important physiological function of Octn2 in humans and mice, preventing excessive loss of this essential cofactor in mitochondrial fatty acid beta-oxidation.

The intestinal uptake of the dietary antioxidant and Octn1 substrate ergothioneine was strongly (~7-fold) decreased in *Octn1*^{-/-} mice, using the everted intestinal sac method and analysis of remaining ergothioneine in the intestinal lumen after oral administration.⁹ Unexpectedly, however, plasma concentrations of oral ergothioneine were increased in *Octn1*^{-/-} mice, instead of decreased. Intravenous administration showed that this could be attributed to a far lower hepatic extraction of ergothioneine in *Octn1*^{-/-} compared to wild-type mice, which more than compensated for the lower oral absorption. Nonetheless, interference with Octn1 activity in the intestine only, for instance by some drugs, might reduce the oral availability of Octn1 substrates.

Octn2 deficiency in Octn2-null mice limited the uptake of L-carnitine in small intestinal enterocytes *in vitro*, both assessed with Ussing chamber transepithelial transport, and with isolated enterocytes.¹⁰ The data suggested that Octn2 contributes to intestinal uptake of L-carnitine, but is not the only uptake process involved. Although the substrate preference of Octn2 for L-carnitine is clearer than that of Octn1, it does transport several drugs *in vitro*.

In summary, therefore, although the data with the compounds ergothioneine and L-carnitine do suggest that Octn1 and Octn2 may be similarly involved in the intestinal absorption of some drugs, direct *in vivo* experimental evidence for this is still lacking.

Intestinal efflux transporters P-glycoprotein (Abcb1a/1b) and Breast cancer resistance protein (Abcg2)

Both these ATP-binding cassette (ABC) efflux transporters reside in the apical membrane of enterocytes, and have a very wide substrate spectrum. They can therefore actively pump many orally administered substrate drugs and other xenobiotics back into the intestinal lumen, thus reducing their oral availability (Figure 1). These important functions as uncovered with knockout mouse models have been extensively reviewed before, and we refer to the article by Fromm et al.¹¹ for a further discussion of their clinical relevance.

P-glycoprotein shares many drug substrates with the drug-metabolizing enzyme cytochrome P450 3A (Cyp3a), that is likewise highly expressed in enterocytes. Combination knockout mice lacking both Abcb1a/1b and Cyp3a were used to unravel the *in vivo* interplay between transporter and metabolizing enzyme.¹² The results revealed efficient collaboration between the two detoxifying systems in reducing the oral availability of shared substrate drugs (Figure 1), but this did not appear to be synergistic in nature.

Multidrug resistance-associated protein 2 (Mrp2, Abcc2)

The multidrug resistance-associated protein 2 (Mrp2; Abcc2) is also an ABC drug efflux transporter for many drugs and drug conjugates. It is expressed in the apical membrane of enterocytes (Figure 1), where it could potentially reduce the intestinal absorption of drug substrates.¹³ As Abcc2 is also expressed in the bile canalicular membrane and in the apical membrane of renal proximal tubular cells it can contribute substantially to the systemic clearance of its substrates, which may affect the interpretation of oral pharmacokinetic studies in knockout mice.

Plasma concentrations after oral administration of the anticancer drug paclitaxel, an Abcb1 and Abcc2 substrate, were unchanged in *Abcc2*^{-/-} compared to wild-type mice, but 1.7-fold increased in *Abcb1a/b;Abcc2*^{-/-} mice compared to *Abcb1a/b*^{-/-} mice, which in their turn showed 8.5-fold higher plasma levels than wild-type mice.¹⁴ This suggests that the contribution of Abcc2 to reducing paclitaxel plasma concentrations only becomes evident in the absence of the highly efficient paclitaxel transporter Abcb1. Similar results were found for docetaxel and etoposide, with a dominant effect of Abcb1 over Abcc2 in restricting plasma AUC after oral drug administration.^{15;16} Further comparison with i.v. administration showed, however, that the oral bioavailability ($AUC_{\text{oral}}/AUC_{\text{i.v.}}$) of paclitaxel and etoposide was not increased by Abcc2 deficiency, whereas that of docetaxel was. This suggests that most of the effect of Abcc2 deficiency on plasma AUC seen for paclitaxel and etoposide was due to reduced systemic clearance, but for docetaxel there may also be an increased intestinal absorption component.

Plasma concentrations of oral methotrexate were not significantly increased in *Abcc2*^{-/-} compared to wild-type mice, but a 1.7-fold increase due to Abcc2 deficiency was seen in the absence of Abcg2, which by itself also caused a 1.7-fold higher plasma AUC compared to wild-type mice.¹⁷ In this case therefore Abcg2 seemed to dominate Abcc2 effects. Interestingly, the effect of Abcc2 was lost in the absence of Abcc3 (see the section on Abcc3 below). Oral bioavailabilities were, however, not changed by the absence or presence of Abcc2, again suggesting that most effects on plasma AUC were mediated through altered systemic clearance.

Collectively, the data indicate that Abcc2 can limit oral plasma levels of drugs, but its effects can easily be obscured by other, dominant transporters. Moreover, plasma concentrations after oral administration of drugs are often increased in the absence of Abcc2 due to decreased systemic elimination rather than increased intestinal uptake. Only for docetaxel is there a clear suggestion of increased intestinal absorption, which would merit further investigation.

Multidrug resistance-associated protein 3 (Mrp3, Abcc3)

Abcc3 is another ABC drug efflux transporter, capable of transporting bile acids¹⁸ and endogenous glucuronide conjugates¹⁹. Unlike Abcc2, Abcc3 is expressed in the basolateral membrane of hepatocytes and enterocytes¹⁹⁻²¹, where it mediates the basolateral efflux of substrates either from enterocytes or hepatocytes into the blood (Figure 1). With respect to xenobiotics, Abcc3 is active in the basolateral efflux of a broad range of glucuronides²², sulfates²³, folates²⁴, etoposide¹⁵ and methotrexate²⁵.

Upon oral administration of methotrexate at 1 mg/kg, the plasma AUC_{0-4hr} was 3.4-fold lower in *Abcc3*^{-/-} mice than in wild-type mice.²⁵ Extensive pharmacokinetic analyses indicated that the bile canalicular clearance of methotrexate from plasma was increased, presumably because of reduced basolateral back-flux of methotrexate from the liver to blood in the absence of Abcc3. Oral bioavailability data, however, suggested reduced intestinal uptake of methotrexate. Everted intestinal sac experiments confirmed that the net intestinal uptake of methotrexate was considerably reduced in the duodenum of the *Abcc3*^{-/-} mice, indicating that Abcc3 normally facilitates the absorptive efflux of methotrexate from the enterocyte to blood (Figure 1). Apparently, the decreased plasma levels of methotrexate in *Abcc3*^{-/-} mice were due to both lower intestinal absorption and lower basolateral hepatic efflux.

In addition, upon oral administration of gemfibrozil, E3040, troglitazone, bisphenol A, and 4-methylumbelliferon, *Abcc3*^{-/-} mice showed a marked reduction in the plasma concentration of glucuronide conjugates of these compounds compared with wild-type mice.²² This suggests that Abcc3 plays a key role in the efflux of these glucuronide conjugates into the systemic circulation. However, it was not further investigated whether this resulted primarily from reduced efflux of these glucuronides from liver hepatocytes or from enterocytes, as glucuronidation can occur in both cell types.

Multidrug resistance-associated protein 4 (Mrp4, *Abcc4*)

The ABC drug efflux transporter Abcc4 can extrude a wide variety of endogenous organic anions and xenobiotics out of the cell, including steroid and bile acid conjugates²⁶, diuretics²⁷, antibiotics²⁸ and antiviral drugs²⁹. Its subcellular localization is cell-type dependent: apical in renal proximal tubular epithelial cells, but basolateral in prostate tubuloacinar cells, hepatocytes, and choroid plexus epithelium.³⁰ It is not exactly clear where Abcc4 resides in the intestine. In the human colonic cell line HT-29-CL19A, Abcc4 was found in both the apical and basolateral membrane, with a higher expression apically.³¹ In Caco-2 enterocyte cells, Abcc4 is apparently localized in the basolateral membrane³² (Figure 1). On the basis of the latter localization, Abcc4 might facilitate the intestinal absorption of drugs.

Upon intrajejunal administration of the polar cephalosporin antibiotic cefadroxil, portal and peripheral blood concentrations were similar in *Abcc4*^{-/-} mice, but approximately 2-fold reduced in *Abcc3;Abcc4*^{-/-} mice compared with wild-type mice. This suggested that the impact of Abcc4 on intestinal absorption of cefadroxil only became apparent in the absence of Abcc3.³³ Ussing chamber experiments with isolated intestinal tissue indicated that Abcc4 deficiency, but not Abcc3 deficiency, resulted in reduced transepithelial absorption of cefadroxil. The data suggest that in mice, Abcc4 is mostly localized in the basolateral membrane of enterocytes, and contributes to absorptive efflux of cefadroxil from enterocyte to blood. Note, however, that the intrajejunal administration data do not exclude that increased biliary clearance of cefadroxil from blood, mainly due to the hepatic Abcc3/Abcc4 deficiency, may also have contributed to the lower cefadroxil blood levels in *Abcc3;Abcc4*^{-/-} mice. This would be analogous to the situation described above for methotrexate in *Abcc3*^{-/-} mice.²⁵

Organic anion-transporting polypeptides (OATP; SLCO) OATP1A and OATP1B

Organic anion-transporting polypeptides (Oatps, Slco) are Na⁺-independent transmembrane transporters that mediate the cellular uptake of a broad range of organic endogenous and exogenous compounds, including many drugs and their conjugates.³⁴ Human OATP1A2 and human and mouse OATP2B1 are thought to be located in the apical membrane of enterocytes, where they could have an important role in intestinal uptake of drugs. In addition, mouse *Oatp1a4* and *Oatp1a5* mRNAs were detected in small intestine, but their protein localization has not been established yet (Figure 1). Although there are no straightforward orthologs between the human and mouse OATP1A and OATP1B family members, mouse intestinal *Oatp1a4* and *Oatp1a5* might have functions analogous to those of the single human OATP1A2 protein.

To date, several knockout and transgenic mouse models have been generated to study the physiological and pharmacological functions of OATP1A and OATP1B transporters *in vivo*.³⁵ Mice lacking all *Oatp1a/1b* genes (*Oatp1a/1b*^{-/-} mice) were generated to avoid any compensation by other *Oatp1a* or *Oatp1b* proteins.³⁶ Pharmacological functions of *Oatp1a* and *Oatp1b* proteins in the liver uptake and thus systemic clearance of several anticancer drugs, organic dyes, estrogen derivatives, antibiotics, statins and toxins could be established in the aforementioned mouse models.³⁵ However, directed studies to assess the impact on intestinal drug absorption of *Oatp1a* and *Oatp1b* proteins have so far only been performed in *Oatp1a/1b*^{-/-} mice, with remarkably little success. Portal vein sampling tests of orally administered methotrexate, fexofenadine, pravastatin, and rosuvastatin have all failed to yield clear indications for reduced intestinal drug uptake due to the absence of *Oatp1a* and *Oatp1b* proteins, whereas the hepatic disposition of all these drugs was clearly affected.³⁶⁻³⁸ These results raise the question whether there may be extensive redundancy for uptake transporters of these drugs in the intestine, possibly including *Oatp2b1* and drug uptake transporters of other families. Additional transporter gene knockout studies may shed light on this question.

Conclusion

Unlike the situation for several apical intestinal efflux transporters, that clearly limit the intestinal uptake of drugs, insight into the intestinal transporters that facilitate intestinal drug absorption is still surprisingly limited. Ongoing and future studies with genetically modified mouse models may further improve these insights, thus supporting the development of optimal orally available drugs.

References

- Lu H, Chen C, Klaassen C. Tissue distribution of concentrative and equilibrative nucleoside transporters in male and female rats and mice. *Drug Metab Dispos* **2004**; 32 (12): 1455-61.
- Govindarajan R, Bakken AH, Hudkins KL, Lai Y, Casado FJ, Pastor-Anglada M, Tse CM, Hayashi J, Unadkat JD. In situ hybridization and immunolocalization of concentrative and equilibrative nucleoside transporters in the human intestine, liver, kidneys, and placenta. *Am J Physiol Regul Integr Comp Physiol* **2007**; 293 (5): R1809-R1822.
- Endres CJ, Moss AM, Govindarajan R, Choi DS, Unadkat JD. The role of nucleoside transporters in the erythrocyte disposition and oral absorption of ribavirin in the wild-type and equilibrative nucleoside transporter 1-/- mice. *J Pharmacol Exp Ther* **2009**; 331 (1): 287-96.
- Moss AM, Endres CJ, Ruiz-Garcia A, Choi DS, Unadkat JD. Role of the equilibrative and concentrative nucleoside transporters in the intestinal absorption of the nucleoside drug, ribavirin, in wild-type and Ent1(-/-) mice. *Mol Pharm* **2012**; 9 (9): 2442-9.
- Han TK, Everett RS, Proctor WR, Ng CM, Costales CL, Brouwer KL, Thakker DR. Organic Cation Transporter 1 (OCT1/mOCT1) Is Localized in the Apical Membrane of Caco-2 Cell Monolayers and Enterocytes. *Mol.Pharmacol.* **2013**; 84 (2): 182-9.
- Koepsell H, Lips K, Volk C. Polyspecific organic cation transporters: structure, function, physiological roles, and biopharmaceutical implications. *Pharm Res* **2007**; 24 (7): 1227-51.
- Jonker JW, Wagenaar E, Mol CA, Buitelaar M, Koepsell H, Smit JW, Schinkel AH. Reduced hepatic uptake and intestinal excretion of organic cations in mice with a targeted disruption of the organic cation transporter 1 (OCT1 [Slc22a1]) gene. *Mol Cell Biol* **2001**; 21 (16): 5471-7.
- Higgins JW, Bedwell DW, Zamek-Gliszczynski MJ. Ablation of both organic cation transporter (OCT)1 and OCT2 alters metformin pharmacokinetics but has no effect on tissue drug exposure and pharmacodynamics. *Drug Metab Dispos* **2012**; 40 (6): 1170-7.
- Sugiura T, Kato S, Shimizu T, Wakayama T, Nakamichi N, Kubo Y, Iwata D, Suzuki K, Soga T, Asano M, Iseki S, Tamai I, Tsuji A, Kato Y. Functional expression of carnitine/organic cation transporter OCTN1/SLC22A4 in mouse small intestine and liver. *Drug Metab Dispos* **2010**; 38 (10): 1665-72.
- Kato Y, Sugiura M, Sugiura T, Wakayama T, Kubo Y, Kobayashi D, Sai Y, Tamai I, Iseki S, Tsuji A. Organic cation/carnitine transporter OCTN2 (Slc22a5) is responsible for carnitine transport across apical membranes of small intestinal epithelial cells in mouse. *Mol Pharmacol* **2006**; 70 (3): 829-37.
- Misaka C, Müller F, Fromm MF. Clinical relevance of drug efflux pumps in the gut. *Curr Opin Pharmacol* **2013**; 13.
- van Waterschoot RA, Schinkel AH. A critical analysis of the interplay between cytochrome P450 3A and P-glycoprotein: recent insights from knockout and transgenic mice. *Pharmacol Rev* **2011**; 63 (2): 390-410.
- Jedlitschky G, Hoffmann U, Kroemer HK. Structure and function of the MRP2 (ABCC2) protein and its role in drug disposition. *Expert Opin Drug Metab Toxicol* **2006**; 2 (3): 351-66.
- Lagas JS, Vlaming ML, van Tellingen O, Wagenaar E, Jansen RS, Rosing H, Beijnen JH, Schinkel AH. Multidrug resistance protein 2 is an important determinant of paclitaxel pharmacokinetics. *Clin Cancer Res* **2006**; 12 (20 Pt 1): 6125-32.
- Lagas JS, Fan L, Wagenaar E, Vlaming ML, van Tellingen O, Beijnen JH, Schinkel AH. P-glycoprotein (P-gp/Abcb1), Abcc2, and Abcc3 determine the pharmacokinetics of etoposide. *Clin Cancer Res* **2010**; 16 (1): 130-40.
- van Waterschoot RA, Lagas JS, Wagenaar E, Rosing H, Beijnen JH, Schinkel AH. Individual and combined roles of CYP3A, P-glycoprotein (MDR1/ABCB1) and MRP2 (ABCC2) in the pharmacokinetics of docetaxel. *Int J Cancer* **2010**; 127 (12): 2959-64.
- Vlaming ML, van Esch A, van de Steeg E, Pala Z, Wagenaar E, van Tellingen O, Schinkel AH. Impact of abcc2 [multidrug resistance-associated protein (MRP) 2], abcc3 (MRP3), and abcg2 (breast cancer resistance protein) on the oral pharmacokinetics of methotrexate and its main metabolite 7-hydroxymethotrexate. *Drug Metab Dispos* **2011**; 39 (8): 1338-44.
- Belinsky MG, Dawson PA, Shchavaleva I, Bain LJ, Wang R, Ling V, Chen ZS, Grinberg A, Westphal H, Klein-Szanto A, Lerro A, Kruh GD. Analysis of the in vivo functions of Mrp3. *Mol Pharmacol* **2005**; 68 (1): 160-8.
- Zelcer N, van de Wetering K, de Waart R, Scheffer GL, Marschall HU, Wielinga PR, Kuil A, Kunne C, Smith A, van der Valk M, Wijnholds J, Elferink RO, Borst P. Mice lacking Mrp3 (Abcc3) have normal bile salt transport, but altered hepatic transport of endogenous glucuronides. *J Hepatol* **2006**; 44 (4): 768-75.
- Rost D, Mahner S, Sugiyama Y, Stremmel W. Expression and localization of the multidrug resistance-associated protein 3 in rat small and large intestine. *Am J Physiol Gastrointest Liver Physiol* **2002**; 282 (4): G720-G726.
- Shoji T, Suzuki H, Kusuhara H, Watanabe Y, Sakamoto S, Sugiyama Y. ATP-dependent transport of organic anions into isolated basolateral membrane vesicles from rat intestine. *Am J Physiol Gastrointest Liver Physiol* **2004**; 287 (4): G749-G756.
- Hirouchi M, Kusuhara H, Onuki R, Ogilvie BW, Parkinson A, Sugiyama Y. Construction of triple-transfected cells [organic anion-transporting polypeptide (OATP) 1B1/multidrug resistance-associated protein (MRP) 2/MRP3 and OATP1B1/

- MRP2/MRP4] for analysis of the sinusoidal function of MRP3 and MRP4. *Drug Metab Dispos* **2009**; 37 (10): 2103-11.
23. Zamek-Gliszczynski MJ, Nezasa K, Tian X, Bridges AS, Lee K, Belinsky MG, Kruh GD, Brouwer KL. Evaluation of the role of multidrug resistance-associated protein (Mrp) 3 and Mrp4 in hepatic basolateral excretion of sulfate and glucuronide metabolites of acetaminophen, 4-methylumbelliferone, and harmol in Abcc3^{-/-} and Abcc4^{-/-} mice. *J Pharmacol Exp Ther* **2006**; 319 (3): 1485-91.
 24. Kitamura Y, Kusuhara H, Sugiyama Y. Basolateral efflux mediated by multidrug resistance-associated protein 3 (Mrp3/Abcc3) facilitates intestinal absorption of folates in mouse. *Pharm Res* **2010**; 27 (4): 665-72.
 25. Kitamura Y, Hirouchi M, Kusuhara H, Schuetz JD, Sugiyama Y. Increasing systemic exposure of methotrexate by active efflux mediated by multidrug resistance-associated protein 3 (mrp3/abcc3). *J Pharmacol Exp Ther* **2008**; 327 (2): 465-73.
 26. Zelcer N, Reid G, Wielinga P, Kuil A, van der Heijden I, Schuetz JD, Borst P. Steroid and bile acid conjugates are substrates of human multidrug-resistance protein (MRP) 4 (ATP-binding cassette C4). *Biochem J* **2003**; 371 (Pt 2): 361-7.
 27. Hasegawa M, Kusuhara H, Adachi M, Schuetz JD, Takeuchi K, Sugiyama Y. Multidrug resistance-associated protein 4 is involved in the urinary excretion of hydrochlorothiazide and furosemide. *J Am Soc Nephrol* **2007**; 18 (1): 37-45.
 28. Ci L, Kusuhara H, Adachi M, Schuetz JD, Takeuchi K, Sugiyama Y. Involvement of MRP4 (ABCC4) in the luminal efflux of ceftizoxime and cefazolin in the kidney. *Mol Pharmacol* **2007**; 71 (6): 1591-7.
 29. Imaoka T, Kusuhara H, Adachi M, Schuetz JD, Takeuchi K, Sugiyama Y. Functional involvement of multidrug resistance-associated protein 4 (MRP4/ABCC4) in the renal elimination of the antiviral drugs adefovir and tenofovir. *Mol Pharmacol* **2007**; 71 (2): 619-27.
 30. Russel FG, Koenderink JB, Masereeuw R. Multidrug resistance protein 4 (MRP4/ABCC4): a versatile efflux transporter for drugs and signalling molecules. *Trends Pharmacol Sci* **2008**; 29 (4): 200-7.
 31. Li C, Krishnamurthy PC, Penmatsa H, Marrs KL, Wang XQ, Zaccolo M, Jalink K, Li M, Nelson DJ, Schuetz JD, Naren AP. Spatiotemporal coupling of cAMP transporter to CFTR chloride channel function in the gut epithelia. *Cell* **2007**; 131 (5): 940-51.
 32. Ming X, Thakker DR. Role of basolateral efflux transporter MRP4 in the intestinal absorption of the antiviral drug adefovir dipivoxil. *Biochem Pharmacol* **2010**; 79 (3): 455-62.
 33. de Waart DR, van de Wetering K, Kunne C, Duijst S, Paulusma CC, Oude Elferink RP. Oral availability of cefadroxil depends on ABCC3 and ABCC4. *Drug Metab Dispos* **2012**; 40 (3): 515-21.
 34. Kalliokoski A, Niemi M. Impact of OATP transporters on pharmacokinetics. *Br J Pharmacol* **2009**; 158 (3): 693-705.
 35. Iusuf D, van de Steeg E, Schinkel AH. Functions of OATP1A and 1B transporters in vivo: insights from mouse models. *Trends Pharmacol Sci* **2012**; 33 (2): 100-8.
 36. van de Steeg E, Wagenaar E, van der Kruijssen CM, Burggraaff JE, de Waart DR, Elferink RP, Kenworthy KE, Schinkel AH. Organic anion transporting polypeptide 1a/1b-knockout mice provide insights into hepatic handling of bilirubin, bile acids, and drugs. *J Clin Invest* **2010**; 120 (8): 2942-52.
 37. Iusuf D, Sparidans RW, van Esch A, Hobbs M, Kenworthy KE, van de Steeg E, Wagenaar E, Beijnen JH, Schinkel AH. Organic anion-transporting polypeptides 1a/1b control the hepatic uptake of pravastatin in mice. *Mol Pharm* **2012**; 9 (9): 2497-504.
 38. Iusuf D, van Esch A, Hobbs MJ, Taylor MA, Kenworthy KE, van de Steeg E, Wagenaar E, Schinkel AH. Murine Oatp1a/1b Uptake Transporters Control Rosuvastatin Systemic Exposure without Affecting Its Apparent Liver Exposure. *Mol Pharmacol* **2013**; 83 (5): 919-29.

P-glycoprotein and Cytochrome P450 3A act together in restricting the oral bioavailability of paclitaxel.

Jeroen J.M.A. Hendrikkx
Jurjen S. Lagas
Hilde Rosing
Jan H.M. Schellens
Jos H. Beijnen
Alfred H. Schinkel

Abstract

Paclitaxel is avidly transported by P-glycoprotein (P-gp/MDR1/ABCB1). This results in low oral bioavailability, which can be boosted by coadministration of P-gp inhibitors. Unlike paclitaxel, docetaxel is extensively metabolized by CYP3A4 and its oral bioavailability can be enhanced in mice and humans by coadministration of the potent CYP3A inhibitor ritonavir. Unexpectedly, ritonavir also enhances the oral bioavailability of paclitaxel in humans. We aimed to resolve the mechanism underlying this enhancement. Using mice lacking Cyp3a and/or P-gp we investigated the combined and separate restricting roles of Cyp3a and P-gp in the oral bioavailability of paclitaxel, and the boosting effect of ritonavir. CYP3A4-humanized mice were used for translation to the human situation. P-gp had a dominant effect (11.6-fold, $P < 0.001$) over Cyp3a (<1.5-fold, n.s.) in limiting plasma concentrations of oral paclitaxel. However, in the absence of P-gp, Cyp3a decreased paclitaxel plasma concentrations twofold ($P < 0.001$). Coadministered ritonavir inhibited Cyp3a-mediated metabolism, but not P-gp-mediated transport of paclitaxel. Owing to the dominant effect of P-gp, ritonavir enhanced only paclitaxel plasma concentrations in P-gp-deficient mice. Mouse liver microsomes metabolized paclitaxel far less efficiently than human or CYP3A4-transgenic liver microsomes, revealing much lower efficiency of paclitaxel metabolism by mouse than by human CYP3As. Accordingly, ritonavir could enhance the oral bioavailability of paclitaxel in CYP3A4-humanized mice, despite the fact that these mice are P-gp-proficient. Our results show that CYP3A4 inhibition most likely underlies the boosting effect of ritonavir on oral paclitaxel bioavailability in humans. Furthermore, CYP3A4-humanized mice allow improved understanding of CYP3A4-mediated paclitaxel metabolism in humans.

Introduction

Paclitaxel (Taxol[®]) was isolated in the early 1970s from the bark of the *Taxus brevifolia* tree and is approved and widely used as an intravenously administered anticancer agent for various malignancies.¹ Paclitaxel has a poor aqueous solubility and upon oral administration, its intestinal uptake is seriously hampered by the ATP-binding cassette (ABC) drug efflux transporter P-glycoprotein (MDR1/ABCB1/P-gp).²⁻⁷ Consequently, the oral bioavailability of paclitaxel is very low.⁸ Nonetheless, as oral administration has many advantages over intravenous (i.v.) administration⁸, the development of an oral paclitaxel formulation remains the subject of preclinical and clinical studies.⁹ In humans, paclitaxel is mainly metabolized by Cytochrome P450 (CYP) 2C8 and by CYP3A4 upon standard i.v. administration. CYP2C8-mediated metabolism leads to the formation of 6 α -hydroxy-paclitaxel, whereas CYP3A4-mediated metabolism leads to the formation of 3'-p-hydroxy-paclitaxel. Both metabolites are further metabolized by CYP3A4 and CYP2C8, respectively, to yield 6 α ,3'-p-dihydroxy-paclitaxel.¹⁰ In addition to MDR1 P-gp, paclitaxel is also transported by the ABC efflux transporters Multidrug resistance-associated protein 2 (MRP2/ABCC2) and MRP7/ABCC10.^{3,5;10;11}

Several studies have shown that the oral bioavailability of paclitaxel can be boosted by combining paclitaxel with an inhibitor of MDR1.^{2;6;7} However, the impact of drug-metabolizing enzymes on the oral bioavailability of paclitaxel is not yet fully elucidated. The oral plasma AUC (area under the plasma concentration-time curve, which is a measure of the systemic exposure upon oral administration) of docetaxel (Taxotere[®]), a structurally related taxane anticancer drug, can be strongly enhanced in both mice and humans by coadministration of the potent CYP3A4 inhibitor ritonavir.^{12;13} This is explained by the fact that docetaxel is extensively metabolized by CYP3A.¹⁰ Interestingly, although the elimination of paclitaxel is thought to be far less dependent on metabolism by CYP3A4, we recently observed that paclitaxel oral bioavailability in humans can also be substantially improved by coadministration of ritonavir: a proof-of-concept study in cancer patients showed that oral coadministration of 100 mg paclitaxel and 100 mg ritonavir resulted in similar plasma paclitaxel AUC as oral coadministration of 100 mg paclitaxel and 15 mg/kg cyclosporin A, an MDR1 and CYP3A inhibitor.^{14;15} Although in this proof-of-concept study the plasma AUC of paclitaxel when combined with either ritonavir or cyclosporin A was not directly compared to paclitaxel alone, comparison with historical data shows that coadministration of paclitaxel and cyclosporin A results in eight to ninefold increased paclitaxel plasma concentrations in patients, with promising antitumor activity.^{4;16;17} The recent data suggest a fivefold boosting effect of ritonavir on oral paclitaxel AUC. Therefore, it seemed of interest to us to study the underlying mechanism of the boosting effect of ritonavir, also because the subtherapeutic boosting dose of 100 mg ritonavir has a far better safety profile than 15 mg/kg of the immunosuppressant cyclosporin A.

Inhibition of intestinal CYP3A by ritonavir might possibly be responsible for the elevated paclitaxel plasma concentrations after coadministration with ritonavir, because in human enterocytes mainly CYP3A and hardly any CYP2C8 (which is thought to primarily metabolize paclitaxel in the liver) is expressed.¹⁸ On the other hand, it has also been reported that ritonavir could inhibit MDR1 P-gp^{19;20}, which might provide an

alternative explanation for its boosting effect. We therefore aimed to resolve the likely cause of the boosting effect of ritonavir on paclitaxel oral bioavailability.

In our study, we used mice lacking Cyp3a and/or Mdr1a/b P-gp, and Cyp3a knockout mice (Cyp3a^{-/-}) transgenically expressing human CYP3A4 to investigate: i) the combined and separate roles of P-gp and Cyp3a in restricting the oral bioavailability of paclitaxel; and ii) whether the boosting effect of ritonavir on the oral bioavailability of paclitaxel can be explained primarily by inhibition of CYP3A, or P-gp, or possibly of both.

Material and Methods

Drugs and chemicals

Paclitaxel, docetaxel and ritonavir were purchased from Sequoia Research Products (Oxford, United Kingdom). Drug-free lithium-heparinized human plasma was obtained from Bioreclamation LLC (New York, NY, USA). All other chemicals were of analytical grade and obtained from commercial sources.

Animals

Mice used in our study were housed and handled according to institutional guidelines complying with Dutch legislation. Mice were kept in a temperature-controlled environment with a 12-hr light / 12-hr dark cycle and received a standard diet (AM-II, Hope Farms, Woerden, The Netherlands) and acidified water *ad libitum*. Strains used in our study were wildtype, Cyp3a^{-/-}²¹, Mdr1a/b knockout (Mdr1a/b^{-/-})²², and combined Cyp3a and Mdr1a/b knockout mice (Cyp3a/Mdr1a/b^{-/-})²³. Also Cyp3a knockout mice with specific expression of human CYP3A4 in liver, intestine or both liver and intestine (Cyp3a^{-/-}Tg-3A4_{Hep}, Cyp3a^{-/-}Tg-3A4_{Int} and Cyp3a^{-/-}Tg-3A4_{Hep/Int}, respectively) were used.²¹ All strains had a >99% FVB genetic background. In all experiments, male mice of 8-16 weeks of age were used.

In vivo analysis of plasma pharmacokinetics

Prior to the experiments, stock solutions containing 6 mg/mL paclitaxel or 7.5 mg/mL ritonavir in ethanol:polysorbate 80 (1:1, v/v) were made and stored at -20° C. On the day of the experiments stock solutions were diluted with water to obtain solutions containing 1 mg/mL paclitaxel or 1.25 mg/mL ritonavir. Animals were fasted 2 hr before oral drug administration to minimize variation in absorption. Paclitaxel was administered orally or intraperitoneally (i.p.) at a dose of 10 mg per kg of bodyweight. Oral administration was performed by gavage into the stomach using a blunt-ended needle. In case of coadministration with ritonavir, a dose of 12.5 mg ritonavir per kg of bodyweight was administered by gavage 15 min prior to oral paclitaxel administration.

Sample collection

Multiple blood samples (~50 µL) were collected from the tail vein at 15 and 30 min and 1, 2, 4, 8 and 16 hr, using heparinized capillary tubes (Oxford Labware, St. Louis, MO, USA). All samples up to 8 hours after administration were derived from the same

mouse. As the 16 hr time-point was added later, these samples were collected from different animals. At the last time-point of sequential sampling (8 hr) and at the 16 hr time-point, blood was taken by cardiac puncture. Blood samples were centrifuged at ambient temperature at 8,000*g* for 5 min and subsequently plasma was collected. All samples were stored at -20°C until analysis.

Microsomal incubations

Pooled human liver and intestinal microsomes and the nicotinamide adenine dinucleotide phosphate (NADPH) regeneration system were obtained from BD Biosciences (Erembodegem, Belgium). Mouse microsomes were collected as described earlier.²⁴ In brief, mouse liver was collected from five different animals per strain and washed with an ice-cold buffer solution A (50 mM Tris-HCl pH 7.4 containing 250 mM sucrose, 1 mM EDTA and 1 tablet Complete® (Protease inhibitor cocktail) per 45 ml). The livers were homogenized in 50 mM Tris-HCl pH 7.4 supplemented with 150 mM KCl, 1 mM EDTA, 1 tablet Complete® per 45 ml and 20% v/v glycerol. After multiple centrifugation steps, the microsomes were resuspended in buffer solution B and stored at -80°C. Microsomal incubations were performed with human liver and intestinal microsomes and with murine liver microsomes of wildtype and *Cyp3a^{-/-}Tg-3A4_{Hep}* mice. A 150 µL sample containing 10 µM paclitaxel or 10 µM docetaxel, microsomes (protein concentration 0.5 mg/mL for liver microsomes and 1 mg/mL for intestinal microsomes), 100 mM phosphate buffer pH = 7.4 and water was preincubated for 5 min at 37°C. To study the effect of ritonavir-mediated CYP inhibition, the samples containing 2.5 µM ritonavir were also prepared. After preincubation, 50 µL of a NADPH regeneration system was added and the samples were incubated for 15 min at 37°C (Thermomixer Comfort, Eppendorf Netheler Hinz GmbH, Hamburg, Germany), while automatically shaken at 1,000 rpm. After incubation the samples were placed on ice and the enzymatic reaction was stopped by adding 100 µL ice-cold acetonitrile. An aliquot of 200 µL supernatant was collected and sample pretreatment as described for plasma samples was started.

Bioanalytical analysis

A previously developed liquid chromatography coupled with tandem mass spectrometry (LC-MS/MS) assay was used to quantify paclitaxel, 3'-p-hydroxy-paclitaxel and 6α-hydroxy-paclitaxel in plasma samples.²⁵ ¹³C₆-labelled paclitaxel and 10-desacetyl-paclitaxel were used as internal standards for paclitaxel and the metabolites, respectively. In summary, mouse plasma samples of 20 µL were diluted with 180 µL of human plasma. Human plasma was used for dilution of the samples as the concentrations in the undiluted mouse plasma were outside the calibration range and also to mimic the calibration standards which were in human plasma. After dilution of the samples, 25 µL of internal standard working solution was added. Subsequently, the samples were mixed briefly, tertiarybutyl methyl ether was added and the samples were shaken for 10 minutes at 1,250 rpm. The samples were centrifuged at 23,000*g*, snap-frozen and the organic layer was collected. After evaporation of the organic layer, the samples were reconstituted with 100 µL of 10 mM ammonium hydroxide pH 5:acetonitrile (1:1, v/v) and an aliquot was injected into the LC-MS/MS system.

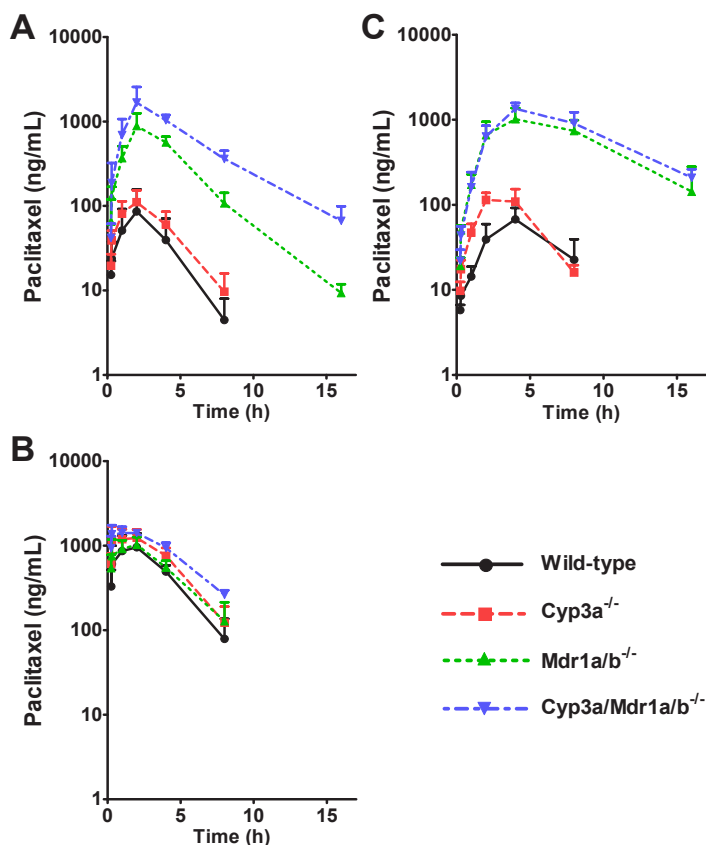


Figure 1. Plasma concentration-time curves in wildtype, Mdr1a/b^{-/-}, Cyp3a^{-/-} and Cyp3a/Mdr1a/b^{-/-} mice, after oral administration of 10 mg/kg paclitaxel without ritonavir (panel A), intraperitoneal administration of 10 mg/kg paclitaxel (panel B) or after oral administration of 10 mg/kg paclitaxel with 12.5 mg/kg ritonavir (panel C).

Calibration standards in human plasma in a range of 0.25-1000 ng/mL or 0.25-100 ng/mL were used for quantification of paclitaxel and metabolites, respectively.

Pharmacokinetic calculations and statistical analysis

Pharmacokinetic parameters, including the area under plasma concentration-time curves (AUCs), were calculated using the software package PK Solutions 2.0.2 (SUMMIT, Research Services, Ashland, OH, USA). One-way ANOVA was used when multiple groups were compared and the Bonferroni posthoc correction was used to accommodate multiple testing. The two-sided unpaired Student's *t* test was used when treatments or differences between two groups were compared. Data that did not show normal distribution were log-transformed to normalize the distribution of the data sets and enable statistical comparison. During all statistical analyses, differences in group sizes were considered in the calculations. Differences were considered statistically significant when $P < 0.05$. All data are presented as mean \pm standard deviation (SD).

Table 1. Plasma pharmacokinetic parameters in wild-type, Mdr1a/b^{-/-}, Cyp3a^{-/-} and Cyp3a/Mdr1a/b^{-/-} mice, after i.p. or oral administration of 10 mg/kg paclitaxel with or without 12.5 mg/kg oral ritonavir.

	Wild-type	Mdr1a/b ^{-/-}	Cyp3a ^{-/-}	Cyp3a/Mdr1a/b ^{-/-}
Intraperitoneal paclitaxel				
Number of animals	6	6	5	6
AUC ₀₋₈ (ng*h/mL)	4036 ± 1084 ^{\$,###,^^^}	4552 ± 606 ^{^^}	5871 ± 829 [*]	7276 ± 945 ^{###,##}
Oral paclitaxel				
Number of animals	10	5	9	5
AUC ₀₋₈ (ng*h/mL)	307 ± 225 ^{###,^^^}	3572 ± 836 ^{###,sss}	446 ± 160 ^{###,^^^}	6934 ± 1901 ^{###,sss}
AUC ₀₋₁₆ (ng*h/mL)		4039 ± 674 ^{^^^}		8645 ± 1701 ^{###}
Oral paclitaxel + ritonavir				
Number of animals	5	5	8	5
AUC ₀₋₈ (ng*h/mL)	322 ± 87 ^{ss,###,^^^}	5896 ± 1652 ^{###,sss,†}	575 ± 153 ^{###,^^^}	6952 ± 1328 ^{###,ss}
AUC ₀₋₁₆ (ng*h/mL)		9205 ± 1780 ^{†††}		11424 ± 2266 ^{††}

Values represent the means ± SD. Symbols correspond with levels of significance as calculated with ANOVA of the Log-transformed data with Bonferroni's post-hoc test. Symbols reflect comparison to Wild-type (*), Mdr1a/b^{-/-} (#), Cyp3a^{-/-} (\$) or Cyp3a/Mdr1a/b^{-/-} (^) mice or to co-administration without ritonavir (†). One, two or three symbols reflect P < 0.05, P < 0.01 and P < 0.001, respectively.

Results

Contribution of Mdr1a/b and Cyp3a to plasma pharmacokinetics of oral paclitaxel.

To study the effect of murine Mdr1a/b P-gp and Cyp3a on paclitaxel exposure after oral administration of paclitaxel (10 mg/kg), we compared paclitaxel plasma concentrations in wildtype, Cyp3a^{-/-}, Mdr1a/b^{-/-} and Cyp3a/Mdr1a/b^{-/-} mice. Although we also screened for 3'-p-OH-paclitaxel and 6α-OH-paclitaxel in all strains, concentrations of these metabolites in plasma were below the lower limit of quantification of the assay (<0.25 ng/mL). In Mdr1a/b^{-/-} mice the area under plasma concentration–time curve from 0 to 8 hr (AUC₀₋₈) was strongly increased (11.6-fold, P < 0.001) relative to wildtype mice (Table 1, Figure 1A). Absence of Cyp3a alone (in Cyp3a^{-/-} mice) caused a 1.5-fold increase in AUC₀₋₈ relative to wildtype, but this was not significant. However, combined absence of Mdr1a/b and Cyp3a resulted in a 22.6-fold increased paclitaxel AUC relative to wildtype mice (P < 0.001). The area under plasma concentration–time curve from 0 to 16 hr (AUC₀₋₁₆) in Cyp3a/Mdr1a/b^{-/-} mice was increased 2.1-fold compared to Mdr1a/b^{-/-} mice (P < 0.001). Comparison of the area under plasma concentration–time curve from 0 extrapolated to infinity (AUC_{0-inf}) gave similar results (see supplementary data 1).

The observation that Mdr1a/b profoundly limits paclitaxel bioavailability after oral administration is in line with the previously described data.^{3,5} Interestingly, however,

the AUC in Cyp3a/Mdr1a/b^{-/-} mice was increased compared to that in Mdr1a/b^{-/-} mice. This demonstrates that, in the absence of Mdr1a/b, murine Cyp3a can also noticeably limit paclitaxel exposure after oral administration.

Our data indicate that the increase in plasma AUC₀₋₈ of paclitaxel in Cyp3a/Mdr1a/b^{-/-} compared to wildtype mice is similar to the combined increases in AUC₀₋₈ in Mdr1a/b^{-/-} and Cyp3a^{-/-} mice (Table 1). Compared to the Cyp3a/Mdr1a/b^{-/-} mice, mice with Mdr1a/b activity and without Cyp3a activity had a 15.5-reduction in AUC₀₋₈, whereas mice without Mdr1a/b activity but with Cyp3a activity had a 1.94-reduction in AUC₀₋₈. As the theoretical product of these two effects (15.5 × 1.94 = 30.1) is slightly higher than the experimentally observed AUC₀₋₈ decrease in wildtype mice (22.6-fold compared to Cyp3a/Mdr1a/b^{-/-} mice), it is clear that there is only an additive, or perhaps even subadditive, effect of Cyp3a and Mdr1a/b in reducing paclitaxel oral exposure.

Contribution of Mdr1a/b and Cyp3a to plasma pharmacokinetics of intraperitoneal paclitaxel.

To discriminate between the Mdr1a/b and the Cyp3a contributions to first-pass clearance in the intestine versus systemic clearance of paclitaxel, we also administered paclitaxel (10 mg/kg) i.p. to the various mouse strains, and thus bypassing the initial intestinal uptake step. In strong contrast to oral paclitaxel administration, in mice lacking Mdr1a/b, paclitaxel plasma AUC₀₋₈ after i.p. administration was not significantly altered compared to wildtype mice (Table 1, Figure 1B). However, in the absence of Cyp3a, plasma AUC of paclitaxel after i.p. administration was 1.5-fold higher compared to that in wildtype mice ($P < 0.05$). Moreover, in Cyp3a/Mdr1a/b^{-/-} mice a 1.8-fold higher paclitaxel plasma AUC compared to wildtype was observed ($P < 0.001$). Paclitaxel plasma AUC₀₋₈ in Cyp3a/Mdr1a/b^{-/-} mice was not significantly increased compared to Cyp3a^{-/-} mice, but it was significantly increased by 1.6-fold ($P < 0.01$) compared to Mdr1a/b^{-/-} mice. These data indicate that after i.p. administration Mdr1a/b does not have a significant impact on paclitaxel plasma concentrations. In contrast, Cyp3a can lower paclitaxel exposure after i.p. administration by 1.5-fold. Again, comparison of the AUC_{0-inf} gave similar results (Supplementary Table 1).

Previously reported i.v. administration of paclitaxel showed a significant difference in plasma AUCs between wildtype and Mdr1a^{-/-} mice⁵, whereas our results after i.p. administration show no difference between wildtype and Mdr1a/b^{-/-} mice. This may relate to the substantial difference in maximal plasma concentrations of paclitaxel obtained after i.p. administration (below ~1,000 ng/mL) versus i.v. administration (exceeding 8,000 ng/mL): the results of Sparreboom et al.⁵ showed similar paclitaxel elimination rates after i.v. administration in wildtype and Mdr1a^{-/-} mice once plasma concentrations went below ~1,000 ng/mL. This is compatible with the absence of a difference between wildtype and Mdr1a/b^{-/-} mice upon i.p. administration, where plasma concentrations did not exceed 1,000 ng/ml (Figure 1B). On the other hand, paclitaxel disappearance from plasma was faster in wildtype mice than in Mdr1a^{-/-} mice whereas plasma concentrations were above ~1,000 ng/ml.⁵ Similar results were observed when paclitaxel was given i.v. to wildtype and Mdr1a/b^{-/-} mice.³ The exact mechanism behind the differences between wildtype and knockout mice in paclitaxel

plasma concentrations arising only above $\sim 1,000$ ng/mL, but not below remains to be determined. It might involve altered distribution and/or elimination of paclitaxel in combination with saturation of non-P-gp paclitaxel clearance mechanisms, that dominate at low plasma concentrations, whereas P-gp dominates at higher plasma concentrations.

Impact of ritonavir on plasma pharmacokinetics of oral paclitaxel.

To investigate the *in vivo* effect of ritonavir on Cyp3a-mediated metabolism and Mdr1-mediated transport of paclitaxel, we orally co-administered paclitaxel (10 mg/kg) and ritonavir (12.5 mg/kg) to the four mouse strains tested above. Paclitaxel plasma AUC_{0-8} was significantly increased (1.65-fold, $P < 0.05$) by ritonavir coadministration only in Mdr1a/b^{-/-} mice, and to a level similar to that seen in Cyp3a/Mdr1a/b^{-/-} mice, with or without ritonavir coadministration (Table 1). The other three strains did not display a significant increase in plasma paclitaxel concentrations (AUC_{0-8} , Table 1, Figure 1C) compared to single paclitaxel administration.

Paclitaxel exposure in Mdr1a/b^{-/-} mice thus appears to be increased through Cyp3a inhibition by ritonavir. However, our results indicate no significant *in vivo* effect of ritonavir on Mdr1a/b-mediated transport of paclitaxel in mice, as paclitaxel plasma AUC_{0-8} in Cyp3a^{-/-} mice was not increased by ritonavir coadministration (Table 1). These results are in line with the data of Bardelmeijer et al¹², which did not demonstrate any effect of ritonavir on *in vitro* transport of docetaxel in human MDR1- and mouse Mdr1a-overexpressing cell lines, whereas paclitaxel transport appeared to be even more difficult to inhibit than docetaxel transport.¹²

In all strains, the time point of reaching maximum plasma concentrations (T_{max}) of paclitaxel was significantly delayed upon coadministration of ritonavir. This observation is likely explained by the reported delaying effect of ritonavir on gastric emptying.^{26;27} This delay did not, however, appear to affect the overall AUC_{0-8} , as indicated by the similar paclitaxel AUCs of Cyp3a/Mdr1a/b^{-/-} mice with and without ritonavir coadministration (Table 1).

Oral coadministration of paclitaxel and ritonavir in CYP3A4-humanized mice

Although murine Cyp3a enzymes are catalytically quite similar to human CYP3A4, there can still be interspecies differences in affinity or metabolic activity towards certain individual substrates or inhibitors. For translation of preclinical data to the human situation, we therefore assessed paclitaxel plasma concentrations after oral administration at 10 mg/kg in mice lacking all murine Cyp3a enzymes, but expressing human CYP3A4. We used the Cyp3a^{-/-} and the humanized Cyp3a^{-/-}Tg-3A4_{Int}, Cyp3a^{-/-}Tg-3A4_{Hep} and Cyp3a^{-/-}Tg-3A4_{Hep/Int} strains, which express human CYP3A4 in intestine, liver, or both intestine and liver, respectively.²¹

Paclitaxel exposure in the two intestinal CYP3A4 transgene-expressing strains was similarly reduced (albeit not statistically significant) compared to that in Cyp3a^{-/-} mice, by 1.4-fold in the Cyp3a^{-/-}Tg-3A4_{Int} mice, and by 1.5-fold in Cyp3a^{-/-}Tg-3A4_{Hep/Int} mice.

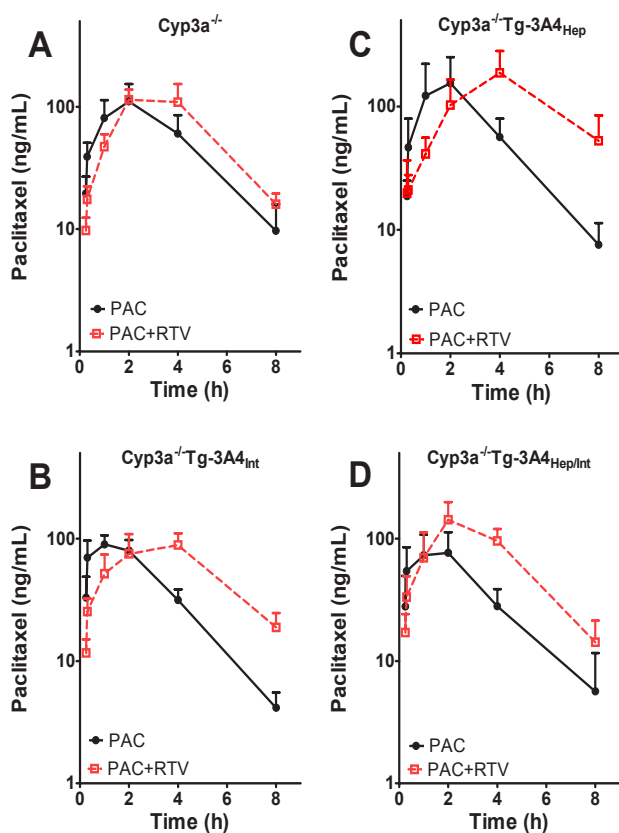


Figure 2. Plasma concentration-time curves after oral administration of 10 mg/kg paclitaxel with or without 12.5 mg/kg ritonavir to *Cyp3a^{-/-}* mice (Panel A), and *Cyp3a^{-/-}* mice expressing human CYP3A4 in liver (panel B), intestine (panel C), or both liver and intestine (panel D). PAC, paclitaxel; RTV, ritonavir.

Table 2. Plasma pharmacokinetic parameters in *Cyp3a^{-/-}* mice expressing human CYP3A4 in liver, intestine, or both, after oral administration of 10 mg/kg paclitaxel with or without 12.5 mg/kg ritonavir.

	<i>Cyp3a^{-/-}</i>	<i>Cyp3a^{-/-}</i> -Tg-3A4 _{Hep}	<i>Cyp3a^{-/-}</i> -Tg-3A4 _{Int}	<i>Cyp3a^{-/-}</i> -Tg-3A4 _{Hep/Int}
Oral paclitaxel				
Number of animals	9	7	5	7
AUC ₀₋₈ (ng*h/mL)	446 ± 160	530 ± 299 [§]	324 ± 30.7	293 ± 77.3*
Oral paclitaxel + ritonavir				
Number of animals	8	6	7	5
AUC ₀₋₈ (ng*h/mL)	575 ± 153	864 ± 291 ^{#†}	467 ± 136 ^{*†}	598 ± 164 ^{††}

Values represent the means ± SD. Symbols correspond with levels of significance as calculated with ANOVA of the Log-transformed data with Bonferroni's post-hoc test. Symbols reflect comparison to *Cyp3a^{-/-}*-Tg-3A4_{Hep} (*), *Cyp3a^{-/-}*-Tg-3A4_{Int} (#), *Cyp3a^{-/-}*-Tg-3A4_{Hep/Int} (\$) or to administration without ritonavir (†). One, two or three symbols reflect $P < 0.05$, $P < 0.01$ and $P < 0.001$, respectively.

Sole hepatic CYP3A4 expression had little impact on the plasma concentrations. (Figure 2, Table 2 and Supplementary Table 2).

In all humanized mouse strains, but not in the *Cyp3a*^{-/-} mice, coadministration of ritonavir resulted in a significant increase in oral paclitaxel plasma AUC₀₋₈: 1.6-fold in the *Cyp3a*^{-/-}Tg-3A4_{Hep} mice ($P < 0.05$), 1.4-fold in the *Cyp3a*^{-/-}Tg-3A4_{Int} mice ($P < 0.05$) and 2.0-fold in the *Cyp3a*^{-/-}Tg-3A4_{Hep/Int} mice ($P < 0.01$) (Figure 2, Table 2). Again, coadministration of ritonavir resulted in a delayed paclitaxel T_{max} in all strains (Figure 2).

Collectively, these data indicate that in the humanized mice inhibition of human CYP3A4 in liver and intestine by ritonavir resulted in modestly increased oral paclitaxel bioavailability. This contrasts with the more limited effect seen in mice only expressing murine *Cyp3a*, where only in the absence of the dominant *Mdr1a/b* P-gp a noticeable increase in paclitaxel AUC could be demonstrated upon ritonavir coadministration (Table 1).

Microsomal incubations with human and murine microsomes

As oral coadministration of paclitaxel and ritonavir did result in increased plasma concentrations of paclitaxel in CYP3A4-humanized mice and in humans, but not in wildtype mice, there might be differences in enzyme activity or substrate specificity of CYP3As between mice and humans. To assess CYP3A activity and substrate specificity for paclitaxel *in vitro*, we incubated paclitaxel with human liver and intestinal microsomes. We compared the obtained results with incubations of paclitaxel with liver microsomes from wildtype mice and from mice expressing human CYP3A4 in the liver (see Figure 3A). As a positive control for activity of the microsomes the metabolism of docetaxel was tested (Figure 3B). The formation of the primary docetaxel metabolites in this

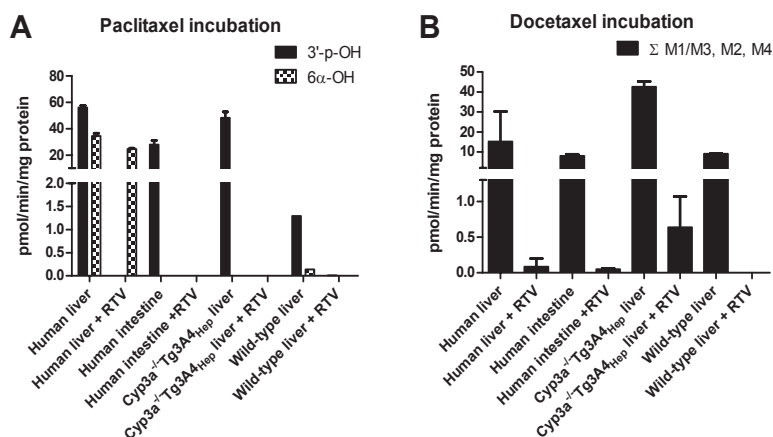


Figure 3. Microsomal incubations with paclitaxel (A) or docetaxel (B) with or without ritonavir (RTV). Metabolite formation in incubation samples with human liver and intestinal microsomes and wildtype and *Cyp3a*^{-/-}Tg3A4_{Hep} murine liver microsomes is presented. For paclitaxel, metabolites 3'-p-hydroxy-paclitaxel (3'-p-OH) and 6α-hydroxy-paclitaxel (6α-OH) were measured and for docetaxel metabolites M1/M3, M2 and M4 were measured and total formation plotted.

experiment was similar to the previously reported metabolite formation²¹, showing that all microsomal preparations used in our experiments were in good condition.

Formation of the CYP3A metabolite 3'-OH-paclitaxel was comparable after incubation with human microsomes and incubation with liver microsomes derived from mice expressing human CYP3A4. With wildtype mouse microsomes, however, only very little paclitaxel metabolite formation was observed (about 1/40th of that observed with human liver microsomes), whereas incubation of docetaxel showed similar levels of metabolite formation in liver microsomes derived from human, wildtype mice and mice expressing human CYP3A4 (Figure 3A and B). These results indicate that murine Cyp3a in wildtype FVB liver metabolizes paclitaxel far less efficiently than human CYP3A4 in either human liver or the CYP3A4-humanized transgenic mouse liver. However, both the murine Cyp3a- and the human CYP3A4-mediated metabolism of paclitaxel was extensively inhibited by ritonavir (Figure 3A). Finally, only upon incubation with human and wildtype mouse liver microsomes we did observe the formation of 6 α -OH-paclitaxel, although this was very low for the mouse liver microsomes (Figure 3A).

Co-incubation with ritonavir resulted in decreased formation of 3'-OH-paclitaxel to concentrations below the detection limit in all the microsomal preparations, both human and mouse, whereas 6 α -OH-paclitaxel formation in human liver microsomes (which is mediated by CYP2C8) was not substantially affected (Figure 3A). As docetaxel metabolites M1/M3, M2 and M4 are all formed through human CYP3A and/or murine Cyp3a^{10;21}, coadministration of the CYP3A inhibitor ritonavir resulted in drastically reduced docetaxel metabolite formation in all the microsomal fractions (Figure 3B).

Discussion

Our data indicate that murine Mdr1a/b and Cyp3a both function to reduce the oral bioavailability of paclitaxel, but Mdr1a/b strongly predominates, and the contribution of Cyp3a comes only to the fore when Mdr1a/b activity is absent. Upon i.p. paclitaxel administration the dominant effect of intestinal Mdr1a/b is circumvented and Cyp3a can noticeably restrict paclitaxel plasma concentrations also in the presence of Mdr1a/b. After oral and i.p. administration, paclitaxel plasma AUC₀₋₈ in the absence of both Cyp3a and Mdr1a/b was very similar. This suggests that, after oral administration at the dosage tested, bioavailability of paclitaxel is primarily limited by Mdr1a/b and Cyp3a, whereas other intestinal drug transporters or metabolic enzymes are of minor importance.

Ritonavir is a potent CYP3A inhibitor in humans and mice, and its coadministration results in increased plasma concentrations of the paclitaxel analogue docetaxel, whereas Mdr1-mediated transport of docetaxel is not affected by ritonavir.^{12;13} Yet, it has been reported that ritonavir is not only a Cyp3a inhibitor, but also a P-gp inhibitor^{19;20}, and coadministration of paclitaxel with other potent P-gp inhibitors in mice results in enhanced bioavailability of paclitaxel.^{2;6;7;28} Some *in vitro* experiments suggest that ritonavir somewhat inhibits Mdr1-mediated transport of paclitaxel²⁹, but *in vivo* inhibition has not been reported so far. Our data show that ritonavir has no noticeable inhibiting effect on Mdr1a/b P-gp mediated transport *in vivo* as paclitaxel plasma AUC

in wildtype and *Cyp3a*^{-/-} mice is not increased after orally co-administered ritonavir. Consistent with the dominant effect of *Mdr1a/b*, inhibition of mouse *Cyp3a* by ritonavir results only in a noticeable effect on the oral bioavailability of paclitaxel in the absence of *Mdr1a/b*. The lack of a noticeable effect of ritonavir on *in vivo* *Mdr1a/b* activity and the dominant effect of *Mdr1a/b* over *Cyp3a* together explain the unchanged paclitaxel plasma AUC₀₋₈ in wildtype mice after coadministration of paclitaxel and ritonavir.

Oral coadministration of ritonavir did significantly increase the oral bioavailability of paclitaxel in transgenic mice overexpressing human CYP3A4 in liver, intestine, or both, but not in *Cyp3a*^{-/-} mice, suggesting that human CYP3A4 in liver and/or intestine reduces paclitaxel bioavailability, albeit modestly. This was noticeable despite the presence of *Mdr1a/b* activity in these strains. We tried to evaluate the relative contribution of liver and intestinal CYP3A to paclitaxel metabolism and its interaction with ritonavir using *Cyp3a*^{-/-}Tg-3A4_{Int} and *Cyp3a*^{-/-}Tg-3A4_{Hep} mice. Interestingly, in both strains paclitaxel plasma AUC₀₋₈ was modestly increased upon ritonavir coadministration, suggesting that ritonavir-mediated CYP3A4 inhibition in both tissues can affect paclitaxel bioavailability.

The difference in ritonavir effect on paclitaxel pharmacokinetics between endogenous murine *Cyp3a* and transgenic CYP3A4 suggested that there is a species difference in CYP3A substrate specificity or enzyme activity. Indeed, the *in vitro* rate of paclitaxel metabolite formation was much higher in human than in mouse liver microsomes. Moreover, in liver microsomes of transgenic mice expressing human CYP3A4, CYP3A4-mediated formation of 3'-p-OH-paclitaxel was similar to that in human liver microsomes. In contrast, metabolite formation rates for docetaxel in liver microsomes from wildtype mice, humans and humanized mice were all in the same range. The difference between wildtype murine and human microsomes in paclitaxel metabolite formation may therefore be owing to a species difference in enzyme activity or affinity towards paclitaxel rather than overall enzyme activity. Experiments comparing paclitaxel behavior in wildtype and *Cyp3a*^{-/-} mice may therefore underestimate the impact of human CYP3A on paclitaxel pharmacokinetics in patients.

In patients it was shown that ritonavir and cyclosporin A can enhance oral paclitaxel exposure to a similar extent.¹⁴ As cyclosporin A is a good P-gp inhibitor with modest CYP3A inhibiting capacity, its boosting effect was primarily attributed to P-gp inhibition.⁴ This was supported by the clinical observation that oral paclitaxel combined with the P-gp inhibitor elacridar (which does not affect CYP3A), yielded similar paclitaxel plasma concentrations in cancer patients as paclitaxel combined with cyclosporin A.^{4,30} Interestingly, our results indicate that (intestinal) CYP3A4 can also seriously hamper the oral paclitaxel bioavailability. Collectively, our data suggest that it is unlikely that the boosting effect of ritonavir on oral paclitaxel bioavailability observed in human patients is due to P-gp inhibition. It seems much more likely that the often substantial levels of intestinal (and hepatic) CYP3A4 in patients significantly contribute to first-pass metabolism of orally administered paclitaxel, and that inhibition of this CYP3A4 by ritonavir explains the boosting effect. In the proof-of-concept study testing oral coadministration of paclitaxel and ritonavir in patients, coadministration of clarithromycin (1,000 mg) and ketoconazole (400 mg) were also tested. These CYP3A4 inhibitors similarly enhanced oral paclitaxel plasma AUCs, confirming the pronounced

restricting role of CYP3A4 in patients.¹⁴ However, because ritonavir can boost paclitaxel uptake at a subtherapeutic dose of 100 mg, this drug has the most favorable safety profile and thus presents the preferable booster.

Our mouse data also add further insight into the cooperation between CYP3A and P-gp in the small intestine. It has been proposed that intestinal P-gp and CYP3A can act together in a synergistic way to reduce oral bioavailability of shared substrate drugs.³¹ Previous studies indicate that intestinal P-gp might improve the efficacy of CYP3A by preventing saturation of the metabolizing enzyme by pumping substrates back into the intestinal lumen.³² A more controversial assertion is that the renewed uptake of those substrates in downstream intestinal cells might lead to repeated and therefore more extensive exposure to Cyp3a-mediated metabolism.³¹ So far, physiologically based pharmacokinetic models have failed to predict the latter effect, and *in vivo* experiments also failed to support this concept.^{23;32} As shown in Results, our present data indicate that murine Mdr1a/b P-gp and Cyp3a function in an additive or subadditive way in reducing the oral bioavailability of paclitaxel. In comparison with the previously analyzed docetaxel²³, paclitaxel is more strongly affected by P-gp than by Cyp3a. Thus, also with this combination of properties, no synergistic effect on paclitaxel bioavailability could be demonstrated. This absence of a noticeable synergistic effect for various drugs with different relative affinities for P-gp and Cyp3a may lead one to question the broader real-life relevance of synergistic Pgp/CYP3A interplay for intestinal drug uptake. Indeed, recent simulation models suggest that only few drugs (2 out of 41 analyzed drugs) might be subject to a noticeable synergistic P-gp/CYP3A interplay, primarily owing to intestinal CYP3A desaturation.³³

Conclusions

In conclusion, our results show that both P-gp and CYP3A are involved in limiting paclitaxel plasma concentrations after oral administration. The boosting effect of ritonavir on oral paclitaxel plasma AUC is caused by CYP3A inhibition and not by Mdr1a/b inhibition. The mechanistic insights from this study may help in improving oral drug formulation strategies for taxanes and related compounds in patients.

References

1. Rowinsky EK, Donehower RC. Paclitaxel (taxol). *N.Engl.J.Med.* **1995**; 332 (15): 1004-14.
2. Bardelmeijer HA, Ouwehand M, Beijnen JH, Schellens JH, van Tellingen O. Efficacy of novel P-glycoprotein inhibitors to increase the oral uptake of paclitaxel in mice. *Invest New Drugs.* **2004**; 22 (3): 219-29.
3. Lagas JS, Vlaming ML, van Tellingen O, Wagenaar E, Jansen RS, Rosing H, Beijnen JH, Schinkel AH. Multidrug resistance protein 2 is an important determinant of paclitaxel pharmacokinetics. *Clin.Cancer Res.* **2006**; 12 (20 Pt 1): 6125-32.
4. Meerum Terwogt JM, Beijnen JH, ten Bokkel Huinink WW, Rosing H, Schellens JH. Coadministration of cyclosporin enables oral therapy with paclitaxel. *Lancet.* **1998**; 352 (9124): 285.
5. Sparreboom A, van Asperen J, Mayer U, Schinkel AH, Smit JW, Meijer DK, Borst P, Nooijen WJ, Beijnen JH, van Tellingen O. Limited oral bioavailability and active epithelial excretion of paclitaxel (Taxol) caused by P-glycoprotein in the intestine. *Proc.Natl.Acad.Sci.U.S.A.* **1997**; 94 (5): 2031-5.
6. van Asperen J, van Tellingen O, Sparreboom A, Schinkel AH, Borst P, Nooijen WJ, Beijnen JH. Enhanced oral bioavailability of paclitaxel in mice treated with the P-glycoprotein blocker SDZ PSC 833. *Br.J.Cancer.* **1997**; 76 (9): 1181-3.
7. van Asperen J, van Tellingen O, van der Valk MA, Rozenhart M, Beijnen JH. Enhanced oral absorption and decreased elimination of paclitaxel in mice cotreated with cyclosporin A. *Clin.Cancer Res.* **1998**; 4 (10): 2293-7.

8. Schellens JHM, Malingre MM, Kruijtzter CM, Bardelmeijer HA, van Tellingen O, Schinkel AH, Beijnen JH. Modulation of oral bioavailability of anticancer drugs: from mouse to man. *Eur.J.Pharm.Sci.* **2000**; 12 (2): 103-10.
9. Koolen SL, Beijnen JH, Schellens JHM. Intravenous-to-oral switch in anticancer chemotherapy: a focus on docetaxel and paclitaxel. *Clin.Pharmacol.Ther.* **2010**; 87 (1): 126-9.
10. Gligorov J, Lotz JP. Preclinical pharmacology of the taxanes: implications of the differences. *Oncologist.* **2004**; 9 (Suppl 2): 3-8.
11. Hopper-Borge EA, Churchill T, Paulose C, Nicolas E, Jacobs JD, Ngo O, Kuang Y, Grinberg A, Westphal H, Chen ZS, Klein-Szanto AJ, Belinsky MG, Kruh GD. Contribution of Abcc10 (Mrp7) to in vivo paclitaxel resistance as assessed in Abcc10(-/-) mice. *Cancer Res.* **2011**; 71 (10): 3649-57.
12. Bardelmeijer HA, Ouwehand M, Buckle T, Huisman MT, Schellens JH, Beijnen JH, van Tellingen O. Low systemic exposure of oral docetaxel in mice resulting from extensive first-pass metabolism is boosted by ritonavir. *Cancer Res.* **2002**; 62 (21): 6158-64.
13. Oostendorp RL, Huitema A, Rosing H, Jansen RS, Ter Heine R, Keessen M, Beijnen JH, Schellens JHM. Coadministration of ritonavir strongly enhances the apparent oral bioavailability of docetaxel in patients with solid tumors. *Clin.Cancer Res.* **2009**; 15 (12): 4228-33.
14. Koolen, S. L. Intravenous-to-oral switch in anticancer chemotherapy. Focus on taxanes and gemcitabine. [Dissertation]. 105-115. 16-2-2011. Utrecht University.
15. Amundsen R, Asberg A, Ohm IK, Christensen H. Cyclosporine A- and tacrolimus-mediated inhibition of CYP3A4 and CYP3A5 in vitro. *Drug Metab Dispos.* **2012**; 40 (4): 655-61.
16. Helgason HH, Kruijtzter CM, Huitema AD, Marcus SG, ten Bokkel Huinink WW, Schot ME, Schornagel JH, Beijnen JH, Schellens JH. Phase II and pharmacological study of oral paclitaxel (Paxoral) plus ciclosporin in anthracycline-pretreated metastatic breast cancer. *Br.J.Cancer.* **2006**; 95 (7): 794-800.
17. Kruijtzter CM, Schellens JH, Mezger J, Scheulen ME, Keilholz U, Beijnen JH, Rosing H, Mathot RA, Marcus S, van TH, Baas P. Phase II and pharmacologic study of weekly oral paclitaxel plus cyclosporine in patients with advanced non-small-cell lung cancer. *J.Clin.Oncol.* **2002**; 20 (23): 4508-16.
18. Thelen K, Dressman JB. Cytochrome P450-mediated metabolism in the human gut wall. *J.Pharm.Pharmacol.* **2009**; 61 (5): 541-58.
19. Drewe J, Gutmann H, Fricker G, Torok M, Beglinger C, Huwyler J. HIV protease inhibitor ritonavir: a more potent inhibitor of P-glycoprotein than the cyclosporine analog SDZ PSC 833. *Biochem.Pharmacol.* **1999**; 57 (10): 1147-52.
20. Holmstock N, Mols R, Annaert P, Augustijns P. In situ intestinal perfusion in knockout mice demonstrates inhibition of intestinal p-glycoprotein by ritonavir causing increased darunavir absorption. *Drug Metab Dispos.* **2010**; 38 (9): 1407-10.
21. van Herwaarden AE, Wagenaar E, van der Kruijssen CM, van Waterschoot RA, Smit JW, Song JY, van der Valk MA, van TO, van der Hoorn JW, Rosing H, Beijnen JH, Schinkel AH. Knockout of cytochrome P450 3A yields new mouse models for understanding xenobiotic metabolism. *J.Clin.Invest.* **2007**; 117 (11): 3583-92.
22. Schinkel AH, Mayer U, Wagenaar E, Mol CA, van DL, Smit JJ, van der Valk MA, Voordouw AC, Spits H, van TO, Zijlmans JM, Fibbe WE, Borst P. Normal viability and altered pharmacokinetics in mice lacking mdr1-type (drug-transporting) P-glycoproteins. *Proc.Natl.Acad.Sci.U.S.A.* **1997**; 94 (8): 4028-33.
23. van Waterschoot RA, Lagas JS, Wagenaar E, van der Kruijssen CM, van Herwaarden AE, Song JY, Rooswinkel RW, van Tellingen O, Rosing H, Beijnen JH, Schinkel AH. Absence of both cytochrome P450 3A and P-glycoprotein dramatically increases docetaxel oral bioavailability and risk of intestinal toxicity. *Cancer Res.* **2009**; 69 (23): 8996-9002.
24. van Waterschoot RA, van Herwaarden AE, Lagas JS, Sparidans RW, Wagenaar E, van der Kruijssen CM, Goldstein JA, Zeldin DC, Beijnen JH, Schinkel AH. Midazolam metabolism in cytochrome P450 3A knockout mice can be attributed to up-regulated CYP2C enzymes. *Mol.Pharmacol.* **2008**; 73 (3): 1029-36.
25. Vainchtein LD, Thijssen B, Stokvis E, Rosing H, Schellens JHM, Beijnen JH. A simple and sensitive assay for the quantitative analysis of paclitaxel and metabolites in human plasma using liquid chromatography/tandem mass spectrometry. *Biomed.Chromatogr.* **2006**; 20 (1): 139-48.
26. Mehendale S, Aung H, Wang CZ, Tong R, Foo A, Xie JT, Yuan CS. Scutellaria baicalensis and a constituent flavonoid, baicalein, attenuate ritonavir-induced gastrointestinal side-effects. *J.Pharm.Pharmacol.* **2007**; 59 (11): 1567-72.
27. Huisman MT, Smit JW, Wiltshire HR, Beijnen JH, Schinkel AH. Assessing safety and efficacy of directed P-glycoprotein inhibition to improve the pharmacokinetic properties of saquinavir coadministered with ritonavir. *J.Pharmacol.Exp.Ther.* **2003**; 304 (2): 596-602.
28. Bardelmeijer HA, Beijnen JH, Brouwer KR, Rosing H, Nooijen WJ, Schellens JH, van Tellingen O. Increased oral bioavailability of paclitaxel by GF120918 in mice through selective modulation of P-glycoprotein. *Clin.Cancer Res.* **2000**; 6 (11): 4416-21.
29. Washington CB, Duran GE, Man MC, Sikic BI, Blaschke TF. Interaction of anti-HIV protease inhibitors with the multidrug transporter P-glycoprotein (P-gp) in human cultured cells. *J.Acquir.Immune.Defic.Syindr.Hum.Retrovirol.* **1998**; 19 (3): 203-9.

30. Malingre MM, Beijnen JH, Rosing H, Koopman FJ, Jewell RC, Paul EM, ten Bokkel Huinink WW, Schellens JH. Coadministration of GF120918 significantly increases the systemic exposure to oral paclitaxel in cancer patients. *Br.J.Cancer.* **2001**; 84 (1): 42-7.
31. Benet LZ. The drug transporter-metabolism alliance: uncovering and defining the interplay. *Mol.Pharm.* **2009**; 6 (6): 1631-43.
32. van Waterschoot RA, Schinkel AH. A critical analysis of the interplay between cytochrome P450 3A and P-glycoprotein: recent insights from knockout and transgenic mice. *Pharmacol.Rev.* **2011**; 63 (2): 390-410.
33. Darwich AS, Neuhoff S, Jamei M, Rostami-Hodjegan A. Interplay of metabolism and transport in determining oral drug absorption and gut wall metabolism: a simulation assessment using the "Advanced Dissolution, Absorption, Metabolism (ADAM)" model. *Curr.Drug Metab.* **2010**; 11 (9): 716-29.

Supplementary table 1. Plasma pharmacokinetic parameters in wild-type, Mdr1a/b^{-/-}, Cyp3a^{-/-} and Cyp3a/Mdr1a/b^{-/-} mice, after i.p. or oral administration of 10 mg/kg paclitaxel with or without 12.5 mg/kg oral ritonavir.

	Wild-type			Cyp3a ^{-/-}		
	Wild-type	Mdr1a/b ^{-/-}	Cyp3a ^{-/-}	Cyp3a/Mdr1a/b ^{-/-}		
Intraperitoneal paclitaxel						
Number of animals	6	6	5	6		
AUC ₀₋₈ (ng*h/mL)	4036 ± 1084 ^{§,^^}	4552 ± 606 ^{^^}	5871 ± 829 [*]	7276 ± 945 ^{***,##}		
AUC _{0-inf} (ng*h/mL)	4332 ± 883	5096 ± 873 ^{^^}	6218 ± 904 [*]	8195 ± 1065 ^{***,##}		
Oral paclitaxel						
Number of animals	10	5	9	5		
AUC ₀₋₈ (ng*h/mL)	307 ± 225 ^{##,^^,^^}	3572 ± 836 ^{***,§§§}	446 ± 160 ^{###,^^,^^}	6934 ± 1901 ^{***,§§§}		
AUC ₀₋₁₆ (ng*h/mL)		4039 ± 674 ^{^^}		8645 ± 1701 ^{##}		
AUC _{0-inf} (ng*h/mL)	320 ± 224 ^{##,^^,^^}	3954 ± 824 ^{***,§§§}	471 ± 174 ^{###,^^,^^}	8830 ± 199 ^{9***,§§§}		
C _{max} (ng/mL)	87.6 ± 70.2 ^{##,^^,^^}	912 ± 327 ^{***,§§§}	112 ± 41 ^{###,^^,^^}	1784 ± 742 ^{***,§§§}		
T _{max} (h)	2.2 ± 0.67	2.4 ± 0.89	1.8 ± 0.44	2.4 ± 0.89		
F _{app} (%)	7.6	78.5	7.6	95.3		
Oral paclitaxel + ritonavir						
Number of animals	5	5	8	5		
AUC ₀₋₈ (ng*h/mL)	322 ± 87 ^{§§,##,^^,^^}	5896 ± 1652 ^{***,§§§,†}	575 ± 153 ^{**,#,^^,^^}	6952 ± 1328 ^{***,§§}		
AUC ₀₋₁₆ (ng*h/mL)		9205 ± 1780 ^{††}		11424 ± 2266 ^{††}		
C _{max} (ng/mL)	67.5 ± 24.2 ^{§§,##,^^,^^}	1058 ± 304 ^{***,§§§}	128 ± 36.7 ^{**,#,##,^^,^^}	1346 ± 230 ^{***,§§§}		
T _{max} (h)	3.6 ± 0.89 [†]	4.0 ± 0.00 ^{††}	2.8 ± 1.04 [†]	4.0 ± 0.00 ^{††}		

Values represent the means ± SD. Symbols correspond with levels of significance as calculated with ANOVA of the Log-transformed data with Bonferroni's post-hoc test. Symbols reflect comparison to wild-type (*), Mdr1a/b^{-/-} (#), Cyp3a^{-/-} (§) or Cyp3a/Mdr1a/b^{-/-} (^) mice or to administration without ritonavir (†). One, two or three symbols reflect P < 0.05, P < 0.01 and P < 0.001, respectively.

Supplementary table 2. Plasma pharmacokinetic parameters in Cyp3a^{-/-} mice expressing human CYP3A4 in liver, intestine, or both, after oral administration of 10 mg/kg paclitaxel with or without 12.5 mg/kg ritonavir.

	Cyp3a ^{-/-}		Cyp3a ^{-/-} Tg-3A4 ^{Hep}		Cyp3a ^{-/-} Tg-3A4 ^{Int}		Cyp3a ^{-/-} Tg-3A4 ^{Hep/Int}	
Number of animals								
paclitaxel	9	7	5	7	5	7	5	7
paclitaxel + ritonavir	8	6	7	6	7	5	6	5
AUC₀₋₈ (ng*h/mL)								
paclitaxel	446 ± 160	530 ± 299 ^s	324 ± 30.7	293 ± 77.3*	324 ± 30.7	293 ± 77.3*	324 ± 30.7	293 ± 77.3*
paclitaxel + ritonavir	575 ± 153	864 ± 291 ^{#,†}	467 ± 136 ^{†,‡}	598 ± 164 ^{††}	467 ± 136 ^{†,‡}	598 ± 164 ^{††}	467 ± 136 ^{†,‡}	598 ± 164 ^{††}
C_{max} (ng/mL)								
paclitaxel	112 ± 41	155 ± 96.5	95.6 ± 18.5	91.0 ± 38.5	95.6 ± 18.5	91.0 ± 38.5	95.6 ± 18.5	91.0 ± 38.5
paclitaxel + ritonavir	128 ± 36.7	204 ± 68.2 [#]	91.9 ± 27.8*	143 ± 55.2	91.9 ± 27.8*	143 ± 55.2	91.9 ± 27.8*	143 ± 55.2
T_{max} (h)								
paclitaxel	1.8 ± 0.44	1.86 ± 0.38	1.20 ± 0.45	1.43 ± 0.54	1.20 ± 0.45	1.43 ± 0.54	1.20 ± 0.45	1.43 ± 0.54
paclitaxel + ritonavir	2.8 ± 1.04	4.33 ± 1.97 ^{††}	2.40 ± 0.89 [†]	3.71 ± 0.76 ^{†††}	2.40 ± 0.89 [†]	3.71 ± 0.76 ^{†††}	2.40 ± 0.89 [†]	3.71 ± 0.76 ^{†††}

Values represent the means ± SD. Symbols correspond with levels of significance as calculated with ANOVA of the Log-transformed data with Bonferroni's post-hoc test. Symbols reflect comparison to Cyp3a^{-/-}Tg-3A4_{Hep} (*), Cyp3a^{-/-}Tg-3A4_{Int} (#), Cyp3a^{-/-}Tg-3A4_{Hep/Int} (\$) or to administration without ritonavir (†). One, two or three symbols reflect P < 0.05, P < 0.01 and P < 0.001, respectively.

Oral co-administration of elacridar
and ritonavir safely enhances
plasma levels of oral paclitaxel and
docetaxel without affecting relative
brain accumulation.

Jeroen J.M.A. Hendrikkx
Jurjen S. Lagas
Els Wagenaar
Hilde Rosing
Jan H.M. Schellens
Jos H. Beijnen
Alfred H. Schinkel

Abstract

The intestinal uptake of the taxanes paclitaxel and docetaxel is seriously hampered by drug efflux through P-glycoprotein (P-gp) and drug metabolism via Cytochrome P450 (CYP) 3A. The resulting low oral bioavailability can be boosted by co-administration of P-gp or CYP3A4 inhibitors. We examined whether it would be feasible and safe to substantially increase the oral availability of taxanes by simultaneous inhibition of P-gp by elacridar and CYP3A by ritonavir using CYP3A4-humanized mice. Oral co-administration of the taxanes with elacridar resulted in complete inhibition of intestinal and hepatic P-gp and increased plasma concentrations of paclitaxel (10.7-fold, $P < 0.001$) and docetaxel (4.0-fold, $P < 0.001$). Co-administration with ritonavir virtually completely inhibited intestinal and hepatic CYP3A4 and resulted in 2.5-fold ($P < 0.001$) and 7.3-fold ($P < 0.001$) increases in plasma concentrations of paclitaxel and docetaxel, respectively. Co-administration with both inhibitors simultaneously resulted in further increased plasma concentrations of paclitaxel (31.9-fold, $P < 0.001$) and docetaxel (37.4-fold, $P < 0.001$). Although boosting of orally applied taxanes with elacridar and ritonavir potentially increases brain accumulation of taxanes, we found that only brain concentrations, but not brain-to-plasma ratios, were increased after co-administration with both inhibitors. This indicates that neither the circulating elacridar levels, nor the increased plasma taxane levels were sufficient to substantially inhibit or saturate the taxane export activity at the blood-brain barrier. We therefore conclude that the oral availability of taxanes can be enhanced by co-administration with oral elacridar and ritonavir, without invoking the risk of increased CNS toxicity of the taxanes.

Introduction

The taxane anticancer agents paclitaxel (Taxol®) and docetaxel (Taxotere®) share the baccatin core ring structure.¹ Currently, paclitaxel and docetaxel are routinely applied intravenously to treat several types of cancer, such as non-small cell lung cancer (NSCLC), ovarian, breast, gastric, prostate and head-and-neck cancer.^{2,3}

The development of oral formulations of paclitaxel and docetaxel is the focus of preclinical and clinical research in our groups because oral administration has many advantages over i.v. administration.^{2,4} Oral administration is more practical and convenient for patients, since oral medication can be taken by the patient at home while i.v. administration requires hospitalisation during infusion. Oral administration in the home situation also reduces treatment cost. Moreover, oral administration enables other dosing schedules like metronomic therapy (e.g. continuous or frequent treatment with low doses of anticancer drugs), which can increase efficacy of taxane treatment and reduce adverse effects caused by high plasma concentrations of docetaxel or paclitaxel.^{5,6}

A major limitation in the concept of oral administration of taxanes is, however, the low oral availability of paclitaxel and docetaxel.^{2,4} Paclitaxel and docetaxel have poor aqueous solubility and upon oral administration, intestinal uptake is seriously hampered by drug efflux through P-glycoprotein (P-gp/MDR1/ABCB1) and systemic exposure is further limited by drug metabolism via Cytochrome P450 (CYP) 3A.⁷⁻¹⁴ P-gp is a member of the ATP-binding cassette (ABC) efflux transporter family and is expressed in multiple tissues like intestine, liver, and kidney, but also at the blood-brain barrier.¹⁵ P-gp-mediated transport limits drug absorption across intestinal cells and brain penetration across the blood-brain barrier (BBB). In enterocytes, P-gp pumps back absorbed taxanes into the intestinal lumen, while at the blood-brain barrier, taxanes are pumped back into the systemic circulation. In liver and kidney, P-gp increases drug excretion by active efflux transport into the bile and urine.¹⁶

CYP3A is a member of the CYP superfamily and CYP enzymes are responsible for most phase-I drug metabolism.¹⁷ CYP enzymes are mainly expressed in the liver, but some CYP members are also expressed in enterocytes. CYP3A is the most abundant CYP enzyme in liver and intestine, representing 40% and 80% of the total CYP enzymes expressed in each tissue, respectively.¹⁸ Docetaxel is primarily metabolized by enzymes of the CYP3A subfamily, while paclitaxel is metabolized by both CYP3A4 and CYP2C8.¹ In contrast to CYP3A, CYP2C8 is only expressed in liver cells.¹⁸

Although docetaxel is a good P-gp substrate, transport of paclitaxel by P-gp is even more efficient. In addition, paclitaxel metabolism is not solely CYP3A dependent. Therefore, it was assumed that oral bioavailability of paclitaxel was primarily limited by P-gp, and that of docetaxel primarily by CYP3A. However, in mice, complete versus single knockout of P-gp and/or Cyp3a genes resulted in further increased plasma exposure of paclitaxel and docetaxel alike after oral administration, suggesting that both systems are important for oral availability of both taxanes.^{13,14} The importance of CYP3A4 for paclitaxel metabolism was further supported by our finding that human

CYP3A4 metabolizes paclitaxel far more efficiently than the mouse Cyp3a enzymes.¹³ Therefore, a promising strategy to boost the oral availability of these taxanes is combining oral formulations of paclitaxel or docetaxel with inhibitors of both P-gp and CYP3A4. In (pre-)clinical studies it has already been demonstrated that the area under the plasma concentration-time curves (AUC) after oral administration of paclitaxel and docetaxel can be strongly enhanced in both mice and humans by co-administration of the potent CYP3A4 inhibitor ritonavir.^{13;19-21} In addition, co-administration of the potent P-gp inhibitor elacridar results in increased oral plasma AUC of paclitaxel in mice and humans.^{22;23}

There are potential risks involved when the oral bioavailability of paclitaxel and docetaxel is increased by inhibition of metabolizing enzymes and drug transporters. For instance, co-administration of oral elacridar in mice resulted in increased brain penetration of intravenously administered paclitaxel by inhibition of P-gp at the blood-brain barrier.²⁴ Therefore, boosting oral uptake of taxanes using an oral P-gp inhibitor might increase the relative risk of CNS toxicity. Furthermore, oral administration of docetaxel or paclitaxel to mice lacking both P-gp and Cyp3a resulted in substantially higher plasma levels than administration of the taxanes to mice lacking either P-gp or Cyp3a alone. Simultaneous inhibition of P-gp and CYP3A by drugs that are co-administered with orally administered taxanes may lead to further increased plasma levels of the taxanes and therefore an increased risk of side effects and toxicity in clinical practice.

In the present preclinical study, we examined whether it would be feasible and safe to substantially increase the oral availability of taxanes by simultaneous inhibition of P-gp and CYP3A using oral co-administration of elacridar and ritonavir, without affecting P-gp transport at the blood-brain barrier.

Materials and Methods

Drugs and chemicals

Paclitaxel, docetaxel, elacridar HCl and ritonavir were purchased from Sequoia Research Products (Oxford, UK). Drug-free lithium-heparinized human plasma was obtained from Bioreclamation LLC (New York, NY, USA). All other chemicals were of analytical grade and obtained from commercial sources.

Animals

Mice used in this study were housed and handled according to institutional guidelines complying with Dutch legislation. Mice were kept in a temperature-controlled environment with a 12-hr light / 12-hr dark cycle and received a standard diet (AM-II, Hope Farms, Woerden, The Netherlands) and acidified water *ad libitum*. In this study Cyp3a knockout mice with specific expression of human CYP3A4 in liver and intestine (Cyp3a^{-/-}Tg-3A4_{Hep/Int}) were used.²⁵ The strain had a >99% FVB genetic background. Cyp3a^{-/-}Tg-3A4_{Hep/Int} mice were used since there is a species difference for paclitaxel in CYP3A substrate specificity or enzyme activity between endogenous murine Cyp3a

and human CYP3A4.¹³ Experiments comparing paclitaxel PK in wild-type mice may therefore underestimate the impact of human CYP3A on paclitaxel pharmacokinetics in patients. The difference between species is minimized using Cyp3a^{-/-}Tg-3A4_{Hep/Int} mice. A basic difference in docetaxel metabolite formation was not observed between human, wild-type mice and Cyp3a^{-/-}Tg-3A4_{Hep/Int} mice.¹³ In all experiments, male mice of 9-14 weeks of age were used.

In vivo analysis of plasma pharmacokinetics

Prior to the experiments, stock solutions containing 6 mg/mL paclitaxel, 6 mg/mL docetaxel, 15 mg/mL elacridar HCl, 7.5 mg/mL ritonavir or 15 mg/mL elacridar HCl and 7.5 mg/mL ritonavir in ethanol:polysorbate 80 (1:1, v/v) were made and stored at -20° C. On the day of the experiments stock solutions were diluted with water (1:5, v/v) to obtain solutions for administration. Animals were fasted 2 hours before oral drug administration to minimize variation in absorption. Paclitaxel and docetaxel were administered orally at a dose of 10 mg per kg of bodyweight, ritonavir was administered orally at a dose of 12.5 mg per kg of bodyweight, and elacridar was administered orally at a dose of 25 mg per kg of bodyweight. Oral administration was performed by gavage into the stomach using a blunt-ended needle. In case of co-administration with ritonavir, elacridar, or ritonavir and elacridar, the booster(s) were orally administered 15 min prior to oral taxane administration.

Sample collection

For determining plasma pharmacokinetics, multiple blood samples (~50 µL) were collected from the tail vein at 15 minutes and at 1, 2, 4, 8 and 24 hours, using heparinized capillary tubes (Oxford Labware, St. Louis, MO, USA). All time point samples were derived from the same mouse. At the last time point of sequential sampling (48 hr), blood was taken by cardiac puncture. Blood samples were centrifuged at ambient temperature at 8,000 *g* for 5 minutes and subsequently plasma was collected. All samples were stored at -20°C until analysis.

For brain accumulation studies, blood samples at 2 hours were taken by cardiac puncture and brain tissue was isolated. Blood samples were centrifuged at ambient temperature at 8,000 *g* for 5 minutes and subsequently plasma was collected. Brain tissue was homogenized in 1% bovine serum albumin. All samples were stored at -20°C until analysis. Brain-to-plasma ratios at *t* = 2 hours were calculated per mouse by dividing the brain concentration by the corresponding plasma concentration.

Bioanalytical analysis

Previously developed liquid chromatography assays coupled with tandem mass spectrometry detection (LC-MS/MS) were used to quantify paclitaxel²⁶ and docetaxel²⁷. Labeled structure analogues were used as internal standards. In summary, mouse plasma samples of 20 µL were diluted with 180 µL of human plasma. Human plasma was used for dilution of the samples as the concentrations in the undiluted mouse plasma were outside the calibration range and also to mimic the calibration standards, which were in human plasma. Brain samples were not diluted since concentrations were too

low to quantify after dilution in some samples. To 200 μL of diluted plasma sample or homogenized brain sample, 25 μL of internal standard working solution was added. Subsequently, the samples were mixed briefly, tertiary-butyl methyl ether was added and the samples were shaken for 10 minutes at 1250 rpm. The samples were centrifuged at 23,000 g , snap-frozen and the organic layer was collected. After evaporation of the organic layer, the samples were reconstituted with reconstitution solvent and an aliquot was injected into the LC-MS/MS system. Calibration standards in human plasma in a range of 0.25-1000 ng/mL or 0.25-500 ng/mL were used for quantification of paclitaxel and docetaxel, respectively.

Pharmacokinetic calculations and statistical analysis

Pharmacokinetic parameters, including the area under the plasma concentration-time curves (AUCs), were calculated using the software package PK Solutions 2.0.2 (SUMMIT, Research Services, Ashland, OH, USA). One-way ANOVA was used when multiple groups were compared and the Bonferroni post-hoc correction was used to accommodate multiple testing. The two-sided unpaired Student's t test was used when treatments or differences between two groups were compared. Data that did not show normal distribution were log-transformed to normalize the distribution of the datasets and enable statistical comparison. During all statistical analyses, differences in group sizes were considered in the calculations. Differences were considered statistically significant when $P < 0.05$. All data are presented as mean \pm SD.

Addition of previously reported data

Previously, we published AUCs of paclitaxel after oral administration of 10 mg/kg paclitaxel with and without 12.5 mg/kg ritonavir to Cyp3a^{-/-}Tg-3A4_{Hep/Int} mice (5 and 7 animals were used, respectively).¹³ These data were compared with plasma concentrations after oral administration of 10 mg/kg paclitaxel with and without 12.5 mg/kg ritonavir obtained in this study (6 and 4 animals were used, respectively). Previously obtained results were not statistically different from the results in the present study (data not shown). Therefore these results were also used to decrease the number of animals needed for this study.

Comparison with previously reported data in knockout mice

To estimate the extent of P-gp inhibition by elacridar and Cyp3a inhibition by ritonavir, plasma exposure after chemical inhibition was compared to plasma exposure after complete knockout of P-gp or Cyp3A. Previously reported plasma AUCs extrapolated to infinity ($\text{AUC}_{0-\text{inf}}$) after oral administration of 10 mg/kg paclitaxel¹³ or 10 mg/kg docetaxel¹⁴ to mice lacking P-gp, Cyp3a, or both, were compared with $\text{AUC}_{0-\text{inf}}$ s after chemical inhibition as obtained in this study. All plasma AUCs were normalized for their matching control group and these relative plasma AUCs were used for comparison.

Results

Paclitaxel exposure after oral co-administration with elacridar and/or ritonavir

To study the effect of the P-gp inhibitor elacridar and the CYP3A inhibitor ritonavir on oral bioavailability of paclitaxel, we orally administered 10 mg/kg paclitaxel to the CYP3A4-humanized $Cyp3a^{-/-}Tg-3A4_{Hep/Int}$ mice and combined paclitaxel administration with 25 mg/kg elacridar and/or 12.5 mg/kg ritonavir.

Oral co-administration of paclitaxel and elacridar or paclitaxel and ritonavir resulted in increased plasma concentrations of paclitaxel (Figure 1). AUC_{0-inf} was 10.7-fold higher after co-administration with elacridar than after single paclitaxel administration ($P < 0.001$). These results in humanized mice are in line with the previously observed 6.6-fold increase in paclitaxel AUC after oral co-administration of paclitaxel and elacridar at the same dose to wild-type mice.²² Co-administration of paclitaxel and ritonavir resulted in an increase in the AUC_{0-inf} of 2.5-fold ($P < 0.001$). However, this boosting effect with ritonavir was clearly less than that of elacridar co-administration. Co-administration of paclitaxel with both elacridar and ritonavir together resulted in further increased plasma concentrations of paclitaxel (31.9-fold higher than single paclitaxel administration; $P <$

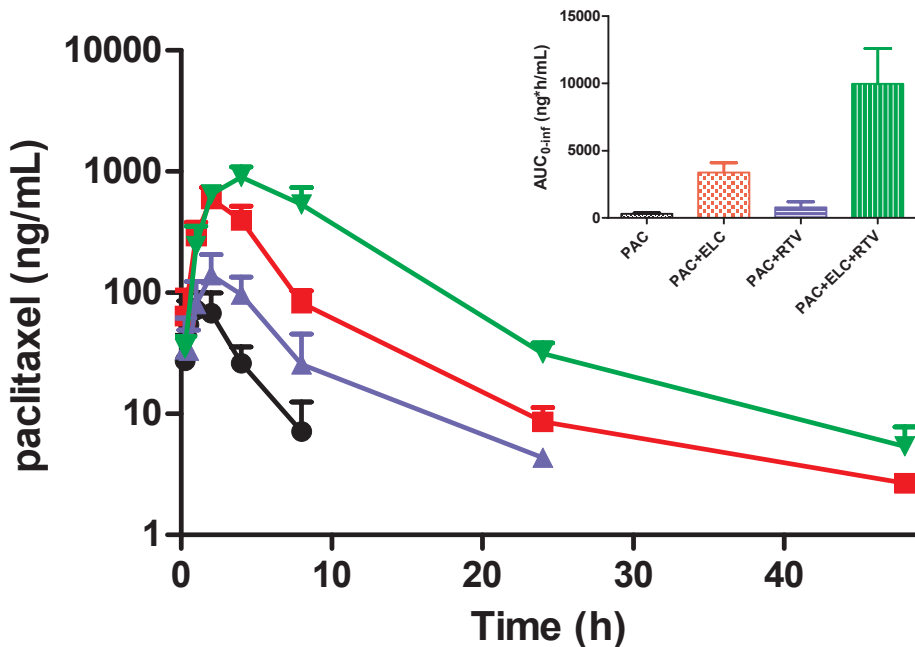


Figure 1. Plasma concentration-time curves in $Cyp3a^{-/-}$ mice expressing human CYP3A4 in liver and intestine ($Cyp3a^{-/-}Tg-3A4_{Hep/Int}$) after oral administration of 10 mg/kg paclitaxel. Paclitaxel was administered alone (●) or co-administered with 25 mg/kg oral elacridar (■), 12.5 mg/kg oral ritonavir (▲) or both elacridar and ritonavir (▼). Insets show the area under the plasma concentration-time curves from 0 extrapolated to infinity (AUC_{0-inf}). Differences in AUC_{0-inf} between all groups were statistically significantly different ($P < 0.001$), unless stated otherwise (NS, $P > 0.05$). Abbreviations: PAC: paclitaxel; ELC: elacridar; RTV: ritonavir.

Table 1. Area under the plasma concentration-time curve of paclitaxel and docetaxel after oral administration of 10 mg/kg paclitaxel or 10 mg/kg docetaxel in Cyp3a^{-/-}Tg-3A4_{Hep/Int} mice. Both drugs were administered as a single dose or co-administered with an oral dose of the CYP3A4 inhibitor ritonavir (12.5 mg/kg), the P-gp inhibitor elacridar (25 mg/kg) or both. Data are compared with previously reported data after oral administration of paclitaxel¹³ or docetaxel¹⁴ to wild-type mice, Mdr1a/b knockout (Mdr1a/b^{-/-}), Cyp3a knockout (Cyp3a^{-/-}), and combined Mdr1a/b and Cyp3a knockout mice (Cyp3a/Mdr1a/b^{-/-}).

	Control group ¹⁾	P-gp inhib./ KO	CYP3A inhib./ KO	CYP3A and P-gp inhib./KO
Oral paclitaxel				
AUC _{0-inf} (ng*h/mL) after inhibition	314 ± 74	3373 ± 725	780 ± 412	10002 ± 2652
Fold vs control	1	10.7	2.5	31.9
AUC_{0-inf} (ng*h/mL) in knockout				
AUC _{0-inf} (ng*h/mL) in knockout	320 ± 224	3954 ± 825	471 ± 174	8830 ± 1999
Fold vs control	1	12.4	1.5	27.6
Oral docetaxel				
AUC _{0-inf} (ng*h/mL) after inhibition	157 ± 67	626 ± 182	1146 ± 281	5869 ± 2520
Fold vs control	1	4.0	7.3	37.4
AUC_{0-inf} (ng*h/mL) in knockout				
AUC _{0-inf} (ng*h/mL) in knockout	228 ± 130	645 ± 272	2627 ± 1011	16466 ± 2020
Fold vs control	1	2.8	11.5	72.2

Values represent the means ± SD. 5-11 animals per group were used.

Abbreviations: AUC_{0-inf}: area under the plasma concentration-time curve from 0 extrapolated to infinity; CYP3A: Cytochrome P450 3A; Cyp3a^{-/-}Tg-3A4_{Hep/Int}: Cyp3a knockout mice with specific expression of human CYP3A4 in liver and intestine; KO: knockout; P-gp: P-glycoprotein (MDR1; ABCB1); SD: standard deviation.

¹⁾ When murine P-gp and human CYP3A are inhibited, the control group reflects single drug administration in Cyp3a^{-/-}Tg-3A4_{Hep/Int} mice. When murine P-gp and murine Cyp3a are knocked out, the control group reflects single drug administration in wild-type mice.

0.001). The increases in oral AUC_{0-inf} of paclitaxel after chemical inhibition with elacridar or ritonavir, alone or in combination, were comparable to the increases in oral AUC_{0-inf} after complete genetic knockout of P-gp or Cyp3a, alone or in combination (Table 1). These data suggest that virtually complete inhibition of both P-gp and CYP3A4 (intestinal and hepatic) was achieved with the combination elacridar and ritonavir.

Docetaxel exposure after oral co-administration with elacridar and/or ritonavir

Parallel to the paclitaxel experiments, we studied the effect of elacridar and/or ritonavir co-administration on the oral bioavailability of docetaxel. In the CYP3A4-humanized mouse model, we observed a 7.3-fold increase in AUC_{0-inf} after oral administration of docetaxel and ritonavir when compared with AUC_{0-inf} after single docetaxel administration (P < 0.001; Figure 2). Oral co-administration of docetaxel and elacridar resulted in a 4.0-fold increase compared to single docetaxel administration (P < 0.001). The AUC_{0-inf} of docetaxel after boosting with elacridar was not significantly different from the AUC_{0-inf} after boosting with ritonavir (P > 0.05). As observed for paclitaxel, co-administration of docetaxel with both elacridar and ritonavir resulted in

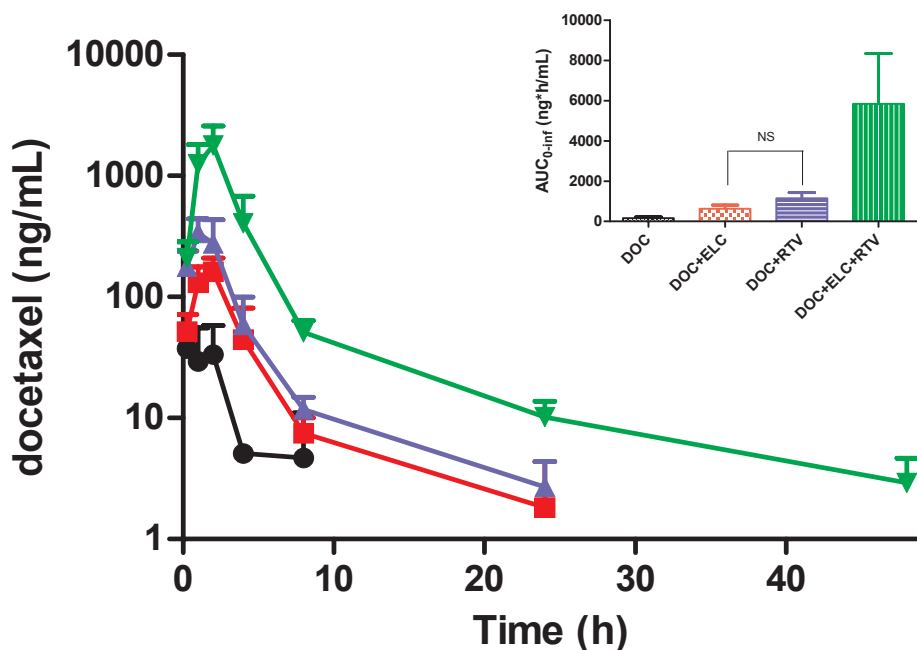


Figure 2. Plasma concentration-time curves in *Cyp3a^{-/-}* mice expressing human CYP3A4 in liver and intestine (*Cyp3a^{-/-}*Tg-3A4_{Hep/Int}) after oral administration of 10 mg/kg docetaxel. Docetaxel was administered alone (●) or co-administered with 25 mg/kg oral elacridar (■), 12.5 mg/kg oral ritonavir (▲) or both elacridar and ritonavir (▼). Insets show the area under the plasma concentration-time curves from 0 extrapolated to infinity (AUC_{0-inf}). Differences in AUC_{0-inf} between all groups were statistically significantly different ($P < 0.001$), unless stated otherwise (NS, $P > 0.05$). Abbreviations: DOC: docetaxel; ELC: elacridar; RTV: ritonavir.

a further increase in AUC_{0-inf} (37.4-fold higher than single docetaxel administration; $P < 0.001$). The increase in oral AUC_{0-inf} of docetaxel after chemical inhibition with elacridar was comparable to the increase in oral AUC_{0-inf} after complete genetic knockout of P-gp. However, the increase after chemical inhibition with ritonavir was modestly, but significantly ($P < 0.01$) lower than after complete genetic knockout of *Cyp3a*, and the same was true for combined CYP3A4 and P-gp inhibition compared to full *Cyp3a* and P-gp knockout ($P < 0.001$; Table 1). These data suggest that for docetaxel in the transgenic mice the inhibition of intestinal and hepatic CYP3A4 by ritonavir was not entirely complete.

Brain concentrations of taxanes after oral co-administration with elacridar and/or ritonavir

Since brain accumulation could potentially be increased after boosting of oral taxanes with a P-gp inhibitor, we measured brain concentrations two hours after oral administration of paclitaxel or docetaxel, i.e., roughly around the plasma T_{max} . Two effects might occur: firstly, increased taxane brain concentrations simply as a consequence of the higher plasma levels of the taxanes; and secondly, a further,

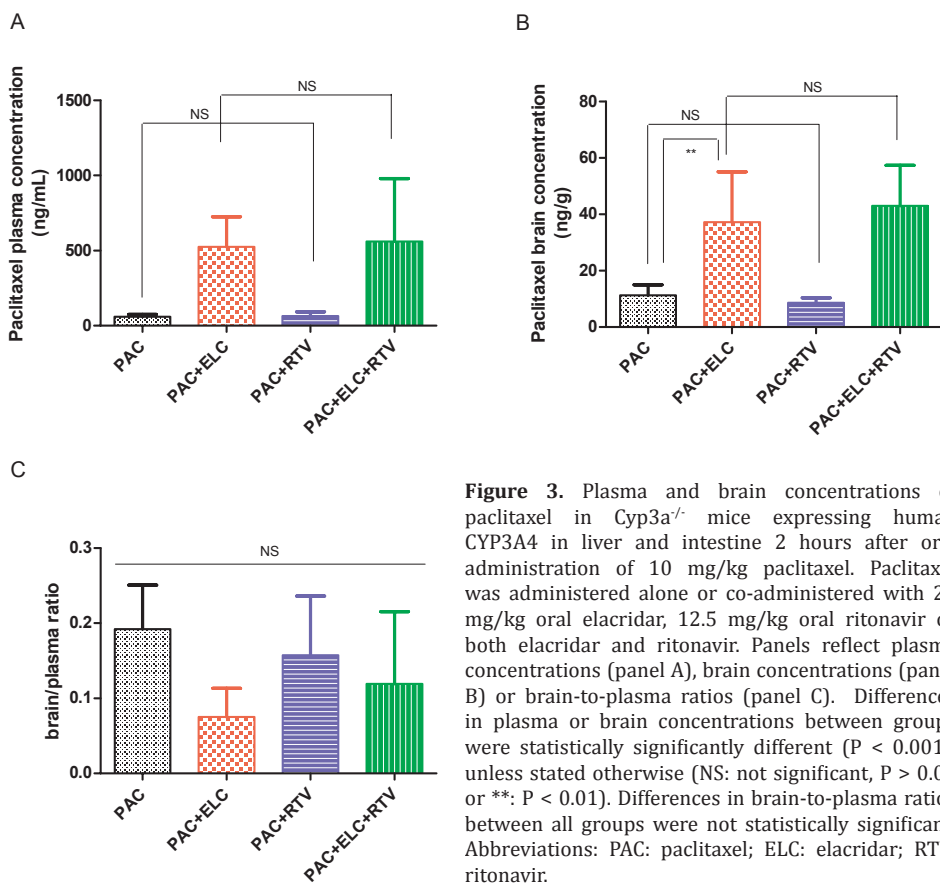


Figure 3. Plasma and brain concentrations of paclitaxel in *Cyp3a^{-/-}* mice expressing human CYP3A4 in liver and intestine 2 hours after oral administration of 10 mg/kg paclitaxel. Paclitaxel was administered alone or co-administered with 25 mg/kg oral elacridar, 12.5 mg/kg oral ritonavir or both elacridar and ritonavir. Panels reflect plasma concentrations (panel A), brain concentrations (panel B) or brain-to-plasma ratios (panel C). Differences in plasma or brain concentrations between groups were statistically significantly different ($P < 0.001$), unless stated otherwise (NS: not significant, $P > 0.05$ or **: $P < 0.01$). Differences in brain-to-plasma ratios between all groups were not statistically significant. Abbreviations: PAC: paclitaxel; ELC: elacridar; RTV: ritonavir.

disproportionate increase in brain concentration relative to the plasma levels due to inhibition of P-gp at the blood-brain barrier, and/or possibly saturation of P-gp activity at the blood-brain barrier due to the much higher plasma taxane levels. The second effects could result in poorly predictable alterations in CNS toxicity of the taxanes. As these effects are most likely to occur when plasma levels of both taxanes and inhibitors are high, we chose the 2-hour time point for sampling. Maximum plasma concentrations of docetaxel and paclitaxel are reached at two to four hours after oral administration. We did not measure plasma concentrations of the inhibitors in this experiment, but maximum plasma concentrations are reached in wild-type mice around two hours after oral administration of elacridar²² or ritonavir (Supplemental Figure 1).

Brain concentrations of paclitaxel were significantly increased after co-administration with elacridar ($P < 0.01$ vs. single paclitaxel administration), but not after co-administration with ritonavir ($P > 0.05$; Figure 3B). Co-administration of paclitaxel with both elacridar and ritonavir resulted in a similar increase in brain concentrations as after co-administration of paclitaxel and elacridar ($P > 0.05$ vs. paclitaxel and elacridar administration; $P < 0.001$ vs. single paclitaxel administration). However, correcting for the increased plasma levels after boosting (Figure 3A), brain-

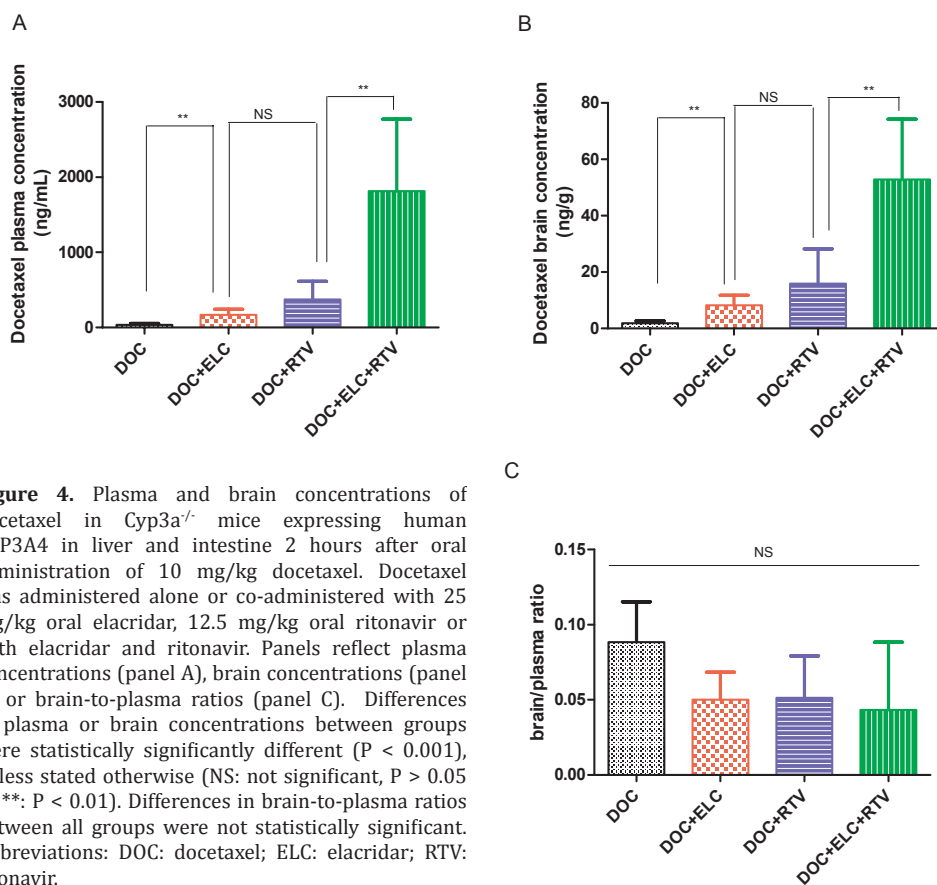


Figure 4. Plasma and brain concentrations of docetaxel in *Cyp3a^{-/-}* mice expressing human CYP3A4 in liver and intestine 2 hours after oral administration of 10 mg/kg docetaxel. Docetaxel was administered alone or co-administered with 25 mg/kg oral elacridar, 12.5 mg/kg oral ritonavir or both elacridar and ritonavir. Panels reflect plasma concentrations (panel A), brain concentrations (panel B) or brain-to-plasma ratios (panel C). Differences in plasma or brain concentrations between groups were statistically significantly different ($P < 0.001$), unless stated otherwise (NS: not significant, $P > 0.05$ or **: $P < 0.01$). Differences in brain-to-plasma ratios between all groups were not statistically significant. Abbreviations: DOC: docetaxel; ELC: elacridar; RTV: ritonavir.

to-plasma ratios were not different between the groups ($P > 0.05$ for all comparisons; Figure 3C). These data suggest that the relative brain accumulation of paclitaxel was not altered by elacridar and ritonavir co-administration, despite the substantially increased plasma levels of paclitaxel and the circulating elacridar levels.

Co-administration with elacridar also increased docetaxel brain concentrations ($P < 0.01$ vs. single docetaxel administration; Figure 4B). In contrast to paclitaxel brain concentrations, docetaxel brain concentrations were substantially increased after co-administration with ritonavir to comparable levels as seen after co-administration with elacridar ($P > 0.05$ vs. docetaxel and elacridar administration; $P < 0.001$ vs. single docetaxel administration), thus more or less following the pattern of effects of the inhibitors on docetaxel plasma concentrations. Brain concentrations of docetaxel were further increased after co-administration with both ritonavir and elacridar ($P < 0.001$ vs. single docetaxel administration). However, the increase in docetaxel brain concentrations was primarily caused by the increased plasma concentrations after boosting (Figure 4A), since brain-to-plasma ratios were not different between any of the treatment groups ($P > 0.05$ for all comparisons; Figure 4C).

Discussion

Our data with CYP3A4-humanized mice show that it is possible to dramatically enhance the plasma AUC of oral paclitaxel and docetaxel (30- to 40-fold) by orally co-administering elacridar and ritonavir. Each inhibitor contributed substantially to the overall AUC increase, although the contribution of elacridar was stronger for paclitaxel, and that of ritonavir for docetaxel. Yet, at the same time, the relative brain accumulation of the taxanes (corrected for the increased plasma levels) was not increased. This indicates that neither the circulating elacridar levels, nor the increased plasma taxane levels were sufficient to substantially inhibit or saturate the taxane export activity at the blood-brain barrier. These data suggest that it may be possible to greatly enhance the oral availability of taxanes in patients by co-administration with oral elacridar and ritonavir, without invoking the risk of increased CNS toxicity of the taxanes.

To estimate the extent of P-gp inhibition by elacridar and CYP3A4 inhibition by ritonavir, plasma exposures after chemical inhibition were compared to plasma exposures after complete knockout of P-gp and/or Cyp3a (Table 1). Plasma AUC_{0-inf} s of paclitaxel and docetaxel were comparable after complete knockout of P-gp and after chemical inhibition of P-gp by elacridar. This suggests that the intestinal and hepatic inhibition of P-gp was complete at the used dose of elacridar.

The plasma AUC_{0-inf} s of paclitaxel were similar after complete gene knockout of Cyp3a and inhibition of CYP3A4 by ritonavir, but the plasma AUC_{0-inf} of docetaxel was slightly lower after ritonavir inhibition than upon Cyp3a knockout. The difference is not substantial (Table 1), but it can probably be attributed to incomplete inhibition of human CYP3A4 in the CYP3A4-humanized mice at later time points, as the ritonavir concentrations likely drop considerably after a few hours. Although not tested in these mice, ritonavir levels in plasma of wild-type mice receiving 12.5 mg/kg oral ritonavir drop substantially after 2 hours (Supplemental Figure 1), which may result in incomplete CYP3A4 inhibition at later time points. The effect may be more obvious for docetaxel than for paclitaxel because docetaxel metabolism is more strongly CYP3A-dependent.¹⁴

Previously reported data showed that complete knockout of both P-gp and Cyp3a resulted in higher plasma concentrations of orally applied taxanes than single knockout of P-gp or Cyp3a.^{13;14} We show here that chemical inhibition of P-gp and CYP3A4 with both elacridar and ritonavir likewise further increased plasma concentrations of orally applied taxanes. In humans, oral formulations of paclitaxel and docetaxel were thus far tested with only one of these boosters. In patients, oral availability of paclitaxel is boosted by elacridar²³ or ritonavir²⁰ and oral availability of docetaxel is boosted by ritonavir.^{21;28} Our results suggest that boosting of orally applied taxanes by both elacridar and ritonavir might further increase plasma exposure of taxanes in patients. Moreover, combined inhibition of P-gp and CYP3A4 may result in decreased interpatient and inpatient variability in taxane pharmacokinetics. Xenobiotics, like other drugs, herbal derivatives or environmental pollutants can cause clinically relevant P-gp and CYP3A4 induction via Pregnane X receptor (PXR) regulation²⁹⁻³¹, but polymorphisms of genes encoding for P-gp and CYP3A4 are currently not related to variability in pharmacokinetics of taxanes.^{32;33} Complete inhibition of both P-gp and CYP3A4 in

intestine and liver by elacridar and ritonavir can eliminate the effects of xenobiotic-related induction and thereby decrease variability in taxane pharmacokinetics after oral administration. Not only CYP3A4 induction, but also incomplete CYP3A4 inhibition by various other co-administered drugs might contribute to variable oral taxane plasma exposure.^{34,35} Complete inhibition of CYP3A by ritonavir might eliminate this risk. It should be noted that, since P-gp and CYP3A4 act at both the intestinal and hepatic level, the risk of interpatient and inpatient variability after oral administration of taxanes is likely higher than after intravenous administration of taxanes, as two potentially variable barriers need to be passed instead of one. This underscores the importance of reducing potential sources of variability by using effective CYP3A and P-gp inhibitors in oral taxane regimens.

Boosting orally applied taxanes with elacridar and ritonavir potentially increases the relative brain penetration of taxanes and would thereby increase the risk of brain toxicity, by either substantial inhibition of BBB P-gp by the circulating elacridar, or saturation of BBB P-gp activity due to the highly increased plasma taxane levels, or a combination of both. We found here that brain concentrations were increased after co-administration of the taxanes with elacridar and ritonavir, but brain-to-plasma ratios were not. This indicates that the increased brain concentrations after oral co-administration of the taxanes with elacridar or ritonavir were merely a consequence of the increased plasma concentrations. Kemper et al.²⁴ showed a 4-fold increase in brain-to-plasma ratios at one hour after administration of 10 mg/kg intravenously administered paclitaxel due to 25 mg/kg orally administered elacridar. This 4-fold increase was comparable with the increase in brain-to-plasma ratios as observed after intravenous administration of paclitaxel to P-gp knockout mice. Brain concentrations were not further increased when the elacridar dose was increased to 100 mg/kg. Both findings suggest that 25 mg/kg oral elacridar can largely, if not completely, inhibit BBB P-gp activity. However, in our experiments we observed no increase in brain-to-plasma ratios after oral co-administration of the same dose of paclitaxel and elacridar. This can most likely be explained by the initially far higher plasma levels of paclitaxel after intravenous administration compared to those after oral administration. When operating close to saturation, P-gp at the blood-brain barrier will be more sensitive to partial inhibition.³⁶ The absence of increased brain-to-plasma ratios in the experiments by Kemper et al.²⁴ at 4 hours after administration of intravenous paclitaxel and oral elacridar (when plasma concentrations of paclitaxel are much lower) further supports this interpretation. Collectively, our data suggest that at modest plasma concentrations of paclitaxel (and presumably also docetaxel), P-gp in the BBB has little or no effect on the relative brain accumulation of taxanes.

Conclusions

Comparison of the results in our study with previously reported data obtained from oral administration of taxanes to knockout mice showed that orally administered elacridar and ritonavir at comparatively low doses can completely (for paclitaxel), or almost completely (for docetaxel) inhibit intestinal and hepatic P-gp and CYP3A4 activity.

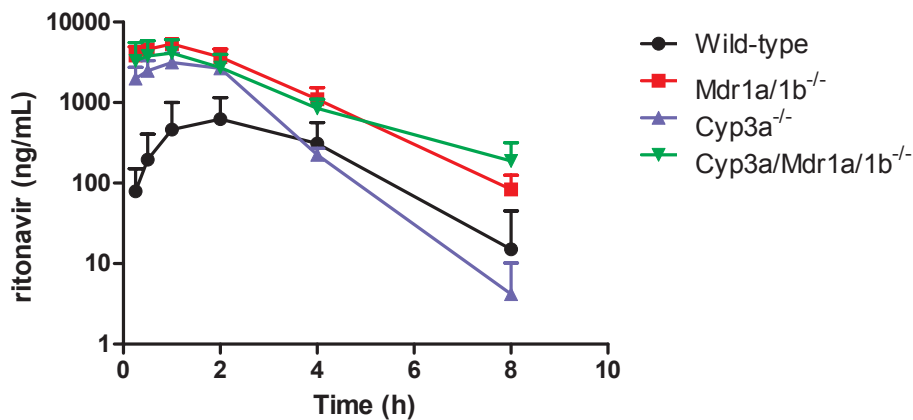
We also demonstrated that co-administration of the taxanes with elacridar and ritonavir simultaneously resulted in a further increase in plasma levels of the taxanes. In contrast, relative brain accumulation of the taxanes was not affected after boosting with oral elacridar. Even at the highly increased plasma concentrations of taxanes after boosting with both elacridar and ritonavir, relative brain accumulation was still similar as seen after boosting with elacridar, or even in otherwise untreated CYP3A4-humanized animals.

We therefore believe that it will be worthwhile testing whether simultaneous inhibition of P-gp and CYP3A may provide a relatively safe strategy to boost plasma exposure of orally applied taxanes in patients, as relative brain exposure is unlikely to be higher than that in the currently used i.v. schedules.

References

1. Vaishampayan U, Parchment RE, Jasti BR, Hussain M. Taxanes: an overview of the pharmacokinetics and pharmacodynamics. *Urology* **1999**; 54 (6A Suppl): 22-9.
2. Koolen SL, Beijnen JH, Schellens JHM. Intravenous-to-oral switch in anticancer chemotherapy: a focus on docetaxel and paclitaxel. *Clin.Pharmacol.Ther.* **2010**; 87 (1): 126-9.
3. Gligorov J, Lotz JP. Preclinical pharmacology of the taxanes: implications of the differences. *Oncologist.* **2004**; 9 Suppl 2): 3-8.
4. Schellens JHM, Malingre MM, Kruijtzter CM, Bardelmeijer HA, van Tellingen O, Schinkel AH, Beijnen JH. Modulation of oral bioavailability of anticancer drugs: from mouse to man. *Eur.J.Pharm.Sci.* **2000**; 12 (2): 103-10.
5. Wu H, Xin Y, Zhao J, Sun D, Li W, Hu Y, Wang S. Metronomic docetaxel chemotherapy inhibits angiogenesis and tumor growth in a gastric cancer model. *Cancer Chemother.Pharmacol.* **2011**; 68 (4): 879-87.
6. Jiang H, Tao W, Zhang M, Pan S, Kanwar JR, Sun X. Low-dose metronomic paclitaxel chemotherapy suppresses breast tumors and metastases in mice. *Cancer Invest.* **2010**; 28 (1): 74-84.
7. Bardelmeijer HA, Ouwehand M, Beijnen JH, Schellens JH, van Tellingen O. Efficacy of novel P-glycoprotein inhibitors to increase the oral uptake of paclitaxel in mice. *Invest New Drugs.* **2004**; 22 (3): 219-29.
8. Lagas JS, Vlaming ML, van Tellingen O, Wagenaar E, Jansen RS, Rosing H, Beijnen JH, Schinkel AH. Multidrug resistance protein 2 is an important determinant of paclitaxel pharmacokinetics. *Clin.Cancer Res.* **2006**; 12 (20 Pt 1): 6125-32.
9. Meerum Terwogt JM, Beijnen JH, ten Bokkel Huinink WW, Rosing H, Schellens JH. Co-administration of cyclosporin enables oral therapy with paclitaxel. *Lancet.* **1998**; 352 (9124): 285.
10. Sparreboom A, van Asperen J, Mayer U, Schinkel AH, Smit JW, Meijer DK, Borst P, Nooijen WJ, Beijnen JH, van Tellingen O. Limited oral bioavailability and active epithelial excretion of paclitaxel (Taxol) caused by P-glycoprotein in the intestine. *Proc.Natl.Acad.Sci.U.S.A.* **1997**; 94 (5): 2031-5.
11. van Asperen J, van Tellingen O, Sparreboom A, Schinkel AH, Borst P, Nooijen WJ, Beijnen JH. Enhanced oral bioavailability of paclitaxel in mice treated with the P-glycoprotein blocker SDZ PSC 833. *Br.J.Cancer.* **1997**; 76 (9): 1181-3.
12. van Asperen J, van Tellingen O, van der Valk MA, Rozenhart M, Beijnen JH. Enhanced oral absorption and decreased elimination of paclitaxel in mice cotreated with cyclosporin A. *Clin.Cancer Res.* **1998**; 4 (10): 2293-7.
13. Hendriks JJ, Lagas JS, Rosing H, Schellens JH, Beijnen JH, Schinkel AH. P-glycoprotein and cytochrome P450 3A act together in restricting the oral bioavailability of paclitaxel. *Int.J.Cancer.* **2013**; 132 (10): 2439-47.
14. van Waterschoot RA, Lagas JS, Wagenaar E, van der Kruijssen CM, Herwaarden AE, Song JY, Rooswinkel RW, van Tellingen O, Rosing H, Beijnen JH, Schinkel AH. Absence of both cytochrome P450 3A and P-glycoprotein dramatically increases docetaxel oral bioavailability and risk of intestinal toxicity. *Cancer Res.* **2009**; 69 (23): 8996-9002.
15. Gottesman MM, Ambudkar SV. Overview: ABC transporters and human disease. *J.Bioenerg.Biomembr.* **2001**; 33 (6): 453-8.
16. Glaeser H, Fromm MF. Animal models and intestinal drug transport. *Expert.Opin.Drug Metab Toxicol.* **2008**; 4 (4): 347-61.
17. Thelen K, Dressman JB. Cytochrome P450-mediated metabolism in the human gut wall. *J.Pharm.Pharmacol.* **2009**; 61 (5): 541-58.
18. Paine MF, Hart HL, Ludington SS, Haining RL, Rettie AE, Zeldin DC. The human intestinal cytochrome P450 "pie". *Drug Metab Dispos.* **2006**; 34 (5): 880-6.
19. Bardelmeijer HA, Ouwehand M, Buckle T, Huisman MT, Schellens JH, Beijnen JH, van Tellingen O. Low systemic exposure

- of oral docetaxel in mice resulting from extensive first-pass metabolism is boosted by ritonavir. *Cancer Res.* **2002**; 62 (21): 6158-64.
20. Koolen, S. L. Intravenous-to-oral switch in anticancer chemotherapy. Focus on taxanes and gemcitabine. [Dissertation]. 105-115. 16-2-2011. Utrecht University.
 21. Oostendorp RL, Huitema A, Rosing H, Jansen RS, Ter Heine R, Keessen M, Beijnen JH, Schellens JHM. Coadministration of ritonavir strongly enhances the apparent oral bioavailability of docetaxel in patients with solid tumors. *Clin.Cancer Res.* **2009**; 15 (12): 4228-33.
 22. Bardelmeijer HA, Beijnen JH, Brouwer KR, Rosing H, Nooijen WJ, Schellens JH, van Tellingen O. Increased oral bioavailability of paclitaxel by GF120918 in mice through selective modulation of P-glycoprotein. *Clin.Cancer Res.* **2000**; 6 (11): 4416-21.
 23. Malingre MM, Beijnen JH, Rosing H, Koopman FJ, Jewell RC, Paul EM, ten Bokkel Huinink WW, Schellens JH. Co-administration of GF120918 significantly increases the systemic exposure to oral paclitaxel in cancer patients. *Br.J.Cancer.* **2001**; 84 (1): 42-7.
 24. Kemper EM, van Zandbergen AE, Cleypool C, Mos HA, Boogerd W, Beijnen JH, van Tellingen O. Increased penetration of paclitaxel into the brain by inhibition of P-Glycoprotein. *Clin.Cancer Res.* **2003**; 9 (7): 2849-55.
 25. van Herwaarden AE, Wagenaar E, van der Kruijssen CM, van Waterschoot RA, Smit JW, Song JY, van der Valk MA, van Tellingen O, van der Hoorn JW, Rosing H, Beijnen JH, Schinkel AH. Knockout of cytochrome P450 3A yields new mouse models for understanding xenobiotic metabolism. *J.Clin.Invest.* **2007**; 117 (11): 3583-92.
 26. Stokvis E, Ouwehand M, Nan LG, Kemper EM, van Tellingen O, Rosing H, Beijnen JH. A simple and sensitive assay for the quantitative analysis of paclitaxel in human and mouse plasma and brain tumor tissue using coupled liquid chromatography and tandem mass spectrometry. *J.Mass Spectrom.* **2004**; 39 (12): 1506-12.
 27. Kuppens IE, van Maanen MJ, Rosing H, Schellens JHM, Beijnen JH. Quantitative analysis of docetaxel in human plasma using liquid chromatography coupled with tandem mass spectrometry. *Biomed.Chromatogr.* **2005**; 19 (5): 355-61.
 28. Marchetti S, Stuurman FE, Koolen SL, Moes JJ, Hendrikx JJ, Thijssen B, Huitema AD, Nuijen B, Rosing H, Keessen M, Voest EE, Mergui-Roelvink M, Beijnen JH, Schellens JH. Phase I study of weekly oral docetaxel (ModraDoc001) plus ritonavir in patients with advanced solid tumors. *ASCO Meeting Abstracts* **2012**; 30 (15_suppl): 2550.
 29. di Masi A, De Marinis E, Ascenzi P, Marino M. Nuclear receptors CAR and PXR: Molecular, functional, and biomedical aspects. *Mol.Aspects Med.* **2009**; 30 (5): 297-343.
 30. Wojnowski L. Genetics of the variable expression of CYP3A in humans. *Ther.Drug Monit.* **2004**; 26 (2): 192-9.
 31. Xu C, Li CY, Kong AN. Induction of phase I, II and III drug metabolism/transport by xenobiotics. *Arch.Pharm.Res.* **2005**; 28 (3): 249-68.
 32. Bosch TM, Meijerman I, Beijnen JH, Schellens JH. Genetic polymorphisms of drug-metabolising enzymes and drug transporters in the chemotherapeutic treatment of cancer. *Clin.Pharmacokinet.* **2006**; 45 (3): 253-85.
 33. Jabir RS, Naidu R, Annuar MA, Ho GF, Munisamy M, Stanslas J. Pharmacogenetics of taxanes: impact of gene polymorphisms of drug transporters on pharmacokinetics and toxicity. *Pharmacogenomics.* **2012**; 13 (16): 1979-88.
 34. Koolen SL, Oostendorp RL, Beijnen JH, Schellens JHM, Huitema AD. Population pharmacokinetics of intravenously and orally administered docetaxel with or without co-administration of ritonavir in patients with advanced cancer. *Br.J.Clin. Pharmacol.* **2010**; 69 (5): 465-74.
 35. Quinney SK, Malireddy SR, Vuppalanchi R, Hamman MA, Chalasani N, Gorski JC, Hall SD. Rate of onset of inhibition of gut-wall and hepatic CYP3A by clarithromycin. *Eur.J.Clin.Pharmacol.* **2013**; 69 (3): 439-48.
 36. Kalvass JC, Polli JW, Bourdet DL, Feng B, Huang SM, Liu X, Smith QR, Zhang LK, Zamek-Gliszczynski MJ. Why clinical modulation of efflux transport at the human blood-brain barrier is unlikely: the ITC evidence-based position. *Clin. Pharmacol.Ther.* **2013**; 94 (1): 80-94.



Supplemental figure 1. Plasma concentration-time curves of ritonavir after oral co-administration of 10 mg/kg paclitaxel and 12.5 mg/kg ritonavir to wild-type, Mdr1a/b knockout (Mdr1a/b^{-/-}), Cyp3a knockout (Cyp3a^{-/-}), and combined Mdr1a/b and Cyp3a knockout mice (Cyp3a/Mdr1a/b^{-/-}). Data are unpublished data from previously reported experiments.¹³

Human OATP1B1, OATP1B3 and OATP1A2 mediate the in vivo uptake of docetaxel.

Jeroen J.M.A. Hendrikk*

Dilek Iusuf*

Anita van Esch

Evita van de Steeg

Els Wagenaar

Jos H. Beijnen

Alfred H. Schinkel

* Both authors contributed equally

Abstract

Purpose: Organic Anion Transporting Polypeptides (human: OATPs, mouse: Oatps) are uptake transporters with important roles in drug pharmacokinetics and toxicity. We aimed to study the *in vivo* impact of mouse and human OATP1A/1B transporters on docetaxel plasma clearance and liver and intestinal uptake.

Experimental Design: Docetaxel was administered to Oatp1a/1b knockout and liver-specific humanized OATP1B1, OATP1B3 and OATP1A2 transgenic mice. Experiments were conducted with a low polysorbate 80 (2.8%) formulation, as 8% polysorbate somewhat inhibited docetaxel plasma clearance after intravenous administration.

Results: After intravenous administration (10 mg/kg) Oatp1a/1b knockout mice had a ~3-fold higher plasma AUC, while the liver concentrations remained unchanged in comparison with wild-type mice. Impaired liver uptake was evident from the significantly reduced (~3-fold) liver-to-plasma ratios after *i.v.* administration. Absence of mouse Oatp1a/1b transporters did not affect the intestinal absorption of orally administered docetaxel (10 mg/kg), while the systemic exposure of docetaxel was again substantially increased due to impaired liver uptake. Most importantly, liver-specific expression of each of the human OATP1B1, OATP1B3 and OATP1A2 transporters provided a nearly complete rescue of the increased plasma levels of docetaxel in Oatp1a/1b-null mice after intravenous administration (10 mg/kg).

Conclusions: One or more of the mouse Oatp1a/1b transporters, and each of the human OATP1A/1B transporters can mediate docetaxel uptake *in vivo*. This might be clinically relevant for OATP1A/1B-mediated tumor uptake of docetaxel and for docetaxel clearance in patients in which the transport activity of OATP1A/1B transporters is reduced due to genetic variation or pharmacological inhibition, leading to potentially altered toxicity.

Introduction

One of the most widely used chemotherapeutic drugs is docetaxel, a microtubule inhibitor approved for the treatment of breast, lung, ovarian, prostate, gastric, and head and neck cancers.¹ An important problem in docetaxel therapy is the inter-patient variability in docetaxel exposure which in turn can lead to unpredictable dose-limiting toxicity (neutropenia, diarrhea) and/or variability in response to treatment.² Factors which control plasma exposure to docetaxel include drug-metabolizing enzymes and drug transporters.² One of the major clearance mechanisms of docetaxel is metabolism by Cytochrome P450 3A (CYP3A), a drug-metabolizing enzyme complex expressed in both the intestine and liver.³ Although there are substantial inter-individual differences in expression and activity of CYP3A enzymes, this alone cannot explain entirely the inter-patient variability after intravenously administered docetaxel.¹ Recent studies pointed to low-activity polymorphic variants of drug transporters involved in the clearance of docetaxel as contributors to the unpredictable systemic exposure of docetaxel.^{1;4;5} These transporters involve efflux transporters from the ATP-binding cassette (ABC) transporter family (ABCB1 or ABCC2), but also uptake transporters of the Organic Anion Transporting Polypeptide (OATP) family.^{1;6}

The OATP superfamily of sodium-independent influx transporters consists of 6 families, of which the OATP1B subfamily is best studied with respect to clinical pharmacogenetics of drugs.⁷ It is important to note that between mouse and human Oatps there are no straightforward orthologs, for example humans have only one OATP1A transporter (OATP1A2), while in mouse there are at least 4 known (Oatp1a1, Oatp1a4, Oatp1a5 and Oatp1a6). In contrast, humans have 2 OATP1B transporters, (OATP1B1 and OATP1B3), while in mouse there is only one (Oatp1b2).⁸

Due to their localization in pharmacokinetically relevant tissues (liver, small intestine and kidney) and their capacity to transport many drugs, OATP1A/1B transporters are thought to play a major role in the distribution, pharmacodynamics and toxicity of many drugs.⁹⁻¹¹ In the liver, OATP1B1 and OATP1B3 are highly expressed on the basolateral membrane of hepatocytes where they mediate the hepatic uptake, and therefore clearance of many xenobiotics.⁸ OATP1A2 is mainly expressed in other tissues, like brain, kidney, and small intestine, while in the liver it is expressed in cholangiocytes but not in hepatocytes. Its role in drug distribution remains to be elucidated.⁸ It is thought that in the small intestine human OATP1A2 and/or mouse Oatp1a proteins are expressed on the apical membrane of enterocytes where they might mediate the intestinal uptake of drugs.¹² In addition to their role in the pharmacokinetics of drugs, many OATPs are expressed in breast, gastrointestinal and lung tumors, where they may contribute to the tumor uptake of anticancer drugs.¹³

Docetaxel has been described as a substrate of human OATP1B1 and OATP1B3, and rat and mouse Oatp1b2 *in vitro*.¹⁴⁻¹⁶ The impact of the functional alterations in uptake capacity of OATP1B1 and/or OATP1B3 on docetaxel pharmacokinetics and toxicity (upon intravenous administration) has been studied in several pharmacogenetic studies, but the results are equivocal^{14;6;14}, while the interaction between OATP1A2 and docetaxel has not been reported yet.

In recent years, substantial efforts have been made to obtain an oral formulation for docetaxel.¹⁷ While oral dosing has substantial advantages over intravenous dosing (more patient-friendly, no hospitalization required, lower healthcare costs), it brings the challenge that the drug must pass an additional biological barrier, the intestinal epithelium. It might be that mouse *Oatp1a* or human OATP1A2 uptake transporters have a role in docetaxel intestinal uptake, while metabolizing enzymes and efflux drug transporters might limit its effective absorption.⁸

Here, we studied the impact of the combined deletion of the mouse *Oatp1a* and *Oatp1b* genes on the disposition of docetaxel after intravenous and oral administration, using *Oatp1a/1b* knockout mice.¹⁸ We further assessed the *in vivo* impact of human OATP1B1, OATP1B3 and OATP1A2 on the uptake of docetaxel using humanized transgenic mice with liver-specific expression of OATP1B1, OATP1B3 or OATP1A2 in an *Oatp1a/1b* knockout background.^{19;20}

Materials and methods

Animals

Animals were housed in groups as far as possible, in a temperature-controlled environment with a 12-hour light/12-hour dark cycle. They received a standard diet (AM-II; Hope Farms) and acidified water *ad libitum*. All mouse experiments were approved by the Animal Experiments Review Board of the Netherlands Cancer Institute (Amsterdam), complying with Dutch legislation and in accordance with European Directive 86/609/EEC. Male wild-type, *Slco1a/1b(-/-)* (*Oatp1a/1b* knockout), *Slco1a/1b(-/-);1B1(Tg)*, *Slco1a/1b(-/-);1B3(Tg)* and *Slco1a/1b(-/-);1A2(Tg)* (i.e., liver-specific OATP1B1, OATP1B3 and OATP1A2 humanized transgenic) mice of comparable genetic background (>99% FVB), between 8 and 14 weeks of age, were used.^{19;21}

Chemicals and reagents

Docetaxel was obtained from Sequoia Research Products (Oxford, UK). Isoflurane (Forane) was purchased from Abbott Laboratories (Queenborough, Kent, UK) and heparin (5,000 IE/ml) was from Leo Pharma BV (Breda, The Netherlands). Bovine serum albumin (BSA), Fraction V was from Roche (Mannheim, Germany) and drug-free lithium-heparinized human plasma was obtained from Bioreclamation LLC (New York, NY, USA). All other reagents were from Sigma-Aldrich (Steinheim, Germany).

Pharmacokinetic studies

For intravenous studies, solutions containing docetaxel (2 mg/mL) were injected in a volume of 5 μ L per g of bodyweight into the tail vein of mice, in order to achieve a dosage of 10 mg/kg. For solutions with low polysorbate concentrations (2.77% of polysorbate 80 in the final solution), docetaxel was dissolved in a mixture of ethanol:polysorbate 80 (50:50) to a concentration of 36 mg/mL, which was further diluted prior to injection with saline to a concentration of 2 mg/mL docetaxel. For solutions containing high polysorbate concentrations (8.3% in the final solution), docetaxel was dissolved in a mixture of ethanol:polysorbate 80 (50:50) to a concentration of 12 mg/mL, which was

further diluted prior to injection with saline to 2 mg/mL docetaxel.

For oral studies, docetaxel (1 mg/mL) was administered to the mice in a volume of 10 μ L per g of bodyweight by oral gavage, in order to achieve a dosage of 10 mg/kg. We used the formulation containing low polysorbate 80 concentrations (2.77%): docetaxel was dissolved in ethanol:polysorbate 80 (50:50) to a concentration of 18 mg/mL, which was further diluted prior to dosing with saline to 1 mg/mL docetaxel.

Experiments were terminated (at $t = 3, 15, 30, 60, 120$ and 240 min after i.v. dosing and $t = 5, 7.5$ and 15 min after oral dosing) by isoflurane anaesthesia and heparin-blood sampling by cardiac puncture, followed by cervical dislocation and tissue collection. For the oral studies, portal vein blood samples were taken prior to cardiac puncture. Blood samples were centrifuged at $5,200g$ for 5 min at $4^{\circ}C$ and plasma was collected and stored at $-30^{\circ}C$ until analysis.

Drug analysis

Concentrations of docetaxel in plasma and livers (homogenized in 3 mL of ice-cold 4% (w/v) BSA) were determined by LC-MS/MS analysis as previously described.²² D₉-labelled docetaxel was used as internal standard for docetaxel. In summary, mouse plasma or tissue homogenate samples of 20 μ L were diluted with 180 μ L of human plasma. Human plasma was used for dilution of the samples as the concentrations in the undiluted mouse plasma were outside the calibration range and also to mimic the calibration standards which were in human plasma. After dilution of the samples, 25 μ L of internal standard working solution was added. Subsequently, the samples were mixed briefly, tertiary-butyl methyl ether was added and the samples were shaken for 10 minutes at 1,250 rpm. The samples were centrifuged at 23,000 g, snap-frozen and the organic layer was collected. After evaporation of the organic layer, the samples were reconstituted with 100 μ L of 10 mM ammonium hydroxide pH 5:acetonitrile (1:1, v/v) and an aliquot was injected into the LC-MS/MS system. Calibration standards in human plasma in a range of 0.25-500 ng/mL were used for quantification of docetaxel.

Pharmacokinetic and statistical analysis

Averaged plasma concentrations for each time point were used to calculate the area under the blood concentration versus time curve (AUC) from $t = 0$ to the last sampling time point by the linear trapezoidal rule; S.E. was calculated by the law of propagation of errors.²³

When variances were not homogeneous, the data were log-transformed in order to obtain equal variances. The two-sided unpaired Student's t -test was used throughout the study to assess the statistical significance of differences between two sets of data. Statistical significance of differences between wild-type and *Slco1a/1b(-/-)*, *Slco1a/1b(-/-);1B1(Tg)*, *Slco1a/1b(-/-);1B3(Tg)* or *Slco1a/1b(-/-);1A2(Tg)* or between *Slco1a/1b(-/-)* mice and *Slco1a/1b(-/-);1B1(Tg)*, *Slco1a/1b(-/-);1B3(Tg)* or *Slco1a/1b(-/-);1A2(Tg)* mice was assessed by one-way ANOVA followed by Tukey's multiple comparison test. Results are presented as the mean \pm S.D. Differences were considered to be statistically significant when $P < 0.05$.¹⁹

Results

Influence of polysorbate 80 concentration on pharmacokinetics of docetaxel

Docetaxel is very poorly soluble in water, and thus the formulation of docetaxel for intravenous administration contains ethanol and polysorbate 80, a detergent used to maintain docetaxel in solution, in concentrations between 0.75-2% in clinical formulations.^{24;25} Recently there has been an increasing number of reports showing that polysorbate 80 might have an inhibitory effect on the transport activity of OATP uptake transporters.^{14;26} Therefore we started by analyzing the effect of polysorbate 80 concentration in the final formulation on the plasma and liver levels of docetaxel after intravenous administration (10 mg/kg) to wild-type mice. We used two docetaxel formulations: one with high (8.3%) and one with a low polysorbate 80 concentration (2.77%). At different time points after dosing, we compared the docetaxel plasma and liver levels and liver-to-plasma ratios in these mice (Figure 1). After dosing with the high polysorbate 80 formulation, the plasma levels of docetaxel at later time points were modestly, but significantly higher than after dosing with the low polysorbate 80 formulation (Figure 1A), suggesting that polysorbate 80 at high concentrations

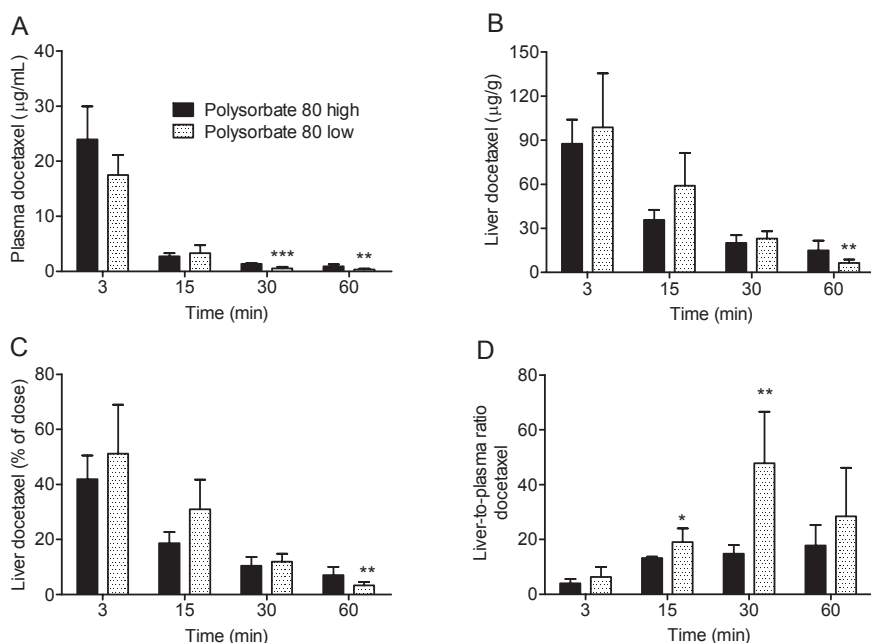


Figure 1. Impact of high (black bars) and low polysorbate (white bars) formulation on plasma and liver levels of docetaxel after administration of 10 mg/kg docetaxel i.v. to male wild-type mice. (A) Plasma concentrations of docetaxel, (B, C) docetaxel liver concentrations as µg/g and % of dose, respectively, and (D) liver-to-plasma ratios were calculated from individual mouse data. Data are presented as mean ± S.D. (n = 5-6, *, P < 0.05; **, P < 0.01; ***, P < 0.001 when compared with wild-type high polysorbate formulation).

has a modest *in vivo* inhibitory effect on plasma clearance of docetaxel. The liver concentrations after high polysorbate concentrations were variably, but mostly not significantly affected by high versus low polysorbate 80 formulation (Figure 1B, C). Assessed by the liver-to-plasma ratios, low polysorbate 80 formulation led to generally higher ratios than the high polysorbate 80 formulation (Figure 1D), suggesting that high concentrations of polysorbate 80 might somewhat inhibit the uptake of docetaxel in the liver. Based on these results, we used the low polysorbate 80 formulation in our subsequent pharmacokinetic studies. Further reduction of polysorbate 80 in the formulation was not compatible with the comparatively high docetaxel dosages given.

Impact of Oatp1a/1b transporters on plasma and liver exposure of docetaxel after intravenous administration

Docetaxel was described as a mouse Oatp1b2 substrate *in vitro* and *in vivo*.¹⁴ We here aimed to study the possible additional roles that mouse Oatp1a transporters may have in the plasma and liver exposure of docetaxel. We therefore made use of Oatp1a/1b knockout mice, which lack all Oatp1a and Oatp1b transporters. After intravenous dosing (10 mg/kg), plasma exposure of docetaxel was significantly increased in the Oatp1a/1b knockout mice in comparison with wild-type mice (Figure 2A). The area

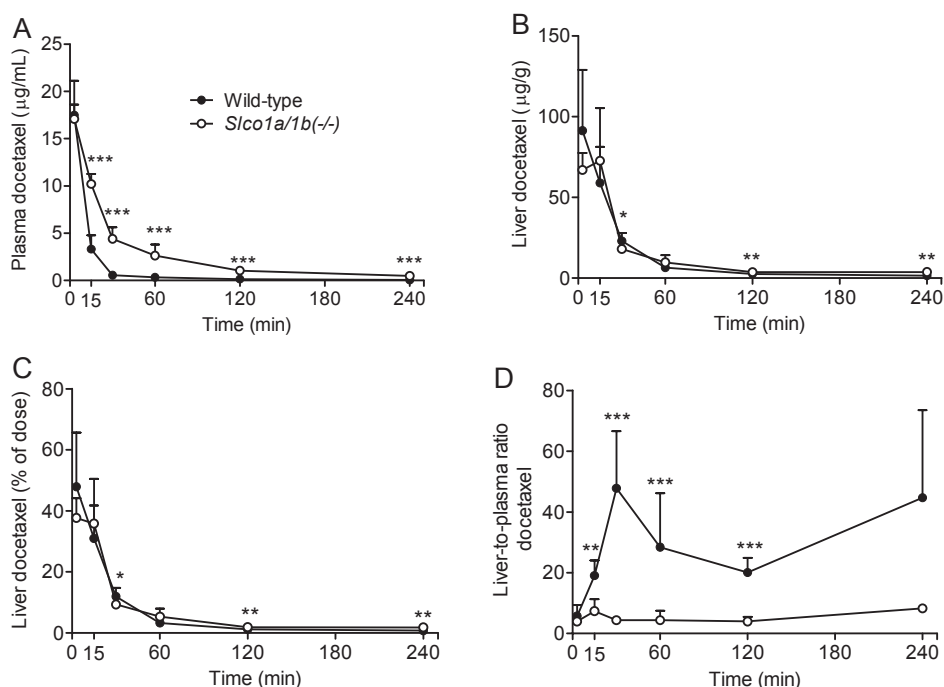


Figure 2. Role of Oatp1a/1b uptake transporters in the plasma and liver exposure of docetaxel after intravenous administration of docetaxel (10 mg/kg) to male wild-type and Oatp1a/1b knockout mice. (A) Plasma concentrations of docetaxel, (B, C) docetaxel liver concentrations as µg/g and % of dose, respectively, and (D) liver-to-plasma ratios of docetaxel. Averaged liver-to-systemic plasma ratios were calculated from individual mouse data. Data are presented as mean ± S.D. (n = 5-6, *, P < 0.05; **, P < 0.01; ***, P < 0.001 when compared with wild-type).

under the curve (AUC) of the plasma concentrations in Oatp1a/1b-null mice was 2.9-fold higher than that in the wild-type mice (608.7 ± 25.2 versus 211.8 ± 19.8 $\mu\text{g}\cdot\text{min}/\text{mL}$, $P < 0.001$), indicating that disposition of docetaxel is impaired in the absence of Oatp1a/1b transporters.

OATP1A/1B transporters mediate mainly the liver uptake of drugs, thus controlling their clearance and disposition. We therefore also measured the liver concentrations. Similar to previous studies with rosuvastatin²⁷, the liver concentrations were not markedly different between the two strains of mice (Figure 2B, C), whereas the liver-to-plasma ratios were clearly reduced at virtually all time points after dosing (Figure 2D). This suggests that liver uptake of docetaxel is substantially impaired in the Oatp1a/1b-null mice.

Oatp1a transporters are not essential for the intestinal absorption of docetaxel

In contrast to Oatp1b2 which is exclusively expressed in the liver, members of the Oatp1a family are also expressed in enterocytes¹² where they are thought to contribute to the intestinal absorption of drugs. We therefore assessed the impact of Oatp1a on the intestinal absorption of docetaxel, again using the low polysorbate 80 formulation (2.77%). We compared portal vein concentrations in Oatp1a/1b knockout and wild-type mice, shortly after oral administration (10 mg/kg) of docetaxel. However, docetaxel portal vein concentrations were substantially higher at all time points in the Oatp1a/1b knockout mice (Figure 3A). These results suggest that Oatp1a transporters are not essential in the intestinal absorption of docetaxel. The increased portal vein concentrations at all time points after dosing likely reflect in part the higher systemic plasma concentrations of docetaxel in the Oatp1a/1b-null mice (Figure 3B) resulting from impaired liver uptake, as seen previously in the intravenous experiment (Figure 3D, E and Figure 2). This impaired liver uptake was evident both in the liver-to-systemic plasma and liver-to-portal vein plasma ratios (Figure 3D, E).

Human OATP1B1, OATP1B3 and OATP1A2 can transport docetaxel in vivo

In the human liver, OATP1B1 and OATP1B3 are expressed on the basolateral membrane of hepatocytes. Although not straightforward homologues of the individual mouse Oatp1a/1b proteins, based on amino acid homology, substrate specificity, and tissue localization, they are considered to fulfill the same roles as the basolateral mouse Oatp1a/1b transporters in the liver.^{19;23;28} We recently generated and characterized humanized mice with hepatocyte-specific expression of OATP1B1, OATP1B3 and OATP1A2 (in an *Slco1a/1b*(-/-) background).^{19;20} Note that *Slco1a/1b*(-/-);*1A2*(Tg) mice do not represent a physiological model for the role of OATP1A2 in hepatic uptake of drugs, as hepatic OATP1A2 in humans is expressed only in cholangiocytes, and not in hepatocytes. Nevertheless, this mouse model has proved to be useful in studying the *in vivo* transport capacity of OATP1A2, which might be relevant for its activity in other healthy or malignant tissues.¹⁹

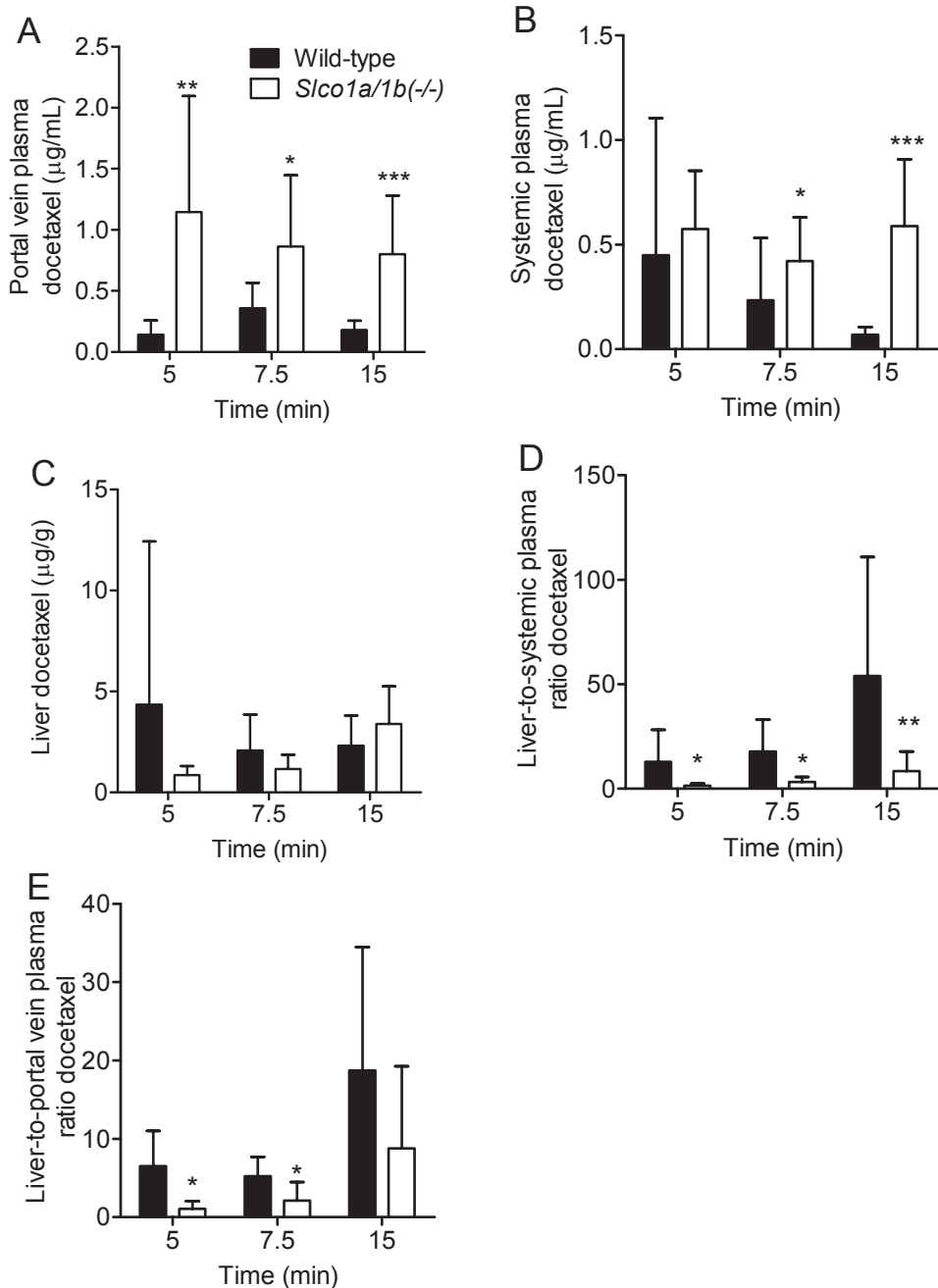


Figure 3. Mouse *Oatp1a* proteins are not essential for the intestinal absorption of docetaxel after oral administration (10 mg/kg) to male wild-type and *Oatp1a/1b* knockout mice. (A), docetaxel portal vein plasma concentrations and (B) docetaxel systemic plasma concentrations, (C) docetaxel liver levels in $\mu\text{g/g}$, (D) liver-to-systemic plasma ratios and (E) liver-to-portal vein plasma ratios. Averaged liver-to-systemic plasma (or liver-to-portal vein plasma) ratios were calculated from individual mouse data. Data are presented as mean \pm SD ($n = 5-6$, *, $P < 0.05$; **, $P < 0.01$ when compared with wild-type).

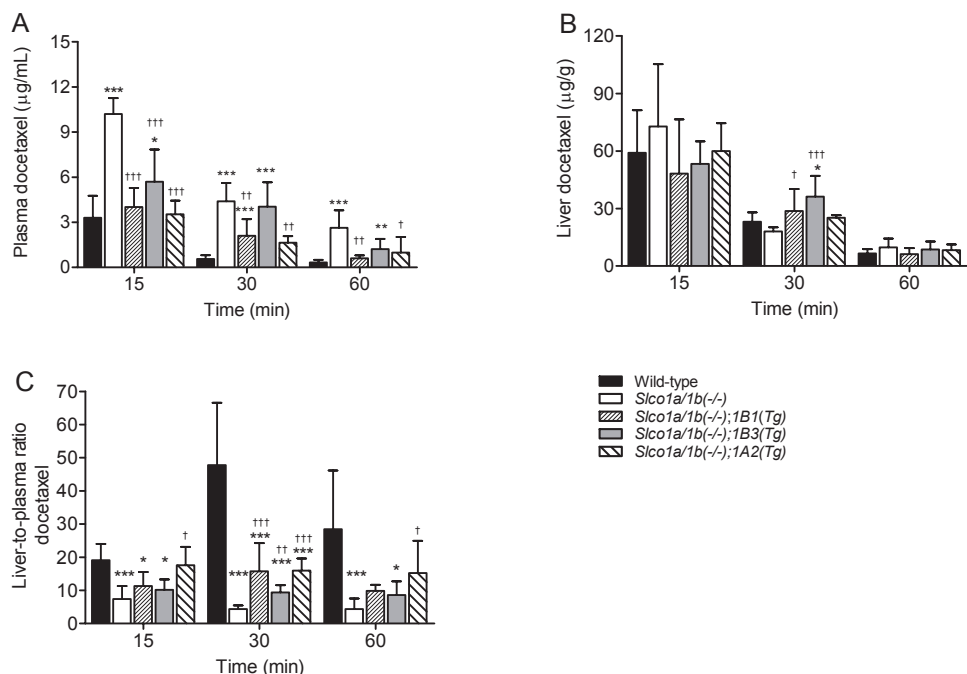


Figure 4. Human OATP1B1, OATP1B3 and OATP1A2 transport docetaxel in vivo after i.v. administration of docetaxel (10 mg/kg) to male wild-type, *Oatp1a/1b* knockout and OATP1B1, -1B3, and -1A2 transgenic mice. (A) Plasma concentrations of docetaxel, (B) docetaxel liver concentrations and (C) liver-to-plasma ratios of docetaxel. Averaged liver-to-systemic plasma ratios were calculated from individual mouse data. Data are presented as mean \pm S.D. ($n = 5-6$, *, $P < 0.05$; **, $P < 0.01$; ***, $P < 0.001$ when compared with wild-type, †, $P < 0.05$; ††, $P < 0.01$; †††, $P < 0.001$ when compared with *Oatp1a/1b* knockout mice).

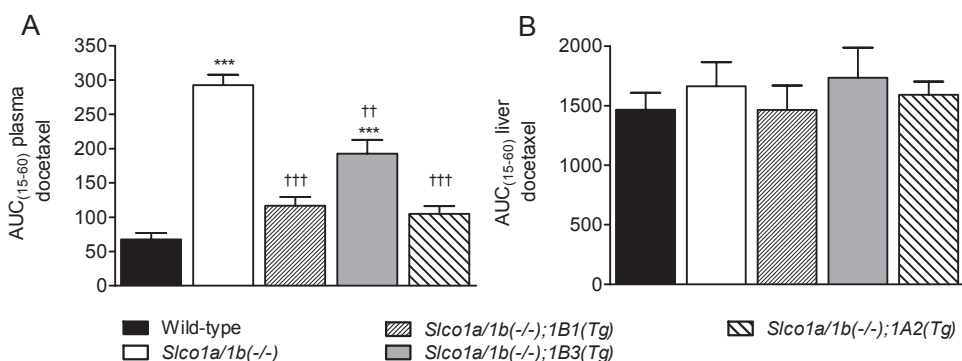


Figure 5. Area under the curve (15 to 60 minutes) of (A) plasma, (B) liver and (C) liver-to-plasma ratios after i.v. administration of docetaxel (10 mg/kg) to male wild-type, *Oatp1a/1b* knockout and OATP1B1, -1B3, and -1A2 transgenic mice. Averaged liver-to-systemic plasma ratios were calculated from individual mouse data. Data are presented as mean \pm S.E.M. ($n = 5-6$, *, $P < 0.05$; ***, $P < 0.001$ when compared with wild-type, †, $P < 0.05$; ††, $P < 0.01$ when compared with *Oatp1a/1b* knockout mice).

We used these models to assess the capacity of the human OATP1A/1B proteins to transport docetaxel *in vivo*. After 10 mg/kg i.v. dosing, the increased docetaxel plasma concentrations in the Oatp1a/1b-null mice were partially or completely brought back to wild-type levels in all the humanized mouse strains (Figure 4A). Only at 30 minutes after dosing, plasma levels in the OATP1B3 humanized mice were as high as in the Oatp1a/1b-null mice, perhaps due to experimental variation (Figure 4A). Also plotted as plasma AUC from 15 till 60 minutes in these strains (Figure 5A), the plasma AUC in the Oatp1a/1b-knockout mice was 4-fold increased in comparison with the wild-type mice. The rescue provided by the presence of OATP1B1 or OATP1A2 was obvious as the plasma AUC values were quite similar to the values in the wild-type mice and significantly lower than in the Oatp1a/1b knockout mice (Figure 5A). The values in the OATP1B3-humanized mice were intermediate between the values in the wild-type and Oatp1a/1b-null mice, most probably due to the high plasma concentrations in this strain at 30 minutes after administration (Figure 4A).

As seen before (Figure 2B), the liver levels were not significantly changed in the Oatp1a/1b-null mice in comparison with wild-type mice, and accordingly shifts in liver concentration due to the role of human OATP1A/1B transporters in rescuing the absence of mouse Oatp1a/1b transporters were modest, albeit significant for OATP1B1 and OATP1B3 at 30 minutes (Figure 4B). However, the liver AUC levels from 15 to 60 min were not significantly altered in any of the tested strains (Figure 5B).

Liver-to-plasma ratios in the humanized mice (in OATP1A2 mice especially) were also significantly higher than in the knockout mice (Figure 4C). However, the liver-to-plasma ratios were not up to the levels seen in wild-type mice (Figure 4C).

This incomplete rescue by human OATP1A/1B transporters in liver-to-plasma ratios is likely an underestimation of the actual OATP1B-mediated liver uptake in humans, as in human liver both OATP1B1 and OATP1B3 function at the same time, likely resulting in additive effects. Nevertheless, these results show that human OATP1B1, OATP1B3 and OATP1A2 can transport docetaxel *in vivo* and that all three transporters can compensate to an extent for the loss of the murine Oatp1a/1b transporters.

Discussion

In the present study we found that mouse Oatp1a/1b transporters contribute to the plasma clearance of docetaxel, even as there was no clear effect on the apparent liver exposure. Still, impaired liver uptake in the absence of Oatp1a/1b transporters was obvious in the markedly reduced liver-to-plasma ratios. Importantly, liver-specific expression of human OATP1B1, OATP1B3 or OATP1A2 provided substantial rescue of the increased plasma levels of docetaxel in Oatp1a/1b knockout mice. Assessed by the liver-to-plasma ratios this rescue was partial. Oatp1a/1b transporters did not appear to contribute to intestinal docetaxel uptake. Our findings indicate that all the human OATP1A/1B uptake transporters, when expressed in hepatocytes, can mediate the liver uptake of docetaxel *in vivo*, and can thus contribute to hepatic docetaxel clearance, and, by implication, possibly docetaxel tumor uptake *in vivo* as well.

Although it has been described that human OATP1B1 and OATP1B3 can transport docetaxel *in vitro*, there is wide variability dependent on the type of cellular uptake system used.^{1,14,15} Our data demonstrate docetaxel transport by OATP1B1 and OATP1B3 in hepatocytes *in vivo*. Transport activity of OATP1B1 or OATP1B3 can be reduced as a consequence of genetic variation (polymorphic variants) or pharmacological inhibition, leading to decreased liver uptake of docetaxel and thus impaired plasma clearance. Yet there are only two clinical studies that show an association between low-activity polymorphisms in the gene encoding OATP1B3 and altered docetaxel pharmacokinetics⁴ or docetaxel-induced neutropenia²⁹, while others investigating the impact of polymorphic variants of OATP1B1 or OATP1B3 on docetaxel pharmacokinetics and toxicity did not find any associations.^{1,6,14,30} Our data suggest that in the case of single polymorphisms affecting only one of the human OATP1B transporters, the remaining OATP1B1 or OATP1B3 could at least partially compensate for the loss of function of the other transporter. Accordingly, single polymorphisms in the OATP1B1 or OATP1B3 genes were not clearly associated with altered docetaxel clearance.¹⁴ This may be different for Rotor syndrome patients, which are deficient in both OATP1B1 and OATP1B3²⁰, and might thus be at risk of developing life-threatening toxicity when treated with docetaxel. Also, clinically relevant drug-drug interactions might occur when docetaxel is co-administered with inhibitors of OATP1B transporters (e.g., rifampicin, cyclosporine, statins) or other OATP1B substrates (e.g., statins, methotrexate, paclitaxel) which might compete for transport into the liver.³¹

To the best of our knowledge, we show here for the first time that OATP1A2 can transport docetaxel *in vivo* and that it can mediate docetaxel liver uptake. Because expression of OATP1A2 in human liver is restricted to cholangiocytes, the epithelial cells of the bile duct, the information provided by our humanized OATP1A2 mice (in which OATP1A2 is expressed in hepatocytes) has only qualitative meaning. Nevertheless, this information is relevant for the function of OATP1A2 in other tissues like small intestine, kidney and the blood-brain barrier, where it might affect the oral uptake, urinary reabsorption or brain penetration of docetaxel.³²⁻³⁴ The role of OATP1A2 in small intestine, and thus in the oral bioavailability of docetaxel remains unclear as in our study we observed that mouse *Oatp1a* transporters are not essential for the intestinal absorption of docetaxel. Importantly, when expressed in tumor cells, OATP1A2 can likely affect the susceptibility of these cells to docetaxel chemotherapy *in vivo* by altering the effective intracellular docetaxel exposure.¹³

OATP1A/1B proteins have been found expressed in tumors of almost all the cancer types which are currently treated with docetaxel: colon, gastric, ovarian, breast and lung cancer (reviewed in^{13,35-37}) and OATP1A2 has also been found in the blood-brain barrier of gliomas.³⁸ Previous studies in our group showed that other anticancer drugs, namely methotrexate and paclitaxel, are also transported *in vivo* by human OATP1A/1B proteins.¹⁹ These data imply that *in vivo* expression and activity of OATP1A/1B transporters in various tumors may affect the tumor drug uptake, and hence influence their sensitivity to certain anticancer drugs.³⁵ Direct studies involving sensitivity to docetaxel in cell lines derived from these tumor types are lacking so far, although there are indications that for paclitaxel and methotrexate, expression and activity of OATP1B1

and/or OATP1B3 transporters can increase sensitivity of tumors cells to these drugs.^{37;39} Moreover, there are several studies trying to correlate the tumor expression levels of OATPs with tumor development and prognosis.^{40;41}

In this study we also aimed to investigate if mouse *Oatp1a* transporters expressed on the basolateral membrane of hepatocytes have an additional role to that of mouse *Oatp1b2*¹⁴ in mediating the liver uptake, and hence plasma clearance of docetaxel. However, in quantitative terms our results are very different from those of de Graan *et al.*¹⁴ We observed a 3-fold higher docetaxel plasma AUC between full *Oatp1a/1b* knockout mice and (FVB) wild-type mice, while de Graan *et al.* noted a 26-fold higher plasma AUC between single *Oatp1b2* knockout mice and their DBA1/lacJ wild-type controls.¹⁴ Comparing the absolute docetaxel plasma AUC levels between the studies, these were quite similar between both knockout strains, but the AUC in wild-type DBA1/lacJ mice was far lower than that in wild-type FVB mice. Assuming that all *Oatp*-dependent docetaxel uptake in the liver is mediated by *Oatp1b2*, this would suggest that this protein is far more active and/or far more highly expressed in DBA1/lacJ mice than in FVB mice. This could theoretically be caused by differences in genetic background, or possibly food and housing conditions between the FVB and DBA1/lacJ wild-type mice. Still, a 26-fold change in plasma AUC is a surprisingly big effect of the knockout of a protein that seems to be a modest docetaxel transporter *in vitro*.¹⁴

Another difference between our data and those of de Graan *et al.* is the unexpected 4.2-fold increase (rather than decrease) in liver AUC in the *Oatp1b2* knockout strain compared to the DBA1/lacJ wild-type strain, as deduced from a 6.2-fold decreased liver-to-plasma AUC ratio and a 26.3-fold increased plasma AUC.¹⁴ In contrast, we observed very similar liver AUCs between FVB wild-type and *Oatp1a/1b* knockout mice (Figure 2B, C). This latter pharmacokinetic behavior is similar to that previously reported for rosuvastatin²⁷, where reduced liver uptake (due to the absence of *Oatp1a/1b* transporters) resulted in marked changes in plasma exposure and liver-to-plasma ratios, without affecting the liver concentrations. This pharmacokinetic behavior is consistent with the physiologically-based pharmacokinetic model of Watanabe *et al.* for drugs with a low renal clearance and for which the liver uptake is the rate-limiting step⁴²⁻⁴⁴, as appears to be the case for pravastatin, rosuvastatin and docetaxel. The 4.2-fold increased liver AUC of docetaxel in DBA1/lacJ *Oatp1b2* knockout mice observed by de Graan *et al.*¹⁴, coinciding with presumably reduced liver uptake rates of docetaxel, therefore remains unexplained. Perhaps additional, as yet unidentified other alterations have contributed to the profoundly changed docetaxel pharmacokinetics in these mice, even though a broad microarray screening of other detoxifying genes did not yield obvious candidates.¹⁴ The model of Watanabe *et al.* would predict an increase in liver AUC primarily as a consequence of diminished canalicular efflux activity.⁴²⁻⁴⁴ Possibly the activity (though not the expression) of one of the ABC transporters involved in docetaxel biliary excretion (ABCB1 or ABCC2)⁴⁴ was compromised in the *Oatp1b2* knockout mice. Clearly, more work will be needed to fully understand all the aspects of *Oatp1a/1b*-mediated hepatic docetaxel clearance.

In line with previous studies^{14;24;26}, we here provide *in vivo* pharmacokinetic evidence that polysorbate 80 at high concentrations can have an inhibitory effect on

the plasma clearance of docetaxel, probably by inhibiting Oatp1a/1b-mediated liver uptake. Perhaps new formulations, which have been studied recently, will provide a better alternative to current polysorbate 80 formulations (reviewed in ^{45;46}).

Taken together, our results suggest that human OATP1A/1B uptake transporters can have multiple effects on the docetaxel therapeutic index, on the one hand by controlling its general plasma and tissue pharmacokinetics and toxicity, but also by possibly mediating its tumor uptake. OATP1A/1B transporters might thus represent a valuable target for modulators in order to improve chemotherapy. Further studies using humanized OATP1A/1B mice may help to better assess the *in vivo* impact of OATP1A/1B transporters on pharmacokinetics, toxicity and therapeutic outcome of anticancer drugs.

References

- Baker SD, Verweij J, Cusatis GA, van Schaik RH, Marsh S, Orwick SJ, Franke RM, Hu S, Schuetz EG, Lamba V, Messersmith WA, Wolff AC, Carducci MA, Sparreboom A. Pharmacogenetic pathway analysis of docetaxel elimination. *Clin Pharmacol Ther.* **2009**; 85 (2): 155-63.
- Baker SD, Sparreboom A, Verweij J. Clinical pharmacokinetics of docetaxel : recent developments. *Clin Pharmacokinet.* **2006**; 45 (3): 235-52.
- van Herwaarden AE, Wagenaar E, van der Kruijssen CM, van Waterschoot RA, Smit JW, Song JY, van der Valk MA, van Tellingen O, van der Hoorn JW, Rosing H, Beijnen JH, Schinkel AH. Knockout of cytochrome P450 3A yields new mouse models for understanding xenobiotic metabolism. *J Clin Invest.* **2007**; 117 (11): 3583-92.
- Chew SC, Singh O, Chen X, Ramasamy RD, Kulkarni T, Lee EJ, Tan EH, Lim WT, Chowbay B. The effects of CYP3A4, CYP3A5, ABCB1, ABCG2, ABCG2 and SLC01B3 single nucleotide polymorphisms on the pharmacokinetics and pharmacodynamics of docetaxel in nasopharyngeal carcinoma patients. *Cancer Chemother Pharmacol.* **2011**; 67 (6): 1471-8.
- Tran A, Jullien V, Alexandre J, Rey E, Rabillon F, Girre V, Dieras V, Pons G, Goldwasser F, Treluyer JM. Pharmacokinetics and toxicity of docetaxel: role of CYP3A, MDR1, and GST polymorphisms. *Clin Pharmacol Ther.* **2006**; 79 (6): 570-80.
- Chew SC, Sandanaraj E, Singh O, Chen X, Tan EH, Lim WT, Lee EJ, Chowbay B. Influence of SLC01B3 haplotype-tag SNPs on docetaxel disposition in Chinese nasopharyngeal cancer patients. *Br J Clin Pharmacol.* **2012**; 73 (4): 606-18.
- Kalliokoski A, Niemi M. Impact of OATP transporters on pharmacokinetics. *Br J Pharmacol.* **2009**; 158 (3): 693-705.
- Iusuf D, van de Steeg E, Schinkel AH. Functions of OATP1A and 1B transporters in vivo: insights from mouse models. *Trends Pharmacol Sci.* **2012**; 33 (2): 100-8.
- Hagenbuch B, Meier PJ. Organic anion transporting polypeptides of the OATP/ SLC21 family: phylogenetic classification as OATP/ SLCO superfamily, new nomenclature and molecular/functional properties. *Pflugers Arch.* **2004**; 447 (5): 653-65.
- Konig J, Seithel A, Gradhand U, Fromm MF. Pharmacogenomics of human OATP transporters. *Naunyn Schmiedebergs Arch Pharmacol.* **2006**; 372 (6): 432-43.
- Niemi M. Role of OATP transporters in the disposition of drugs. *Pharmacogenomics.* **2007**; 8 (7): 787-802.
- Klaassen CD, Aleksunes LM. Xenobiotic, bile acid, and cholesterol transporters: function and regulation. *Pharmacol Rev.* **2010**; 62 (1): 1-96.
- Cutler MJ, Choo EF. Overview of SLC22A and SLCO families of drug uptake transporters in the context of cancer treatments. *Curr Drug Metab.* **2011**; 12 (8): 793-807.
- de Graan AJ, Lancaster CS, Obaidat A, Hagenbuch B, Elens L, Friberg LE, de Bruijn P, Hu S, Gibson AA, Bruun GH, Corydon TJ, Mikkelsen TS, Walker AL, Du G, Loos WJ, van Schaik RH, Baker SD, Mathijssen RH, Sparreboom A. Influence of polymorphic OATP1B-type carriers on the disposition of docetaxel. *Clin Cancer Res.* **2012**; 18 (16): 4433-40.
- Smith NF, Acharya MR, Desai N, Figg WD, Sparreboom A. Identification of OATP1B3 as a high-affinity hepatocellular transporter of paclitaxel. *Cancer Biol Ther.* **2005**; 4 (8): 815-8.
- Yamaguchi H, Kobayashi M, Okada M, Takeuchi T, Unno M, Abe T, Goto J, Hishinuma T, Mano N. Rapid screening of antineoplastic candidates for the human organic anion transporter OATP1B3 substrates using fluorescent probes. *Cancer Lett.* **2008**; 260 (1-2): 163-9.
- Moes JJ, Koolen SL, Huitema AD, Schellens JH, Beijnen JH, Nuijen B. Pharmaceutical development and preliminary clinical testing of an oral solid dispersion formulation of docetaxel (ModraDoc001). *Int J Pharm.* **2011**; 420 (2): 244-50.

18. van de Steeg E, van Esch A, Wagenaar E, van der Kruijssen CM, van Tellingen O, Kenworthy KE, Schinkel AH. High impact of Oatp1a/1b transporters on in vivo disposition of the hydrophobic anticancer drug paclitaxel. *Clin Cancer Res.* **2011**; 17 (2): 294-301.
19. van de Steeg E, van Esch A, Wagenaar E, Kenworthy KE, Schinkel AH. Influence of human OATP1B1, OATP1B3, and OATP1A2 on the pharmacokinetics of methotrexate and paclitaxel in humanized transgenic mice. *Clin Cancer Res.* **2013**; 19 (4): 821-32.
20. van de Steeg E, Stranecky V, Hartmannova H, Noskova L, Hrebicek M, Wagenaar E, van Esch A, de Waart DR, Oude Elferink RP, Kenworthy KE, Sticova E, al Edreesi M, Knisely AS, Kmoch S, Jirsa M, Schinkel AH. Complete OATP1B1 and OATP1B3 deficiency causes human Rotor syndrome by interrupting conjugated bilirubin reuptake into the liver. *J Clin Invest.* **2012**; 122 (2): 519-28.
21. van de Steeg E, Wagenaar E, van der Kruijssen CM, Burggraaff JE, de Waart DR, Elferink RP, Kenworthy KE, Schinkel AH. Organic anion transporting polypeptide 1a/1b-knockout mice provide insights into hepatic handling of bilirubin, bile acids, and drugs. *J Clin Invest.* **2010**; 120 (8): 2942-52.
22. Kuppens IE, van Maanen MJ, Rosing H, Schellens JH, Beijnen JH. Quantitative analysis of docetaxel in human plasma using liquid chromatography coupled with tandem mass spectrometry. *Biomed Chromatogr.* **2005**; 19 (5): 355-61.
23. Iusuf D, Sparidans RW, van Esch A, Hobbs M, Kenworthy KE, van de Steeg E, Wagenaar E, Beijnen JH, Schinkel AH. Organic anion-transporting polypeptides 1a/1b control the hepatic uptake of pravastatin in mice. *Mol Pharm.* **2012**; 9 (9): 2497-504.
24. Ten Tije AJ, Loos WJ, Verweij J, Baker SD, Dinh K, Figg WD, Sparreboom A. Disposition of polyoxyethylated excipients in humans: implications for drug safety and formulation approaches. *Clin Pharmacol Ther.* **2003**; 74 (5): 509-10.
25. van Tellingen O, Beijnen JH, Verweij J, Scherrenburg EJ, Nooijen WJ, Sparreboom A. Rapid esterase-sensitive breakdown of polysorbate 80 and its impact on the plasma pharmacokinetics of docetaxel and metabolites in mice. *Clin Cancer Res.* **1999**; 5 (10): 2918-24.
26. Engel A, Oswald S, Siegmund W, Keiser M. Pharmaceutical excipients influence the function of human uptake transporting proteins. *Mol Pharm.* **2012**; 9 (9): 2577-81.
27. Iusuf D, van Esch A, Hobbs MJ, Taylor MA, Kenworthy KE, van de Steeg E, Wagenaar E, Schinkel AH. Murine Oatp1a/1b Uptake Transporters Control Rosuvastatin Systemic Exposure without Affecting Its Apparent Liver Exposure. *Mol Pharmacol.* **2013**; 83 (5): 919-29.
28. Iusuf D, van de Steeg E, Schinkel AH. Hepatocyte hopping of OATP1B substrates contributes to efficient hepatic detoxification. *Clin Pharmacol Ther.* **2012**; 92 (5): 559-62.
29. Kiyotani K, Mushiroda T, Kubo M, Zembutsu H, Sugiyama Y, Nakamura Y. Association of genetic polymorphisms in SLC01B3 and ABCG2 with docetaxel-induced leukopenia. *Cancer Sci.* **2008**; 99 (5): 967-72.
30. Lewis LD, Miller AA, Owzar K, Bies RR, Markova S, Jiang C, Kroetz DL, Egorin MJ, McLeod HL, Ratain MJ. The relationship of polymorphisms in ABCG2 and SLC01B3 with docetaxel pharmacokinetics and neutropenia: CALGB 60805 (Alliance). *Pharmacogenet. Genomics.* **2013**; 23 (1): 29-33.
31. Karlgren M, Vildhede A, Norinder U, Wisniewski JR, Kimoto E, Lai Y, Haglund U, Artursson P. Classification of inhibitors of hepatic organic anion transporting polypeptides (OATPs): influence of protein expression on drug-drug interactions. *J Med Chem.* **2012**; 55 (10): 4740-63.
32. Gao B, Hagenbuch B, Kullak-Ublick GA, Benke D, Aguzzi A, Meier PJ. Organic anion-transporting polypeptides mediate transport of opioid peptides across blood-brain barrier. *J Pharmacol Exp Ther.* **2000**; 294 (1): 73-9.
33. Glaeser H, Bailey DG, Dresser GK, Gregor JC, Schwarz UI, McGrath JS, Jolicoeur E, Lee W, Leake BF, Tirona RG, Kim RB. Intestinal drug transporter expression and the impact of grapefruit juice in humans. *Clin Pharmacol Ther.* **2007**; 81 (3): 362-70.
34. Lee W, Glaeser H, Smith LH, Roberts RL, Moeckel GW, Gervasini G, Leake BF, Kim RB. Polymorphisms in human organic anion-transporting polypeptide 1A2 (OATP1A2): implications for altered drug disposition and central nervous system drug entry. *J Biol Chem.* **2005**; 280 (10): 9610-7.
35. Obaidat A, Roth M, Hagenbuch B. The expression and function of organic anion transporting polypeptides in normal tissues and in cancer. *Annu Rev Pharmacol Toxicol.* **2012**; 52: 135-51.
36. Sissung TM, Reece KM, Spencer S, Figg WD. Contribution of the OATP1B subfamily to cancer biology and treatment. *Clin Pharmacol Ther.* **2012**; 92 (5): 658-60.
37. Svoboda M, Wlcek K, Taferner B, Hering S, Steiger B, Tong D, Zeillinger R, Thalhammer T, Jager W. Expression of organic anion-transporting polypeptides 1B1 and 1B3 in ovarian cancer cells: relevance for paclitaxel transport. *Biomed Pharmacother.* **2011**; 65 (6): 417-26.
38. Bronger H, Konig J, Kopplow K, Steiner HH, Ahmadi R, Herold-Mende C, Keppler D, Nies AT. ABCG2 drug efflux pumps and organic anion uptake transporters in human gliomas and the blood-tumor barrier. *Cancer Res.* **2005**; 65 (24): 11419-28.
39. Abe T, Kakyo M, Tokui T, Nakagomi R, Nishio T, Nakai D, Nomura H, Unno M, Suzuki M, Naitoh T, Matsuno S, Yawo H. Identification of a novel gene family encoding human liver-specific organic anion transporter LST-1. *J Biol Chem.* **1999**; 274 (24): 17159-63.

40. Maeda T, Irokawa M, Arakawa H, Kuraoka E, Nozawa T, Tateoka R, Itoh Y, Nakanishi T, Tamai I. Uptake transporter organic anion transporting polypeptide 1B3 contributes to the growth of estrogen-dependent breast cancer. *J Steroid Biochem Mol Biol.* **2010**; 122 (4): 180-5.
41. Pressler H, Sissung TM, Venzon D, Price DK, Figg WD. Expression of OATP family members in hormone-related cancers: potential markers of progression. *PLoS One.* **2011**; 6 (5): e20372.
42. Watanabe T, Kusuhara H, Sugiyama Y. Application of physiologically based pharmacokinetic modeling and clearance concept to drugs showing transporter-mediated distribution and clearance in humans. *J Pharmacokinet Pharmacodyn.* **2010**; 37 (6): 575-90.
43. Yoon I, Han S, Choi YH, Kang HE, Cho HJ, Kim JS, Shim CK, Chung SJ, Chong S, Kim DD. Saturable sinusoidal uptake is rate-determining process in hepatic elimination of docetaxel in rats. *Xenobiotica.* **2012**; 42 (11): 1110-9.
44. Watanabe T, Kusuhara H, Maeda K, Shitara Y, Sugiyama Y. Physiologically based pharmacokinetic modeling to predict transporter-mediated clearance and distribution of pravastatin in humans. *J Pharmacol Exp Ther.* **2009**; 328 (2): 652-62.
45. Engels FK, Mathot RA, Verweij J. Alternative drug formulations of docetaxel: a review. *Anticancer Drugs.* **2007**; 18 (2): 95-103.
46. Hennenfent KL, Govindan R. Novel formulations of taxanes: a review. Old wine in a new bottle? *Ann Oncol.* **2006**; 17 (5): 735-49.

Ritonavir inhibits intratumoral
docetaxel metabolism and enhances
docetaxel anti-tumor efficacy in a
mouse model for hereditary breast
cancer.

Jeroen J.M.A. Hendrikx
Jurjen S. Lagas
Ji-Ying Song
Hilde Rosing
Jan H.M. Schellens
Jos H. Beijnen
Sven Rottenberg
Alfred H. Schinkel

Abstract

Docetaxel (Taxotere®) is currently used intravenously for treatment of several types of cancer. Bioavailability of orally administered docetaxel is limited by Cytochrome P450 3A (CYP3A), but can be enhanced by co-administration of the HIV protease inhibitor ritonavir, a strong CYP3A4 inhibitor. Possible anticancer effects of ritonavir itself have been recently described. We here aimed to test whether ritonavir co-administration could increase the anti-tumor efficacy of docetaxel in a syngeneic mouse model for hereditary breast cancer.

Spontaneously arising *K14cre;Brca1^{-/-};p53^{-/-}* mouse mammary tumors were orthotopically implanted in syngeneic female mice lacking Cyp3a (*Cyp3a^{-/-}*), to circumvent increased docetaxel plasma levels due to systemic Cyp3a inhibition by ritonavir. Over three weeks, docetaxel (20 mg/kg) was administered intravenously once weekly, while ritonavir (12.5 mg/kg) was administered orally for 5 subsequent days per week. Untreated mice were used as control for tumor growth.

Ritonavir treatment alone did not significantly affect the median time of survival (14 vs 10 days). Median time of survival in docetaxel-treated mice was 54 days. Ritonavir co-treatment significantly increased this median time to 66 days, and substantially reduced average tumor size. Tumors did not display qualitative histological differences with and without ritonavir treatment. Concentrations of the major docetaxel metabolite M2 in tumor tissue were lower when docetaxel was co-administered with ritonavir, while RNA expression of Cyp3a in the tumors was unaltered.

In this model for BRCA1-mutated breast cancer, we observed no direct antitumor effect of ritonavir itself, but we found enhanced efficacy of docetaxel treatment when combined with oral ritonavir. Our data suggest that Cyp3a inhibition in tumor tissue by ritonavir results in decreased docetaxel metabolism in the tumor, possibly contributing to the observed increased antitumor efficacy of docetaxel when coadministered with ritonavir.

Introduction

Docetaxel (Taxotere®) is a semi-synthetic taxane, originating from the European yew *Taxus baccata*. It is currently used as anticancer agent for several types of cancer, among which lung, breast, gastric and prostate cancer.^(1,2,3,4) The development of an oral formulation of docetaxel is the focus of preclinical and clinical research in our groups. A major limitation in the concept of oral administration of docetaxel is its low oral availability due to its handling by P-glycoprotein (P-gp; MDR1) and Cytochrome P450 (CYP) 3A.^(5,6) Co-administration of the oral formulation of docetaxel with the HIV protease inhibitor and strong CYP3A4 inhibitor ritonavir in mice and humans results in markedly increased docetaxel plasma concentrations.^(7,8)

Possible anticancer effects of protease inhibitors, among which ritonavir, have been incidentally described. Ritonavir also causes DNA damage and cell death in human endothelial cells.⁽⁹⁾ It is also reported that ritonavir decreases the production of factors that contribute to tumor neovascularisation in Kaposi sarcoma.⁽¹⁰⁾ Based on the inhibitory effect on endothelial cell invasion, ritonavir might inhibit angiogenesis.⁽¹¹⁾

In vivo, ritonavir treatment decreased tumor growth in an HIV-independent Kaposi sarcoma mouse model.⁽¹⁰⁾ Preclinical anti-tumor effects of ritonavir were also described for other types of cancer such as mouse lymphoma⁽¹²⁾, human head and neck carcinoma⁽¹³⁾ and human breast cancer.⁽¹⁴⁾ On the other hand, no antitumor effect of ritonavir was observed for glioblastoma in preclinical and clinical studies.^(15,16) In a mouse xenograft model of human prostate cancer, ritonavir co-administration increased docetaxel antitumor efficacy and blocked docetaxel-induced upregulation of CYP3A.⁽¹⁷⁾ However, this study did not analyze docetaxel plasma levels. Therefore, the increased efficacy might also be related to the likely highly increased exposure to docetaxel due to impaired Cyp3a-mediated metabolism of docetaxel by ritonavir. Van Waterschoot et al.⁽¹⁸⁾ showed that plasma levels of intravenously administered docetaxel are 5-fold increased when Cyp3a is absent. Ritonavir completely blocked docetaxel metabolism at a concentration of ~2.5 μM in *in vitro* experiments with mouse liver microsomes.⁽¹⁹⁾ This concentration is most likely reached in the *in vivo* situation as 30 minutes after single oral administration of 40 mg/kg ritonavir, liver concentrations over 40 nmol/g (~40 μM) were observed.⁽²⁰⁾ Since Ikezoe et al.⁽¹⁷⁾ administered 12.5 mg/kg ritonavir for 5 subsequent days a week, inhibition of docetaxel metabolism is likely to be almost complete, probably resulting in up to 5 times higher plasma concentrations in the docetaxel/ritonavir co-treated group than in the docetaxel-treated group.

In the present study, we aimed to investigate whether ritonavir co-administration increases anti-tumor efficacy of docetaxel in a syngeneic mouse model for hereditary breast cancer. We hypothesized that ritonavir co-administration not only affects angiogenesis, but also increases docetaxel levels in the circulation and in tumor tissue. Increased docetaxel exposure in tumors due to ritonavir co-administration could also be caused by inhibition of Cyp3a already inherently expressed in tumors. It is further reported that docetaxel treatment can induce expression of Cyp3a in tumor tissue.⁽²¹⁾ Since it is possible that ritonavir can reduce Cyp3a activity to normal levels⁽¹⁷⁾, co-administration of ritonavir might also result in decreased docetaxel metabolism by

blockage of docetaxel-induced enhancement of Cyp3a expression. In our study we used mice lacking Cyp3a as hosts for the transplanted tumors to rule out increased plasma exposure of docetaxel due to general Cyp3a inhibition by ritonavir outside of the tumor as a cause of altered docetaxel therapy response.

Materials and Methods

Drugs and chemicals

Docetaxel and ritonavir were purchased from Sequoia Research Products (Oxford, UK). Drug-free lithium-heparinized human plasma was obtained from Bioreclamation LLC (New York, NY, USA). All other chemicals were of analytical grade and obtained from commercial sources.

Animals

All mouse experiments were approved by the Animal Experiments Review Board of the Netherlands Cancer Institute (Amsterdam), complying with Dutch legislation and in accordance with European Directive 86/609/EEC. Mice were kept in a temperature-controlled environment with a 12-hr light / 12-hr dark cycle and received a standard diet (AM-II, Hope Farms, Woerden, The Netherlands) and acidified water *ad libitum*. Crushed and moistened food was made available for additional support of mice during treatment. Since we implanted a mouse breast tumor, female mice were selected. In this study, Cyp3a knockout mice (*Cyp3a*^{-/-}) in a >99% FVB genetic background⁽²²⁾ were used as host to eliminate differences in docetaxel metabolism between single docetaxel treatment and co-administration of docetaxel and ritonavir. In experiments to test for the maximum tolerable dose, mice of 8-14 weeks of age were used. For tumor implantations, mice of 7-11 weeks of age were used.

Drug solutions

Prior to the experiments, stock solutions containing 18, 24, 30, 36 or 42 mg/mL docetaxel or 7.5 mg/mL ritonavir in ethanol:polysorbate 80 (1:1, v/v) were made and stored at -20° C. On the day of the experiments docetaxel stock solutions were diluted with saline (1:5, v/v) to obtain solutions for intravenous (i.v.) administration. Solutions containing docetaxel were injected in a volume of 5 µL per g of bodyweight into the tail vein of the mice, in order to achieve a dosage of 15, 20, 25, 30 or 35 mg/kg docetaxel. Ritonavir stock solutions were diluted with water (1:5, v/v) to obtain solutions for oral administration. Ritonavir was orally administered in a volume of 10 µL per g of bodyweight to the mice, in order to achieve a dosage of 12.5 mg/kg ritonavir. Oral administration was performed by gavage into the stomach using a blunt-ended needle.

Maximum Tolerable dose

Prior to tumor treatment, the maximum tolerable dose of docetaxel and ritonavir for *Cyp3a*^{-/-} mice was determined. The maximum tolerable dose was defined as the maximum dose at which mice maintained at least 80% of their initial bodyweight and at which mice did not show signs of little to moderate discomfort (e.g. inactivity, general

weakness/illness or neglected coat). Mice were treated with 15, 20, 25, 30 or 35 mg/kg intravenously administered docetaxel or 12.5 mg/kg orally administered ritonavir. Docetaxel was administered once a week, while ritonavir was administered for 5 subsequent days per week. Tolerability of the doses was determined during treatment with docetaxel and/or ritonavir for 3 subsequent weeks.

Tumor implantation

Small tumor pieces (1-2 mm) derived from the *K14cre;Brca1^{F/F};p53^{F/F}* mouse model⁽²⁴⁾ for hereditary breast cancer were grafted orthotopically in the mammary fat pad of syngeneic female *Cyp3a^{-/-}* mice as described before.⁽²³⁾ A tumor with basal expression of *Cyp3a*, *Mdr1a/b* and *Bcrp* was selected to compare response after docetaxel treatment with and without ritonavir. In screening experiments, the selected tumor showed a decreased tumor volume after treatment with docetaxel and was therefore considered as docetaxel-sensitive. After implantation, tumor size was measured *in situ* in the living animal by caliper (volume = 0.5 x length x width²).^(25,26) One observer measured all tumors to reduce variation in tumor measurement.⁽²⁵⁾

Tumor treatment and sample collection

Tumor treatment was started (day 1) when tumors reached a volume of ~200 mm³. Mice were divided randomly over 4 groups. Group I was not treated and used as control for tumor growth. Group II was treated with 12.5 mg/kg oral ritonavir, group III was treated with 20 mg/kg intravenous (i.v.) docetaxel, and group IV was treated with both 20 mg/kg i.v. docetaxel and 12.5 mg/kg oral ritonavir (Supplemental figure 1). Docetaxel was administered once a week, while ritonavir was administered for 5 subsequent days per week. Mice were treated for 3 subsequent weeks or until tumors reached a volume of ~1500 mm³. After three weeks, treatment was stopped and mice were monitored until a tumor volume of ~1500 mm³ was reached. Tumor volumes were measured daily in all groups. At a tumor volume of ~1500 mm³, mice were sacrificed and blood was taken by cardiac puncture and tumors collected. Blood samples were centrifuged at ambient temperature at 8,000 *g* for 5 minutes and subsequently plasma was collected. After tumor isolation, the tumor was cut over its length axis. One half was used for histological analysis and the other half was used for analysis of drug concentrations and RNA expression. Additional mice were used for tumor and plasma sampling on day 2 and 9. In groups III and IV, samples were also collected on day 16. All samples were taken approximately 24 hours after drug administration on the day before.

Histological analysis

Tumor samples for histological analysis were fixed in EAF fixative (ethanol/acetic acid/formaldehyde/saline at 40:5:10:45 v/v) and embedded in paraffin. Sections were cut at 2 μm from the paraffin blocks and stained with hematoxylin and eosin (HE) according to standard procedures. The sections were reviewed with a Zeiss Axioskop2 Plus microscope (Carl Zeiss Microscopy, Jena, Germany) equipped with Plan-Apochroma and Plan-Neofluar objectives. Images were captured with a Zeiss AxioCam HRc digital camera and processed with AxioVision 4 software (both from Carl Zeiss Vision, Munich, Germany).

RNA expression levels

After isolation, tumor samples were stored in RNeasy[®] (Qiagen, Venlo, The Netherlands) until RNA was extracted using the RNeasy mini kit (Qiagen) according to the manufacturer's protocol for the purification of total RNA from animal tissues. Subsequently, cDNA was generated using 5 µg of total RNA in a synthesis reaction using random hexamers (Applied Biosystems, Foster City, CA, USA) and superscript II reverse transcriptase (Invitrogen, Carlsbad, CA, USA), according to the supplier's protocols. The reverse transcription reaction was performed for 60 min at 42°C with a deactivation step of 15 min at 70°C.

Real-time (RT)-PCR was performed on an Applied Biosystems 7500 real-time cycler system according to the manufacturer's protocol. Specific primers (Qiagen) for the individual mouse genes *Cyp3a11*, *Cyp3a13*, *Cyp3a16*, *Mdr1a*, *Mdr1b* and *Bcrp* were used. Briefly, in a MicroAmp Fast Optical 96-well reaction plate (Applied Biosystems), 10 µl reaction mixtures containing 2.5 µl cDNA (0.1 ng/µl), 5 µl SyBr Green PCR master mix, 1 µl sample primer mix (QuantiTect Primer Assays, Qiagen) and 1.5 µl aqua Braun were pipetted. After sealing the plate with optical adhesive film (Applied Biosystems), the plates were briefly centrifuged. The cycling conditions were initiated at 50°C for 2 min with an enzyme activation step of 95°C for 10 min, followed by 45 PCR cycles of denaturation at 95°C for 15 s, and annealing/extension at 60°C for 1 min. Dissociation curves were analyzed to ensure only a single product was amplified. Analysis of the results was done by the comparative Ct method as described previously.⁽²⁷⁾ Quantitation of the target cDNAs in all samples was normalized to GAPDH cDNA ($Ct_{\text{target}} - Ct_{\text{GAPDH}} = \Delta Ct$). Statistics were performed on ΔCt values.⁽²⁸⁾

Drug concentrations

Previously developed liquid chromatography assays coupled with tandem mass spectrometry detection (LC-MS/MS) were used to quantify docetaxel, ritonavir and docetaxel metabolites M1/M3, M2 and M4 in plasma and tumor homogenates.^(29,30) Labeled structure analogues of docetaxel and ritonavir were used as internal standards. Tumor samples were homogenized in 4% of bovine serum albumin phosphate in buffered saline - pH 7.4 (w/v). A 200 µL sample of plasma or homogenized tumor was used for quantification of the analytes. For quantification of docetaxel, homogenized tumor samples were 20-fold diluted with human plasma as the concentrations in the undiluted samples were outside the calibration range. Ritonavir and metabolites of docetaxel were quantified in undiluted homogenized tumor samples. 25 µL of internal standard working solution was added to the samples. Subsequently, the samples were mixed briefly, tertiary-butyl methyl ether was added and the samples were shaken for 10 minutes at 1250 rpm. They were centrifuged at 23,000 g, snap-frozen and the organic layer was collected. After evaporation of the organic layer, the samples were reconstituted with reconstitution solvent and an aliquot was injected into the LC-MS/MS system. Calibration standards in human plasma were used for quantification. Concentrations in homogenized tumor samples were back-calculated to concentrations in tumor tissue. Limits of quantification for docetaxel and its metabolites in plasma and tumor tissue were 0.5 ng/mL and 0.5 ng/g, respectively, and 2 ng/mL and 2 ng/g for ritonavir.

Statistical analysis

The Mann-Whitney U test was used when differences in drug levels between two groups were compared. Differences were considered statistically significant when $P < 0.05$. For RNA expression levels, one-way ANOVA with Dunnett's correction was used to accommodate multiple testing and to compare expression levels to the control group. Differences were considered statistically significant when $P < 0.05$. All data are presented as mean \pm SD. Survival curves were compared using a Log-rank (Mantel-Cox) test. As a correction for multiple comparisons, differences between survival curves were considered statistically significant when $P < 0.00833$. To compare the period to development of a critical tumor volume (1500 mm^3), one-way ANOVA was used and the Bonferroni post-hoc correction was used to accommodate multiple testing. Differences were considered statistically significant when $P < 0.05$.

Results

Maximum tolerable dose of docetaxel and ritonavir

Initially, tolerability of i.v. docetaxel in female *Cyp3a*^{-/-} mice was assessed. At all tested doses, no other signs of little to moderate discomfort were observed than a decrease in bodyweight. Weekly administration of doses up to 25 mg/kg i.v. docetaxel were well tolerated for 3 weeks ($n = 3$ per dose level; data not shown). Administration of 30 or 35 mg/kg i.v. docetaxel resulted in a drop in bodyweight near to 80% of the initial bodyweight for all mice after the third administration of docetaxel ($n = 2$ per dose level). As a result, 25 mg/kg was considered to be the maximum tolerable dose of docetaxel.

Oral administration of 12.5 mg/kg ritonavir (daily, 5 times per week) was also tolerated for 3 weeks ($n = 3$). However, the combination of 25 mg/kg i.v. docetaxel and 12.5 mg/kg ritonavir resulted in an unacceptable decrease in bodyweight ($<80\%$ of the initial bodyweight) during the third week of treatment ($n = 4$), despite additional support of the mice with crushed and moistened food during treatment. A dose of 15 ($n = 4$) or 20 mg/kg ($n = 5$) i.v. docetaxel co-administered with 12.5 mg/kg oral ritonavir was tolerated when using additional support with crushed and moistened food during treatment. Therefore, 20 mg/kg i.v. docetaxel and 12.5 mg/kg oral ritonavir was selected as the maximum tolerable dose combination of docetaxel and ritonavir and used for tumor treatment (Supplemental figure 1).

Effects of drug treatment on tumor growth

At a tumor volume of $\sim 200 \text{ mm}^3$, the drug treatments were started (Supplemental figure 1). Treatment was given for 3 subsequent weeks. Since tumors of mice receiving single ritonavir treatment reached a volume of $\sim 1500 \text{ mm}^3$ within 3 weeks, mice were sacrificed before the end of the initially planned period of treatment. The median time to reach a tumor volume of $\sim 1500 \text{ mm}^3$ was 10 days in the control group and 14 days in the ritonavir-treated group (Figure 1). Mean times to reach 1500 mm^3 were 10.8 (SD: 2.2) days and 12.4 (SD: 3.1) days, respectively (Supplemental figure 2). Although the tumors in the ritonavir-treated group tended to grow slightly more slowly, there was no

statistically significant difference between the survival curves of the ritonavir-treated group and the untreated group.

As expected, docetaxel treatment resulted in a reduction of tumor volume. After three weeks of treatment the tumor volume was reduced to ~70% of the tumor volume at the start of the treatment (Figure 2). However, after co-treatment with ritonavir the tumor volume was further reduced to ~30% of the initial tumor volume ($P < 0.01$). In line with this stronger effect of the co-treatment, the median time to reach a tumor volume of ~1500 mm³ was 54 days (mean \pm SD: 53.6 \pm 1.5) in the docetaxel group and 66 days (mean \pm SD: 65.6 \pm 8.6) in the docetaxel and ritonavir group (Figure 1; Supplemental figure 1). Interestingly, a statistically significant difference ($P = 0.0025$) was observed between the survival curves of the docetaxel-treated group and the docetaxel and ritonavir co-treated group (Figure 1). Thus, oral co-administration of ritonavir increased the efficacy of docetaxel treatment in our model.

Histological analysis

Tumor tissue derived from the control group on day 2 was considered representative for initial tumor tissue. Histological analysis of these samples showed a solid and moderately differentiated adenocarcinoma with thin fibro-vascular stroma (Figure 3). The tumor cells were round and moderate in size with very poor cell boundaries. Mitotic cells were abundantly present and apoptotic cells were readily seen. Necrosis

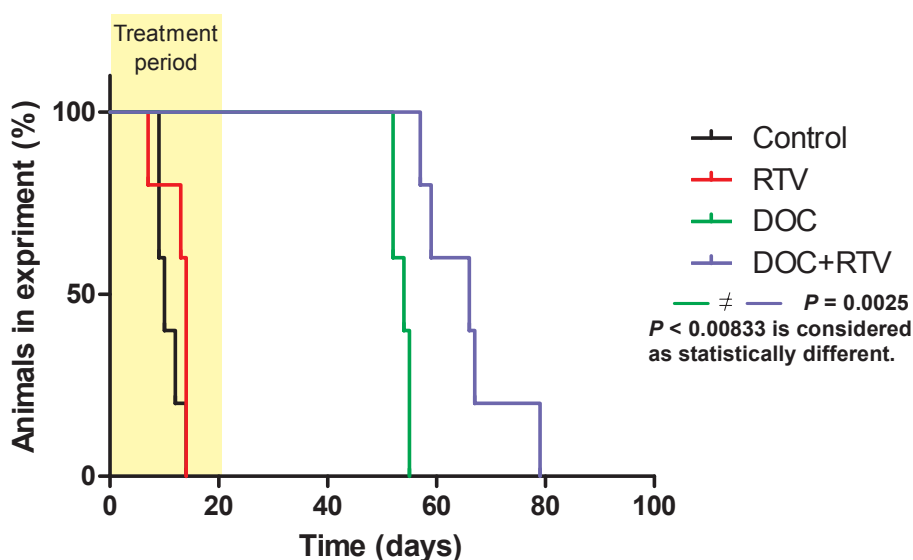


Figure 1. Effect of docetaxel/ritonavir co-administration on survival of *Cyp3a*^{-/-} mice (n = 5 per group) with orthotopically implanted syngeneic mouse mammary tumors. Mice were treated for 3 weeks with 20 mg/kg i.v. docetaxel and/or 12.5 mg/kg oral ritonavir. Docetaxel was administered once a week, while ritonavir was administered for 5 subsequent days per week. Untreated mice were used as a control group. Treatment was started at a tumor volume of 200 mm³ and mice were sacrificed when a tumor volume of ~1500 mm³ was reached. Note that differences between survival curves were considered statistically significant when $P < 0.00833$, in view of the multiple (4) groups compared.

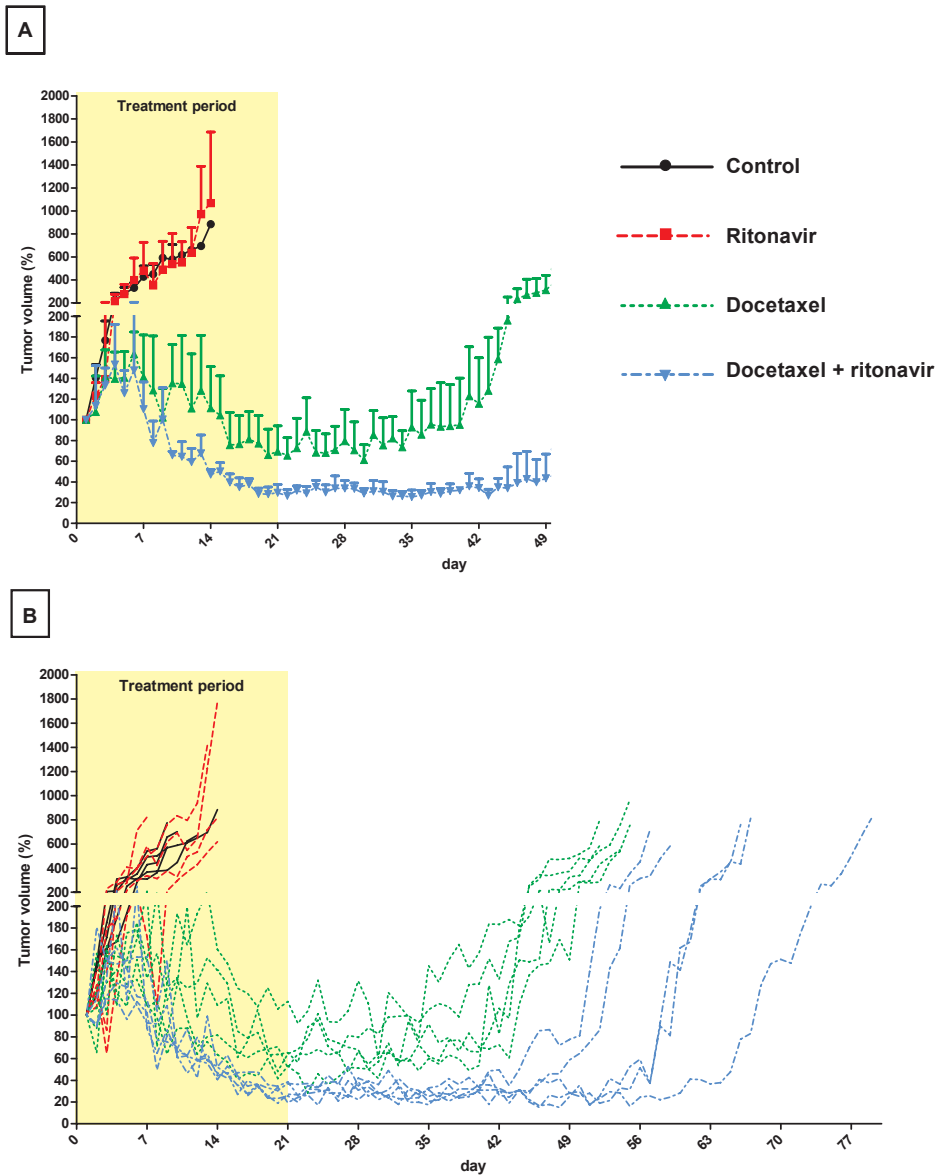


Figure 2. Tumor volumes after docetaxel/ritonavir co-administration to *Cyp3a*^{-/-} mice (n = 5 per group) with orthotopically implanted syngeneic mouse mammary tumors. Tumor volumes are presented as percentage of the tumor volume at start of treatment. Mice were treated for 3 weeks with 20 mg/kg i.v. docetaxel and/or 12.5 mg/kg oral ritonavir. Docetaxel was administered once a week, while ritonavir was administered for 5 subsequent days per week. Untreated mice were used as a control group. Treatment was started at a tumor volume of 200 mm³ and mice were sacrificed when a tumor volume of ~1500 mm³ was reached. Panel A shows the mean tumor volumes with standard deviations per treatment group over the first 7 weeks. Beyond this period, differential loss of individual mice between groups would result in biased means; these were therefore not plotted. Panel B shows the curves of individual mice over the full monitoring period. Curves of different colors represent different treatment groups.

was locally observed in the tumor tissue. On day 9, necrosis in tumor tissue of the control group was more extensive and the tumor stroma showed an increased amount of collagen. At a tumor volume of $\sim 1500 \text{ mm}^3$, necrosis of tumor tissue of the control group was even more readily observed than in tumor tissue collected on day 9. Tumor tissue collected from ritonavir-treated mice was similar to tissue from the control group for days 2 and 9, and at a tumor volume of $\sim 1500 \text{ mm}^3$. On day 2, tumor tissue in docetaxel-treated mice showed more apoptosis than tumor tissue in untreated mice. On day 9, tumor cells of docetaxel-treated mice showed a great deal of pleomorphism (variability in the size and shape of cells) and tumor stroma was expanded with fibrotic changes. In these samples, mitotic cells were readily seen, although not as frequently as in untreated tumor tissue. Apoptotic cells were abundantly present and no necrosis was observed in tumor tissue of docetaxel-treated mice on day 9. On day 16, the number of mitotic cells was further reduced and atrophic cells were observed. Tumor tissue of ritonavir and docetaxel co-treated mice was very similar to tumor tissue of docetaxel-treated mice. There was no obvious difference in the histopathology of all the tumors once they reached a size of $\sim 1500 \text{ mm}^3$ (i.e., when fully grown out, and at least 4 weeks after termination of drug treatment when applied).

RNA expression levels

The observed difference in tumor growth between the docetaxel-treated group and the docetaxel and ritonavir co-treated group might be related to an altered expression profile of metabolizing or drug-transporting enzymes (e.g. Cyp3a or P-gp) between the groups. We therefore measured RNA expression levels in all tumor tissue samples derived on day 2, 9 and 16. Tissue samples derived from the control group on day 2 were considered as initial expression levels in tumor tissue. Although a primer set was used for *Cyp3a13*, expression levels of this gene were too low for reliable quantification. Expression levels of all other tested genes were unchanged over time in the control group (Figure 4). Single treatment with orally administered ritonavir or intravenously administered docetaxel expression levels of the genes encoding for *Cyp3a11*, *Cyp3a16* or *Bcrp*. However, repeated single administration of docetaxel resulted in increased expression levels of genes encoding for *Mdr1a* and *1b* on day 9 and 16 (figure 4, panel C and D). This increase in gene expression during the drug administration period was transient, since expression of *Mdr1a* and *1b* in tumors at a volume of $\sim 1500 \text{ mm}^3$ was again similar to initial expression levels. After administration of docetaxel with and without ritonavir, expression levels of the genes encoding for *Cyp3a11*, *Cyp3a16* or *Bcrp* were not statistically different. Expression levels of *Mdr1a* and *1b* on day 2 were significantly higher after co-administration of docetaxel and ritonavir, however, expression levels were again similar on day 9 and 16 and in tumors at a volume of $\sim 1500 \text{ mm}^3$.

Since expression levels of the tested genes on day 9 and 16 were not different between docetaxel treatment with and without ritonavir, these results suggest that the increased efficacy of docetaxel when co-administered with ritonavir can not be explained by a difference in expression levels of *Cyp3a*, *Mdr1* or *Bcrp* as a result of ritonavir co-administration.

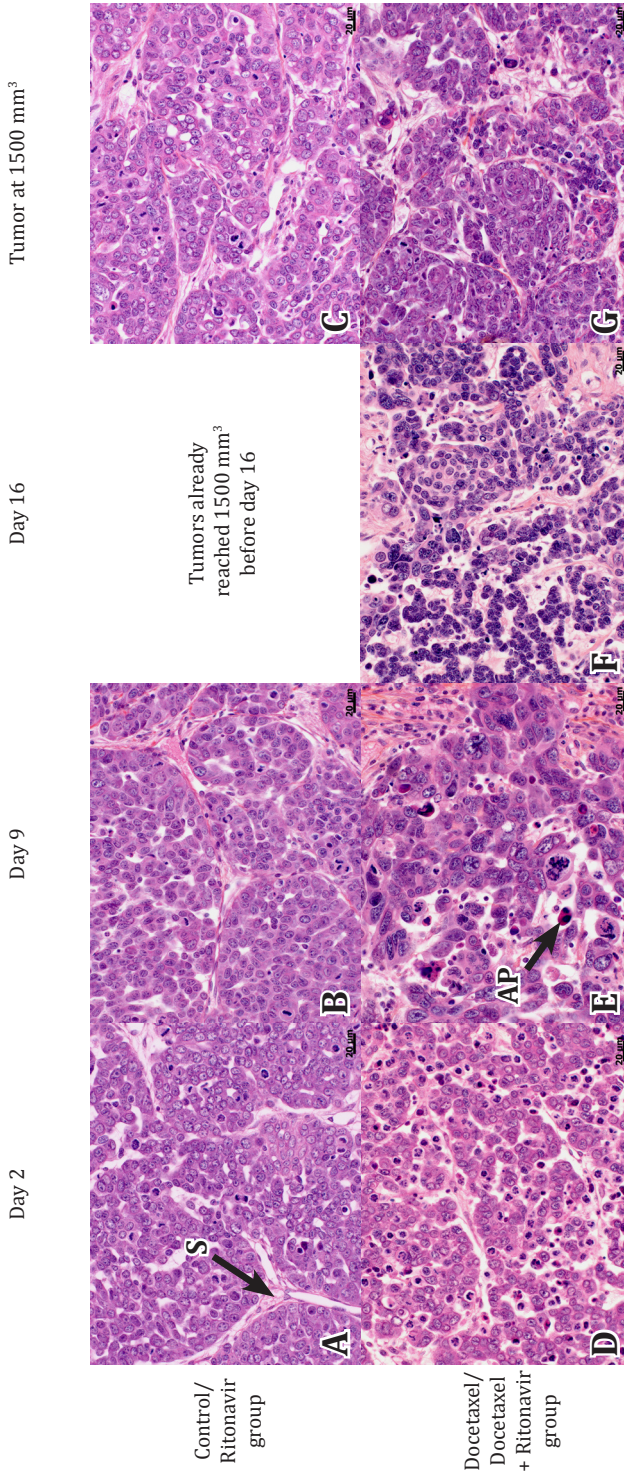


Figure 3. Photomicrographs of representative HE sections of tumor tissue after docetaxel/ritonavir co-administration to *Cyp3a1*^{-/-} mice (n = 5 per group) with orthotopically implanted syngeneic mouse mammary tumors. Tumor tissues of untreated mice and mice treated with 12.5 mg/kg ritonavir for 5 subsequent days a week looked very similar and representative images are therefore shown in the upper panels. Tumor tissue of mice treated with 20 mg/kg docetaxel once a week looked similar with or without co-administration of ritonavir and representative images are shown in the lower panels. Mice were sacrificed for pathological examination on days 2 and 9, and at a tumor volume of ~1500 mm³. Docetaxel-treated mice were also sacrificed at day 16. Tumor tissue derived from the control group at day 2 was considered as representative for initial tumor tissue (Panel A). Over time, necrosis in tumor tissue was more extensive and the tumor stroma showed an increased amount of collagen (Panels B and C). On day 2, tumor tissue in docetaxel-treated mice showed more apoptosis than tumor tissue in untreated mice (Panel D). During docetaxel treatment, tumor cells showed a great deal of pleomorphism (variability in the size and shape of cells) and the tumor stroma was expanded (Panels E and F). Mitotic cells were readily seen, while apoptotic cells were abundantly present (Panel F). Tumor tissue of tumors of ~1500mm³, when fully grown out, and thus either untreated or at least 4 weeks after the last docetaxel treatment, were not different between untreated mice and mice treated with docetaxel (Panel G). Arrows mark tumor stroma (S), and apoptosis (AP). (Original magnification 40x).

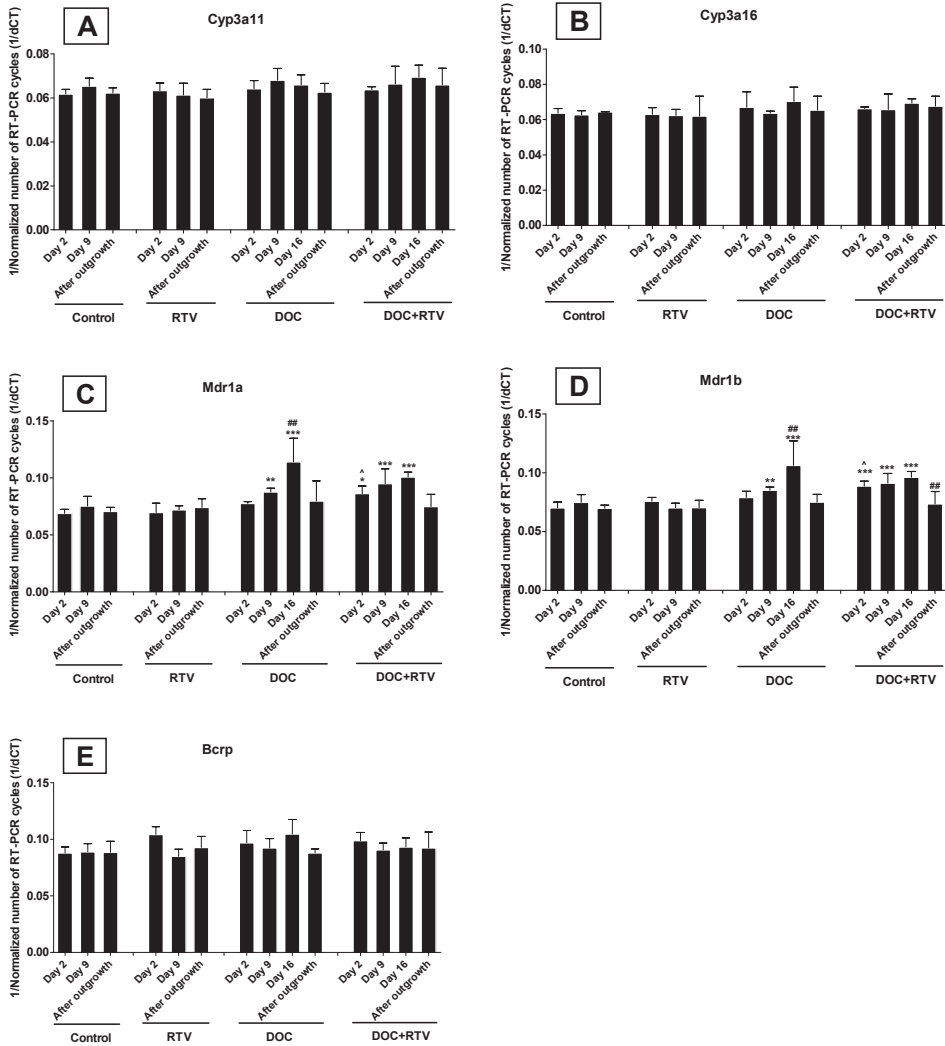


Figure 4. RNA expression levels in tumor tissue (n = 5 per group). Panels reflect expression of *Cyp3a11* (panel A), *Cyp3a16* (panel B), *Mdr1a* (panel C), *Mdr1b* (panel D) and *Bcrp* (panel E). Expression of *Cyp3a13* was too low to detect. *Cyp3a1*^{-/-} mice were implanted with syngeneic mouse mammary tumors and treated for 3 weeks with 20 mg/kg i.v. docetaxel and/or 12.5 mg/kg oral ritonavir. Docetaxel was administered once a week, while ritonavir was administered for 5 subsequent days per week. Untreated mice were used as a control group. Samples were collected on day 2, day 9 and after outgrowth (tumor volume ~1500 mm³). Samples were also collected on day 16 for the docetaxel and docetaxel + ritonavir treated group. Data reflect 1 divided by the number of RT-PCR cycles. Data are presented as mean ± S.D. Cycles are normalized for *GAPDH* expression. Data are not statistically different from samples taken on day 2 in the control group, unless otherwise specified (**P* < 0.05, ***P* < 0.01 and ****P* < 0.001). Other symbols reflect a statistical difference between day 2 and another day in that group (## *P* < 0.01) or a difference between docetaxel treatment with or without ritonavir (^ *P* < 0.05). Abbreviations: DOC: docetaxel; RTV: ritonavir.

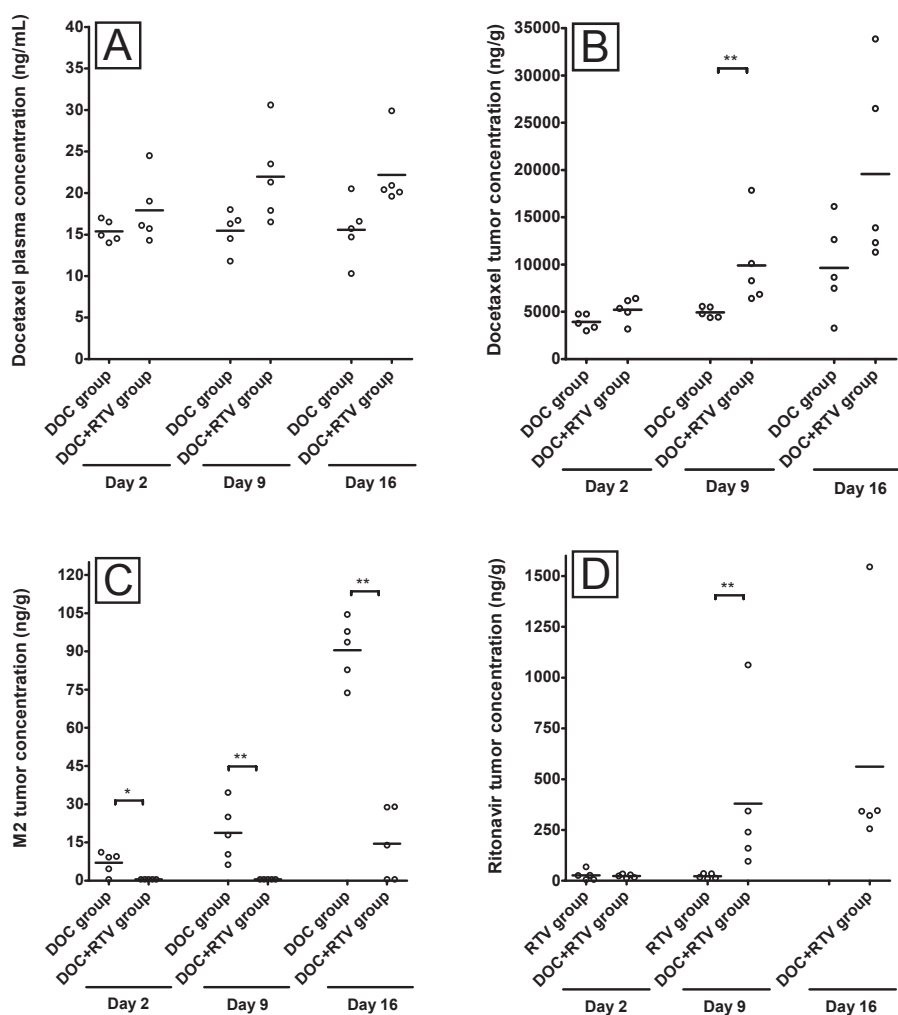


Figure 5. Drug concentrations in plasma and tumor tissue ($n = 5$ per group) on days 2, 9 and 16. Samples were taken approximately 24 hr after the last administration of ritonavir and docetaxel. Panels reflect plasma (panel A), and tumor (panel B) concentrations of docetaxel, tumor concentrations of docetaxel metabolite M2 (panel C), and tumor concentrations of ritonavir (panel D). Ritonavir and metabolite M2 were not detected in plasma (limit of detection was 2 ng/mL and 0.5 ng/mL, respectively). *Cyp3a1*^{-/-} mice were implanted with syngeneic mouse mammary tumors and treated for 3 weeks with 20 mg/kg i.v. docetaxel and/or 12.5 mg/kg oral ritonavir. Docetaxel was administered once a week, while ritonavir was administered for 5 subsequent days per week. Untreated mice were used as a control group. Samples were collected on days 2 and 9. Samples were also collected on day 16 for the docetaxel and docetaxel + ritonavir treated group. Data are presented as individual data points and lines represent the mean. Statistical significance was tested using the Mann-Whitney U test. The limit of detection (0.5 ng/g) was used for statistical calculations when tumor concentrations of M2 were below the limit of detection. Differences between single drug treatment and co-treatment of docetaxel and ritonavir are not statistically different, unless otherwise specified (** $P < 0.01$) Abbreviations: DOC: docetaxel; NS: not significant; RTV: ritonavir.

Drug concentrations in plasma and tumors

On day 2, 9 and 16, plasma concentrations of ritonavir were below the limit of detection. These samples were taken approximately 24 hours after oral administration of 12.5 mg/kg ritonavir on the day before. Docetaxel metabolites could also not be detected in plasma in samples taken on day 2, 9 and 16 (approximately 24 hours after i.v. administration of 20 mg/kg docetaxel). In contrast, docetaxel plasma concentrations were detectable throughout, but not significantly different after administration of i.v. docetaxel with or without oral ritonavir ($P > 0.05$, figure 5, panel A).

In tumor tissue on day 2, 24 hr after the first drug administration, both ritonavir and docetaxel concentrations were comparable between single and co-administration of the drugs ($P > 0.05$; figure 5, panel B and D). However, on day 9, concentrations of ritonavir and docetaxel in tumor tissue were higher when docetaxel was co-administered with ritonavir than after single drug administration ($P < 0.001$). On day 16, although not statistically significant ($P = 0.15$), tumor concentrations of docetaxel also tended to be increased in the co-treated group. Interestingly, tumor concentrations of the major docetaxel metabolite M2 after docetaxel and ritonavir co-administration were significantly lower than after single docetaxel administration at all sampled time points ($P < 0.05$ to $P < 0.01$; figure 5, panel C), suggesting substantially decreased metabolism of docetaxel.

Discussion

Our data in *Cyp3a*^{-/-} mice with an orthotopically transplanted mouse mammary tumor model showed an additional inhibiting effect on tumor growth when oral ritonavir was co-administered with i.v. docetaxel. No effect of ritonavir administration alone was observed and histological analysis of tumors showed no qualitative difference between docetaxel treatment with and without ritonavir. Therefore, it is likely that in our experiments the antitumor efficacy of docetaxel was enhanced by ritonavir after co-administration, instead of reflecting a direct antitumor effect of ritonavir itself.

Previously, effects of ritonavir treatment were assessed in multiple mouse models.^(12,17,13,14) However, most of these mouse models used human xenografts in immunocompromised mice and the predictive value of such models for the clinical setting is often questioned.^(31,32) The use of genetically engineered mouse models (GEMMs) developing certain well-defined tumors might be better to predict clinical efficacy of anticancer drugs, since GEMM-derived tumors evolve in immune-proficient physiological conditions and use representative tumor-stromal interactions.^(33,32) An example of a GEMM for breast cancer is the *BRCA1*- and *p53*-deficient mouse model we used here. Mammary tumors in this model exhibit dramatic genomic instability, and their molecular signatures resemble those of human *BRCA1*-mutated breast cancers.⁽²⁴⁾ Rottenberg et al. observed that spontaneous tumors of this GEMM showed a similar response to docetaxel when different parts of the same tumor were orthotopically transplanted into syngeneic wild-type mice (FVB genetic background).⁽³⁴⁾ In our experiment we used these spontaneous *K14cre;Brca1*^{-/-};*p53*^{-/-} mouse mammary tumors implanted in a syngeneic *Cyp3a*^{-/-} strain. We could study a spontaneously

arising mammary tumor from a GEM model that resembles *BRCA1*-mutated human breast cancer and that maintains its characteristics when implanted in the mammary fat pad of syngeneic mice. In addition, absence of *Cyp3a* in the host strain avoids a strong increase in docetaxel plasma concentrations as a result of inhibition of systemic Cyp3a metabolism by ritonavir. In this combined GEM model, we observed no direct antitumor effect of ritonavir itself, but found enhanced antitumor effects of docetaxel treatment when combined with oral ritonavir. Our results are in line with the results of Ikezoe et al⁽¹⁷⁾ and suggest that the observed increased efficacy of docetaxel after co-administration with oral ritonavir in their xenograft model for prostate cancer was not only due to a difference in plasma exposure to docetaxel.

We aimed to understand the observed additional inhibiting effect on tumor growth when oral ritonavir was co-administered with i.v. docetaxel and studied drug concentrations in plasma and tumor tissue as well as mRNA expression in tumor tissue. After i.v. administration of docetaxel in *Cyp3a*^{-/-} mice, plasma concentrations (approximately 24 hours after drug administration) were not significantly different with and without oral co-administration of ritonavir (Figure 5, panel A), albeit that there was a trend towards slightly higher plasma levels in the ritonavir co-treated mice. Plasma concentrations of ritonavir and docetaxel metabolites were below the limit of detection in all measured samples.

In tumor tissue, docetaxel concentrations on day 9 were significantly higher (mean about 2.0-fold increased) when docetaxel was co-administered with ritonavir than after single drug administration (Figure 5B). Also on day 16 there was a 2.0-fold higher mean tumor docetaxel concentration in the co-treated group, although this was not statistically significant. Also for ritonavir on day 9 there were markedly and significantly higher tumor concentrations (Figure 5D).

Ritonavir concentrations in tumor tissue on day 9 were significantly higher when ritonavir and docetaxel were co-administered than after single ritonavir concentration. However, for ritonavir one should be cautious with interpretation of tumor concentrations on day 9 since this comparison might be biased by the difference in tumor volume in the ritonavir-treated group and docetaxel and ritonavir co-treated group (~770 mm³ versus ~170 mm³, respectively). Moreover, histology of tumors was different between tumors treated with and without docetaxel. This concern is less of a problem for docetaxel and docetaxel metabolite M2 concentrations, since histology of docetaxel-treated tumors was comparable between groups treated with and without ritonavir. Tumor sizes on day 9 were also more similar between the docetaxel-treated and co-treated groups.

The amount of the primary docetaxel metabolite M2 in tumor tissue was clearly much lower when docetaxel was co-administered with ritonavir on all days of measurement (Figure 5, panel C). Docetaxel is metabolized via Cyp3a into metabolite M2 and this metabolite is further metabolized into other metabolites.^(35,36,37) Metabolite M2 exhibits some cytotoxicity, however its cytotoxic effects are much lower than the cytotoxic effects of docetaxel. The other metabolites show no relevant cytotoxic activity.⁽³⁸⁾ A decrease in docetaxel tumor concentrations can be caused by both docetaxel metabolism and

docetaxel efflux from the tumor tissue by drug transporters like P-gp. Given this, M2 tumor concentrations are a good parameter for assessment of altered docetaxel metabolism, since M2 formation is a direct functional result of docetaxel metabolism. Lower M2 tumor concentrations in docetaxel and ritonavir co-treated mice suggest that docetaxel metabolism in the tumor was lower when docetaxel was co-administered with ritonavir than after single docetaxel administration. Decreased metabolism of docetaxel in the tumor could also explain the observed higher parent docetaxel concentrations in the tumor when docetaxel is co-administered with ritonavir (Figure 5, panel B).

Docetaxel metabolism might be altered due to Cyp3a inhibition in the tumor by ritonavir or by altered *Cyp3a* expression in tumor tissue. Ritonavir could be detected and quantified in tumor tissue, indicating that Cyp3a inhibition in tumors by ritonavir is a possibility. As we did not observe a change in *Cyp3a11*, *-3a13* or *-3a16* expression in tumors, altered docetaxel metabolism seems not to be caused by a shift in *Cyp3a* expression. *Mdr1a* and *1b* expression in tumors was increased after repeated single docetaxel treatment (Figure 4C and D), but co-administration of docetaxel and ritonavir resulted in similar changes in expression levels on day 9 and 16. It cannot be excluded that the increased expression of *Mdr1a* and *Mdr1b* after docetaxel (co)treatment is related to selection of tumor cells with comparatively higher *Mdr1a* and *Mdr1b* expression. Intracellular exposure of cells to docetaxel will be reduced when intrinsic expression of *Mdr1a* and *Mdr1b* is higher. This can result in a survival benefit for such cells and thus in a relatively high abundance of tumor cells with a high expression of *Mdr1*. Moreover, theoretically the observed increase in expression of *Mdr1a* and *1b* in docetaxel treated tumors could also be related to the relative increase in tumor stroma in these tumors, as they are responding to the docetaxel therapy, in case stroma has higher *Mdr1a* and *1b* expression than the initial tumor cells. Expression of *Mdr1* genes in stroma will become more important if the number of tumor cells decreases and the stroma is relatively expanded. Nonetheless, based on similar expression levels of *Mdr1* in docetaxel-treated mice with and without ritonavir co-treatment, it is not likely that *Mdr1a* and *1b* activity are a factor in the increased antitumor efficacy as observed after co-administration of docetaxel and ritonavir.

During the first week of treatment, tumor volumes were comparable in mice treated with docetaxel and in mice treated with both docetaxel and ritonavir. During the second week of treatment, we started to observe differences in tumor volume between these groups. An increased antitumor efficacy of docetaxel and ritonavir co-treatment was clearly visible during the third and last week of treatment. This is in line with the observed differences in tumor concentrations of docetaxel and M2 over time (Figure 5). On day 2, tumor concentrations of M2 were low in docetaxel-treated mice and not detectable in docetaxel and ritonavir co-treated mice. While M2 was still undetectable on day 9 and 16 in tumor tissue of co-treated mice, tumor concentrations of M2 increased over time after single docetaxel administration. In line with these observations, parent docetaxel concentrations were about 2-fold increased in the tumors. This suggests decreased docetaxel metabolism in tumors upon co-administration with ritonavir. Since detectable concentrations of ritonavir were still observed in tumor tissue 24 hr after administration, it is likely that ritonavir can extensively inhibit intratumoral

Cyp3a. Given the absence of antitumor efficacy of single ritonavir treatment in our model, Cyp3a inhibition in the tumor by ritonavir may be primarily responsible for the observed increase in docetaxel efficacy when docetaxel is co-administered with ritonavir.

Conclusions

We showed that antitumor efficacy of intravenously administered docetaxel in a GEM model for *BRCA1*-mutated breast cancer is substantially increased by co-administration of orally administered ritonavir. Since we used mice lacking Cyp3a, this increase in efficacy is unlikely to be caused by altered systemic clearance of docetaxel. Although we screened for an underlying mechanism for the increased efficacy of docetaxel when coadministered with ritonavir, this is not yet fully explained. We could exclude a differential shift in gene expression of Cyp3a and P-gp as a result of coadministration with ritonavir. Our data indicate that Cyp3a inhibition in tumor tissue by ritonavir may cause decreased docetaxel metabolism in the tumor and this may have contributed to the observed increased antitumor efficacy of docetaxel when coadministered with ritonavir.

Since ritonavir is currently used in clinical phase I trials to increase the plasma exposure of orally applied docetaxel in patients⁽³⁹⁾, these results reveal an additional advantage of co-administration of docetaxel and ritonavir. Although we administered docetaxel intravenously in this experiment, the increased antitumor efficacy might also be observed after oral administration. We therefore believe that it will be worthwhile to test in patients whether oral co-administration of docetaxel and ritonavir will result in a higher anti-tumor efficacy than that of the currently used i.v. schedules of docetaxel without co-administration of ritonavir.

Acknowledgements

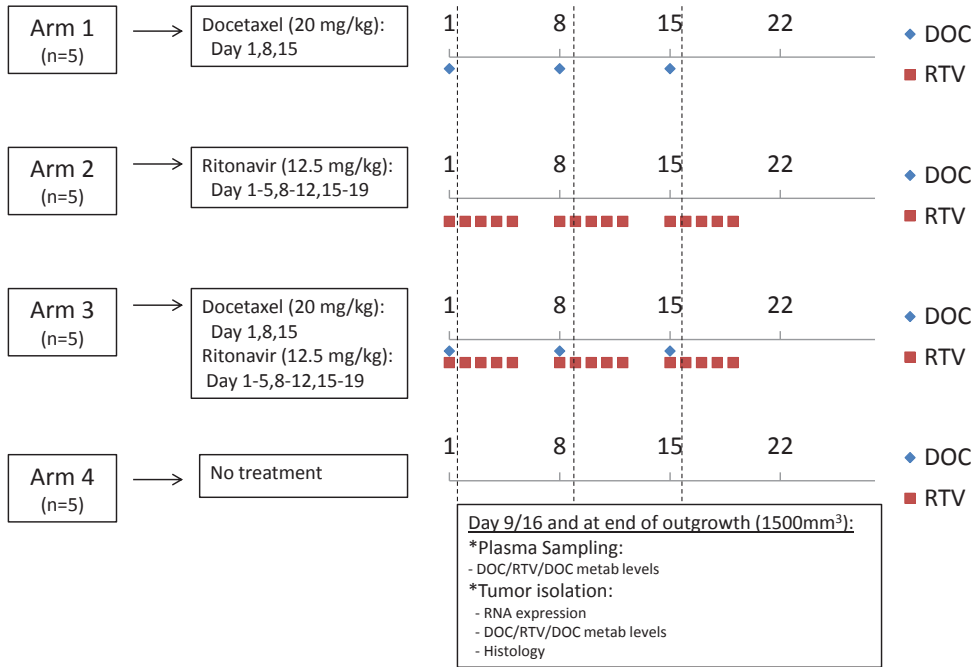
We thank Wendy Sol for her help during tumor implantations and Anita van Esch for her help during RT-PCR analysis.

References

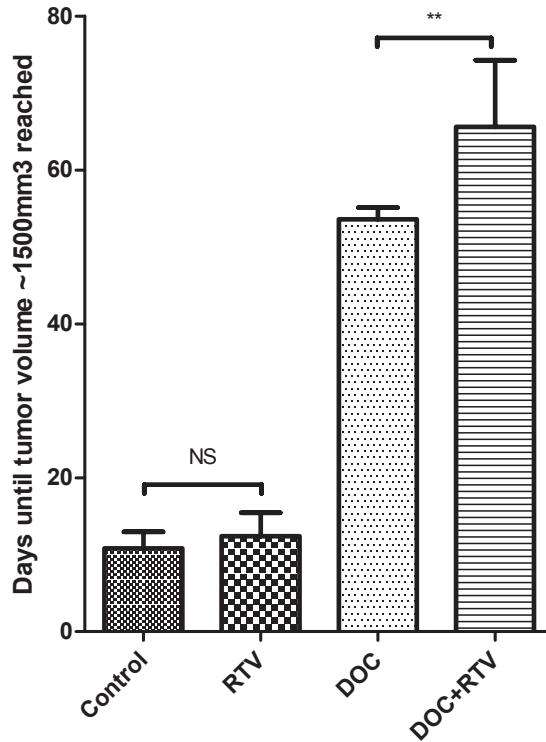
1. Grossi F, Kubota K, Cappuzzo F *et al*: Future scenarios for the treatment of advanced non-small cell lung cancer: focus on taxane-containing regimens. *Oncologist*. **2010**; 15 (10): 1102-12.
2. Nishiyama M, Wada S: Docetaxel: its role in current and future treatments for advanced gastric cancer. *Gastric.Cancer*. **2009**; 12 (3): 132-41.
3. Belfiglio M, Fanizza C, Tinari N, Ficorella C, Iacobelli S, Natoli C: Meta-analysis of phase III trials of docetaxel alone or in combination with chemotherapy in metastatic breast cancer. *J.Cancer Res.Clin.Oncol*. **2012**; 138 (2): 221-29.
4. Cheetham P, Petrylak DP: Tubulin-targeted agents including docetaxel and cabazitaxel. *Cancer J*. **2013**; 19 (1): 59-65.
5. Koelen SL, Beijnen JH, Schellens JHM: Intravenous-to-oral switch in anticancer chemotherapy: a focus on docetaxel and paclitaxel. *Clin.Pharmacol.Ther*. **2010**; 87 (1): 126-29.
6. Schellens JHM, Malingre MM, Kruijtzter CM *et al*: Modulation of oral bioavailability of anticancer drugs: from mouse to man. *Eur.J.Pharm.Sci*. **2000**; 12 (2): 103-10.
7. Bardelmeijer HA, Ouweland M, Buckle T *et al*: Low systemic exposure of oral docetaxel in mice resulting from extensive first-pass metabolism is boosted by ritonavir. *Cancer Res*. **2002**; 62 (21): 6158-64.
8. Oostendorp RL, Huitema A, Rosing H *et al*: Coadministration of ritonavir strongly enhances the apparent oral

- bioavailability of docetaxel in patients with solid tumors. *Clin.Cancer Res.* **2009**; 15 (12): 4228-33.
9. Zhong DS, Lu XH, Conklin BS *et al*: HIV protease inhibitor ritonavir induces cytotoxicity of human endothelial cells. *Arterioscler.Thromb.Vasc.Biol.* **2002**; 22 (10): 1560-66.
 10. Pati S, Pelsler CB, Dufraine J, Bryant JL, Reitz MS, Jr, Weichold FF: Antitumorigenic effects of HIV protease inhibitor ritonavir: inhibition of Kaposi sarcoma. *Blood.* **2002**; 99 (10): 3771-79.
 11. Sgadari C, Monini P, Barillari G, Ensoli B: Use of HIV protease inhibitors to block Kaposi's sarcoma and tumour growth. *Lancet Oncol.* **2003**; 4 (9): 537-47.
 12. Gaedicke S, Firat-Geier E, Constantiniu O *et al*: Antitumor effect of the human immunodeficiency virus protease inhibitor ritonavir: induction of tumor-cell apoptosis associated with perturbation of proteasomal proteolysis. *Cancer Res.* **2002**; 62 (23): 6901-08.
 13. Maggiorella L, Wen B, Frascogna V, Opolon P, Bourhis J, Deutsch E: Combined radiation sensitizing and anti-angiogenic effects of ionizing radiation and the protease inhibitor ritonavir in a head and neck carcinoma model. *Anticancer Res.* **2005**; 25 (6B): 4357-62.
 14. Srirangam A, Mitra R, Wang M *et al*: Effects of HIV protease inhibitor ritonavir on Akt-regulated cell proliferation in breast cancer. *Clin.Cancer Res.* **2006**; 12 (6): 1883-96.
 15. Ahluwalia MS, Patton C, Stevens G *et al*: Phase II trial of ritonavir/lopinavir in patients with progressive or recurrent high-grade gliomas. *J.Neurooncol.* **2011**; 102 (2): 317-21.
 16. Laurent N, de Bouard S, Guillamo JS *et al*: Effects of the proteasome inhibitor ritonavir on glioma growth in vitro and in vivo. *Mol.Cancer Ther.* **2004**; 3 (2): 129-36.
 17. Ikezoe T, Hisatake Y, Takeuchi T *et al*: HIV-1 protease inhibitor, ritonavir: a potent inhibitor of CYP3A4, enhanced the anticancer effects of docetaxel in androgen-independent prostate cancer cells in vitro and in vivo. *Cancer Res.* **2004**; 64 (20): 7426-31.
 18. van Waterschoot RA, Lagas JS, Wagenaar E *et al*: Absence of both cytochrome P450 3A and P-glycoprotein dramatically increases docetaxel oral bioavailability and risk of intestinal toxicity. *Cancer Res.* **2009**; 69 (23): 8996-9002.
 19. Hendriks JJ, Lagas JS, Rosing H, Schellens JH, Beijnen JH, Schinkel AH: P-glycoprotein and cytochrome P450 3A act together in restricting the oral bioavailability of paclitaxel. *Int.J.Cancer.* **2013**; 132 (10): 2439-47.
 20. Li F, Wang L, Guo GL, Ma X: Metabolism-mediated drug interactions associated with ritonavir-boosted tipranavir in mice. *Drug Metab Dispos.* **2010**; 38 (5): 871-78.
 21. Harmsen S, Meijerman I, Beijnen JH, Schellens JH: Nuclear receptor mediated induction of cytochrome P450 3A4 by anticancer drugs: a key role for the pregnane X receptor. *Cancer Chemother.Pharmacol.* **2009**; 64 (1): 35-43.
 22. van Herwaarden AE, Wagenaar E, van der Kruijssen CM *et al*: Knockout of cytochrome P450 3A yields new mouse models for understanding xenobiotic metabolism. *J.Clin.Invest.* **2007**; 117 (11): 3583-92.
 23. Rottenberg S, Nygren AO, Pajic M *et al*: Selective induction of chemotherapy resistance of mammary tumors in a conditional mouse model for hereditary breast cancer. *Proc.Natl.Acad.Sci.U.S.A.* **2007**; 104 (29): 12117-22.
 24. Liu X, Holstege H, van der Gulden H *et al*: Somatic loss of BRCA1 and p53 in mice induces mammary tumors with features of human BRCA1-mutated basal-like breast cancer. *Proc.Natl.Acad.Sci.U.S.A.* **2007**; 104 (29): 12111-6.
 25. Euhus DM, Hudd C, LaRegina MC, Johnson FE: Tumor measurement in the nude mouse. *J.Surg.Oncol.* **1986**; 31 (4): 229-34.
 26. Romijn JC, Verkoelen CF, Schroeder FH: Measurement of the survival of human tumor cells after implantation in athymic nude mice. *Int.J.Cancer.* **1986**; 38 (1): 97-101.
 27. Livak KJ, Schmittgen TD: Analysis of relative gene expression data using real-time quantitative PCR and the 2(-Delta Delta C(T)) Method. *Methods.* **2001**; 25 (4): 402-8.
 28. Yuan JS, Reed A, Chen F, Stewart CN, Jr: Statistical analysis of real-time PCR data. *BMC.Bioinformatics.* **2006**; 7 (85): 85.
 29. Hendriks JJ, Hillebrand MJ, Thijssen B *et al*: A sensitive combined assay for the quantification of paclitaxel, docetaxel and ritonavir in human plasma using liquid chromatography coupled with tandem mass spectrometry. *J.Chromatogr.B Analyt.Technol.Biomed.Life Sci.* **2011**; 879 (28): 2984-90.
 30. Hendriks JJ, Dubbelman AC, Rosing H, Schinkel AH, Schellens JH, Beijnen JH: Quantification of docetaxel and its metabolites in human plasma by liquid chromatography/tandem mass spectrometry. *Rapid Commun.Mass Spectrom.* **2013**; 27 (17): 1925-34.
 31. Kerbel RS: Human tumor xenografts as predictive preclinical models for anticancer drug activity in humans: better than commonly perceived-but they can be improved. *Cancer Biol.Ther.* **2003**; 2 (4 Suppl 1): S134-9.
 32. Suggitt M, Bibby MC: 50 years of preclinical anticancer drug screening: empirical to target-driven approaches. *Clin.Cancer Res.* **2005**; 11 (3): 971-81.
 33. Sharpless NE, Depinho RA: The mighty mouse: genetically engineered mouse models in cancer drug development. *Nat.Rev.Drug Discov.* **2006**; 5 (9): 741-54.
 34. Rottenberg S, Vollebergh MA, de Hoon B *et al*: Impact of intertumoral heterogeneity on predicting chemotherapy response of BRCA1-deficient mammary tumors. *Cancer Res.* **2012**; 72 (9): 2350-61.

35. Bardelmeijer HA, Roelofs AB, Hillebrand MJ, Beijnen JH, Schellens JH, van Tellingen O: Metabolism of docetaxel in mice. *Cancer Chemother.Pharmacol.* **2005**; 56 (3): 299-306.
36. Marre F, Sanderink GJ, de Sousa G, Gaillard C, Martinet M, Rahmani R: Hepatic biotransformation of docetaxel (Taxotere) in vitro: involvement of the CYP3A subfamily in humans. *Cancer Res.* **1996**; 56 (6): 1296-1302.
37. Shou M, Martinet M, Korzekwa KR, Krausz KW, Gonzalez FJ, Gelboin HV: Role of human cytochrome P450 3A4 and 3A5 in the metabolism of taxotere and its derivatives: enzyme specificity, interindividual distribution and metabolic contribution in human liver. *Pharmacogenetics* **1998**; 8 (5): 391-401.
38. Sparreboom A, van Tellingen O, Scherrenburg EJ *et al*: Isolation, purification and biological activity of major docetaxel metabolites from human feces. *Drug Metab Dispos.* **1996**; 24 (6): 655-58.
39. Marchetti S, Stuurman FE, Koolen SL *et al*: Phase I study of weekly oral docetaxel (ModraDoc001) plus ritonavir in patients with advanced solid tumors. *ASCO Meeting Abstracts.* **2012**; 30 (15_suppl): 2550.

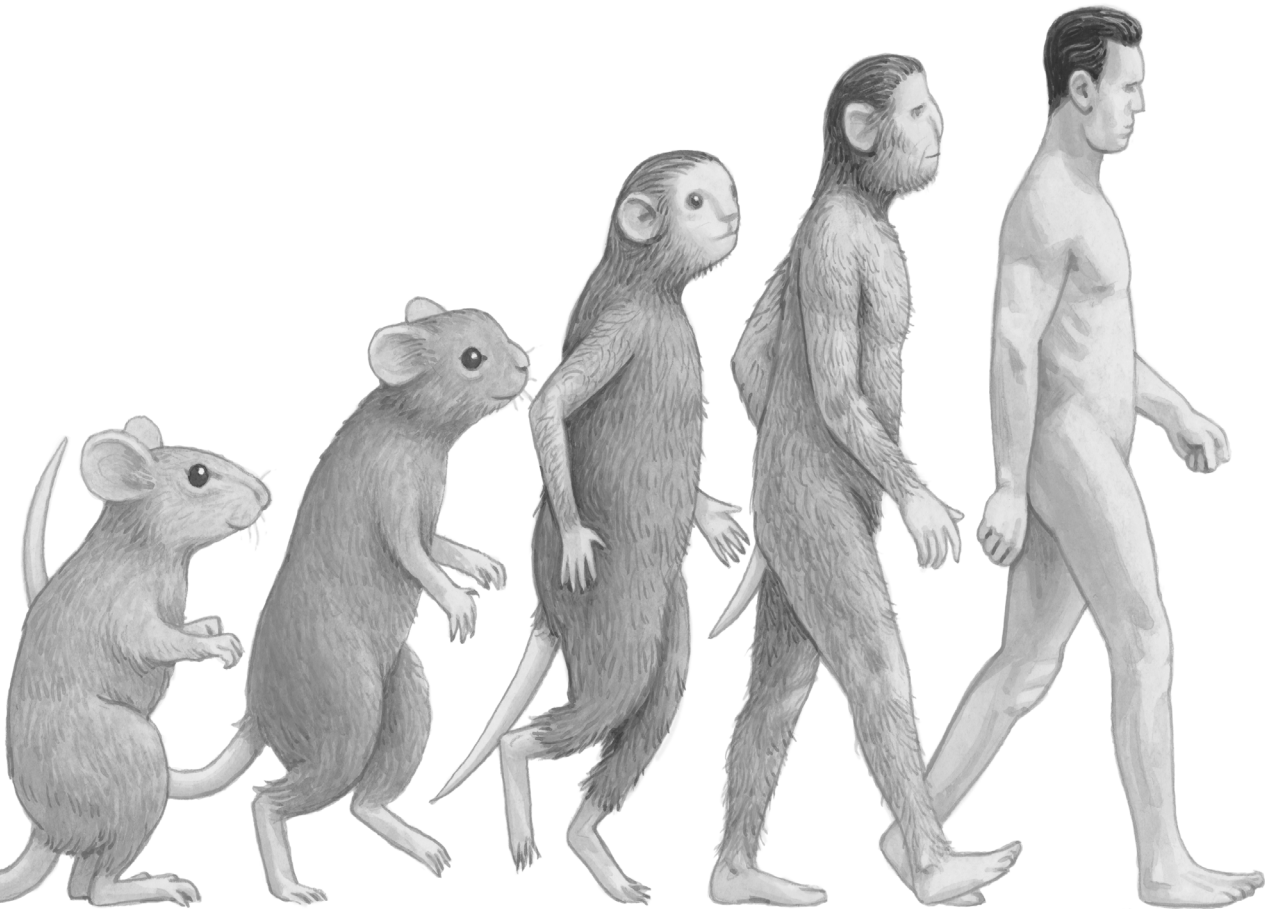
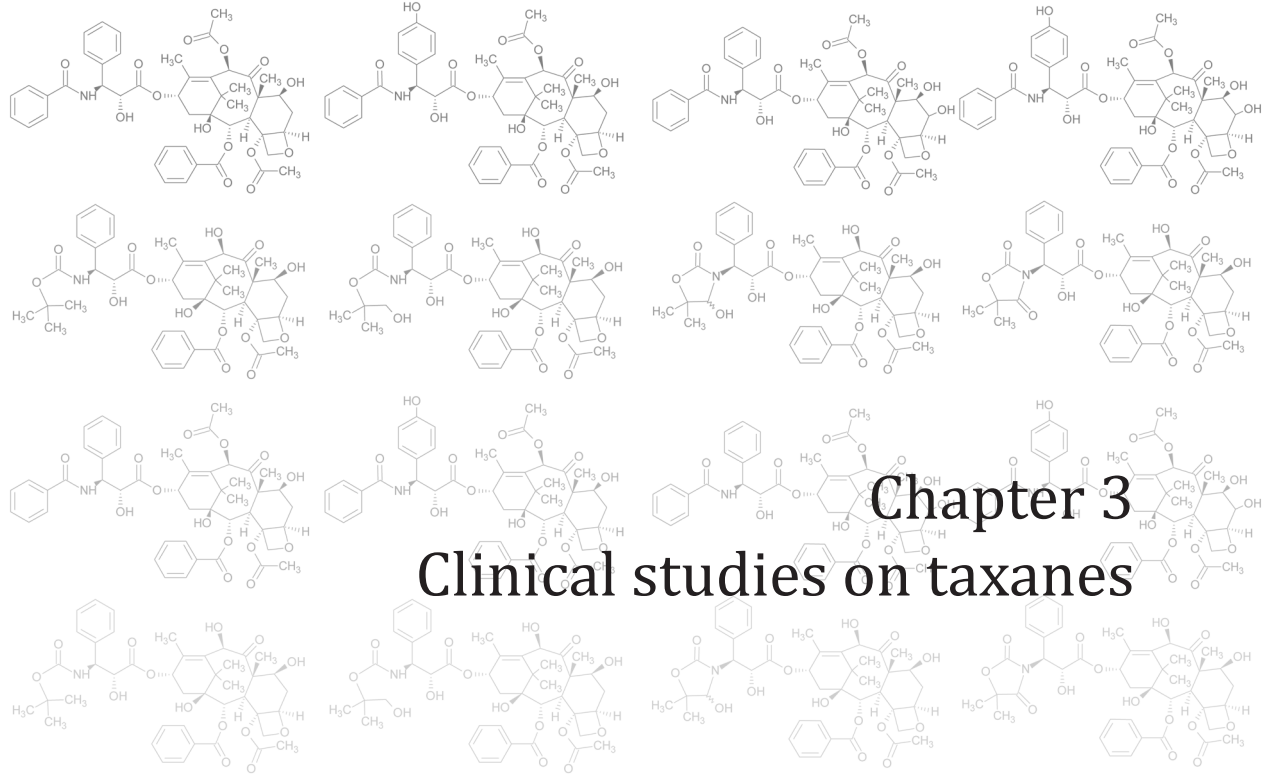


Supplemental figure 1. Treatment schedules used in this experiment. *Cyp3a*^{-/-} mice implanted with syngeneic mouse mammary tumors were treated for 3 weeks with 20 mg/kg i.v. docetaxel and/or 12.5 mg/kg oral ritonavir. Docetaxel was administered once a week, while ritonavir was administered for 5 subsequent days per week. Untreated mice were used as a control group. Treatment was started at a tumor volume of 200 mm³ and mice were sacrificed when a tumor volume of ~1500 mm³ was reached. Abbreviations: DOC: docetaxel; RTV: ritonavir.



Supplemental figure 2. Effect of ritonavir/docetaxel co-treatment on period to development of a critical tumor volume. Days passed until a tumor volume of $\sim 1500 \text{ mm}^3$ was reached ($n = 5$ per group). *Cyp3a*^{-/-} mice were implanted with mouse mammary tumors and treated for 3 weeks with 20 mg/kg i.v. docetaxel and/or 12.5 mg/kg oral ritonavir. Docetaxel was administered once a week, while ritonavir was administered for 5 subsequent days per week. Untreated mice were used as a control group. Treatment was started at a tumor volume of 200 mm^3 and mice were sacrificed when a tumor volume of $\sim 1500 \text{ mm}^3$ was reached. Differences between groups were statistically significantly different ($P < 0.001$), unless stated otherwise (NS: not significant, $P > 0.05$ or **: $P < 0.01$). Levels of significance as calculated with ANOVA. Logarithmic transformation was used to correct for different variances between groups and the Bonferroni post-hoc correction was used to accommodate multiple testing.





Relationship between systemic exposure to docetaxel and severe intestinal toxicity after oral docetaxel administration in mice and patients.

Jeroen J.M.A. Hendrikk*
Rik E. Stuurman*
Ji-Ying Song
Jurjen S. Lagas
Hilde Rosing
Serena Marchetti
Jos H. Beijnen
Alfred H. Schinkel
Jan H.M. Schellens

* Both authors contributed equally

Abstract

Oral administration of docetaxel in combination with CYP3A4 and P-glycoprotein boosters is used in clinical trials to improve oral bioavailability of docetaxel. The most common and dose-limiting toxicity of oral docetaxel was diarrhea. This study combined preclinical and clinical data and focused on incidence, severity and cause of oral docetaxel induced diarrhea. We examined intestinal toxicity in mice lacking Cyp3a and mice lacking both Cyp3a and P-glycoprotein after oral and intraperitoneal administration of docetaxel. Data were compared with results from clinical studies conducted in humans who received docetaxel orally. Intestinal toxicity in mice was similar after oral and intraperitoneal administration of docetaxel and included severe degeneration of large and small intestinal mucosa. This indicated that intestinal toxicity by docetaxel was caused by systemic exposure to docetaxel rather than by a direct local effect of docetaxel. In human, severity and onset of diarrhea was used as parameter for intestinal toxicity. Plasma exposure to docetaxel was higher in patients that suffered from diarrhea than in patients without diarrhea. Higher plasma exposure tended to be associated with increased severity of diarrhea. The administered dose and maximal observed plasma concentrations were not higher in patients with diarrhea than in patients without diarrhea. Our data indicate that the onset of severe diarrhea after oral co-administration of docetaxel in humans is probably caused by the level of docetaxel in the systemic blood circulation. Severe diarrhea after oral docetaxel is reversible and is not related to the route of administration of docetaxel.

Introduction

Docetaxel (Taxotere®) is a semi-synthetic derivative of a paclitaxel analogue originally obtained from the *Taxus baccata* and currently used as an anticancer agent in several types of cancer, such as non-small cell lung cancer (NSCLC), breast, gastric, prostate and head and neck cancer.¹ Docetaxel undergoes complex detoxification, involving both ABC drug transporters and drug-metabolizing enzymes, which results in low bioavailability after oral administration.² In vivo, both P-glycoprotein (P-gp/ABCB1/MDR1) and Cytochrome P450 (CYP) 3A are involved in the pharmacokinetics (PK) of docetaxel by decreasing exposure to docetaxel.^{3,4} Due to the poor water solubility of docetaxel and its handling by P-gp and CYP3A, the oral bioavailability of docetaxel is limited and several studies have explored the usefulness of enhancers in combination with oral formulations to increase the bioavailability.⁵ One of the applied boosting agents is the CYP3A inhibitor ritonavir (Norvir®). Low doses of ritonavir are widely used as a booster to increase the bioavailability of protease inhibitors in HIV therapy.⁶ Similarly, a low dose of ritonavir was shown to enhance the systemic exposure to oral docetaxel resulting in an apparent bioavailability of approximately 60%.⁷

These results encouraged us to perform a phase I dose escalation study to determine the feasibility of this concept with oral docetaxel in combination with ritonavir.⁸ This study started with docetaxel as a drinking solution and during the study denoted ModraDoc001 10 mg capsules, containing docetaxel as a solid dispersion without the use of polysorbate 80, were introduced.⁹ Oral docetaxel in combination with either 100 mg or 200 mg ritonavir, however, resulted in a modified toxicity profile of docetaxel compared to its intravenous administration. The most common and dose-limiting toxicity of oral docetaxel was diarrhea, while the most common treatment-related adverse events after intravenous administration of docetaxel were alopecia, anemia, leucocytopenia and neutropenia.^{8,10} This increase of intestinal toxicity after oral administration of docetaxel was also seen in another dose escalation study with oral docetaxel and ritonavir and in several proof of principle studies with oral docetaxel boosted by one of each of the CYP3A inhibitors ritonavir, ketoconazole, grapefruit juice and clarithromycin.¹¹

Similarly, severe intestinal toxicity in mice was observed after oral administration of 10 mg/kg docetaxel in mice lacking murine P-gp (Mdr1a/b P-gp) and Cyp3a.¹² Pathological examination of these mice revealed degeneration and necrosis of the intestinal mucosa three days after docetaxel administration.

Damage to the intestinal mucosa can lead to an imbalance between absorption and secretion of fluids leading to diarrhea. This damage could be an effect of mitotic arrest of intestinal crypt cells caused by exposure to chemotherapeutic agents in the systemic circulation as observed after administration of 5-fluorouracil¹³, or it can be a direct local effect of intestinal luminal drug on the intestinal or colonic epithelium as it is believed to be the case after irinotecan administration.^{14,15} In the case of the applied oral docetaxel formulation, both clinical and preclinical data suggest intestinal toxicity by oral docetaxel as major etiology. Therefore it is important to understand the mechanism behind the development of this toxicity and possible measures to prevent it.

In this study, we examined mice lacking Cyp3a and mice lacking both Cyp3a and Mdr1a/b P-gp, in order to mimic the clinical conditions wherein Cyp3a and possibly P-gp are inhibited. Clinical data of two phase I trials with oral docetaxel were selected to investigate the severity and the duration of intestinal toxicity after oral administration of the drug. Our study aimed to elucidate 1) whether the intestinal toxicity caused by docetaxel is a direct local effect or related to the docetaxel concentration in the systemic circulation, and 2) whether the intestinal toxicity is related to the amount of docetaxel present in the lumen of the gastrointestinal tract. The data obtained from the mouse experiments were compared to the data derived from clinical studies with orally administered docetaxel.

Materials and Methods

Drugs and chemicals

Docetaxel and ritonavir for mice studies were purchased from Sequoia Research Products (Oxford, UK). Drug-free lithium-heparinized human plasma was obtained from Bioreclamation LLC (New York, NY, USA). All other chemicals were of analytical grade and obtained from commercial sources.

In patient studies, docetaxel was administered to patients as drinking solution (i.v. formulation, Taxotere[®], Rhone-Poulenc Rorer/Aventis) or capsules (ModraDoc001 10 mg capsules, Department of Pharmacy & Pharmacology, Slotervaart Hospital/The Netherlands Cancer Institute). CYP3A inhibitors employed were ritonavir (Norvir[®]; Abbott, Illinois, USA), ketoconazole (Nizoral[®]; Janssen-Cilag, Tilburg, The Netherlands), grapefruit juice (Coolbest[®] pink grapefruit juice: Royal Friesland Foods N.V. Meppel, The Netherlands) and clarithromycin (Klacid[®]; Abbott, Illinois, USA).

Animals

Mice were housed and handled according to institutional guidelines complying with Dutch legislation. Mice were kept in a temperature-controlled environment with a 12-hr light / 12-hr dark cycle and received a standard diet (AM-II, Hope Farms, Woerden, The Netherlands) and acidified water *ad libitum*. Strains used in this study were Cyp3a knockout (Cyp3a^{-/-})¹⁶ and combined Cyp3a and Mdr1a/b P-gp knockout mice (Cyp3a/Mdr1a/b^{-/-})¹². All strains had a >99% FVB genetic background. In all experiments, male mice of 8-14 weeks of age were used. For dose-finding experiments 4-5 mice per group were used and toxicity was determined in 6-9 mice per group.

Docetaxel plasma pharmacokinetics for mice studies

Prior to the experiments, stock solutions containing 1, 3, 6, 9 and 36 mg/mL docetaxel in ethanol:polysorbate 80 (1:1, v/v) were prepared and stored at -20° C. On the day of the experiments stock solutions were diluted with water to obtain solutions containing various concentrations of docetaxel in ethanol:polysorbate 80:water (1:1:10, v/v). Animals were fasted 2 hours before oral drug administration to minimize variation in absorption. Docetaxel was administered orally or intraperitoneally at various doses using a total volume of 10 μ L per kg of body weight. Oral administration was performed

by gavage into the stomach using a blunt-ended needle. Intraperitoneal administration was performed by injection into the peritoneal cavity. Multiple blood samples (~50 µL) were collected from the tail vein at 15 and 30 minutes and 1, 2, 4, 8 and 24 hours after administration, using heparinized capillary tubes (Oxford Labware, St. Louis, MO, USA). Blood samples were centrifuged at ambient temperature at 8,000 *g* for 5 minutes and subsequently plasma was collected. All samples were stored at -20°C until analysis.

Histological analysis for mice studies

Three days after oral or intraperitoneal administration of docetaxel to mice, total body necropsy was performed and tissues and organs were fixed in EAF fixative (ethanol/acetic acid/formaldehyde/saline at 40:5:10:45 v/v) and embedded in paraffin. Sections were cut at 2 µm from the paraffin blocks and stained with hematoxylin and eosin (HE) according to standard procedures. The sections were reviewed with a Zeiss Axioskop2 Plus microscope (Carl Zeiss Microscopy, Jena, Germany) equipped with Plan-Apochroma and Plan-Neofluar objectives. Images were captured with a Zeiss AxioCam HRc digital camera and processed with AxioVision 4 software (both from Carl Zeiss Vision, Munich, Germany).

Clinical trials

The PK data in humans were obtained from two clinical studies which have been extensively described elsewhere.^{8;11;17} Briefly, the first study was a phase I study with weekly once daily oral docetaxel in combination with different CYP3A inhibitors. This study included 73 patients in several cohorts, including a dose escalation cohort with ritonavir and proof of principle cohorts with ritonavir, ketoconazole, grapefruit juice and clarithromycin. In the dose escalating cohort of the study docetaxel was administered as drinking solution in the first dose level (30 mg docetaxel, n=5) and as ModraDoc001 capsules (n=43) in the other dose levels. The once weekly doses of the other dose levels were 40, 60 and 80 mg docetaxel in combination with 100 mg or 200 mg ritonavir. Patients received the treatment until progressive disease or until unacceptable toxicity despite dose reduction. In additional cohorts, a total of 25 patients received 30 mg docetaxel as ModraDoc001 capsules in combination with 100 mg ritonavir or another CYP3A inhibitor in a cross-over design (ketoconazole, grapefruit juice and clarithromycin). Patients continued in the subsequent weeks with 30 mg or 40 mg docetaxel as drinking solution (n=6) or as ModraDoc001 capsules (n=17) in combination with 100 mg RTV until progressive disease or adverse events were observed, that required dose modifications or discontinuation of therapy.

The second study was a dose escalation study with oral docetaxel (as ModraDoc001 capsules) in combination with ritonavir with a comparable design as the dose escalation cohort in the first study. In this second study both docetaxel and ritonavir were given once a week in a bi-daily schedule. This study included 17 patients treated at three dose levels. The once weekly doses were 40, 60 and 80 mg docetaxel as ModraDoc001 capsules and 200 mg ritonavir. The demographic and baseline characteristics of the patients and treatment schedules of the different studies and cohorts are described in Table 1.

Table 1. Patient demographics and study details of two clinical studies used for PK data in humans.

	QD dose escalation ⁸		Proof of concept cohorts ¹¹		BID dose escalation ¹⁷		Total	
Number of patients	48		25		17		90	
Sex (male/female)	28/20		15/10		9/8		52/38	
Median age (range)	59 (36-79)		61 (46-74)		66 (41-77)		60 (36-79)	
Dosage form	Drinking solution (n=5) ModraDoc001 (n=43)		Drinking solution (n=6) ModraDoc001 (n=17)*		ModraDoc001 (n=17)			
Daily docetaxel dose	30, 40, 60, 80 mg		30, 40 mg		40, 60, 80 mg			
Daily ritonavir dose	100, 200 mg		100 mg*		200 mg			
Schedule	QD		QD		BID			
PK assessments	Week 1 and 2		Week 1, 2 and 3		Week 1 and 3			
	N	%	N	%	N	%	N	%
WHO status								
0	21	44%	8	32%	8	47%	37	41%
1	22	46%	12	48%	8	47%	42	47%
2	5	10%	5	20%	1	6%	11	12%
Ethnic origin								
Caucasian	44	92%	25	100%	16	94%	85	94%
Asian	2	4%	0	0%	0	0%	2	2%
African Descent	2	4%	0	0%	1	6%	3	3%
Tumor characteristics								
NSCLC	22	46%	6	24%	11	65%	39	43%
UCC	4	8%	6	24%	3	18%	13	14%
Ovary	3	6%	3	12%	1	6%	7	8%
Primary unknown	3	6%	3	12%	0	0%	6	7%
Other	16	34%	7	28%	2	12%	25	28%
Stage of cancer								
Locally advanced	2	4%	0	0%	0	0%	2	2%
Metastatic	46	96%	25	400%	17	100%	88	98%
Prior Treatment								
Chemotherapy	47	98%	25	100%	17	100%	89	99%
Radiotherapy	33	69%	11	44%	9	53%	53	59%
Surgery	26	54%	18	72%	7	41%	51	57%

The first study was a phase I study with weekly once daily (QD) oral docetaxel in combination with different CYP3A inhibitors, including a dose escalation cohort with ritonavir and proof of principle cohorts with ritonavir, ketoconazole, grapefruit juice and clarithromycin. The second study was a dose escalation study with weekly bi-daily (BID) oral docetaxel in combination with ritonavir: (*= treatment in subsequent weeks after the cross-over phase).

In all studies patients were fasted two hours before and one hour after oral drug administration to minimize variation in absorption. Optional pre-treatment consisted of 1 mg granisetron orally one hour prior to treatment. The adverse events were determined using the National Cancer Institute's Common Terminology Criteria for AEs criteria (NCI-CTCAE v3.0). All clinical studies were approved by the Medical Ethics Committee of the Netherlands Cancer Institute and written informed consent was obtained from all patients prior to study entry. The studies were registered under identifier NCT01173913 (NIH register) and under identifier ISRCTN32770468 (ISRCTN register).

The PK of docetaxel were monitored according to various schedules in the different cohorts and studies during the first 24 or 48 hours (Table 1). Blood samples were collected in heparinized tubes and centrifuged at 4°C at 1500 *g* for 10 minutes. Subsequently, plasma was collected and stored at -20°C until the time of analysis.

Patients

The clinical studies had similar inclusion and exclusion criteria. Patients were eligible if they had a histological or cytological proof of cancer, if there were no standard treatment options available and if docetaxel treatment was considered appropriate. Other inclusion criteria were age ≥ 18 years, performance status of 0, 1 or 2 according to the WHO Performance Status (PS) scale, life expectancy longer than 3 months, and adequate bone marrow, hematological and biological functions (neutrophil count of $\geq 1.5 \times 10^9/L$ and platelets of $\geq 100 \times 10^9/L$; alanine transaminase (ALT) and aspartate transaminase (AST) ≤ 2.5 times institutional upper limit of normal (ULN), bilirubin of ≤ 1.5 times of the ULN; serum creatinine ≤ 1.5 of the upper limit of the ULN or creatinine clearance ≥ 50 mL/min by Cockcroft-Gault formula).

Patients with known alcoholism, drug addiction and/or psychotic disorders were considered not suitable for adequate follow up, and thus excluded. Patients were not allowed to concomitantly use P-gp and CYP3A modulating drugs, H₂-receptor antagonists or proton pump inhibitors. Other exclusion criteria were uncontrolled infectious disease, bowel obstructions that might influence drug absorption, neurologic disease, pre-existing neuropathy higher than grade 1, symptomatic cerebral or leptomeningeal metastases, pregnancy, breastfeeding, refusal to use adequate contraception and previous anticancer therapy within 4 weeks prior to the first dose of oral docetaxel.

Drug analysis

Previously developed LC-MS/MS assays were used to quantify docetaxel in plasma samples of mice and humans.^{18;19} D₉-labelled docetaxel was used as internal standard for docetaxel. Mouse plasma samples of 20 μ L were diluted with 180 μ L of drug-free human plasma prior to sample pre-treatment. Human plasma was used for dilution of the samples as the concentrations in the undiluted mouse plasma were outside the calibration range and also to mimic the calibration standards that were prepared in human plasma. Sample pre-treatment of human plasma and diluted mouse plasma was started by adding a small volume of internal standard working solution to the samples. Subsequently, the samples were mixed briefly, tertiary-butyl methyl ether was added

and the samples were shaken for 10 minutes at 1250 rpm. The samples were centrifuged at 23,000 *g*, snap-frozen and the organic layer was collected. After evaporation of the organic layer, the samples were reconstituted with 100 μ l reconstitution solvent and an aliquot was injected into the LC-MS/MS system.

Pharmacokinetic calculations and statistical analysis

Pharmacokinetic parameters in mice, including the area under plasma concentration-time curves (AUCs), were calculated using the software package PK Solutions 2.0.2 (SUMMIT, Research Services, Ashland, OH, USA). The individual pharmacokinetic parameters of the patients were analyzed using descriptive non-compartmental pharmacokinetic methods and validated R scripts (R version 2.13.1). The AUCs were estimated by the linear trapezoidal (absorption phase) and logarithmic trapezoidal rule (elimination phase). The areas under the plasma concentration-time curves to infinite time (AUC_{inf}) were calculated by extrapolation. All PK data of the animal and human studies are presented as mean \pm SD.

For statistical testing in animal experiments, one-way ANOVA was used when multiple groups were compared and the Bonferroni post-hoc correction was used to accommodate multiple testing. The two-sided unpaired Student's *t* test was used when treatments or differences between two groups were compared. Data that did not show normal distribution were log-transformed to normalize the distribution of the datasets for statistical comparison. During all statistical analyses in animal experiments, differences in group sizes were considered in the calculations. The Mann-Whitney-Wilcoxon test is used for statistical testing in clinical studies. Differences were considered statistically significant when $P < 0.05$.

Results

Dose finding of docetaxel in mice

In our experiments, the plasma AUC in Cyp3a/Mdr1a/b^{-/-} mice was 27-fold higher than in Cyp3a^{-/-} mice after an oral dose of 10 mg/kg docetaxel (Figure 1). Previously, severe toxicity (including intestinal toxicity) was observed three days after single oral administration of 10 mg/kg docetaxel to Cyp3a/Mdr1a/b^{-/-} mice, but no toxicity was observed after administration of the same dose to Cyp3a^{-/-} mice.¹² This difference in toxicity might be caused by differences in docetaxel exposure in enterocytes and plasma between the two strains. To differentiate between the amount of docetaxel present in the intestine and the amount of docetaxel that is absorbed and reaches the systemic circulation within the different strains, various doses of orally administered docetaxel were given, plasma concentrations were measured, and AUCs were calculated. It was observed that an oral dose higher than 60 mg/kg docetaxel in Cyp3a^{-/-} mice did not result in a further increase in AUC compared to a dose of 60 mg/kg (data not shown). This is most likely due to the limited water solubility of docetaxel. Because of the limited volume in the intestinal tract, docetaxel could precipitate and therefore not be absorbed efficiently from the intestinal lumen.

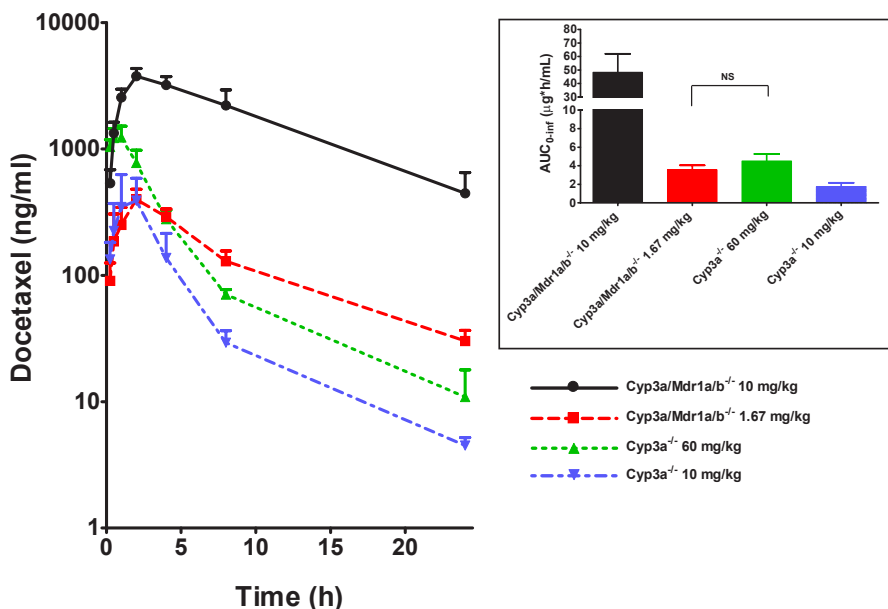


Figure 1. Plasma concentration-time curves obtained after oral administration of docetaxel to *Cyp3a*^{-/-} and *Cyp3a/Mdr1a/b*^{-/-} mice. Values represent the mean \pm SD. Inset shows the area under the plasma concentration-time curves extrapolated from zero to infinity (AUC_{inf}). All AUC_{inf} s differ mutually significantly ($P < 0.001$) as calculated with ANOVA of the Log-transformed data with Bonferroni's post-hoc test, unless otherwise specified (NS).

A dose of 10 mg/kg orally administered docetaxel in *Cyp3a/Mdr1a/b*^{-/-} mice resulted in the highest AUC and the highest maximal plasma concentration (C_{max}) used in these experiments (Figure 1). In *Cyp3a*^{-/-} mice, the highest observed AUC was after administration of 60 mg/kg docetaxel. This AUC was comparable to the AUC after administration of 1.67 mg/kg in *Cyp3a/Mdr1a/b*^{-/-} mice, although the C_{max} was lower in the latter group. Administration of 10 mg/kg in *Cyp3a*^{-/-} mice resulted in a similar C_{max} as observed after a dose of 1.67 mg/kg in *Cyp3a/Mdr1a/b*^{-/-} mice. Although the observed C_{max} was similar, administration of 10 mg/kg docetaxel in *Cyp3a*^{-/-} mice resulted in the lowest AUC used in these experiments. The difference in shape of the plasma concentration-time curve between *Cyp3a*^{-/-} and *Cyp3a/Mdr1a/b*^{-/-} mice is caused by the *Mdr1a/b* P-gp effect on the elimination of docetaxel.⁴

Various doses of intraperitoneally administered docetaxel were also tested in both strains. For each strain, we aimed for an AUC that was similar to the highest AUC as obtained after oral administration. This resulted in an intraperitoneal dose of 12 mg/kg docetaxel used for *Cyp3a/Mdr1a/b*^{-/-} mice and an intraperitoneal dose of 5 mg/kg docetaxel used for *Cyp3a*^{-/-} mice (Figure 2). The difference in oral over intraperitoneal dose ratio between the strains illustrates the impact of intestinal *Mdr1a/b* P-gp in reducing oral bioavailability of docetaxel.

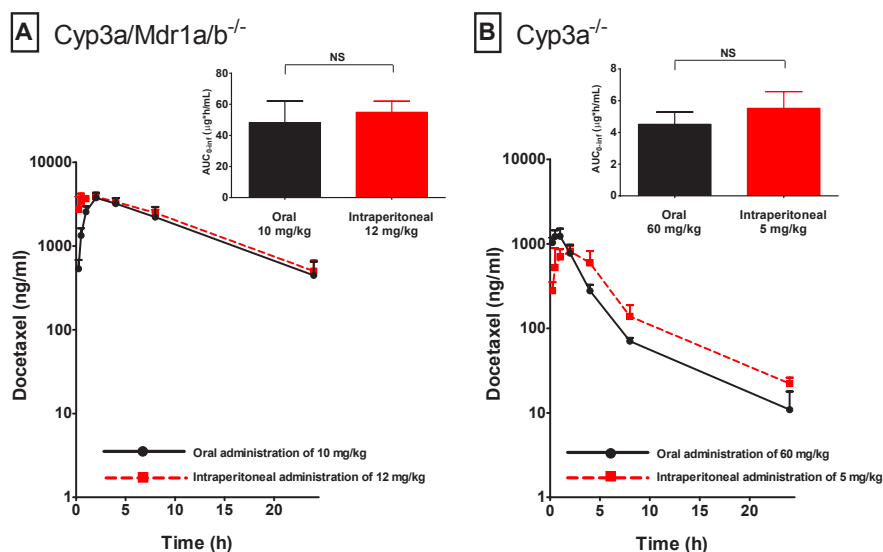


Figure 2. Plasma concentration-time curves after oral or intraperitoneal administration of docetaxel to Cyp3a/Mdr1a/b^{-/-} (panel A) and Cyp3a^{-/-} (panel B) mice. Values represent the mean \pm SD. Insets show the area under the plasma concentration-time curves extrapolated from zero to infinity (AUC_{inf}). AUCs_{inf} between oral and intraperitoneal administration do not differ significantly per strain as calculated with a two-sided unpaired Student's t-test (NS).

Toxicity after oral and intraperitoneal administration of docetaxel in mice

For toxicity experiments, docetaxel was administered orally once at doses of 1.67 and 10 mg/kg in Cyp3a/Mdr1a/b^{-/-} mice and at doses of 10 and 60 mg/kg in Cyp3a^{-/-} mice. Plasma AUCs were similar after administration of 1.67 mg/kg docetaxel to Cyp3a/Mdr1a/b^{-/-} mice and 60 mg/kg docetaxel to Cyp3a^{-/-} mice (Figure 1). Intraperitoneally administered doses were 12 mg/kg in Cyp3a/Mdr1a/b^{-/-} mice and 5 mg/kg in Cyp3a^{-/-} mice. This resulted in similar plasma AUCs as an oral dose of 10 mg/kg in Cyp3a/Mdr1a/b^{-/-} mice and 60 mg/kg in Cyp3a^{-/-} mice, respectively (Figure 1 and 2). The different dosages and administration routes were used to allow comparison of docetaxel toxicity between the strains at similar plasma levels. Pathological examination performed 72 hours after oral administration of 10 mg/kg docetaxel to Cyp3a/Mdr1a/b^{-/-} mice revealed a significant reduction of hematopoietic cells in spleen and bone marrow (see Table 2 and Figure 3), which did not occur after a low dose of docetaxel (1.67 mg/kg). The intestinal toxicity observed at 10 mg/kg was severe degeneration of the large and small intestinal mucosa with depletion of the crypts and inflammatory infiltrations. This toxicity was found in all mice in this group and was similar to previously observed toxicity after administration of the same dose of oral docetaxel in this strain.¹² After oral administration of the same dose (10 mg/kg docetaxel) to Cyp3a^{-/-} mice no signs of severe toxicity were observed, but the mean AUC in these mice was almost 28-fold lower than in Cyp3a/Mdr1a/b^{-/-} mice after the same dose. Even at the maximum achievable AUC in Cyp3a^{-/-} mice after an oral dose of 60 mg/kg docetaxel, only mild toxicity in the intestinal cells and spermatogenic cells was observed (Table 2). However, the maximum

Table 2. Overview of toxicity observed after various doses of docetaxel, administered orally or intraperitoneally to Cyp3a/Mdr1a/b^{-/-} and Cyp3a^{-/-} mice.

	Cyp3a/Mdr1a/b ^{-/-} mice	Cyp3a ^{-/-} mice
IP dose	Dose: 12 mg/kg AUC_{inf}: 54.9 ± 7.1 µg/mL*h C_{max}: 3880 ± 356 ng/mL Toxicity: severe toxicity. Observations: Depletion of crypts in mucosa of intestine and colon, intestinal inflammation, edema in mucosa of colon, depletion of hematopoietic cells in bone marrow, reduced hematopoietic activity in spleen	Dose: 5 mg/kg AUC_{inf}: 5.5 ± 1.0 µg/mL*h C_{max}: 817 ± 137 ng/mL Toxicity: little toxicity. Observations: Increase in mitosis and apoptosis in intestinal mucosa, incidental depletion of hematopoietic cells in bone marrow, incidentally reduced hematopoietic activity in spleen and incidental testicular degeneration.
High oral dose	Dose: 10 mg/kg AUC_{inf}: 48.3 ± 13.8 µg/mL*h C_{max}: 3766 ± 572 ng/mL Toxicity: severe toxicity. Observations: Depletion of crypts in mucosa of intestine and colon, intestinal inflammation, edema in mucosa of colon, depletion of hematopoietic cells in bone marrow, reduced hematopoietic activity in spleen	Dose: 60 mg/kg AUC_{inf}: 4.5 ± 0.8 µg/mL*h C_{max}: 1234 ± 281 ng/mL Toxicity: little toxicity. Observations: Increase in mitosis and apoptosis in intestinal mucosa and necrosis of spermatogenic cells.
Low oral dose	Dose: 1.67 mg/kg AUC_{inf}: 3.6 ± 0.5 µg/mL*h C_{max}: 400 ± 80 ng/mL Toxicity: no toxicity. Observations: Lesions in testis and testicular degeneration incidentally observed (likely to be FVB-strain background pathology)	Dose: 10 mg/kg AUC_{inf}: 1.7 ± 0.4 µg/mL*h C_{max}: 391 ± 196 ng/mL Toxicity: no toxicity. Observations: No abnormalities detected

AUC in Cyp3a^{-/-} mice was still 10.7-fold lower than the AUC in Cyp3a/Mdr1a/b^{-/-} mice after oral administration of 10 mg/kg. The observed toxicity in Cyp3a^{-/-} mice after a dose of 60 mg/kg docetaxel was characterized as increased mitosis and apoptosis of cells in the mucosa of the small intestine in four out of nine mice and necrosis of spermatogenic cells in three out of nine mice. Administration of a low oral dose of 1.67 mg/kg docetaxel in Cyp3a/Mdr1a/b^{-/-} mice did not result in signs of toxicity. Lesions and testicular degeneration observed in one testis of one out of six mice were likely to be FVB-strain background pathology. The mean AUC in these mice was comparable to the mean AUC after a dose of 10 mg/kg docetaxel in Cyp3a^{-/-} mice.

In contrast to the diarrhea often observed in patients receiving oral docetaxel, in none of the mice of both strains diarrhea was observed after oral administration of docetaxel. In Cyp3a/Mdr1a/b^{-/-} mice, a loss of body weight was observed after administration of 10 mg/kg docetaxel. The average body weight of these mice was decreased to 88% of the initial body weight in three days. The body weight after three days of all other mouse groups was 99-105% of the initial body weight.

After intraperitoneal administration of 5 mg/kg docetaxel in Cyp3a^{-/-} mice, similar mild toxicity was observed as after oral administration of 60 mg/kg docetaxel to these

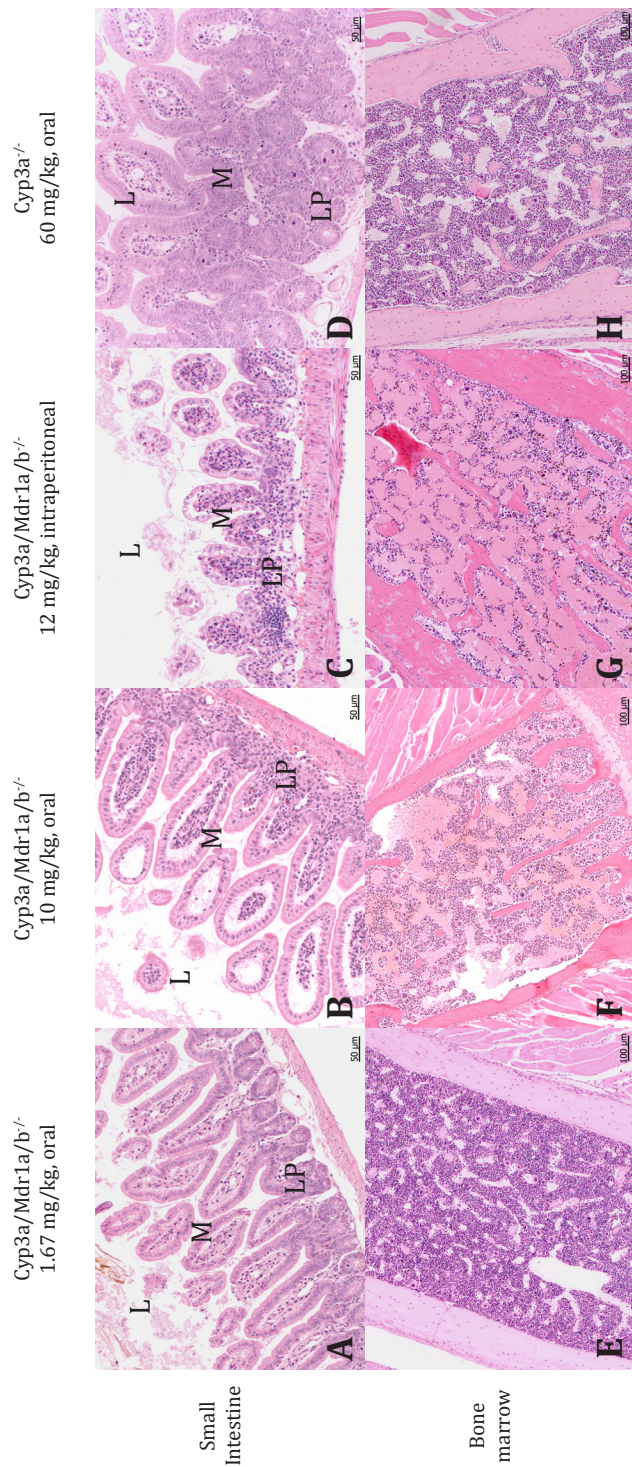


Figure 3. Microphotograph of a typical HE section of the ileum (upper panels, original magnification 20x) and bone marrow (lower panels, original magnification 10x) of Cyp3a/Mdr1a/b^{-/-} and Cyp3a^{-/-} mice after single oral or intraperitoneal administration of docetaxel. Mice were sacrificed for pathological examination 72 hours after docetaxel administration. The Cyp3a/Mdr1a/b^{-/-} mice showed no toxicity after oral administration of 1.67 mg/kg (panel A and E), but showed severe toxicity after oral administration of 10 mg/kg (B and F) or intraperitoneal administration of 12 mg/kg (C and G). The severe toxicity observed in Cyp3a/Mdr1a/b^{-/-} mice was depletion of crypts in small intestine (B and C) and depletion of hematopoietic cells in bone marrows (F and G). Cyp3a^{-/-} mice showed an increase in mitosis and apoptosis in intestinal mucosa, but no changes in bone marrow after oral administration of 60 mg/kg (D and H). Abbreviations: L: intestinal lumen; M: mucosa; LP: lamina propria. Arrows indicate deep crypts.

mice (Table 2). Plasma AUCs and C_{\max} values were similar under these conditions (Figure 2B). Changes in the mucosa of the small intestine were observed in four out of six mice. Incidentally, depletion of hematopoietic cells in bone marrow and reduced hematopoietic activity in spleen or testicular degeneration were observed in one out of six mice. Strikingly, in Cyp3a/Mdr1a/b^{-/-} mice, toxicity was also similar after intraperitoneal administration of 12 mg/kg docetaxel and oral administration of 10 mg/kg (Table 2). Again, plasma AUCs and C_{\max} values were similar under these conditions (Figure 2A). The toxicity included severe degeneration of intestinal mucosa and depletion of the crypts combined with inflammatory infiltrations. In all mice of both strains, no diarrhea was observed after intraperitoneal administration of docetaxel. The mean body weight after three days was 87% and 95% of the initial body weight in Cyp3a/Mdr1a/b^{-/-} and Cyp3a^{-/-} mice, respectively.

Toxicity after oral administration of docetaxel in humans

To quantify the intestinal toxicity in humans, two phase I studies were selected. By combining these studies, we could compare the diarrhea at multiple daily dose-levels of docetaxel and increase the number of evaluable patients. The results of the studies could be combined, since the inclusion and exclusion criteria of these studies were identical. In the studies the range of the daily doses of docetaxel was 20-80 mg, and the PK parameters of docetaxel were determined in all patients. Therefore, the results in mice could also be compared to the results in patients. In humans the intestinal toxicity was measured by the severity of diarrhea and the number of patients with diarrhea, since no pathologic observations of the intestines were performed during the study.

Out of 90 patients, 12 patients (13%) had suffered from diarrhea, considered unrelated to the study treatment, and 49 patients (54%) had suffered from 150 events of diarrhea considered related to study drug. Patients with an event of unrelated diarrhea were excluded from the analyses. Life-threatening or disabling diarrhea (grade 4) was not seen during the studies. Most of the related events of diarrhea (89%) lasted not more than one week and for most patients (63%) the worst event of diarrhea started within three weeks after the start of treatment. In total 40% of the patients (n=31) had diarrhea up to grade 1, and 13% of the patients (n=10) reported grade 2 diarrhea. For most of this last group of patients (80%) grade 2 diarrhea started during the first two weeks of treatment. In case of grade 1- 2 diarrhea, patients were advised to use loperamide, except on the day of administration since loperamide is metabolized via CYP3A4.^{20;21} No dose interruption neither reduction was implemented. The mean duration of grade 2 diarrhea was eight days (range, 1-21 days) and in most cases (70%) patients recovered fully from diarrhea after loperamide treatment.

Eight patients (10%) suffered from diarrhea up to grade 3. Grade 3 diarrhea started in all patients during the first two weeks of treatment and one patient had a second event in the sixth week. Seven patients were directly hospitalized and therefore this grade 3 diarrhea was labeled as serious adverse event. During an event of grade 3 diarrhea, loperamide was given and docetaxel was withheld by protocol until recovery to \leq grade 1 and restarted at a lower dose. The mean duration of grade 3 diarrhea was four days (range, 1-12 days) and in most cases (75%) patients recovered fully from

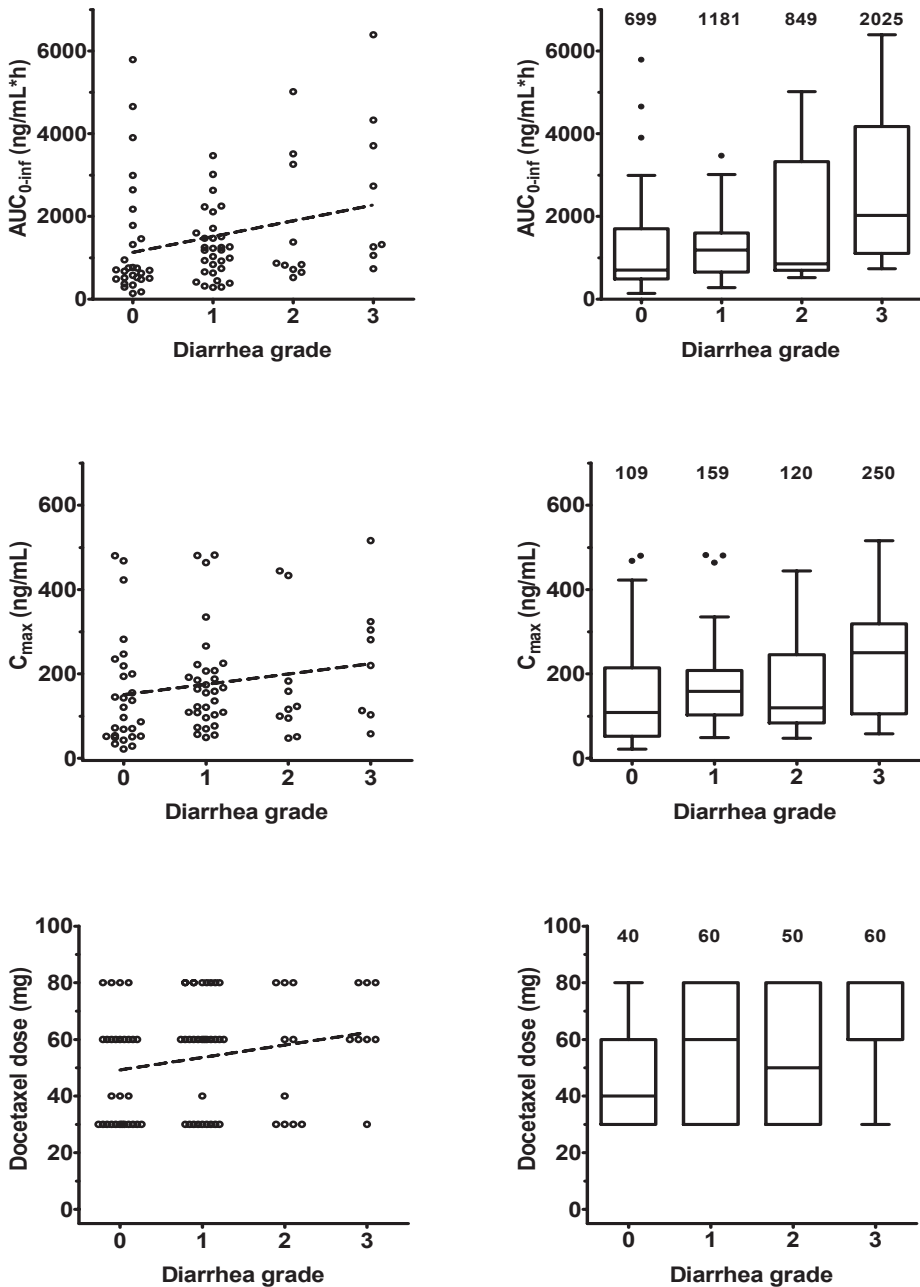


Figure 4. Relationship between the severity of diarrhea after oral administration of docetaxel and AUC_{0-inf} of docetaxel, C_{max} and the daily dose given as events and boxplot. Grade 4 diarrhea is not seen in the clinical studies. Numbers are the median values; line is the linear regression.

diarrhea after this period. Three patients discontinued treatment, the others continued with a dose reduction.

Most of the moderate and severe events of diarrhea (grade 2 and 3) occurred during the first three weeks of treatment and therefore the PK characteristics of docetaxel related to these events were known. The highest grade of the diarrhea observed per patient was coupled to the corresponding AUC_{inf} , C_{max} and daily dose. For the diarrhea events without corresponding PK characteristics, the maximum observed AUC_{inf} and the corresponding C_{max} of that patient were used.

In figure 4 the severity of the diarrhea events is plotted against the AUC_{inf} , the corresponding C_{max} and the daily dose. The AUC_{inf} of the patients who suffered from any grade of diarrhea was significantly higher than the AUC_{inf} of patients without diarrhea (Mann-Whitney-Wilcoxon Test, $p=0.04$). This difference might be underestimated, since the follow up ended within a week after start of treatment in two out of six patients without diarrhea and with an AUC_{inf} above $2 \mu\text{g}/\text{mL}\cdot\text{h}$. These patients died because of progression of disease and therefore events of diarrhea could have been missed in these patients. Another patient was hospitalized in the third week of treatment. This patient had no diarrhea, but other signs of intestinal toxicity, which were considered related to oral docetaxel (grade 3 gastritis and grade 3 duodenal ulcer). There was a tendency towards association of the severity of diarrhea with the AUC_{inf} .

In patients with diarrhea, C_{max} was not statistically significantly higher than in patients without diarrhea. Also the daily administered dose was not higher in patients with diarrhea than in patients without diarrhea. Moreover, it was observed that the median administered daily dose was similar in all patients with diarrhea of any grade. There was no tendency towards association of the administered daily dose or the C_{max} with the severity of diarrhea.

Discussion

A limitation in the treatment with most oral anti-cancer drugs is the development of gastrointestinal disorders. For several orally administered anti-cancer drugs, development of diarrhea is the major cause for treatment discontinuation and its severity sometimes represents a dose-limiting toxic event.²² During development of a novel oral formulation of docetaxel significant diarrhea was encountered. This led to the execution of preclinical studies to unravel the mechanism of this toxicity.

We used mice lacking Cyp3a with and without intact Mdr1a/b P-gp expression to investigate the cause of the intestinal toxicity as observed in patients after oral administration of docetaxel. The Cyp3a deficient mice are used to reflect the co-administration of docetaxel with the CYP3A inhibitor ritonavir in humans. Although human CYP3A has no clear direct murine orthologues²³, there is a broad functional overlap between human CYP3A and murine Cyp3a for the metabolism of docetaxel.^{16;24} Human MDR1 function is covered by murine Mdr1a and Mdr1b.²⁵ Despite these limitations associated with extrapolation of preclinical data, mice lacking Cyp3a with

and without functional Mdr1a/b expression might be used as a model for oral co-administration of docetaxel and ritonavir in humans.²⁶

In our study, Cyp3a/Mdr1a/b^{-/-} mice and Cyp3a^{-/-} mice received high and low doses of oral docetaxel. Each strain also received an intraperitoneal dose which resulted in comparable plasma exposures as the high oral doses. This enabled us to discriminate between local versus systemic exposure in relation to toxicity. Severe intestinal and bone marrow toxicity was observed after the high oral dose in Cyp3a/Mdr1a/b^{-/-} mice (10 mg/kg docetaxel). However, also after intraperitoneal administration of a dose of 12 mg/kg, similarly severe intestinal and bone marrow toxicity was observed in this strain. By intraperitoneal administration of docetaxel, the intestinal uptake step is circumvented. Since both administration routes of docetaxel resulted in comparable plasma AUCs, it is likely that the observed intestinal toxicity is caused by docetaxel in the systemic circulation rather than by a direct effect on the intestinal mucosal cells of docetaxel during absorption from the gut lumen. After both routes of administration, depletion of cells in the deep crypts of the intestine was observed at histological investigation. These crypt cells are not directly involved in drug absorption. The depletion of the deep crypt

Table 3. Incidence and severity of diarrhea in various published trials in humans after intravenous administration of docetaxel compared to incidence and severity of diarrhea in humans after oral administration of docetaxel.

	Dose	Tumor	N	Overall	gr 1 -2	gr 3 - 4	Ref
Intravenous docetaxel, every 3 weeks							
	80 mg/m ²	Breast	56	30%	30%	0%	32
	75 mg/m ²	NSCLC	110	21%	18%	3%	28
	75 mg/m ²	Breast	54	37%	26%	11%	34
	75 mg/m ²	Prostate	176	46%	44%	2%	29
Intravenous docetaxel, every 2 weeks:							
	50 mg/m ²	Prostate	170	37%	36%	1%	29
Intravenous docetaxel, every week:							
	33.3 mg/m ²	NSCLC	110	26%	23%	3%	28
	30 mg/m ²	Breast	48	45%	27%	8%	34
	40 mg/m ²	Breast	20	>30%*	>25%*	5%	31
	36 mg/m ²	NSCLC	30	>24%*	>10%*	14%	30
	35 mg/m ²	NSCLC	36	9%	3%	6%	33
Oral docetaxel**							
		***	46	62%	56%	6%	8,11,17

Abbreviation: NSCLC = non-small cell lung cancer, gr = grade refers to the severity of diarrhea, Ref = reference

* Grade 1 toxicity was not reported

** Daily doses of 60/100, 80/100, 40/200 and 60/200 mg docetaxel and ritonavir, respectively (every week)

*** Different tumor types, patients were eligible if they were diagnosed with a histological or cytological proof of cancer, if there were no standard curative or palliative treatment options available and if docetaxel treatment was appropriate for further treatment.

cells supports the hypothesis that intestinal toxicity is caused by systemic exposure to docetaxel, since similar findings (mitotic arrest and apoptosis in crypts of the mucosa) have been reported in the literature with other systemically applied anticancer drugs. For instance, after intraperitoneal administration of cisplatin, Allan et al observed decreased crypt cell production rates²⁷, leading to reduced height of the villi and loss of mucosal function.

The toxicity data in humans showed that patients with diarrhea had a higher AUC_{inf} than patients without diarrhea. On the basis of indirect comparison, the overall incidence of treatment-related diarrhea of any grade after i.v. treatment was two-fold lower than at the highest tolerable dose-levels of oral docetaxel in two dose escalation studies²⁸⁻³⁴ (Table 3). However, the incidence of grade 3/4 diarrhea after oral docetaxel administration was in the same range as after i.v. treatment, indicating that severe diarrhea is most probably caused by docetaxel in the systemic circulation rather than by local exposure in the intestinal tract. This hypothesis is supported by the observation that plasma AUCs in patients after oral administration of these doses of docetaxel were comparable to those after i.v. administration of standard doses of docetaxel.^{8;35;36} The higher incidence of mild and moderate diarrhea (grade 1 and 2) after oral administration of docetaxel versus after i.v. administration explains the observed two-fold higher overall incidence of diarrhea of any grade after oral administration of docetaxel.

The lack of intestinal toxicity after oral administration of 60 mg/kg docetaxel to Cyp3a^{-/-} mice shows that the absolute amount of docetaxel present in the intestinal lumen is not directly related to the development of toxicity. In Cyp3a/Mdr1a/b^{-/-} mice, an orally administered dose of only 10 mg/kg docetaxel already resulted in severe toxicity including intestinal toxicity. This indicates that docetaxel must be absorbed to cause intestinal toxicity. In Cyp3a^{-/-} mice this absorption is blocked by Mdr1a/b P-gp. In patients, the severity of diarrhea does not appear to be related to the orally administered dose (i.e. amount of docetaxel present in the gastrointestinal tract). Therefore, incomplete absorption of an oral formulation of docetaxel most likely does not increase the risk of severe diarrhea, or of other types of intestinal toxicity.

Our mice data show that a high AUC of docetaxel in the systemic blood circulation is responsible for degeneration of the intestinal mucosa and depletion of the crypts combined with inflammatory infiltrations. Despite the severe changes in the intestinal mucosa, no diarrhea was observed. Based on the body weight loss in mice with severe toxicity, it is possible that the mice did not develop diarrhea, because the mice stopped eating and drinking early after the development of toxicities in the gastrointestinal tract. It is also possible that diarrhea would have developed after the three days used in our study as observed for 5-FU treatment by Wu et al.³⁷ In humans, death of colonic crypt cells can result in a cascade of effects whereby immature crypt cells release more secretory compounds and thereby cause diarrhea.³⁸ The damaged colonic crypts are also not able to absorb chloride, the driving force of water absorption in the colon. Degeneration of intestinal mucosa and inflammatory infiltrations can also lead to inflammatory diarrhea.^{39;40} This is also seen during colonoscopy and in colon biopsies of patients who had developed docetaxel-induced pseudo-membranous colitis.^{41;42} Therefore, it is

likely that the onset of severe diarrhea in humans after docetaxel treatment is caused by malfunction of the intestinal tract due to similar structural changes of the intestinal mucosa as observed in mice.

Although these results indicate that severe toxicity in the intestine is caused by the amount of docetaxel in the systemic circulation and not by a direct local effect, the increase of mild and moderate diarrhea (grade 1 and 2) after oral administration of docetaxel is not explained. Unlike severe diarrhea, the incidence of mild and moderate diarrhea in patients after oral co-administration of docetaxel and ritonavir was two-fold higher compared to i.v. treatment with docetaxel. These events of mild and moderate diarrhea after oral administration often occur during the evening after treatment, but also some days later. Since oral administration of docetaxel is only explored in a few clinical studies, limited data is available regarding the pathophysiology of these mild and moderate toxicities. Short-term locally high docetaxel concentrations in the human enterocyte might cause apoptosis of intestinal epithelial cells, although apoptosis of epithelial cells is not observed in our mouse experiments. Cell death in the epithelial cells can cause synthesis of inflammatory cytokines, which eventually can cause mucositis.^{39,40} It is also reported that ritonavir can induce apoptosis in human intestinal epithelial cells and thereby decrease barrier function of the epithelial layer.⁴³ The loss of epithelial cells might cause the observed onset of diarrhea, which is also seen after ritonavir treatment of HIV patients at low doses of 100-400 mg a day.⁴⁴ Since the patients in our study received the other CYP3A inhibitors for only one week in the proof of principle cohorts, we could not distinguish between the contribution of docetaxel and ritonavir in the onset of mild and moderate diarrhea. After single oral administration of docetaxel or ritonavir, the intestinal villi could be damaged. This damage could lead to a reduced surface area for absorption resulting in diarrhea via secretory mechanisms.^{38,44} The higher incidence of mild and moderate diarrhea after oral co-administration of docetaxel and ritonavir than after i.v. administration of docetaxel can therefore be caused by both ritonavir and docetaxel. These events can be treated by prompt management with loperamide, but should be carefully monitored by the treating physicians.³⁸

In conclusion, our data indicate that diarrhea upon oral docetaxel administration is not directly related to the amount of docetaxel present in the lumen of the gastrointestinal tract. Moreover, in contrast to mild diarrhea the onset of severe diarrhea after oral co-administration of docetaxel and ritonavir in humans is probably caused by the level of docetaxel in the systemic blood circulation, is reversible and is not related to the route of administration of docetaxel.

References

1. Gligorov J, Lotz JP. Preclinical pharmacology of the taxanes: implications of the differences. *Oncologist*. **2004**; 9 Suppl 2): 3-8.
2. Schellens JHM, Malingre MM, Kruijtzter CM, Bardelmeijer HA, van Tellingen O, Schinkel AH, Beijnen JH. Modulation of oral bioavailability of anticancer drugs: from mouse to man. *Eur.J.Pharm.Sci*. **2000**; 12 (2): 103-10.
3. Vaishampayan U, Parchment RE, Jasti BR, Hussain M. Taxanes: an overview of the pharmacokinetics and pharmacodynamics. *Urology*. **1999**; 54 (6A Suppl): 22-9.
4. van Waterschoot RA, Lagas JS, Wagenaar E, Rosing H, Beijnen JH, Schinkel AH. Individual and combined roles of CYP3A, p-glycoprotein (MDR1/ABCB1) and MRP2 (ABCC2) in the pharmacokinetics of docetaxel. *Int.J.Cancer*. **2010**; 127 (12): 2954-64.
5. Koolen SL, Beijnen JH, Schellens JHM. Intravenous-to-oral switch in anticancer chemotherapy: a focus on docetaxel and paclitaxel. *Clin.Pharmacol.Ther*. **2010**; 87 (1): 126-9.
6. Cooper CL, van Heeswijk RP, Gallicano K, Cameron DW. A review of low-dose ritonavir in protease inhibitor combination therapy. *Clin.Infect.Dis*. **2003**; 36 (12): 1585-92.
7. Oostendorp RL, Huitema A, Rosing H, Jansen RS, Ter Heine R, Keessen M, Beijnen JH, Schellens JHM. Coadministration of ritonavir strongly enhances the apparent oral bioavailability of docetaxel in patients with solid tumors. *Clin.Cancer Res*. **2009**; 15 (12): 4228-33.
8. Marchetti S, Stuurman FE, Koolen SL, Moes JJ, Hendriks JJ, Thijssen B, Huitema AD, Nuijen B, Rosing H, Keessen M, Voest EE, Mergui-Roelvink M, Beijnen JH, Schellens JH. Phase I study of weekly oral docetaxel (ModraDoc001) plus ritonavir in patients with advanced solid tumors. *ASCO Meeting Abstracts*. **2012**; 30 (15 suppl): 2550.
9. Moes JJ, Koolen SL, Huitema AD, Schellens JH, Beijnen JH, Nuijen B. Pharmaceutical development and preliminary clinical testing of an oral solid dispersion formulation of docetaxel (ModraDoc001). *Int.J.Pharm*. **2011**; 420 (2): 244-50.
10. European Medicines Agency: Taxotere-Summary of Product Characteristics (SPC). http://www.ema.europa.eu/docs/en_GB/document_library/EPAR_-_Product_Information/human/000073/WC500035264.pdf. Visited 3-9-2012.
11. Koolen, S. L. Intravenous-to-oral switch in anticancer chemotherapy. Focus on taxanes and gemcitabine. [Dissertation]. 105-115. 16-2-2011. Utrecht University.
12. van Waterschoot RA, Lagas JS, Wagenaar E, van der Kruijssen CM, van Herwaarden AE, Song JY, Rooswinkel RW, van Tellingen O, Rosing H, Beijnen JH, Schinkel AH. Absence of both cytochrome P450 3A and P-glycoprotein dramatically increases docetaxel oral bioavailability and risk of intestinal toxicity. *Cancer Res*. **2009**; 69 (23): 8996-9002.
13. Inomata A, Horii I, Suzuki K. 5-Fluorouracil-induced intestinal toxicity: what determines the severity of damage to murine intestinal crypt epithelia? *Toxicol.Lett*. **2002**; 133 (2-3): 231-40.
14. Ikuno N, Soda H, Watanabe M, Oka M. Irinotecan (CPT-11) and characteristic mucosal changes in the mouse ileum and cecum. *J.Natl.Cancer Inst*. **1995**; 87 (24): 1876-83.
15. Sandmeier D, Chaubert P, Bouzourene H. Irinotecan-induced colitis. *Int.J.Surg.Pathol*. **2005**; 13 (2): 215-8.
16. van Herwaarden AE, Wagenaar E, van der Kruijssen CM, van Waterschoot RA, Smit JW, Song JY, van der Valk MA, van Tellingen O, van der Hoorn JW, Rosing H, Beijnen JH, Schinkel AH. Knockout of cytochrome P450 3A yields new mouse models for understanding xenobiotic metabolism. *J.Clin.Invest*. **2007**; 117 (11): 3583-92.
17. Stuurman, F.E. Clinical pharmacology of novel anticancer drug formulations [Dissertation]. 71-87. 18-9-2013. Utrecht University.
18. Hendriks JJ, Hillebrand MJ, Thijssen B, Rosing H, Schinkel AH, Schellens JH, Beijnen JH. A sensitive combined assay for the quantification of paclitaxel, docetaxel and ritonavir in human plasma using liquid chromatography coupled with tandem mass spectrometry. *J.Chromatogr.B Analyt.Technol.Biomed.Life Sci*. **2011**; 879 (28): 2984-90.
19. Kuppens IE, van Maanen MJ, Rosing H, Schellens JHM, Beijnen JH. Quantitative analysis of docetaxel in human plasma using liquid chromatography coupled with tandem mass spectrometry. *Biomed.Chromatogr*. **2005**; 19 (5): 355-61.
20. Kim KA, Chung J, Jung DH, Park JY. Identification of cytochrome P450 isoforms involved in the metabolism of loperamide in human liver microsomes. *Eur.J.Clin.Pharmacol*. **2004**; 60 (8): 575-81.
21. Marechal JD, Yu J, Brown S, Kapelioukh I, Rankin EM, Wolf CR, Roberts GC, Paine MJ, Sutcliffe MJ. In silico and in vitro screening for inhibition of cytochrome P450 CYP3A4 by comedications commonly used by patients with cancer. *Drug Metab Dispos*. **2006**; 34 (4): 534-8.
22. Lorient Y, Perlemuter G, Malka D, Penault-Llorca F, Boige V, Deutsch E, Massard C, Armand JP, Soria JC. Drug insight: gastrointestinal and hepatic adverse effects of molecular-targeted agents in cancer therapy. *Nat.Clin.Pract.Oncol*. **2008**; 5 (5): 268-78.
23. Nelson DR, Zeldin DC, Hoffman SM, Maltais LJ, Wain HM, Nebert DW. Comparison of cytochrome P450 (CYP) genes from the mouse and human genomes, including nomenclature recommendations for genes, pseudogenes and alternative-splice variants. *Pharmacogenetics*. **2004**; 14 (1): 1-18.

24. van Waterschoot RA, Schinkel AH. A critical analysis of the interplay between cytochrome P450 3A and P-glycoprotein: recent insights from knockout and transgenic mice. *Pharmacol.Rev.* **2011**; 63 (2): 390-410.
25. Schinkel AH, Jonker JW. Mammalian drug efflux transporters of the ATP binding cassette (ABC) family: an overview. *Adv. Drug Deliv.Rev.* **2003**; 55 (1): 3-29.
26. Koolen SL, van Waterschoot RA, van TO, Schinkel AH, Beijnen JH, Schellens JH, Huitema AD. From mouse to man: predictions of human pharmacokinetics of orally administered docetaxel from preclinical studies. *J.Clin.Pharmacol.* **2012**; 52 (3): 370-80.
27. Allan SG, Smyth JF. Small intestinal mucosal toxicity of cis-platinum--comparison of toxicity with platinum analogues and dexamethasone. *Br.J.Cancer.* **1986**; 53 (3): 355-60.
28. Gridelli C, Gallo C, Di MM, Barletta E, Illiano A, Maione P, Salvagni S, Piantedosi FV, Palazzolo G, Caffo O, Ceribelli A, Falcone A, Mazzanti P, Brancaccio L, Capuano MA, Isa L, Barbera S, Perrone F. A randomised clinical trial of two docetaxel regimens (weekly vs 3 week) in the second-line treatment of non-small-cell lung cancer: The DISTAL 01 study. *Br.J.Cancer.* **2004**; 91 (12): 1996-2004.
29. Kellokumpu-Lehtinen PL, Harmenberg U, Joensuu T, McDermott R, Hervonen P, Ginman C, Luukka M, Nyandoto P, Hemminki A, Nilsson S, McCaffrey J, Asola R, Turpeenniemi-Hujanen T, Laestadius F, Tasmuth T, Sandberg K, Keane M, Lehtinen I, Luukkaala T, Joensuu H. 2-Weekly versus 3-weekly docetaxel to treat castration-resistant advanced prostate cancer: a randomised, phase 3 trial. *Lancet Oncol.* **2013**; 14 (2): 117-24.
30. Lilenbaum RC, Schwartz MA, Seigel L, Belette F, Blaustein A, Wittlin FN, Davila E. Phase II trial of weekly docetaxel in second-line therapy for nonsmall cell lung carcinoma. *Cancer.* **2001**; 92 (8): 2158-63.
31. Mey U, Gorschluter M, Ziske C, Kleinschmidt R, Glasmacher A, Schmidt-Wolf IG. Weekly docetaxel in patients with pretreated metastatic breast cancer: a phase II trial. *Anticancer Drugs.* **2003**; 14 (3): 233-8.
32. Rugo HS, Stopeck AT, Joy AA, Chan S, Verma S, Lluch A, Liau KF, Kim S, Bycott P, Rosbrook B, Bair AH, Soulieres D. Randomized, placebo-controlled, double-blind, phase II study of axitinib plus docetaxel versus docetaxel plus placebo in patients with metastatic breast cancer. *J.Clin.Oncol.* **2011**; 29 (18): 2459-65.
33. Serke M, Schoenfeld N, Lodenkemper R. Weekly docetaxel as second-line chemotherapy in advanced non-small cell lung cancer: phase II trial. *Anticancer Res.* **2004**; 24 (2C): 1211-6.
34. Stemmler HJ, Harbeck N, Groll dr, I, Vehling KU, Rauthe G, Abenhardt W, Artmann A, Sommer H, Meerpohl HG, Kiechle M, Heinemann V. Prospective multicenter randomized phase III study of weekly versus standard docetaxel (D2) for first-line treatment of metastatic breast cancer. *Oncology.* **2010**; 79 (3-4): 197-203.
35. Baker SD, Zhao M, Lee CK, Verweij J, Zabelina Y, Brahmer JR, Wolff AC, Sparreboom A, Carducci MA. Comparative pharmacokinetics of weekly and every-three-weeks docetaxel. *Clin.Cancer Res.* **2004**; 10 (6): 1976-83.
36. Bruno R, Hille D, Riva A, Vivier N, ten Bokkel Huinnink WW, van Oosterom AT, Kaye SB, Verweij J, Fossella FV, Valero V, Rigas JR, Seidman AD, Chevallier B, Fumoleau P, Burris HA, Ravdin PM, Sheiner LB. Population pharmacokinetics/pharmacodynamics of docetaxel in phase II studies in patients with cancer. *J.Clin.Oncol.* **1998**; 16 (1): 187-96.
37. Wu Z, Han X, Qin S, Zheng Q, Wang Z, Xiang D, Zhang J, Lu H, Wu M, Zhu S, Yu Y, Wang Y, Han W. Interleukin 1 receptor antagonist reduces lethality and intestinal toxicity of 5-Fluorouracil in a mouse mucositis model. *Biomed.Pharmacother.* **2011**; 65 (5): 339-44.
38. Gibson RJ, Keefe DM. Cancer chemotherapy-induced diarrhoea and constipation: mechanisms of damage and prevention strategies. *Support.Care Cancer.* **2006**; 14 (9): 890-900.
39. Sonis ST. The pathobiology of mucositis. *Nat.Rev.Cancer.* **2004**; 4 (4): 277-84.
40. Sultani M, Stringer AM, Bowen JM, Gibson RJ. Anti-inflammatory cytokines: important immunoregulatory factors contributing to chemotherapy-induced gastrointestinal mucositis. *Chemother.Res.Pract.* **2012**; 2012:490804.
41. Ibrahim NK, Sahin AA, Dubrow RA, Lynch PM, Boehnke-Michaud L, Valero V, Buzdar AU, Hortobagyi GN. Colitis associated with docetaxel-based chemotherapy in patients with metastatic breast cancer. *Lancet.* **2000**; 355 (9200): 281-3.
42. Stemmler HJ, Kenngotte S, Diepolder H, Heinemann V. Gastrointestinal toxicity associated with weekly docetaxel treatment. *Ann.Oncol.* **2002**; 13 (6): 978-81.
43. Bode H, Lenzner L, Kraemer OH, Kroesen AJ, Bendfeldt K, Schulzke JD, Fromm M, Stoltenburg-Didinger G, Zeitz M, Ullrich R. The HIV protease inhibitors saquinavir, ritonavir, and nelfinavir induce apoptosis and decrease barrier function in human intestinal epithelial cells. *Antivir.Ther.* **2005**; 10 (5): 645-55.
44. MacArthur RD, DuPont HL. Etiology and pharmacologic management of noninfectious diarrhea in HIV-infected individuals in the highly active antiretroviral therapy era. *Clin.Infect.Dis.* **2012**; 55 (6): 860-7.

Plasma levels of docetaxel metabolites in humans after oral administration of docetaxel with and without ritonavir.

Jeroen J.M.A. Hendrikkx
Stijn L.W. Koolen
Rik E. Stuurman
Hilde Rosing
Alfred H. Schinkel
Serena Marchetti
Jos H. Beijnen
Jan H.M. Schellens

Abstract

Docetaxel is metabolised by Cytochrome P450 (CYP) 3A enzymes into four metabolites, identified as M2, M4 and the stereoisomers M1 and M3. Metabolite levels in plasma are usually low after intravenous administration of docetaxel. Currently, oral co-administration of docetaxel and the CYP3A inhibitor ritonavir is tested in clinical trials. Both the oral route of administration of docetaxel and co-administration with ritonavir might alter docetaxel metabolite concentrations in plasma, compared with standard intravenous administration.

In this study, microsome incubations were used to investigate metabolite formation of docetaxel with and without ritonavir. Metabolite concentrations in human plasma were measured after oral administration of docetaxel with and without ritonavir and compared to metabolite concentrations after intravenous administration of docetaxel with ritonavir.

Co-incubation of docetaxel and ritonavir with human liver microsomes resulted in decreased docetaxel metabolism but did not result in the formation of other metabolites than M1/M3, M2 or M4. Metabolite M2 was more abundant in plasma during the first hours after oral administration than after intravenous administration of docetaxel. Plasma levels of docetaxel metabolites decreased at a higher dose of ritonavir, but were not changed at a variable dose of docetaxel.

We demonstrated that oral co-administration of ritonavir and docetaxel resulted in low plasma concentrations of docetaxel metabolites due to CYP3A inhibition by ritonavir. Therefore, it is concluded that the boosting effect of ritonavir on the bioavailability of docetaxel is caused by inhibition of the metabolism of docetaxel. We showed that the metabolite profile in plasma is different after oral and i.v. administration of docetaxel when co-administered with ritonavir. According to FDA recommendations, further testing of docetaxel metabolite safety is not required for oral co-administration of docetaxel and ritonavir due to a low plasma exposure to the metabolites.

Introduction

Docetaxel (Taxotere®) is a semi-synthetic taxane, originating from the *Taxus baccata* and is currently used as anticancer agent in several types of cancer, among which lung, breast, gastric, prostate and head and neck cancer.¹ In humans, docetaxel is metabolised by Cytochrome P450 (CYP) 3A enzymes into four metabolites.^{2,3} The affinity of docetaxel for CYP3A4 is higher than for CYP3A5, but the maximal transformation rate is comparable.³ The first step in docetaxel metabolism is hydroxylation of the synthetic isobutoxy side chain into metabolite M2 (Figure 1). Oxidation of M2 leads to the formation of an unstable aldehyde intermediate metabolite, which is immediately cyclized into the stereo isomers M1 and M3.^{2,3} Further oxidation of M1 and M3 results in the formation of M4.² Metabolite M2 exhibits some cytotoxicity, however its cytotoxic effects are much lower than the cytotoxic effects of docetaxel. The other metabolites show no relevant cytotoxic activity.⁴

In human plasma, no metabolites were observed after injection of a low non-therapeutic dose of radioactive-labelled docetaxel.⁵ After one hour infusion of 45 and 100 mg docetaxel/m², low levels of docetaxel metabolites were observed in plasma at the end of the infusion time.^{6,7} Liver dysfunction is shown to result in higher docetaxel metabolite levels in plasma.⁷ Overall, data on docetaxel metabolites in human plasma are limited, since metabolite concentrations are much lower than docetaxel concentrations after intravenous (i.v.) administration of docetaxel and U.S. Food and Drug Administration (FDA) guidelines on Safety Testing on Metabolites (MIST) only recommend further safety testing if metabolite exposure exceeds 10% of the parent drug exposure.⁸

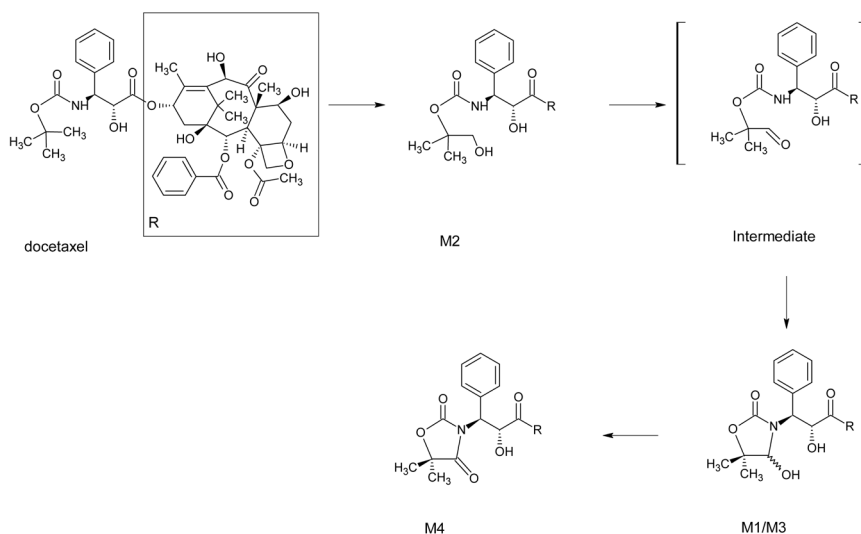


Figure 1. Chemical structures of docetaxel and metabolites.

The development of oral formulations of docetaxel is subject of preclinical and clinical research because oral administration has many advantages over i.v. administration.^{9,10} Oral administration would be more practical and convenient for patients, since oral medication can be easily taken by the patient at home while i.v. administration requires hospitalisation during infusion. Oral administration at home also results in reduced costs of the treatment. Moreover, allergic reactions caused by Chremophor EL[®] (polyoxyethylated castor oil) in paclitaxel formulations are reduced since this pharmaceutical additive is not used in oral formulations. Furthermore, oral administration enables other dosing schedules like metronomic therapy, which could increase efficacy of taxane treatment, and reduce adverse effects due to high plasma concentrations of docetaxel or paclitaxel.

A major limitation in the concept of oral administration of docetaxel is the low oral availability of the drug due to the poor water solubility of docetaxel and its handling by P-gp and CYP3A.^{9,10} Co-administration of the oral formulations of docetaxel and the CYP3A4 inhibitor ritonavir in mice and humans resulted in increased plasma concentrations of docetaxel.^{11,12} After oral administration of docetaxel with and without cyclosporin A, another CYP3A inhibitor, alterations in the docetaxel/metabolite ratios were observed in murine faeces.¹² This raises the question if metabolite concentrations in humans are altered – or if even other metabolites are formed – after co-administration of docetaxel and ritonavir. Moreover, metabolite concentrations in plasma may also be altered upon a switch from intravenous (i.v.) to oral administration of docetaxel due to a first-pass effect after oral administration of docetaxel. In this study we aimed to show that ritonavir boosts bioavailability of docetaxel by inhibiting its metabolism in humans. We used microsomal incubations to investigate metabolite formation of docetaxel after co-incubation with and without ritonavir. We hypothesized that metabolite concentrations in plasma were low after oral co-administration of docetaxel and ritonavir and wanted to test if docetaxel metabolite profiles were changed after oral administration of docetaxel compared to intravenous administration.

Materials and Methods

Chemicals

Docetaxel and ritonavir were purchased from Sequoia Research Products (Oxford, United Kingdom) and used for microsomal incubations. Pooled human liver microsomes (BD UltraPool™ HLM 150), pooled human intestinal microsomes (BD Gentest™) and reduced nicotinamide adenine dinucleotide phosphate (NADPH) regeneration system were obtained from BD Biosciences (Erembodegem, Belgium). Drug-free lithium-heparinized human plasma was obtained from Bioreclamation LLC (New York, NY, USA). Docetaxel was intravenously administered to patients as Taxotere[®] (Rhone-Poulenc Rorer/Aventis) and orally as drinking solution (i.v. formulation, Taxotere[®], Rhone-Poulenc Rorer/Aventis) and capsules (ModraDoc001 10 mg capsules¹³, Department of Pharmacy & Pharmacology, Slotervaart Hospital/The Netherlands Cancer Institute). Ritonavir was orally administered as Norvir[®] (Abbott, Illinois, USA). All other chemicals were of analytical grade and obtained from commercial sources.

In vitro docetaxel metabolism

Microsome incubations were performed with human liver or intestinal microsomes. A 150- μ L sample contained 10 μ M docetaxel, microsomes (protein concentration 0.5 mg/mL for liver microsomes or 1 mg/mL for intestinal microsomes), 100 mM phosphate buffer, pH 7.4, and water. The sample was spiked with 2 μ L 250 μ M ritonavir in methanol or 2 μ L methanol and preincubated for 5 min at 37°C. After preincubation, 50 μ L of an NADPH regeneration system was added and the samples were incubated for 15 min at 37°C (Thermomixer Comfort, Eppendorf Netheler Hinz GmbH, Hamburg, Germany), while automatically shaken at 1,000 rpm. After incubation, the samples were placed on ice and the enzymatic reaction was stopped by adding 100 μ L ice-cold acetonitrile. An aliquot of 200 μ L supernatant was collected and docetaxel and metabolites were quantified by liquid chromatography coupled with tandem mass spectrometry detection (LC-MS/MS).

For screening of docetaxel metabolite formation in the presence and absence of ritonavir, microsome incubations were performed with human liver microsomes. A 940- μ L sample contained 10 μ M docetaxel, microsomes (protein concentration 0.5 mg/mL), 100 mM phosphate buffer, pH 7.4, and water. The sample was spiked with 5 μ L 1000 μ M ritonavir in methanol or 5 μ L methanol and preincubated for 5 min at 37°C. After preincubation, 60 μ L of an NADPH regeneration system was added and the samples were incubated for 4 hours at 37°C (Thermomixer Comfort, Eppendorf Netheler Hinz GmbH, Hamburg, Germany), while automatically shaken at 1,000 rpm. After incubation, the samples were placed on ice and the enzymatic reaction was stopped by adding 450 μ L ice-cold acetonitrile. The samples were vortex-mixed for 10 s and centrifuged for 3 min at 23,000 g. The supernatant was collected and a volume of 25 μ L was injected on a previously developed UV-system for quantification of docetaxel and its metabolites.¹⁴ Molar absorption of docetaxel and metabolites was measured at a wavelength of 227 nm.

In vivo docetaxel metabolism

Human plasma samples were obtained from a clinical phase I study with weekly oral or i.v. docetaxel.¹⁵ Docetaxel administration was combined with oral ritonavir. During this study docetaxel was administered intravenously at a low dose (n=7) and orally as a drinking solution (n=2) and as ModraDoc001 capsules (n=34). The daily doses were 20, 30, 60 and 80 mg docetaxel combined with 0, 100 and 200 mg ritonavir. Patients were fasted two hours before and one hour after oral drug administration to minimize variation in absorption. Blood samples were collected predose and during 48 h after intravenous or oral administration of docetaxel with or without ritonavir. Blood samples were collected in lithium heparinized tubes, immediately placed on ice and centrifuged within 1 h at 1500 g for 10 min at 4°C. Plasma was stored at -20°C until the time of analysis. The phase I study was approved by the Medical Ethics Committee of the Netherlands Cancer Institute and written informed consent was obtained from all patients prior to study entry. The study was registered under identifier ISRCTN32770468 (ISRCTN register).

Patient Characteristics

Patients were eligible if they had histological or cytological proof of cancer, if there were no standard curative or palliative treatment options available and if docetaxel treatment was considered appropriate. Patients were aged at least 18 years and had a performance status of 0, 1 or 2 according to the WHO Performance Status (PS) scale. The life expectancy was longer than 3 months and the bone marrow, hematological and biological functions were adequate (neutrophil count of $\geq 1.5 \times 10^9/L$ and platelets of $\geq 100 \times 10^9/L$; alanine transaminase (ALT) and aspartate transaminase (AST) ≤ 2.5 times institutional upper limit of normal (ULN), bilirubin of ≤ 1.5 times of the ULN; serum creatinine ≤ 1.5 of the ULN or creatinine clearance ≥ 50 ml/min by Cockcroft-Gault formula).

Patients with known alcoholism, drug addiction and/or psychotic disorders were considered not suitable for adequate follow up, and thus excluded. Patients were not allowed to concomitantly use P-glycoprotein (P-gp) and CYP3A modulating drugs, H₂-receptor antagonists or proton pump inhibitors. Other exclusion criteria were uncontrolled infectious disease, bowel obstructions that may influence drug absorption, neurologic disease, pre-existing neuropathy higher than grade 1, symptomatic cerebral or leptomeningeal metastases, pregnancy, breastfeeding, refusal to use adequate contraception and previous anticancer therapy within 4 weeks prior to the first dose of oral docetaxel.

Quantification of docetaxel and metabolites

A previously developed LC-MS/MS assay was used to quantify docetaxel, M2, M1/M3, and M4 in plasma and incubation samples.¹⁴ D₉-labeled docetaxel was used as internal standard. In summary, to 200 μ L samples, 25 μ L of internal standard working solution was added. Subsequently, the samples were mixed briefly, tertiarybutyl methyl ether was added and the samples were shaken for 10 min at 1,250 rpm. The samples were centrifuged at 23,000g, snap-frozen and the organic layer was collected. After evaporation of the organic layer, the samples were reconstituted with 100 μ L of 10 mM ammonium hydroxide pH 5:acetonitrile (1:1, v/v) and an aliquot was injected into the LC-MS/MS system. Calibration standards of docetaxel in human plasma in a range of 0.25–500 ng/mL were used for quantification of docetaxel and its metabolites.

Data analysis

The individual pharmacokinetic parameters of the patients were analyzed using descriptive non-compartmental pharmacokinetic methods and validated R scripts (R version 2.10.0). The area under the plasma concentration-time curve (AUC) was estimated for docetaxel by the linear (absorption phase) and logarithmic (elimination phase) trapezoidal rule. The AUCs to infinite time (AUC_{inf}) were calculated for docetaxel by extrapolation. The maximum observed plasma concentration (C_{max}) was reported for docetaxel and its metabolites. Plasma concentration-time curves over the first 10 hours after administration were plotted by non-linear regression of the individual data points using GraphPad (GraphPad Prism version 5.01). For regression after i.v. administration of docetaxel, curves were fitted using the two compartment model for

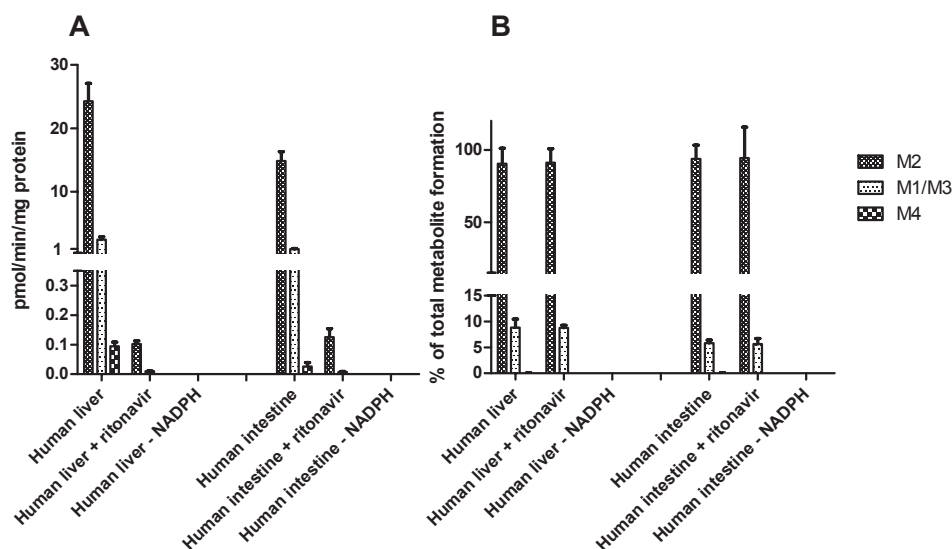


Figure 2. Microsome incubations with pooled human liver microsomes and pooled human intestinal microsomes. Docetaxel was incubated with and without ritonavir. Incubation without reduced nicotinamide adenine dinucleotide phosphate (NADPH) was used as control for cytochrome P450 (CYP) mediated metabolism of docetaxel. Panels show metabolite formation (A) and metabolite formation relative to the total amount of metabolites formed (B).

single intravenous bolus administration. For regression after oral administration of docetaxel and regression of metabolites, curves were fitted using the two compartment model for single oral administration.¹⁶

Results

Docetaxel metabolism in vitro

Incubation of docetaxel with human liver and intestinal microsomes resulted in formation of the known metabolites M1/M3, M2 and M4 (Figure 2). As expected, co-incubation of docetaxel and ritonavir resulted in decreased formation of these docetaxel metabolites. However, the relative abundances of the metabolites were not changed by ritonavir co-incubation (Figure 2B). Screening for docetaxel metabolites using HPLC with UV-detection showed only peaks of docetaxel and its known metabolites in the UV chromatogram after docetaxel and ritonavir co-incubation. No additional peaks in the UV chromatogram were observed that could possibly be related to formation of other metabolites of docetaxel during incubation.

Docetaxel metabolism in vivo

Plasma samples were obtained from a total of 43 individuals, distributed over 7 dose regimes (Table 1). After oral administration, maximum plasma concentrations of metabolites of docetaxel were reached around the C_{max} of docetaxel. After intravenous

Table 1. Overview of the pharmacokinetic parameters of docetaxel and its metabolites. C_{max} of the metabolites is presented as percentage of the C_{max} of docetaxel as calculated for the individual patient.

Dose	n	Docetaxel	M2	M1/M3	M4	
		AUC_{inf} (ng*mL/h)	C_{max} (ng/mL)	C_{max} (% of C_{max} docetaxel)	C_{max} (ng/mL)	C_{max} (% of C_{max} docetaxel)
20 mg docetaxel iv +						
100 mg ritonavir po	7	541 ± 232	520 ± 338 (E0I)	<LLQ-4.51	0.445-5.80	0.14-0.6%
					<LLQ-1.00	<LLQ-0.14%
30 mg docetaxel po +						
0 mg ritonavir po	7	40.1 ± 27.8	25.2 ± 27.4	<LLQ-2.96	<LLQ-1.41	<LLQ-5.44%
100 mg ritonavir po	9	729 ± 637	116 ± 135	<LLQ-19.3	<LLQ-1.98	<LLQ-2.88%
200 mg ritonavir po	4	733 ± 141	82.8 ± 34.7	<LLQ	<LLQ-0.331	<LLQ-0.26%
					<LLQ	<LLQ
60 mg docetaxel po +						
100 mg ritonavir po	3	1228 ± 794	256 ± 148	<LLQ-0.942	<LLQ-0.930	<LLQ-0.22%
200 mg ritonavir po	10	1536 ± 932	159 ± 88.4	<LLQ-2.36	<LLQ-2.50	<LLQ-0.79%
					<LLQ-0.582	<LLQ-0.16%
80 mg docetaxel po +						
200 mg ritonavir po	3	4710 ± 2140	336 ± 157	<LLQ	0.305-0.328	0.06-0.13%
					<LLQ	<LLQ

Abbreviations: n: number of patients; M1/M3: docetaxel metabolites M1/M3; M2: docetaxel metabolite M2; M4: docetaxel metabolite M4; AUC_{inf} : Area under the plasma-concentration curve, extrapolated to infinity; C_{max} : maximal observed plasma concentration; E0I: end of infusion; iv: intravenous administration; po: oral administration; <LLQ: below lower limit of quantification of the assay. Data are presented as mean±SD. Mean and SD could not be calculated for docetaxel metabolites since some samples had concentrations below the lower limit of quantification. Therefore, instead of mean±SD the range minimum-maximum is given. The range of the C_{max} of the metabolites as percentage of the docetaxel C_{max} was calculated for the individual patient.

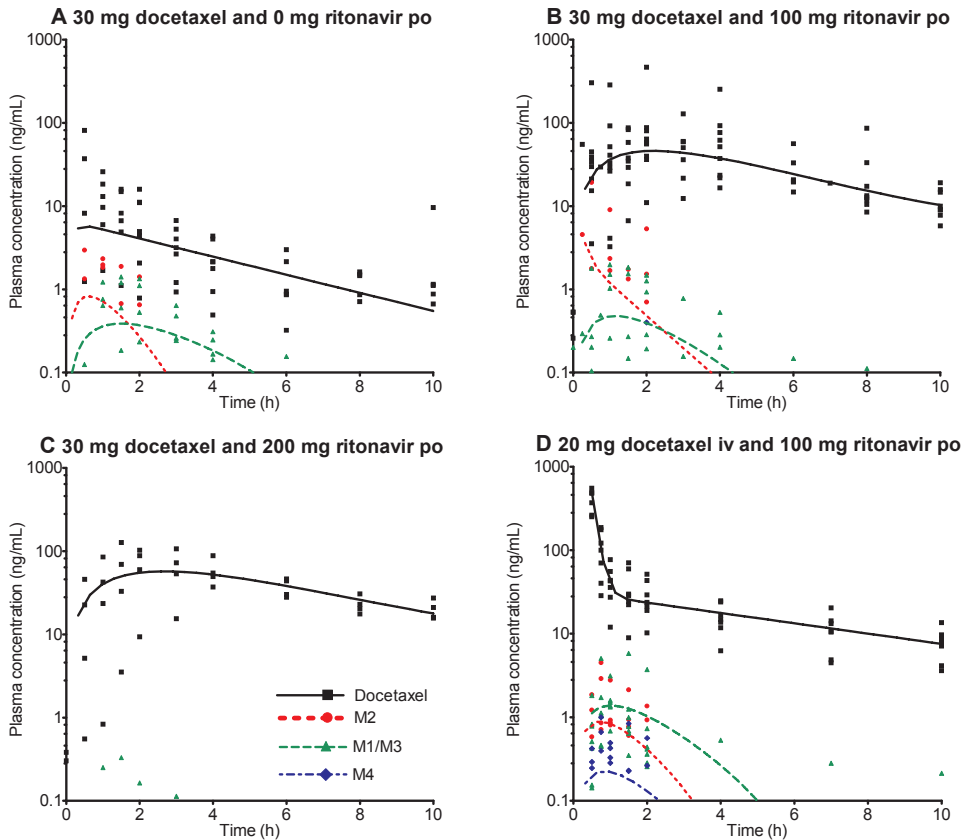


Figure 3. Plasma concentration-time curves of docetaxel and its metabolites after oral or intravenous administration of docetaxel in patients with and without ritonavir. Individual data points were plotted and curves were fitted using nonlinear regression of the individual data. For regression after oral administration of docetaxel and regression of metabolites, curves were fitted using the two compartment model for single oral administration. For regression after i.v. administration of docetaxel, curves were fitted using the two compartment model for single intravenous bolus administration. Docetaxel was administered orally in doses of 30 mg (panel A, B and C) and intravenously in a dose of 20 mg (panel D). Ritonavir was co-administered orally in doses of 100 mg (panel B and D), 200 mg (panel C) or not co-administered (panel A). Abbreviations: po: per os/orally; iv: intravenously.

administration of docetaxel, maximum metabolite levels were reached at the end of the infusion time. In all patients at all dose regimes, metabolite concentrations showed a high variation, but individual metabolite profiles were similar within each regimen. At all dose levels and administration routes, metabolites M1/M3 and M2 were often observed in plasma, while metabolite M4 was hardly observed (Table 1 and Figure 3).

AUCs_{inf} of docetaxel were similar after 30 mg orally administered docetaxel and after 20 mg i.v. administered docetaxel, both combined with 100 mg of ritonavir. However, metabolite concentrations were different. Plasma concentrations of M2 were higher after oral administration of docetaxel than after iv administration, while M1/M3 and M4 levels were lower after oral administration (Table 1, Figure 3B and 3D). When metabolite plasma concentrations are corrected for the difference in C_{max} of docetaxel, plasma levels of M2 and M1/M3 are higher after oral than after i.v. administration.

Metabolite concentrations in plasma after oral administration of 30 mg docetaxel with and without 100 mg ritonavir were in the same range, although plasma concentrations of docetaxel were much higher after co-administration with 100 mg ritonavir (Table 1, Figure 3A and 3B). Increasing the co-administered ritonavir dose to 200 mg, oral administration of 30 mg docetaxel resulted in lower plasma concentrations of the metabolites while docetaxel plasma concentrations were comparable to co-administration of 100 mg ritonavir (Figure 3B and 3C). A similar trend was observed when 60 mg of docetaxel was administered with 100 or 200 mg ritonavir (Table 1).

When 100 mg ritonavir was co-administered with 60 mg oral docetaxel, the docetaxel plasma concentration was 1.7-fold higher than after co-administration with 30 mg oral docetaxel. However, after doubling the docetaxel dose, the plasma concentrations of M1/M3 were hardly changed and plasma concentrations of M2 were even decreased (Table 1). A similar trend was observed when 200 mg ritonavir was co-administered with 30 or 60 mg oral docetaxel. Although metabolites could hardly be detected after oral co-administration of 200 mg ritonavir and 30 mg docetaxel, plasma concentrations of M1/M3 were comparable after co-administration of 200 mg ritonavir with 60 or 80 mg oral docetaxel (Table 1).

After i.v. administration of 20 mg docetaxel with 100 mg ritonavir, metabolites M1/M3 were the most abundant in plasma, while M4 was the least abundant (Figure 3D). After oral administration of 30 mg docetaxel without ritonavir, M2 was the most abundant metabolite in plasma during the first two hours after administration, while M1/M3 was the most abundant during two to four hours after administration. Metabolite M4 could not be detected (Figure 3A). A similar pattern was observed after oral co-administration of 30 mg docetaxel with 100 mg ritonavir (Figure 3B). Similar to i.v. administration of docetaxel, M1/M3 was the most abundant metabolite in plasma after oral co-administration of 100 mg ritonavir and 60 mg docetaxel (Figure 3D) and after oral co-administration of 200 mg ritonavir and 30, 60 or 80 mg docetaxel (Table 1). After oral administration of docetaxel, metabolite M4 could hardly be detected in plasma of patients.

Discussion

Docetaxel metabolism and metabolite concentrations in human plasma after intravenous administration have been described before^{6,7}, however oral administration or co-administration with ritonavir is not yet investigated and might result in an altered metabolite profile.

Using human microsomes, we observed that docetaxel co-incubation with ritonavir did not result in the formation of previously unreported metabolites. This experiment could be considered as an amplification of the P450-mediated metabolism *in vivo* and we cannot exclude that metabolites other than M1/M3, M2 and M4 are formed after co-incubation with ritonavir, albeit at very low and undetectable concentrations. We anticipate that in patients co-administration of ritonavir does not result in clinically relevant formation of metabolites other than M1/M3, M2 or M4.

Even though ritonavir co-incubation decreased the concentration of metabolites formed, the relative concentrations of the metabolites remained constant. In patient samples, we observed that oral administration of 30 mg docetaxel with and without 100 mg ritonavir resulted in a similar metabolite profile. Both *in vitro* and *in vivo* data show that the relative proportions of docetaxel metabolites did not change by combining docetaxel with ritonavir. This makes accumulation of docetaxel metabolites in plasma due to inhibited CYP3A metabolism by ritonavir unlikely.

After oral administration of docetaxel, we observed a different metabolite profile than after i.v. administration. In the first hours after oral administration of 30 mg docetaxel and 100 mg ritonavir metabolite M2 was more abundant than M1/M3 in plasma, whereas after i.v. administration of 20 mg docetaxel and 100 mg ritonavir metabolites M1/M3 were more abundant. This difference in metabolite profile is most likely related to the first-pass metabolism of docetaxel. After oral administration of docetaxel, the drug must be absorbed in the intestine and pass the liver to reach the systemic circulation, whereas after i.v. administration only hepatic metabolism is involved. Preclinical studies with mice expressing human CYP3A4 showed that docetaxel absorption after oral administration is limited by both intestinal and hepatic CYP3A4, whereby intestinal CYP3A4 is more dominant.¹⁷

Metabolite concentrations were lower after oral co-administration of docetaxel and 100 mg ritonavir than after single administration of the same dose of oral docetaxel. Metabolite concentrations were further decreased when the ritonavir dose was increased to 200 mg. Interestingly, after co-administration of oral docetaxel and 200 mg ritonavir, metabolite M2 is not the most abundant metabolite in the first period after administration. Probably the higher dose of ritonavir results in further decreased intestinal metabolism of docetaxel and therefore the metabolite profile in plasma is more similar to the profile after i.v. administration of docetaxel and ritonavir.

At a fixed dose of ritonavir and variable doses of docetaxel, metabolite plasma levels are hardly changed. Thus, plasma levels of docetaxel metabolites seem to be related to the ritonavir dose and not to the docetaxel dose. This indicates that the *in vivo* inhibition of docetaxel metabolism via CYP3A by ritonavir is dependent on ritonavir binding and

not influenced by binding competition between docetaxel and ritonavir. This *in vivo* observation is in line with previously reported irreversible binding of ritonavir to CYP3A4 resulting in inactivation of CYP3A4.¹⁸

This study provides important information about metabolite plasma levels after oral administration of docetaxel with and without ritonavir. Although we used a sensitive assay for quantification of the metabolites, metabolite concentrations in some of the samples were too low to quantify. This hampers the interpretation of the results and observed differences between dose levels. However, the absence of high metabolite concentrations in plasma answers shows that after oral administration of docetaxel with and without ritonavir, metabolite levels are low and in a similar range as after i.v. administration of docetaxel and ritonavir. The levels of metabolites of docetaxel in plasma after oral co-administration of docetaxel and ritonavir did not exceed 5% of the maximum observed levels of docetaxel. The FDA recommends further testing of metabolite safety when the exposure of the metabolite exceeds 10% of the exposure of the parent compound.⁸ Exposure is generally based on AUC, but the FDA states that it sometimes may be more appropriate to use C_{\max} . Since metabolite concentrations after oral co-administration of docetaxel and ritonavir are very low and metabolites are only detected in samples taken in the first hours after administration, we used C_{\max} to compare exposure of docetaxel and its metabolites. Our results indicate that further testing of docetaxel metabolite safety is not required.

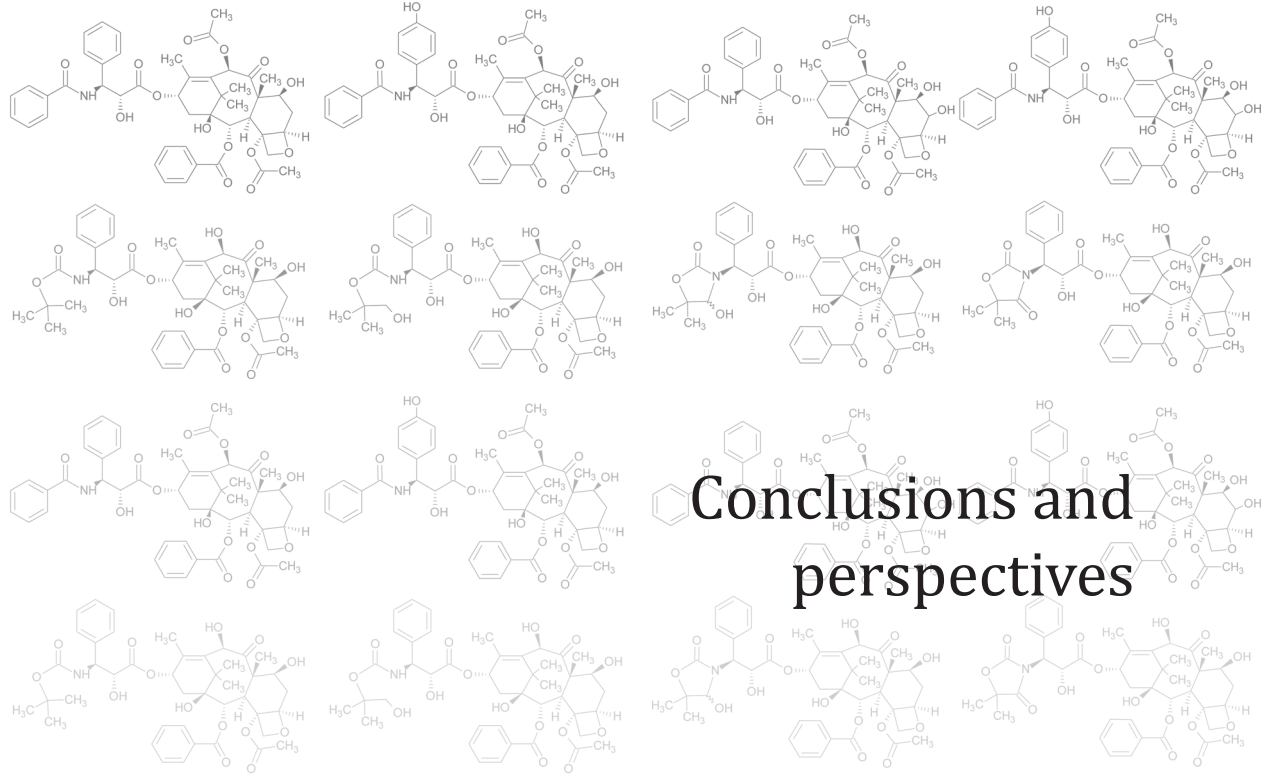
Conclusion

We demonstrated that oral co-administration of ritonavir and docetaxel to humans resulted in low plasma concentrations of docetaxel metabolites due to CYP3A inhibition by ritonavir. Therefore, it is concluded that the boosting effect of ritonavir on the bioavailability of docetaxel is caused by inhibition of the metabolism of docetaxel. We showed that in the first hours after oral administration of 30 mg docetaxel and 100 mg ritonavir metabolite M2 is more abundant than M1/M3 in plasma, whereas after i.v. administration of 20 mg docetaxel and 100 mg ritonavir metabolites M1/M3 are more abundant. Thus, the metabolite profile in plasma is different after oral and i.v. administration of docetaxel when co-administered with ritonavir. Plasma concentrations of the metabolites were decreased when the administered dose of ritonavir was increased, but plasma concentrations were not changed when the administered dose of docetaxel is changed. *In-vitro* experiments with human liver microsomes showed that CYP3A inhibition by ritonavir did not result in relevant formation of other metabolites than M1/M3, M2 or M4. Since metabolite proportions do not change after ritonavir co-incubation or co-administration, metabolite accumulation after oral co-administration of docetaxel and ritonavir is not likely. Based on FDA recommendations, we conclude that further safety testing of metabolites of docetaxel is not required for oral co-administration of docetaxel and ritonavir.

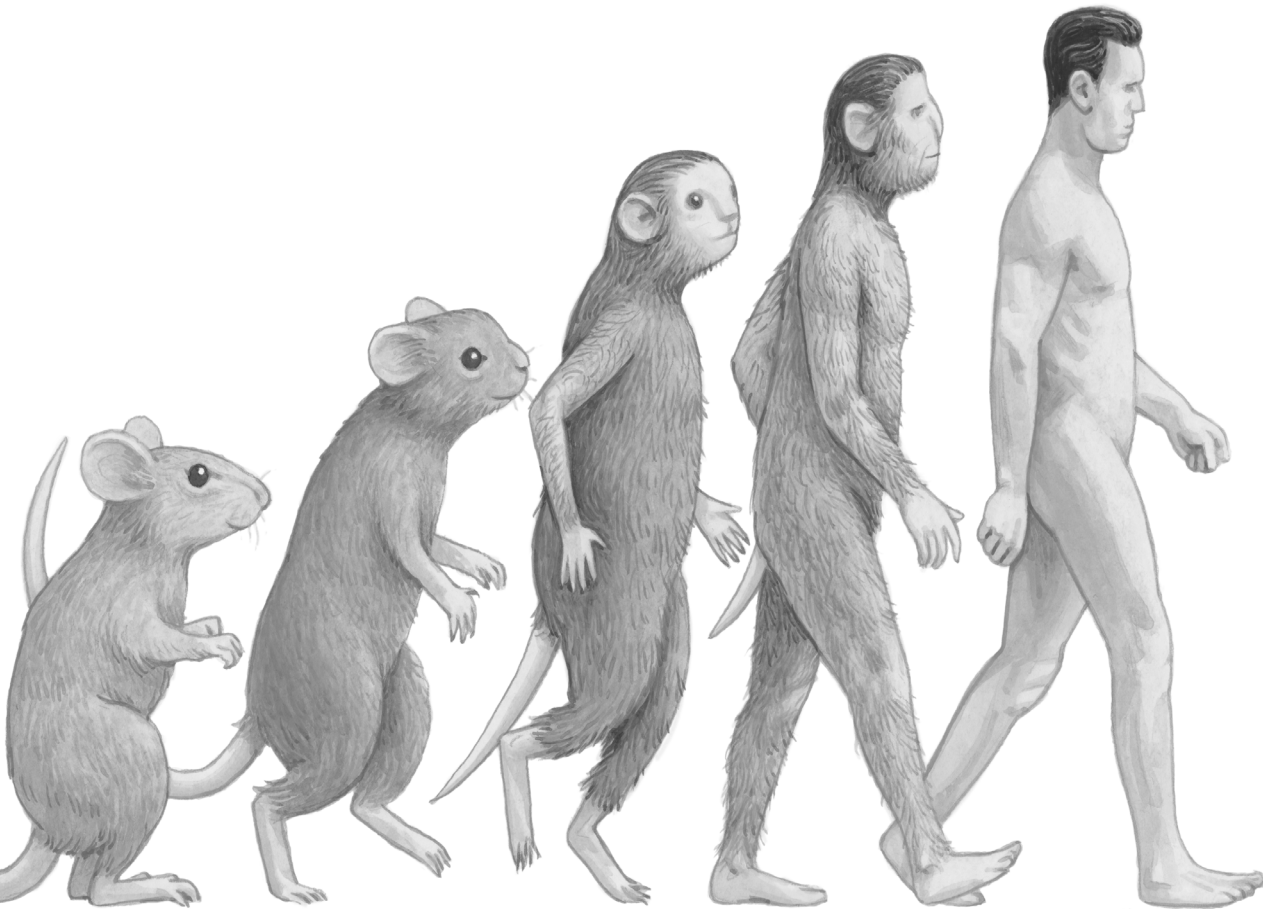
References

1. Gligorov J, Lotz JP. Preclinical pharmacology of the taxanes: implications of the differences. *Oncologist*. **2004**; 9 Suppl 2): 3-8.
2. Marre F, Sanderink GJ, de Sousa G, Gaillard C, Martinet M, Rahmani R. Hepatic biotransformation of docetaxel (Taxotere) in vitro: involvement of the CYP3A subfamily in humans. *Cancer Res*. **1996**; 56 (6): 1296-302.
3. Shou M, Martinet M, Korzekwa KR, Krausz KW, Gonzalez FJ, Gelboin HV. Role of human cytochrome P450 3A4 and 3A5 in the metabolism of taxotere and its derivatives: enzyme specificity, interindividual distribution and metabolic contribution in human liver. *Pharmacogenetics* **1998**; 8 (5): 391-401.
4. Sparreboom A, van Tellingen O, Scherrenburg EJ, Boesen JJ, Huizing MT, Nooijen WJ, Versluis C, Beijnen JH. Isolation, purification and biological activity of major docetaxel metabolites from human feces. *Drug Metab Dispos*. **1996**; 24 (6): 655-8.
5. van der Veldt AA, Hendrikse NH, Smit EF, Mooijer MP, Rijnders AY, Gerritsen WR, van der Hoeven JJ, Windhorst AD, Lammertsma AA, Lubberink M. Biodistribution and radiation dosimetry of (11)C-labelled docetaxel in cancer patients. *Eur.J.Nucl.Med.Mol.Imaging* **2010**. 37 (10): 1950-8
6. Guitton J, Cohen S, Tranchand B, Vignal B, Droz JP, Guillaumont M, Manchon M, Freyer G. Quantification of docetaxel and its main metabolites in human plasma by liquid chromatography/tandem mass spectrometry. *Rapid Commun.Mass Spectrom*. **2005**; 19 (17): 2419-26.
7. Rosing H, Lustig V, van Warmerdam LJ, Huizing MT, ten Bokkel Huinink WW, Schellens JH, Rodenhuis S, Bult A, Beijnen JH. Pharmacokinetics and metabolism of docetaxel administered as a 1-h intravenous infusion. *Cancer Chemother. Pharmacol*. **2000**; 45 (3): 213-8.
8. U.S. Food and Drug Administration, Center for Drug Evaluation and Research, Guidance for industry: Safety Testing of Drug Metabolites. <http://www.fda.gov/downloads/Drugs/GuidanceComplianceRegulatoryInformation/Guidances/ucm079266.pdf>. Visited 3-9-2012.
9. Koolen SL, Beijnen JH, Schellens JHM. Intravenous-to-oral switch in anticancer chemotherapy: a focus on docetaxel and paclitaxel. *Clin.Pharmacol.Ther*. **2010**; 87 (1): 126-9.
10. Schellens JHM, Malingre MM, Kruijtzter CM, Bardelmeijer HA, van Tellingen O, Schinkel AH, Beijnen JH. Modulation of oral bioavailability of anticancer drugs: from mouse to man. *Eur.J.Pharm.Sci*. **2000**; 12 (2): 103-10.
11. Oostendorp RL, Huitema A, Rosing H, Jansen RS, Ter Heine R, Keessen M, Beijnen JH, Schellens JHM. Coadministration of ritonavir strongly enhances the apparent oral bioavailability of docetaxel in patients with solid tumors. *Clin.Cancer Res*. **2009**; 15 (12): 4228-33.
12. Bardelmeijer HA, Ouwehand M, Buckle T, Huisman MT, Schellens JH, Beijnen JH, van Tellingen O. Low systemic exposure of oral docetaxel in mice resulting from extensive first-pass metabolism is boosted by ritonavir. *Cancer Res*. **2002**; 62 (21): 6158-64.
13. Moes JJ, Koolen SL, Huitema AD, Schellens JH, Beijnen JH, Nuijen B. Pharmaceutical development and preliminary clinical testing of an oral solid dispersion formulation of docetaxel (ModraDoc001). *Int.J.Pharm*. **2011**; 420 (2): 244-50.
14. Hendriks JJ, Dubbelman AC, Rosing H, Schinkel AH, Schellens JH, Beijnen JH. Quantification of docetaxel and its metabolites in human plasma by liquid chromatography/tandem mass spectrometry. *Rapid Commun.Mass Spectrom*. **2013**; 27 (17): 1925-34.
15. Marchetti S, Stuurman FE, Koolen SL, Moes JJ, Hendriks JJ, Thijssen B, Huitema AD, Nuijen B, Rosing H, Keessen M, Voest EE, Mergui-Roelvink M, Beijnen JH, Schellens JH. Phase I study of weekly oral docetaxel (ModraDoc001) plus ritonavir in patients with advanced solid tumors. *ASCO Meeting Abstracts* **2012**; 30 (15_suppl): 2550.
16. Dubois, A., Bertrand, J., and Mentré, F. Mathematical Expressions of the Pharmacokinetic and Pharmacodynamic Models implemented in the PFIM software. www.pfim.biostat.fr/PFIM_PKPD_library.pdf. 2011.
17. van Herwaarden AE, Wagenaar E, van der Kruijssen CM, van Waterschoot RA, Smit JW, Song JY, van der Valk MA, van Tellingen O, van der Hoorn JW, Rosing H, Beijnen JH, Schinkel AH. Knockout of cytochrome P450 3A yields new mouse models for understanding xenobiotic metabolism. *J.Clin.Invest*. **2007**; 117 (11): 3583-92.
18. Sevrioukova IF, Poulos TL. Structure and mechanism of the complex between cytochrome P4503A4 and ritonavir. *Proc.Natl.Acad.Sci.U.S.A*. **2010**; 107 (43): 18422-7.





Conclusions and perspectives



Conclusions and perspectives

The aim of this thesis was to obtain mechanistic insights in the boosting effect of ritonavir on orally administered taxanes and to support clinical development of oral formulations of paclitaxel and docetaxel. In this chapter, we discuss several aspects of the development of oral formulations of taxanes that are addressed in previous chapters of this thesis. Successively, main results on bioanalysis of taxanes, preclinical studies and clinical studies are depicted and put into a wider context.

Bioanalysis of taxanes

During clinical drug development reliable and sensitive bioanalytical assays for quantification of these drugs are prerequisites to support trials. High Performance Liquid Chromatography (HPLC) or Ultra Performance Liquid Chromatography (UPLC) coupled with tandem mass spectrometry (MS/MS) is most frequently used for quantification of taxanes and results in sensitive, selective and reliable assays (**chapter 1.1**). When bioanalytical assays are described in scientific literature, method development and optimization is often extensively discussed. Based on previously reported results, there seems to be an overlap in behaviour of taxanes during sample pre-treatment and the influence of mobile phase composition and interference on quantification in developed LC-MS/MS assays. In general, sample pre-treatment using liquid-liquid extraction with tertiary-butylmethylether or on-line solid-phase extraction is advised. These pre-treatment methods can be fast and often result in high sensitivity at low costs. Usually, a mobile phase containing at least 50% of organic phase and volatile components is used to quantify taxanes in MS/MS assays. Ammonium-containing additives in the mobile phase and an alkaline pH can increase the response, thus unbuffered ammonium hydroxide is advised as additive to the mobile phase.

Combined analysis of taxanes with other compounds can increase sample throughput, and thus accelerate clinical development, when multiple drugs are co-administered. However, this results in the need for further optimisation during method development, especially when compounds behave differently. During method development of combined assays for quantification of paclitaxel, docetaxel and ritonavir in human matrices, we observed that ionisation of ritonavir is more efficient than ionisation of the taxanes (**chapters 1.2 and 1.3**). Ritonavir was not only a better responder, but the desired concentration range of ritonavir was also 4-fold higher. Consequently obtaining sensitivity of docetaxel and paclitaxel at low drug concentrations resulted in saturation of the response of ritonavir at high drug concentrations. Suboptimal mass spectrometry settings for ritonavir resulted in the most accurate and precise quantification of ritonavir, despite the differences in ionisation and target concentration ranges between ritonavir and the taxanes.

Before bioanalytical assays are used to support preclinical and clinical studies, assay performance is usually tested during a validation program. Although guidelines for validation of assays are published by state institutions like the U.S. Food and Drug Administration (FDA)¹, one is at liberty to deviate from these guidelines at justified motives. One of these motives can be the switch of matrix in which the

analytes are quantified. Although at first glance the change is minor, the impact can be underestimated. We observed that the response of paclitaxel, docetaxel and ritonavir is different in processed samples originating from plasma, feces homogenate or urine (**chapters 1.2 and 1.3**). To avoid unexpected issues, a full validation program was executed when the sample matrix was changed from human plasma to human feces or urine. During validation of the assay (**chapter 1.3**), we observed that quantification of docetaxel, paclitaxel, ritonavir -and maybe also other drugs- in feces samples of patients might be biased when homogenized samples are stored in large portions and when aliquots for quantification are taken after storage. In urine samples, we observed that quantification of the analytes after spiking of these compounds in a small volume resulted in underestimation of the concentration, indicating that adsorption to the container wall takes place when analytes are spiked to urine. These observations after the switch from human plasma to human feces or urine underline that one should be reserved to execute a partial validation program for bioanalytical assays that are based on previously validated assays.

Another motive to deviate from governmental guidelines can be the lack of availability of reference compounds. The development and validation of bioanalytical assays according to FDA guidelines requires the use of chemically pure reference standards¹, while during drug development, compounds like metabolites are usually commercially not -or hardly- available at chemically pure quality. We described an approach to quantify docetaxel metabolites by LC-MS/MS using docetaxel calibration samples and thus avoiding the need for chemical pure substances of docetaxel metabolites (**chapter 1.4**). With head-to-head comparison of both UV and MS/MS detection we calculated correction factors and showed that our method was accurate and precise. The concept of this approach was proved using human plasma samples containing paclitaxel and this approach may be used in general to quantify metabolites of other agents by LC-MS/MS using parent drug calibration standards.

Preclinical aspects of orally administered taxanes

Prior to the start of clinical studies, drug candidates are tested in the preclinical setting.² During preclinical testing, *in vitro* and *in vivo* experiments are set up to test efficacy and safety prior to administration to humans. When clinical studies with promising drug candidates are ongoing, new research questions often arise and additional preclinical testing is started. For instance, insight into the intestinal transporters that facilitate intestinal drug absorption is still surprisingly limited (**chapter 2.1**). Ongoing and future studies with genetically modified mouse models may further improve these insights, thus supporting the development of optimal orally available drugs.

Using knock-out mouse models, we addressed the role of some intestinal drug transporting or metabolizing enzymes in absorption of orally administered taxanes. We showed that both P-glycoprotein (P-gp) and Cytochrome P450 (CYP) 3A are involved in limiting paclitaxel plasma concentrations after oral administration and that the boosting effect of ritonavir on oral paclitaxel plasma exposure is caused by CYP3A inhibition and not by P-gp inhibition (**chapter 2.2**). Our data indicate that for

intestinal absorption of paclitaxel, enzymes other than P-gp and CYP3A are not relevant. For intestinal absorption of docetaxel, we showed that the uptake transporter Organic Anion-transporting Polypeptide (OATP) 1a is not essential (**chapter 2.4**). These insights in the roles of drug transporting or metabolizing enzymes in limiting oral absorption of taxanes, provide new points of application for improvement of oral taxane formulations in patients.

One of the possible ways to improve oral absorption of taxanes is simultaneous inhibition of P-gp and CYP3A by coadministered drugs. We tested the effect of coadministration of paclitaxel and docetaxel with the P-gp inhibitor elacridar and the CYP3A inhibitor ritonavir (**chapter 2.3**). We observed an increase in plasma exposure of orally applied taxanes when coadministered with either oral elacridar or ritonavir. Oral coadministration of the taxanes with both elacridar and ritonavir resulted in even further increased plasma exposure. Although oral absorption of taxanes is increased after boosting with both elacridar and ritonavir, there are potential risks involved in this combination. For instance, coadministration of oral elacridar in mice resulted in increased brain penetration of intravenously administered paclitaxel by inhibition of P-gp at the blood-brain barrier.³ However, we also demonstrated that relative brain accumulation of the taxanes was not affected after boosting with oral elacridar. Even at the highly increased plasma concentrations of taxanes after boosting with both elacridar and ritonavir, relative brain accumulation was still similar as seen after single taxane administration. We therefore believe that it will be worth testing whether simultaneous inhibition of P-gp and CYP3A may provide a relatively safe strategy to boost plasma exposure of orally applied taxanes in patients, as relative brain exposure is unlikely to be higher than that in the currently used i.v. schedules.

Ritonavir administration may not only increase oral absorption of taxanes⁴⁻⁶, but possible anticancer effects are also described.⁷⁻¹⁵ In this thesis, we showed that antitumor efficacy of intravenously administered docetaxel is increased by coadministration of orally administered ritonavir (**chapter 2.5**). Our data indicate that Cyp3a inhibition in tumor tissue by ritonavir results in decreased docetaxel metabolism in the tumor. This could result in prolonged tumor exposure to docetaxel and, therefore, this could have caused the observed increase in antitumor efficacy of docetaxel when coadministered with ritonavir. In our experiment, we administered ritonavir orally for five subsequent days per week with weekly administered i.v. docetaxel, while in current clinical studies, oral ritonavir is coadministered once a week with oral docetaxel formulations.¹⁶ Therefore, more preclinical testing is needed to assess if the increased antitumor efficacy of docetaxel is still observed when ritonavir is administered in a weekly schedule.

Clinical aspects of orally administered taxanes

During early clinical evaluation of cytotoxic agents, the focus is usually on drug safety and to determine the recommended dose for efficacy studies. Therefore, toxicity is an essential endpoint when anticancer agents are evaluated for the first time in patients.¹⁷ In the first studies with oral docetaxel, the most common and dose-limiting toxicity was diarrhea.¹⁶ We combined preclinical and clinical data to gain more insight in the onset of diarrhea (**chapter 3.1**). Chemotherapy-induced diarrhea is the

result of damage to the intestinal mucosa. This damage causes an imbalance between absorption and secretion of fluids in the intestinal tract.¹⁸ We showed that the amount of docetaxel present in the lumen of the gastrointestinal tract was not related to the onset of intestinal damage and that intestinal damage in mice was caused by systemic exposure to docetaxel. Evaluation of clinical data showed that patients with diarrhea had a higher docetaxel plasma exposure than patients without diarrhea. Moreover, the incidence of severe diarrhea after oral docetaxel administration was in the same range as after i.v. treatment, indicating that severe diarrhea is most probably caused by docetaxel in the systemic circulation rather than by local exposure in the intestinal tract. We conclude that the onset of severe diarrhea after oral coadministration of docetaxel and ritonavir in humans is probably caused by the level of docetaxel in the systemic blood circulation and that severe diarrhea is reversible and not related to the route of administration of docetaxel. Although severe diarrhea is very inconvenient and may even cause life threatening situations, our data indicate that dose reductions can be effective to minimize (severe) diarrhea during treatment with oral docetaxel. In contrast with commonly observed adverse effects after intravenous administration of docetaxel (e.g. anemia, leucocytopenia and neutropenia¹⁹), diarrhea is easily recognized by non-medically trained persons and has not to be confirmed in laboratory. This makes diarrhea an adverse effect of orally applied docetaxel that is manageable in daily clinical practice.

Early clinical evaluation of new drugs or drug formulations focuses not only on safety of the parent compounds, but also on formed metabolites. FDA guidelines on Safety Testing on Metabolites (MIST) recommend further safety testing if metabolite exposure exceeds 10% of the parent drug exposure.²⁰ Metabolite plasma concentrations after intravenous administration of docetaxel are much lower than docetaxel plasma concentrations²¹⁻²³, but metabolite concentrations can be altered – or even other metabolites can be formed- after coadministration of docetaxel and ritonavir. Moreover, due to a first-pass effect after oral administration of docetaxel, metabolite concentrations in plasma may also be altered due to a switch from intravenous (i.v.) to oral administration of docetaxel. We showed that docetaxel metabolite concentrations after oral coadministration of docetaxel and ritonavir are very low and only detected in samples taken in the first hours after administration (**chapter 3.2**). Our results indicate that further testing of docetaxel metabolite safety is not required.

Perspectives

The use of oral taxanes in daily practice is not yet feasible. We addressed multiple important questions in this thesis that arose during early clinical testing of oral formulations of taxanes. Safety and proof-of-concept of oral administration of taxanes to patients is shown, but clinical efficacy has still to be established. In future studies efficacy of orally administered taxanes must be determined in a large cohort of patients. Since efficacy of intravenously administered taxanes is already proven²⁴⁻²⁶, it is likely that an antitumor response will be observed after oral co-administration of taxanes and ritonavir. However, the tumor response after administration of orally boosted taxanes must be compared to the response after intravenous administration of taxanes. Moreover, oral formulations make other dosing schedules possible and prior to general

use of oral taxanes, the optimal schedule must be determined.

This thesis addressed questions related to the development of orally administered taxanes. However, the impact of the results exceeds this topic. The publication of FDA guidelines on Safety Testing of Drug Metabolites²⁰ in 2008 underlined the importance of early detection of drug metabolites. Drug metabolites may show pharmacologic activity and thus possibly cause toxic effects. Moreover, discovery of drug metabolites at an early stage during drug development may also result in modification of the chemical structure of a drug to reduce the risk of adverse drug reactions during clinical application.²⁷ Our work attributed to the early quantification of drug metabolites by presenting a method to quantify drug metabolites without chemically pure drug reference compounds. We showed the feasibility of correction factors for the quantification of docetaxel metabolites using docetaxel calibration standards. This approach can be used for the quantification of any drug metabolite and may thus provide targeted information about metabolites at an early stage.

As discussed in our review about genetically modified mouse models in chapter 2.1, the role of the efflux transporter P-gp in the intestinal uptake of drugs is much more identified than the role of intestinal transporters that facilitate intestinal drug absorption. But not only the role of P-gp in intestinal uptake is extensively documented, also its role in brain uptake is frequently studied.²⁸ We showed that intestinal P-gp was completely inhibited by elacridar and increased the intestinal absorption of taxanes. However, P-gp in the blood-brain barrier was not completely inhibited and brain penetration of the oral taxanes was not increased. When oral taxanes are co-administered with oral elacridar, it is not likely that co-administration will increase the brain penetration. These findings conflict with efforts to increase brain penetration of anticancer drugs by coadministration of elacridar for treatment of brain metastases.²⁹ But taxanes are considered as very good substrates of P-gp^{3,30} and other experiments showed improved brain penetration of other chemotherapeutic agents.^{31,32} Thus, co-administration of elacridar will not improve brain penetration of all drugs. Most likely, multiple factors will determine if P-gp inhibition by elacridar is sufficient to increase brain penetration. Plasma concentrations of elacridar are most relevant, since at lower elacridar concentrations, P-gp transport is not completely inhibited.³³ Thereby affinity of a substrate for P-gp transport is important. A substrate with a higher affinity will require almost complete inhibition of P-gp, while transport of a weaker substrate will already be affected at non-complete inhibition. At last, the plasma concentration of the substrate might be relevant. This can explain the observed difference between brain penetration of oral (**chapter 2.1**) and iv³ paclitaxel when coadministered with 25 mg/kg oral elacridar. Thus, multiple factors must be taken into account when trying to increase brain penetration with co-administration of elacridar and future clinical studies to improve penetration of chemotherapeutic agents should focus on coadministration of a high dose of elacridar with moderate substrates of P-gp. Our results also show that intestinal P-gp can already be inhibited by a low dose of oral elacridar and thus, oral absorption of P-gp substrates can be boosted with low doses of elacridar without the risk of increased brain penetration.

In vitro experiments can give mechanistic insights or even predict drug-drug

interactions based on inhibition of CYP-mediated metabolism.³⁴ However, when the drug of interest is a substrate for both drug transporters and metabolizing enzymes, prediction of the *in vivo* interplay based on *in vitro* experiments is difficult.^{34;35} In such case, animal models can be used to predict pharmacokinetics and pharmacodynamics in patients. Previously, it is reported that there is a species difference in paclitaxel metabolism, resulting in the formation of different metabolites.³⁶ Paclitaxel metabolites 3'*p*-hydroxypaclitaxel and 6 α -hydroxypaclitaxel are formed in both mice and human, but in mice, also other metabolites are formed.³⁷ This implicates that wild-type mice are not the best model to assess *in vivo* interplay between drug transporters and metabolizing enzymes for paclitaxel. Our results in chapter 2.2 and 2.3 showed that mice expressing human CYP3A4 are a better model to assess paclitaxel metabolism than mice expressing murine Cyp3a enzymes. Moreover, administration of paclitaxel to wild-type mice with and without ritonavir did not result in a difference in plasma exposure of paclitaxel, while coadministration of paclitaxel with ritonavir to humanized mice showed an increase in plasma exposure. This increase in plasma exposure of paclitaxel is also observed in patients when paclitaxel and ritonavir are coadministered.⁶ This underlines the importance of selecting the right animal model to study the *in vivo* interplay. Especially for prediction of drug-drug interactions, one should select a model that reflects the human situation and our data showed that humanized mouse models may be a better tool than wild-type mice.

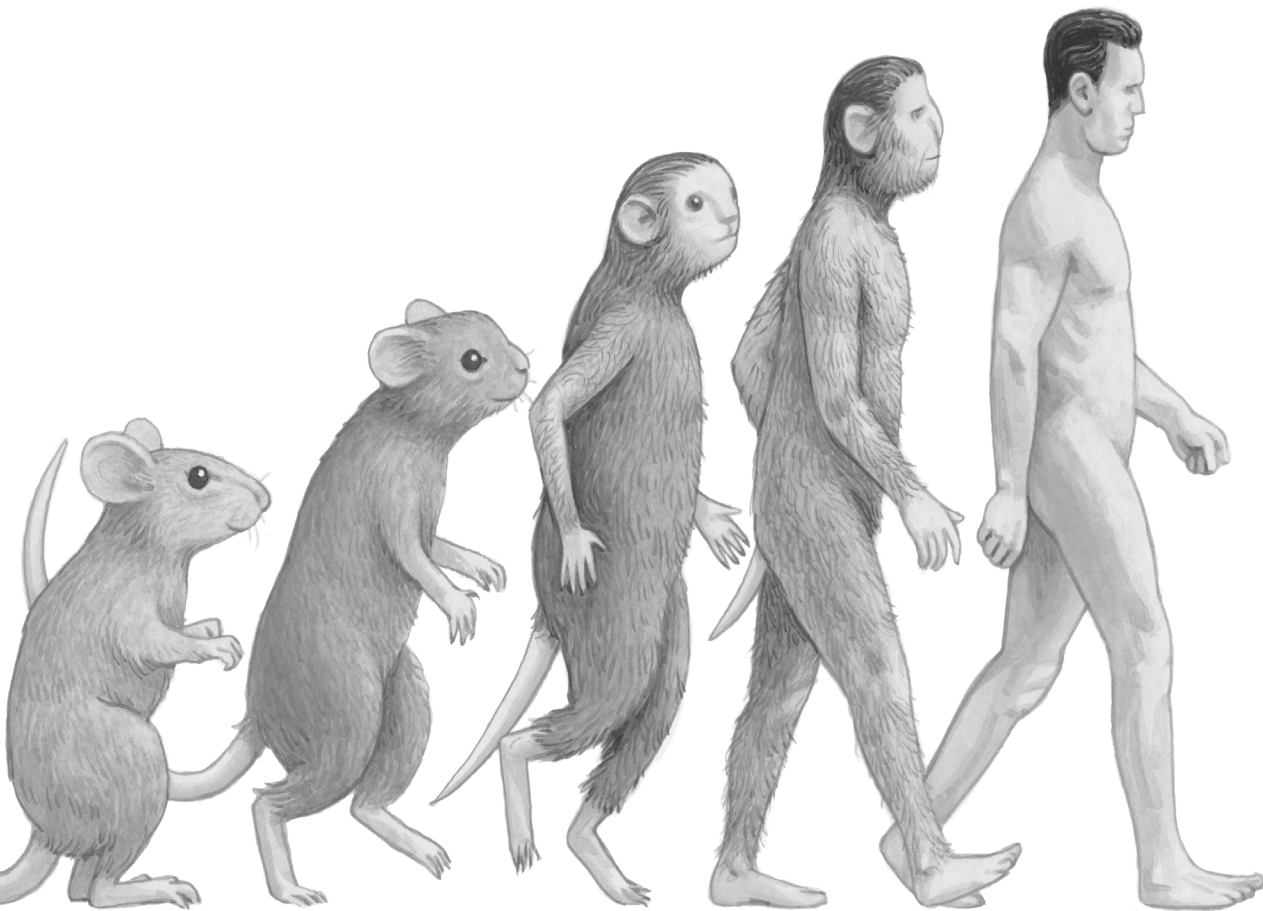
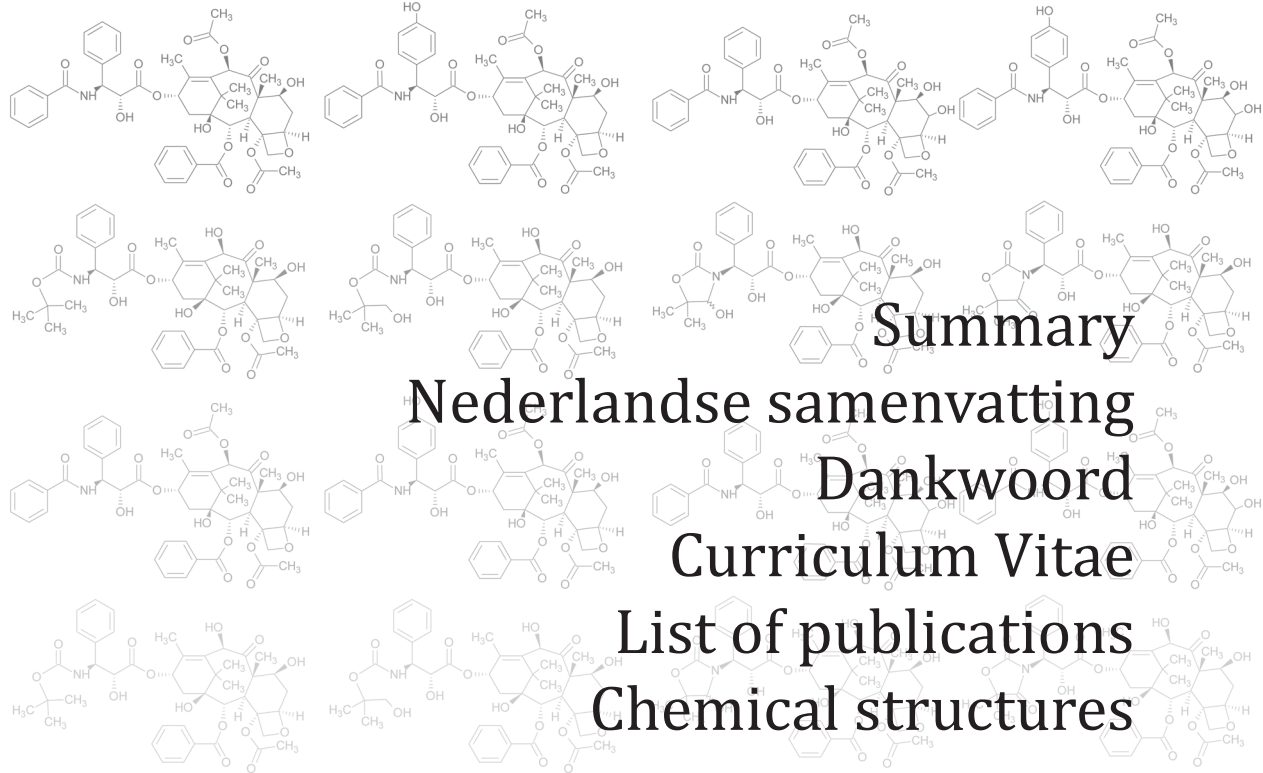
Overall, in this thesis we described multiple aspects that are involved in the development of oral formulations of taxanes. We addressed the development of bioanalytical assays for quantification of taxanes and showed applicability of assays for the combined quantification of taxanes and ritonavir in human plasma, feces and urine. Moreover, we described an approach to quantify docetaxel metabolites by LC-MS/MS using docetaxel calibration samples, which can be applied to other metabolites when chemically pure substances are not available. Using knock-out and humanized mouse models, we discussed the roles of drug metabolizing and transporting enzymes after oral administration of taxanes. Our data showed that boosting with both elacridar and ritonavir is a relatively safe strategy to boost plasma exposure of orally applied taxanes, as relative brain exposure is unlikely to be higher than that in the currently used *i.v.* schedules. We also observed that coadministration of docetaxel and ritonavir caused increased anti-tumor efficacy of docetaxel in a mouse model for hereditary breast cancer. Our data suggest that this could be caused by intratumoral Cyp3a inhibition. In this thesis, we looked not only at bioanalytical and preclinical aspects, but also at clinical aspects of orally applied taxanes. The onset of diarrhea in patients after administration of oral formulations of docetaxel was explained by combining preclinical and clinical data. Finally, our data indicate that docetaxel metabolites are hardly found in plasma after oral coadministration of docetaxel and ritonavir and, therefore, further testing of docetaxel metabolite safety is not required for the development of oral formulations of taxanes.

References

1. U.S. Food and Drug Administration. Center for Drug Evaluation and Research, Guidance for Industry Bioanalytical Method Validation, 2001. <http://www.fda.gov/downloads/Drugs/GuidanceComplianceRegulatoryInformation/Guidances/UCM070107.pdf>. Visited 18-2-2011.
2. DeGeorge JJ, Ahn CH, Andrews PA, Brower ME, Giorgio DW, Goheer MA, Lee-Ham DY, McGuinn WD, Schmidt W, Sun CJ, Tripathi SC. Regulatory considerations for preclinical development of anticancer drugs. *Cancer Chemother. Pharmacol.* **1998**; 41 (3): 173-85.
3. Kemper EM, van Zandbergen AE, Cleypool C, Mos HA, Boogerd W, Beijnen JH, van Tellingen O. Increased penetration of paclitaxel into the brain by inhibition of P-Glycoprotein. *Clin. Cancer Res.* **2003**; 9 (7): 2849-55.
4. Bardelmeijer HA, Ouweland M, Buckle T, Huisman MT, Schellens JH, Beijnen JH, van Tellingen O. Low systemic exposure of oral docetaxel in mice resulting from extensive first-pass metabolism is boosted by ritonavir. *Cancer Res.* **2002**; 62 (21): 6158-64.
5. Oostendorp RL, Huitema A, Rosing H, Jansen RS, Ter Heine R, Keessen M, Beijnen JH, Schellens JHM. Coadministration of ritonavir strongly enhances the apparent oral bioavailability of docetaxel in patients with solid tumors. *Clin. Cancer Res.* **2009**; 15 (12): 4228-33.
6. Koolen, S. L. Intravenous-to-oral switch in anticancer chemotherapy. Focus on taxanes and gemcitabine. [Dissertation]. 105-115. 16-2-2011. Utrecht University. 16-2-2011.
7. Srirangam A, Milani M, Mitra R, Guo Z, Rodriguez M, Kathuria H, Fukuda S, Rizzardi A, Schmechel S, Skalik DG, Pelus LM, Potter DA. The human immunodeficiency virus protease inhibitor ritonavir inhibits lung cancer cells, in part, by inhibition of survivin. *J. Thorac. Oncol.* **2011**; 6 (4): 661-70.
8. Ahluwalia MS, Patton C, Stevens G, Tekautz T, Angelov L, Vogelbaum MA, Weil RJ, Chao S, Elson P, Suh JH, Barnett GH, Peereboom DM. Phase II trial of ritonavir/lopinavir in patients with progressive or recurrent high-grade gliomas. *J. Neurooncol.* **2011**; 102 (2): 317-21.
9. Ikezoe T, Bandobashi K, Yang Y, Takeuchi S, Sekiguchi N, Sakai S, Koeffler HP, Taguchi H. HIV-1 protease inhibitor ritonavir potentiates the effect of 1,25-dihydroxyvitamin D3 to induce growth arrest and differentiation of human myeloid leukemia cells via down-regulation of CYP24. *Leuk. Res.* **2006**; 30 (8): 1005-11.
10. Maggiora L, Wen B, Frascogna V, Opolon P, Bourhis J, Deutsch E. Combined radiation sensitizing and anti-angiogenic effects of ionizing radiation and the protease inhibitor ritonavir in a head and neck carcinoma model. *Anticancer Res.* **2005**; 25 (6B): 4357-62.
11. Laurent N, de Boudard S, Guillaume JS, Christov C, Zini R, Jouault H, Andre P, Lotteau V, Peschanski M. Effects of the proteasome inhibitor ritonavir on glioma growth in vitro and in vivo. *Mol. Cancer Ther.* **2004**; 3 (2): 129-36.
12. Sgadari C, Monini P, Barillari G, Enoli B. Use of HIV protease inhibitors to block Kaposi's sarcoma and tumour growth. *Lancet Oncol.* **2003**; 4 (9): 537-47.
13. Gaedicke S, Firat-Geier E, Constantiniu O, Lucchiari-Hartz M, Freudenberg M, Galanos C, Niedermann G. Antitumor effect of the human immunodeficiency virus protease inhibitor ritonavir: induction of tumor-cell apoptosis associated with perturbation of proteasomal proteolysis. *Cancer Res.* **2002**; 62 (23): 6901-8.
14. Zhong DS, Lu XH, Conklin BS, Lin PH, Lumsden AB, Yao Q, Chen C. HIV protease inhibitor ritonavir induces cytotoxicity of human endothelial cells. *Arterioscler. Thromb. Vasc. Biol.* **2002**; 22 (10): 1560-6.
15. Pati S, Pelser CB, Dufraigne J, Bryant JL, Reitz MS, Jr, Weichold FF. Antitumorogenic effects of HIV protease inhibitor ritonavir: inhibition of Kaposi sarcoma. *Blood.* **2002**; 99 (10): 3771-9.
16. Marchetti S, Stuurman FE, Koolen SL, Moes JJ, Hendriks JJ, Thijssen B, Huitema AD, Nuijen B, Rosing H, Keessen M, Voest EE, Mergui-Roelvink M, Beijnen JH, Schellens JH. Phase I study of weekly oral docetaxel (ModraDoc001) plus ritonavir in patients with advanced solid tumors. *ASCO Meeting Abstracts* **2012**; 30 (15_suppl): 2550.
17. Le Tourneau C, Dieras V, Tresca P, Cacheux W, Paoletti X. Current challenges for the early clinical development of anticancer drugs in the era of molecularly targeted agents. *Target Oncol.* **2010**; 5 (1): 65-72.
18. Solomon R, Cherny NI. Constipation and diarrhea in patients with cancer. *Cancer J.* **2006**; 12 (5): 355-64.
19. European Medicines Agency: Taxotere-Summary of Product Characteristics (SPC). http://www.ema.europa.eu/docs/en_GB/document_library/EPAR_-_Product_Information/human/000073/WC500035264.pdf. Visited 27-11-2013.
20. U.S. Food and Drug Administration, Center for Drug Evaluation and Research, Guidance for industry: Safety Testing of Drug Metabolites, 2008. <http://www.fda.gov/downloads/Drugs/GuidanceComplianceRegulatoryInformation/Guidances/ucm079266.pdf>. Visited 3-9-2012.
21. Guittou J, Cohen S, Tranchand B, Vignal B, Droz JP, Guillaumont M, Manchon M, Freyer G. Quantification of docetaxel and its main metabolites in human plasma by liquid chromatography/tandem mass spectrometry. *Rapid Commun. Mass Spectrom.* **2005**; 19 (17): 2419-26.
22. Rosing H, Lustig V, van Warmerdam LJ, Huizing MT, ten Bokkel Huinink WW, Schellens JH, Rodenhuis S, Bult A, Beijnen JH. Pharmacokinetics and metabolism of docetaxel administered as a 1-h intravenous infusion. *Cancer Chemother.*

- Pharmacol.* **2000**; 45 (3): 213-8.
23. van der Veldt AA, Hendrikse NH, Smit EF, Mooijer MP, Rijnders AY, Gerritsen WR, van der Hoeven JJ, Windhorst AD, Lammertsma AA, Lubberink M. Biodistribution and radiation dosimetry of [¹¹C]-labelled docetaxel in cancer patients. *Eur.J.Nucl.Med.Mol.Imaging* **2010**.
 24. Mattos-Arruda L, Cortes J. Advances in first-line treatment for patients with HER-2+ metastatic breast cancer. *Oncologist.* **2012**; 17 (5): 631-44.
 25. Bookman MA. First-line chemotherapy in epithelial ovarian cancer. *Clin.Obstet.Gynecol.* **2012**; 55 (1): 96-113.
 26. Maluf FC, Smaletz O, Herchenhorn D. Castration-resistant prostate cancer: systemic therapy in 2012. *Clinics.(Sao Paulo).* **2012**; 67 (4): 389-94.
 27. Baranczewski P, Stanczak A, Kautiainen A, Sandin P, Edlund PO. Introduction to early in vitro identification of metabolites of new chemical entities in drug discovery and development. *Pharmacol.Rep.* **2006**; 58 (3): 341-52.
 28. Amin ML. P-glycoprotein Inhibition for Optimal Drug Delivery. *Drug Target Insights.* **2013**; 19;7:27-34.): 27-34.
 29. Breedveld P, Beijnen JH, Schellens JH. Use of P-glycoprotein and BCRP inhibitors to improve oral bioavailability and CNS penetration of anticancer drugs. *Trends Pharmacol.Sci.* **2006**; 27 (1): 17-24.
 30. Kemper EM, Verheij M, Boogerd W, Beijnen JH, van Tellingen O. Improved penetration of docetaxel into the brain by co-administration of inhibitors of P-glycoprotein. *Eur.J.Cancer.* **2004**; 40 (8): 1269-74.
 31. Durmus S, Sparidans RW, Wagenaar E, Beijnen JH, Schinkel AH. Oral availability and brain penetration of the B-RAFV600E inhibitor vemurafenib can be enhanced by the P-GLYCOprotein (ABCB1) and breast cancer resistance protein (ABCG2) inhibitor elacridar. *Mol.Pharm.* **2012**; 9 (11): 3236-45.
 32. Chuan Tang S, Nguyen LN, Sparidans RW, Wagenaar E, Beijnen JH, Schinkel AH. Increased oral availability and brain accumulation of the ALK inhibitor crizotinib by coadministration of the P-glycoprotein (ABCB1) and breast cancer resistance protein (ABCG2) inhibitor elacridar. *Int.J.Cancer.* **2013**): 10.
 33. den Ouden D, van den Heuvel M, Schoester M, van Rens G, Sonneveld P. In vitro effect of GF120918, a novel reversal agent of multidrug resistance, on acute leukemia and multiple myeloma cells. *Leukemia.* **1996**; 10 (12): 1930-6.
 34. Tang C, Prueksaritanont T. Use of in vivo animal models to assess pharmacokinetic drug-drug interactions. *Pharm.Res.* **2010**; 27 (9): 1772-87.
 35. van Waterschoot RA, Schinkel AH. A critical analysis of the interplay between cytochrome P450 3A and P-glycoprotein: recent insights from knockout and transgenic mice. *Pharmacol.Rev.* **2011**; 63 (2): 390-410.
 36. Vaclavikova R, Soucek P, Svobodova L, Anzenbacher P, Simek P, Guengerich FP, Gut I. Different in vitro metabolism of paclitaxel and docetaxel in humans, rats, pigs, and minipigs. *Drug Metab Dispos.* **2004**; 32 (6): 666-74.
 37. Bardelmeijer HA, Roelofs AB, Hillebrand MJ, Beijnen JH, Schellens JH, van Tellingen O. Metabolism of docetaxel in mice. *Cancer Chemother.Pharmacol.* **2005**; 56 (3): 299-306.





Summary

Cancer is one of the leading causes of death worldwide. Therefore, the onset and behavior of cancer is studied by many research groups. The increase in knowledge of the onset and behavior of cancer is accompanied by new therapeutic options and treatment strategies. In our research group, the focus is on the development of new oral formulations of taxanes, a group of widely used anticancer agents that are currently administered intravenously (i.v.). A major limitation in the concept of oral administration of the taxanes paclitaxel (Taxol[®]) and docetaxel (Taxotere[®]), is the low oral availability. Paclitaxel and docetaxel have poor aqueous solubility and upon oral administration, intestinal uptake can be seriously hampered by drug efflux through P-glycoprotein (P-gp/MDR1/ABCB1) and by drug metabolism via Cytochrome P450 (CYP) 3A. Several studies by our group have shown that the oral bioavailability of paclitaxel and docetaxel can be enhanced by combining the taxanes with the CYP3A4 inhibitor ritonavir (Norvir[®]).

The aim of this thesis was to obtain mechanistic insights into the boosting effect of ritonavir on orally administered taxanes and to support clinical development of oral pharmaceutical formulations of paclitaxel and docetaxel.

Bioanalysis of taxanes

During drug development reliable and sensitive bioanalytical assays for quantification of these drugs are prerequisites to support preclinical and clinical trials. Assays to support trials with oral formulations of docetaxel and paclitaxel are described in Chapter 1 of this thesis. In **Chapter 1.1**, an overview is presented of publications that describe method development and validation of assays used to quantify taxanes in biological matrices such as plasma, tissue, feces and urine. Currently, liquid chromatography (LC) coupled with ultraviolet detection (UV) or tandem mass spectrometry detection (MS/MS) are mostly used for quantification of the taxanes. LC-MS/MS provides more sensitivity and selectivity compared to LC-UV. The increased selectivity of LC-MS/MS requires less sample pre-treatment and can reduce run time since less chromatographic separation is required. Therefore, when sensitivity or high sample throughput is required, LC-MS/MS is the best choice for quantification of taxanes in biological samples. Since interfering signals are increased after protein precipitation, liquid-liquid extraction with tertiary-butylmethylether or on-line solid-phase extraction is advised when high sensitivity and selectivity are needed. Selectivity is further increased with a mobile phase containing at least 50% of organic phase. Moreover, addition of ammonium to the mobile phase increases sensitivity of MS/MS detection.

A combined assay for the quantification of paclitaxel, docetaxel and ritonavir in human plasma is described in **Chapter 1.2**. Method development including optimisation of the mass transitions and response, mobile phase optimisation and column selection are discussed. During method development, it was observed that ionisation of ritonavir is more efficient than ionisation of the taxanes. This, however, resulted in saturation of the response of ritonavir at high drug concentrations. Suboptimal mass spectrometry settings for ritonavir resulted in decreased saturation and the quantification of the

taxanes and ritonavir could thus be combined. The method was validated according to US Food and Drug Administration (FDA) guidelines and the principles of Good Laboratory Practice (GLP). The described method was successfully applied in clinical studies with oral administration of docetaxel or paclitaxel in combination with ritonavir.

In **Chapter 1.3**, method development and validation of an assay for the quantification of paclitaxel, docetaxel and ritonavir in human feces and urine are described. During development, it was observed that quantification of docetaxel, paclitaxel, ritonavir -and maybe also other drugs- in feces samples of patients might be biased when homogenized samples are stored in large portions and when aliquots for quantification are taken after storage. Apparently, thawing a homogenized sample after storage at -20° C results in non-uniform distribution of the analytes in the sample. This can be circumvented by taking aliquots for quantification immediately after homogenization of samples, prior to storage. In urine samples, we observed that quantification of the analytes after spiking of these compounds in a small volume resulted in underestimation of the concentration, indicating that adsorption to the container wall takes place when analytes are spiked to urine. Therefore, samples should be diluted prior to storage. After storage of both feces and urine samples, sample pre-treatment should be performed in the same tubes as used for storage. The assay for combined quantification of the taxanes and ritonavir in feces and urine was validated according to FDA guidelines and the principles of GLP. This assay can be used to test absorption and excretion of orally administered taxane and ritonavir formulations.

During drug development, plasma concentrations of both the parent compound and its metabolites are studied. Accurate quantification of metabolites in biological samples using mass spectrometry is, however, often hampered by the lack of metabolites of chemically pure quality. An approach to quantify metabolites of docetaxel in human plasma by LC-MS/MS without using chemically pure substances of the metabolites is described in **Chapter 1.4**. Metabolites M2, M4 and the stereoisomers M1 and M3 were quantified using docetaxel calibration standards. The concept of quantification of structural analogues, like metabolites, using a calibration curve of the parent drug and applying a correction factor was tested using paclitaxel as test compound. The assay was tested during a partial validation program based on the FDA guidelines on bioanalytical method validation. The same approach may be used for quantification of metabolites of other drugs by LC-MS/MS when chemically pure reference substances are unavailable.

Preclinical studies on taxanes

In Chapter 2, mouse models are used to obtain further mechanistic insights into the limited intestinal absorption of paclitaxel and docetaxel. Intestinal absorption is an essential step in the therapeutic use of most orally administered drugs. In **Chapter 2.1**, the role of intestinal drug transporting systems in drug absorption and disposition is discussed and the genetically modified mouse models that are used to study them. Ongoing and future studies with genetically modified mouse models may further improve these insights, thus supporting the development of optimal orally available drugs.

In **Chapter 2.2**, the mechanism underlying the enhancement of the oral bioavailability of paclitaxel in humans by co-administration of ritonavir was studied. Our results showed that both P-gp and CYP3A are involved in limiting paclitaxel plasma concentrations after oral administration. Our data indicate that for intestinal absorption of paclitaxel, enzymes other than P-gp and CYP3A are not relevant. Co-administered ritonavir inhibited CYP3A-mediated metabolism, but not P-gp-mediated transport of paclitaxel. It was observed that mouse liver microsomes metabolized paclitaxel far less efficiently than human or CYP3A4-transgenic liver microsomes, revealing much lower efficiency of paclitaxel metabolism by mouse than by human CYP3As. Therefore, CYP3A4-humanized mice allow improved understanding of CYP3A4-mediated paclitaxel metabolism in humans.

In **Chapter 2.3**, it is examined whether it would be feasible and safe to substantially increase the oral availability of taxanes by simultaneous inhibition of P-gp and CYP3A by elacridar and ritonavir, respectively. An increase in plasma exposure of orally applied taxanes was observed when co-administered with either oral elacridar or ritonavir. Oral co-administration of the taxanes with both elacridar and ritonavir resulted in even further increased plasma exposure. The results were compared with previously reported data obtained from oral administration of taxanes to knock-out mice. This showed that orally administered elacridar and ritonavir at comparatively low doses can completely (for paclitaxel), or almost completely (for docetaxel) inhibit intestinal and hepatic P-gp and CYP3A4 activity. In contrast, relative brain accumulation of the taxanes was not affected after boosting with oral elacridar. Therefore it was concluded that the oral availability of taxanes can be enhanced by co-administration with oral elacridar and ritonavir, without evoking the risk of increased toxicity of the taxanes in the central nervous system (CNS).

In **Chapter 2.4**, the *in vivo* impact of mouse and human Organic Anion Transporting Polypeptide (OATP) 1A/1B transporters on docetaxel plasma clearance and liver and intestinal uptake is studied in genetically engineered mouse models. Absence of mouse *Oatp1a/1b* transporters resulted in impaired liver uptake of docetaxel, but did not affect the intestinal absorption after oral administration. Liver-specific expression of each of the human OATP1B1, OATP1B3 and OATP1A2 transporters provided a nearly complete rescue of the impaired liver uptake of docetaxel in *Oatp1a/1b*-null mice.

The anti-tumor efficacy of docetaxel and ritonavir in a mouse model for hereditary breast cancer is described in **Chapter 2.5**. Growth of implanted mouse mammary tumors was decreased by single docetaxel treatment but not by single ritonavir treatment. Tumor growth was further reduced when docetaxel was co-administered with ritonavir, showing increased efficacy of docetaxel when co-administered with ritonavir. Our data indicate that *Cyp3a* inhibition in tumor tissue by ritonavir resulted in decreased docetaxel metabolism in the tumor. This most likely contributed to the observed increased antitumor efficacy of docetaxel when co-administered with ritonavir.

Clinical studies on taxanes

In Chapter 3, safety of orally co-administered docetaxel and ritonavir in patients is discussed. The most common and dose-limiting toxicity of oral docetaxel was diarrhea. In **chapter 3.1**, preclinical and clinical data are combined and incidence, severity and cause of oral docetaxel induced diarrhea are studied. Our data indicate that the onset of severe diarrhea after oral co-administration of docetaxel and ritonavir in humans is probably caused by the level of docetaxel in the systemic blood circulation and is not related to the route of administration of docetaxel.

Early clinical evaluation of new drugs or drug formulations focuses not only on safety of the parent compounds, but also on formed metabolites. FDA guidelines on Safety Testing on Metabolites (MIST) recommend further safety testing if metabolite exposure exceeds 10% of the parent drug exposure. In **Chapter 3.2**, plasma concentrations of metabolites of docetaxel after oral co-administration of docetaxel and ritonavir are described. Both the oral route of administration of docetaxel and co-administration with ritonavir might alter docetaxel metabolite concentrations in plasma, compared with standard intravenous administration. It was observed that the metabolite profile in plasma was different after oral and i.v. administration of docetaxel when co-administered with ritonavir. However, CYP3A inhibition by ritonavir resulted in low plasma concentrations of metabolites of docetaxel and thus further testing of the safety of the metabolites is not required.

Overall, in this thesis multiple aspects involved in the development of oral formulations of taxanes are described. The development of bioanalytical assays for quantification of taxanes are addressed; the roles of drug metabolizing and transporting enzymes after oral administration of taxanes using knock-out and humanized mouse models are discussed; and increased anti-tumor efficacy of docetaxel is shown when ritonavir is co-administered. Moreover, the onset of severe diarrhea and the abundance of metabolites of docetaxel in patients is studied after oral co-administration of docetaxel and ritonavir. Hopefully, this thesis will further contribute to the development of oral taxanes.

Samenvatting

Kanker is wereldwijd gezien één van de belangrijkste doodsoorzaken. Er wordt dan ook veel onderzoek gedaan naar het ontstaan van kanker en het achterliggende ziekteproces. De toenemende kennis over het ziekteproces draagt bij aan de ontdekking van nieuwe aangrijpingspunten voor geneesmiddelen en aan de ontwikkeling van nieuwe strategieën in de behandeling. Onze onderzoeksgroep richt zich op de ontwikkeling van nieuwe orale toedieningsvormen van taxanen. De verzamelnaam taxanen verwijst naar een groep geneesmiddelen die veelvuldig gebruikt wordt bij de behandeling van kanker. Taxanen worden momenteel via een intraveneus infuus toegediend aan patiënten. Een belangrijke beperking in de orale toediening van de taxanen paclitaxel (Taxol®) en docetaxel (Taxotere®) is echter de lage biologische beschikbaarheid. Dit wordt veroorzaakt doordat paclitaxel en docetaxel slecht wateroplosbare stoffen zijn. Bovendien worden deze middelen na opname in de darm teruggepompt naar de darminhoud door het eiwit P-glycoproteïne (P-gp/MDR1/ABCB1) of afgebroken door Cytochroom P450 (CYP) 3A eiwitten in de darmwand. Verschillende studies uit onze onderzoeksgroep laten zien dat de biologische beschikbaarheid van paclitaxel en docetaxel na orale toediening wordt verhoogd als deze taxanen met ritonavir (Norvir®), een remmer van CYP3A, worden ingenomen

Het doel van dit proefschrift was inzicht te verkrijgen in het mechanisme dat ten grondslag ligt aan de verhoging van de biologische beschikbaarheid van oraal toegediende taxanen wanneer deze middelen worden toegediend in combinatie met ritonavir.

Bioanalyse van taxanen

Tijdens de ontwikkeling van geneesmiddelen zijn betrouwbare en gevoelige bioanalytische methoden nodig om geneesmiddelconcentraties te meten voor preklinische en klinische studies. In hoofdstuk 1 van dit proefschrift zijn methoden voor taxanen beschreven. Meerdere wetenschappelijke publicaties beschrijven de ontwikkeling en validatie van methoden die gebruikt worden om taxanen te kwantificeren in biologisch materiaal (zoals bloedplasma, orgaanweefsel, feces en urine). In **hoofdstuk 1.1** wordt een overzicht gegeven van deze wetenschappelijke publicaties. De meeste methoden maken gebruik van vloeistofchromatografie (LC) gekoppeld aan ultraviolet detectie (UV) of gekoppeld aan tandem massaspectrometrie (MS/MS). Voor een gevoelige en snelle methode heeft MS/MS de voorkeur boven UV. Vloeistof-vloeistof extractie en vaste-fase extractie zijn het meest geschikt als monstervoorbewerking voor een gevoelige en selectieve methode. Voor de vloeistof chromatografie geeft het gebruik van een mobiele fase met tenminste 50% organisch oplosmiddel de beste selectiviteit. De toevoeging van ammoniumzouten aan de mobiele fase geeft bovendien een verbetering van de gevoeligheid bij MS/MS detectie.

In **hoofdstuk 1.2** wordt een methode beschreven voor de gecombineerde bepaling van paclitaxel, docetaxel en ritonavir in humaan bloedplasma. De ontwikkeling van de methode, inclusief de optimalisatie van de massa transities, analiet respons en mobiele fase, en de keuze van de kolom worden besproken. Tijdens de ontwikkeling

van de methode bleek dat de ionisatie van ritonavir in de ionisatiebron van de massaspectrometer efficiënter verloopt dan de ionisatie van de taxanen. Dit resulteerde in verzadiging van de detector in het hoge concentratie bereik van ritonavir. De verschillende middelen konden in één bepaling gecombineerd worden door het kiezen van suboptimale parameters voor de ionisatie van ritonavir. De methode werd gevalideerd volgens de eisen van de Amerikaanse voedsel en geneesmiddel autoriteit (FDA) en de principes van Goede Laboratorium Praktijken (GLP). De beschreven methode werd succesvol toegepast bij de ondersteuning van klinische studies met orale toediening van docetaxel of paclitaxel in combinatie met ritonavir.

In **hoofdstuk 1.3** wordt een methode beschreven voor de gecombineerde bepaling van paclitaxel, docetaxel en ritonavir in feces en urine. Tijdens de ontwikkeling van deze methode werd vastgesteld dat de middelen niet meer homogeen verdeeld waren over het monster als feces homogenaat ontdooid werd na invriezen. Hierdoor konden de geneesmiddelen niet meer precies en nauwkeurig gekwantificeerd worden in de monsters. De onjuiste bepaling kan worden voorkomen door het monster voor invriezen al te verdelen over verschillende porties voor de analyse. De urine monsters moesten ook al voor invriezen verdeeld worden in meerdere porties. Dit komt doordat de slecht-wateroplosbare stoffen adsorberen aan de wand van de plastic buis. Door de porties na het invriezen op te werken in dezelfde buis, kunnen de geneesmiddelen toch precies gekwantificeerd worden. De methode werd gevalideerd volgens de eisen van de FDA en de principes van GLP en is geschikt om de opname en uitscheiding van taxanen en ritonavir na orale toediening te onderzoeken.

Tijdens de ontwikkeling van een geneesmiddel worden niet alleen de concentraties van het geneesmiddel in het bloed bestudeerd, maar ook concentraties van de metaboliëten die ontstaan na afbraak van het geneesmiddel. Voor een nauwkeurige bepaling van deze metaboliëten met massaspectrometrie zijn echter chemisch zuivere referentiestoffen nodig, echter deze verbinden zijn in de vroege fase van de geneesmiddelontwikkeling niet altijd beschikbaar. In **hoofdstuk 1.4** wordt een procedure beschreven om metaboliëten van docetaxel te bepalen met LC-MS/MS zonder gebruik te maken van chemisch zuivere referentiestoffen van de metaboliëten. Voor de bepaling van de metaboliëten M2, M4 en de stereoisomeren M1 en M3 werd chemisch zuiver docetaxel gebruikt als referentiestof voor de kalibratielijnen. Het concept om een chemisch zuivere stof en een correctiefactor toe te passen om structuuranalogen, zoals metaboliëten, te bepalen werd getest met paclitaxel. De methode werd getest tijdens een partiële validatie die gebaseerd is op de eisen van de FDA. De procedure kan ook gebruikt worden om metaboliëten van andere geneesmiddelen te meten met LC-MS/MS als er geen chemisch zuivere referentiestoffen beschikbaar zijn.

Preklinische studies met taxanen

In hoofdstuk 2 wordt gebruik gemaakt van muismodellen om meer inzicht te krijgen in de beperkte opname van paclitaxel en docetaxel in de darm. De opname in de darm is een belangrijke stap om oraal toegediende geneesmiddelen te kunnen gebruiken bij therapeutische behandelingen. In **hoofdstuk 2.1** wordt de rol besproken die transport eiwitten in de darm spelen bij de absorptie en verdeling van geneesmiddelen. Daarbij

worden ook genetisch gemodificeerde muismodellen besproken die gebruikt worden om deze transportsystemen te bestuderen. Deze muismodellen kunnen gebruikt worden om een beter inzicht te krijgen in de opname en verdeling van geneesmiddelen. Dit inzicht kan bijdragen aan de verdere ontwikkeling van orale toediening van nieuwe en bestaande geneesmiddelen.

Hoofdstuk 2.2 is gericht op het verklaren van het mechanisme waardoor ritonavir de orale biologische beschikbaarheid van paclitaxel verhoogt in patiënten. Onze resultaten laten zien dat zowel P-gp als CYP3A een rol spelen in het beperken van de paclitaxel concentraties in bloed na orale toediening van paclitaxel. Andere transportsystemen leveren echter geen relevante bijdrage aan het beperken van de biologische beschikbaarheid van oraal toegediend paclitaxel. Als de orale toediening van paclitaxel wordt gecombineerd met de toediening van ritonavir, neemt de biologische beschikbaarheid van paclitaxel toe doordat CYP3A wordt geremd door ritonavir. Ritonavir heeft echter geen invloed op het transport van paclitaxel door P-gp. Het metabolisme van paclitaxel in muizen is verder bestudeerd door gebruik te maken van microsomen. Er werd gezien dat microsomen uit de lever van muizen minder goed zijn in het afbreken van paclitaxel dan microsomen uit de lever van muizen met humaan CYP3A of uit de lever van mensen. Dit betekent dat Cyp3a eiwitten van muizen minder efficiënt zijn in het afbreken van paclitaxel dan CYP3A eiwitten van mensen. Door in preklinische studies gebruik te maken van genetisch gemodificeerde muizen met humaan CYP3A, kan er een beter beeld gevormd worden van de afbraak van paclitaxel door CYP3A in de mens.

In **hoofdstuk 2.3** is onderzocht of het mogelijk -en veilig- was om de biologische beschikbaarheid van taxanen te verhogen door gelijktijdig de werking van P-gp en CYP3A eiwitten te blokkeren. Elacridar is gebruikt om P-gp te blokkeren en ritonavir om CYP3A te blokkeren. Zowel de toediening van elacridar als de toediening van ritonavir verhoogde de biologische beschikbaarheid van de taxanen paclitaxel en docetaxel. Gelijktijdige toediening van elacridar en ritonavir zorgde voor een verdere verhoging van de biologische beschikbaarheid. De resultaten uit deze studie zijn vergeleken met eerdere resultaten uit studies waarin knock-out muizen zijn gebruikt. Deze knock-out muizen zijn genetisch gemodificeerd, waardoor ze geen P-gp of CYP3A eiwitten tot expressie brengen. Deze vergelijking liet zien dat elacridar en ritonavir de werking van respectievelijk P-gp en CYP3A eiwitten (bijna) volledig blokkeerden in de lever en de darm. De penetratie van de taxanen in de hersenen werd echter niet beïnvloed door de gelijktijdige toediening van de taxanen met de lage dosering elacridar. Hieruit kan geconcludeerd worden dat de biologische beschikbaarheid van de taxanen na orale toediening kan worden verhoogd door gelijktijdige orale toediening van elacridar en ritonavir. Hierbij is er bij de orale toediening van taxanen met elacridar en ritonavir geen verhoogd risico op toxiciteit in het centrale zenuwstelsel ten opzichte van intraveneuze toediening van de taxanen.

In **hoofdstuk 2.4** zijn transporteiwitten die organische anionen in de muis en de mens transporteren (OATPs) bestudeerd. De rol van de subtypen 1A en 1B in de opname van docetaxel in de darm en de klaring van docetaxel uit bloedplasma en leverweefsel is onderzocht in genetisch gemodificeerde muizen. De afwezigheid van

Oatp1a/1b eiwitten resulteerde in een verminderde opname van docetaxel in de lever, maar had geen invloed op de absorptie van docetaxel in de darm. Het aanbrengen van humaan OATP1B1, OATP1B3 en OAPT1A2 door genetische modificatie in de lever van muizen zonder Oatp1a/1b eiwitten zorgde ervoor dat de opname van docetaxel in de lever weer normaal was.

In **hoofdstuk 2.5** is het effect van docetaxel en ritonavir op de tumorgroei bestudeerd in een muismodel voor erfelijke borstkanker. De groei van geïmplanteerde tumoren werd niet geremd door behandeling met ritonavir, maar wel door behandeling met docetaxel. De tumorgroei werd bovendien sterker geremd door gelijktijdige behandeling met docetaxel en ritonavir. Onze resultaten duiden erop dat remming van Cyp3a door ritonavir in de tumor zorgt voor een lokaal verminderde afbraak van docetaxel. Dit heeft waarschijnlijk bijgedragen aan de sterkere remming van de tumorgroei als de behandeling met docetaxel werd aangevuld met ritonavir.

Klinische studies met taxanen

In Hoofdstuk 3 wordt de veiligheid van de gelijktijdige orale toediening van docetaxel en ritonavir beschreven. Diarree is de meest voorkomende bijwerking die ervoor zorgt dat de dosering van oraal toegediend docetaxel niet verhoogd kan worden. In hoofdstuk 3.1 zijn gegevens uit preklinische en klinische studies gekoppeld om te bestuderen wat de oorzaak is van diarree na orale toediening van docetaxel, hoe ernstig de diarree is en hoe vaak diarree voorkomt. Onze resultaten duiden erop dat het ontstaan van ernstige diarree na gelijktijdige orale toediening van docetaxel en ritonavir waarschijnlijk wordt veroorzaakt door de hoeveelheid docetaxel in het bloed. Het ontstaan van ernstige diarree is niet gerelateerd aan de toedieningsroute van docetaxel.

Tijdens de ontwikkeling van geneesmiddelen wordt niet alleen gekeken naar de veiligheid van het geneesmiddel, maar ook naar de veiligheid van de metabolieten die ontstaan na afbraak van het geneesmiddel. De richtlijnen van de FDA stellen dat er onderzoek naar de veiligheid van de metabolieten moet plaatsvinden als de blootstelling aan de metabolieten hoger wordt dan 10% van de blootstelling aan het geneesmiddel. In **hoofdstuk 3.2** zijn de concentraties van de metabolieten van docetaxel in het bloed bestudeerd na gelijktijdige orale toediening van docetaxel en ritonavir. Zowel de orale toedieningsroute van docetaxel als de gelijktijdige toediening van docetaxel met ritonavir kunnen mogelijk de concentraties van de metabolieten in het bloed veranderen ten opzichte van de intraveneuze toediening van docetaxel. De metabolietprofielen die gezien worden in bloedplasma zijn verschillend na orale en intraveneuze toediening van docetaxel. Echter de concentraties van de metabolieten in bloedplasma zijn laag na gelijktijdige orale toediening van docetaxel en ritonavir als gevolg van de remming van CYP3A door ritonavir. Daarom zijn verdere studies naar de veiligheid van de metabolieten niet nodig.

In dit proefschrift zijn verschillende aspecten beschreven van de ontwikkeling van orale toedieningsvormen van taxanen. Allereerst is de ontwikkeling van bioanalytische methoden voor de bepaling van taxanen behandeld. Vervolgens zijn knock-out en

gehumaniseerde muizen gebruikt om te onderzoeken wat de rol is van eiwitten die geneesmiddelen transporteren of afbreken als taxanen oraal toegediend worden. Bovendien is in een muismodel voor erfelijke borstkanker aangetoond dat de tumorgroei sterker wordt geremd als ritonavir wordt toegevoegd aan de behandeling met docetaxel. Tot slot is het ontstaan van ernstige diarree en de aanwezigheid van metabolieten van docetaxel in bloedplasma bestudeerd na orale toediening van docetaxel in combinatie met ritonavir. Hopelijk levert dit proefschrift een verdere bijdrage aan de ontwikkeling van orale taxanen.

Dankwoord

Na bijna vier jaar onderzoek is mijn proefschrift gereed. Ik heb genoten van deze periode en ben trots op het eindresultaat. Dit proefschrift is niet alleen het resultaat van mijn werk, maar is mede geworden zoals het is door de steun en toewijding van anderen.

Allereerst wil ik de patiënten bedanken die hebben meegewerkt aan de klinische studies die beschreven worden in dit proefschrift. Zonder hun deelname aan de studies had ik niet de beschikking over de vele samples en data die geanalyseerd zijn.

Ik wil ook mijn dank uitspreken aan mijn co-promotoren en promotoren. Hilde, ik heb erg veel gehad aan je steun op het gebied van de bioanalyse van taxanen. Je hebt me veel bijgebracht over bioanalyse en GLP en we hebben mooie assays ontwikkeld! Ik heb genoten van onze samenwerking en ben er van overtuigd dat dit de komende jaren niet veranderd. Alfred, bedankt voor je kritische blik en je uitleg bij de diverse muizenstudies. Ik vond het erg prettig om met je samen te werken en heb veel geleerd over de wereld van de drugtransporters. Gedurende mijn promotie heb je me altijd geweldig ondersteund bij de opzet van de experimenten, ook als ze buiten je reguliere onderzoeksgebieden vielen. Jos, ik wil je bedanken dat je me de mogelijkheid hebt geboden om promotieonderzoek te doen. Je gaf me altijd veel vrijheid in de projecten en ik heb veel geleerd van je kritische blik op onderzoek. Jan, bedankt voor de mogelijkheid om naast mijn onderzoek de opleiding tot klinisch farmacoloog te volgen. Hierdoor heb ik veel meegekregen over het uitvoeren van klinische studies en de dagelijkse praktijk in de kliniek.

De leden van mijn leescommissie wil ik bedanken voor het doornemen van mijn leesmap: prof. Gert Folkerts, prof. Berend Olivier, prof. Emile Voest, dr. Sven Rottenberg en prof. Ron Matthijssen.

Cynthia en Perry, fijn dat jullie mijn paranimfen willen zijn! Perry, we hebben lief en leed gedeeld in Huize Oskar en al tijdens de studie een gedeelde interesse gevonden in de wetenschap. Op naar een vruchtbare samenwerking als arts en apotheker in de toekomst! Cynthia, ik heb genoten van onze periode als kamergenoten en de discussies over bioanalyse, massabalans en minder wetenschappelijke onderwerpen. Je droge constatering en ergernissen over de alledaagse besommeringen zal ik missen. Beiden succes met het afronden van jullie eigen promotie.

Ik wil ook alle mede-onderzoekers bedanken voor de geweldige tijd! Rik, ik heb genoten van de gezamenlijke projecten en de goede samenwerking. Coen, bedankt voor de discussies over statistiek en nespresso. Stijn, bedankt voor het inwerken binnen de Modrastudies. Nynke, bedankt voor het nalezen van diverse manuscripten. Tine, bedankt voor de gezellige tijd als kamergenote. Ook alle andere (oud-)OIO's bedankt voor de discussies, goede werksfeer en gezellige OIO weekenden.

Dear people of the Schinkelgroup and H5 (formerly known as P2), thanks for the warm welcome as "guest" at the NKI! Anita, bedankt voor alle hulp bij de diverse PCR assays. Els, bedankt voor de fok voor al mijn experimenten. Sven, thanks for our

collaboration during the tumor response experiment. I would also like to thank all the other people, especially Dilek, Selvi en Seng Chuan.

Mijn dank gaat ook uit naar alle mensen in de apotheek waar ik de afgelopen jaren met plezier heb gewerkt. Jurjen, bedankt voor je hulp bij de opzet van de muisexperimenten. Bas, bedankt voor je hulp als studieleider. Abadi, Niels en Lianda, bedankt voor de hulp bij de taxaanalyses. Ook de rest van het lab, QA en de apotheek, bedankt voor de goede werksfeer in de afgelopen periode en dat het maar zo mag blijven in de komende periode.

Ik wil ook de proefdierverzorgers van G3, Olaf en Ji-Ying Song bedanken voor de hulp bij de diverse muisexperimenten..

Mijn dank gaat ook uit naar allen met wie ik samengewerkt heb in de afgelopen jaren, maar die ik niet bij naam genoemd heb.

Pap, mam, Martijn en Sander, bedankt voor de steun de afgelopen jaren en de geweldige familiesfeer. Jullie hebben mij mede gemaakt zoals ik ben. It's all in the family.

Nina, last but not least! Bedankt voor je interesse en steun de afgelopen jaren. Je hebt vele verhalen aangehoord en vele stukken gelezen. Fijn dat ik dit promotietraject zo met je kon delen. *Det weej nog lang van ein meuge genete en des dich nog lang mien stuur meugs blieve. Ik halt van dich!*

Curriculum Vitae

Jeroen Hendriks werd geboren op 19 februari 1983 te Grubbenvorst. Hij behaalde in 2001 zijn gymnasium diploma aan het Dendron College te Horst, Limburg. Aansluitend begon hij aan de studie Farmacie aan de Universiteit Utrecht, waar in 2005 het bachelor diploma werd behaald. Als onderdeel van de masteropleiding werd een wetenschappelijke stage uitgevoerd bij het Departement Biomedische Analyse aan de Universiteit Utrecht onder supervisie van Dr. R.W. Sparidans. Tijdens deze stage zijn twee bioanalytische methoden ontwikkeld en gevalideerd voor de bepaling van midazolam en de metaboliëten van midazolam. In mei 2009 behaalde Jeroen zijn masterdiploma Farmacie met de profielkeuze



“Patiënt en Complexe medicatie”. Gelijktijdig begon hij als projectapotheker bij de Apotheek van het Academisch Medisch Centrum (AMC) te Amsterdam op de afdelingen Productie en Laboratorium. In mei 2010 startte hij met het promotieonderzoek dat is beschreven in dit proefschrift bij de Apotheek van het Slotervaart ziekenhuis en de afdelingen Klinische Farmacie en Moleculaire Oncologie van het Nederlands Kanker Instituut te Amsterdam. Het onderzoek werd uitgevoerd onder begeleiding van Prof. Dr. J.H. Beijnen, Prof. Dr. J.H.M. Schellens, Dr. A.H. Schinkel en Dr. H. Rosing. Naast het promotieonderzoek volgde Jeroen de opleiding tot klinisch farmacoloog, waarvoor in december 2013 de certificering werd toegekend door de Nederlandse Vereniging voor Klinische Farmacie & Biofarmacie (NVKFB). Sinds januari 2014 is Jeroen in opleiding tot ziekenhuisapotheker bij de apotheek van het Antoni van Leeuwenhoek ziekenhuis en het Slotervaart Ziekenhuis te Amsterdam.

Curriculum Vitae

Jeroen Hendriks was born on February 19th 1983 in Grubbenvorst, The Netherlands. In 2001 he finished secondary school at the Dendron College in Horst, Limburg, The Netherlands. Subsequently, he started studying Pharmaceutical Sciences at Utrecht University, where he received his BSc degree in 2005. During the Masters programme a scientific internship was performed at the Department of Biomedical Analysis of Utrecht University under supervision of Dr. R.W. Sparidans. Two bioanalytical assays for the quantification of midazolam and its metabolites were developed and validated during this internship. In May 2009, Jeroen obtained his MSc degree in Pharmacy with specialization "Pharmaceutical care". At the same time he started working as pharmacist at the Formulations Department and the Laboratory Department of the Pharmacy of the Academic Medical Centre (AMC), Amsterdam. In May 2010, he started with his PhD project described in this thesis at the Department of Pharmacy and Pharmacology of the Slotervaart Hospital, Amsterdam and at the Department of Clinical Pharmacology and the Division of Molecular Oncology of the Netherlands Cancer Institute, Amsterdam. The PhD project was supervised by Prof. Dr. J.H. Beijnen, Prof. Dr. J.H.M. Schellens, Dr. A.H. Schinkel and Dr. H. Rosing. During the PhD program, Jeroen followed a training for clinical pharmacologist and certification was granted in December 2013 by the Dutch Society for Clinical Pharmacology & Biopharmacy. Since January 2014 Jeroen is trained to be a Hospital Pharmacist at the Pharmacy of the Antoni van Leeuwenhoek hospital and the Slotervaart Hospital, Amsterdam.

Publications

Hendriks JJMA, Rosing H, Schinkel AH, Schellens JHM, Beijnen JH. *Quantification of taxanes in biological matrices: A review of bioanalytical assays and recommendations for development of new assays* Bioanalysis. **2014**; accepted

Mooiman K, Maas-Bakker R, **Hendriks JJMA**, Bank P, Rosing H, Beijnen JH, Schellens JHM, Meijerman, I. *The effect of Complementary and Alternative Medicines (CAM) on CYP3A4-mediated metabolism of three different substrates: 7-benzyloxy-4-trifluoromethyl-coumarin (BFC), midazolam and docetaxel*. J Pharm & Pharmacol. **2014** doi: 10.1111/jphp.12208

Hendriks JJMA, Rosing H, Schinkel AH, Schellens JHM, Beijnen JH. Combined quantification of paclitaxel, docetaxel and ritonavir in human feces and urine using LC-MS/MS. Biomed Chromatogr. **2014**; 28 (2): 302-10

Tang SC*, **Hendriks JJMA***, Beijnen JH, Schinkel AH. *Genetically modified mouse models for oral drug absorption and disposition*. Curr Opin Pharmacol. **2013**; 13 (6): 853-8. *Contributed equally

Hendriks JJMA, Dubbelman AC, Rosing H, Schinkel AH, Schellens JHM, Beijnen JH. *Quantification of docetaxel and its metabolites in human plasma by liquid chromatography/tandem mass spectrometry*. Rapid Commun.Mass Spectrom. **2013**; 27 (17): 1925-34.

Hendriks JJMA, Lagas JS, Rosing H, Schellens JHM, Beijnen JH, Schinkel AH. *P-glycoprotein and cytochrome P450 3A act together in restricting the oral bioavailability of paclitaxel*. Int.J.Cancer. **2013**; 132 (10): 2439-47.

Moes JJ, Stuurman FE, **Hendriks JJMA**, Marchetti S, Huitema ADR, Beijnen JH, Schellens JHM, Nuijen B. *Pharmacokinetic evaluation of three oral formulations of docetaxel boosted with ritonavir: two single-drug formulations vs. a fixed-dose combination tablet*. Drug Del Transl Res **2013**; 3 (3): 243-51.

Hendriks JJMA, Hillebrand MJX, Thijssen B, Rosing H, Schinkel AH, Schellens JHM, Beijnen JH. *A sensitive combined assay for the quantification of paclitaxel, docetaxel and ritonavir in human plasma using liquid chromatography coupled with tandem mass spectrometry*. J.Chromatogr.B Analyt.Technol.Biomed.Life Sci. **2011**; 879 (28): 2984-90.

Hendriks JJMA, Beijnen JH, Schellens JHM. *Methylnaltrexone*. Oncologist. **2009**; 14 (7): 679-82.

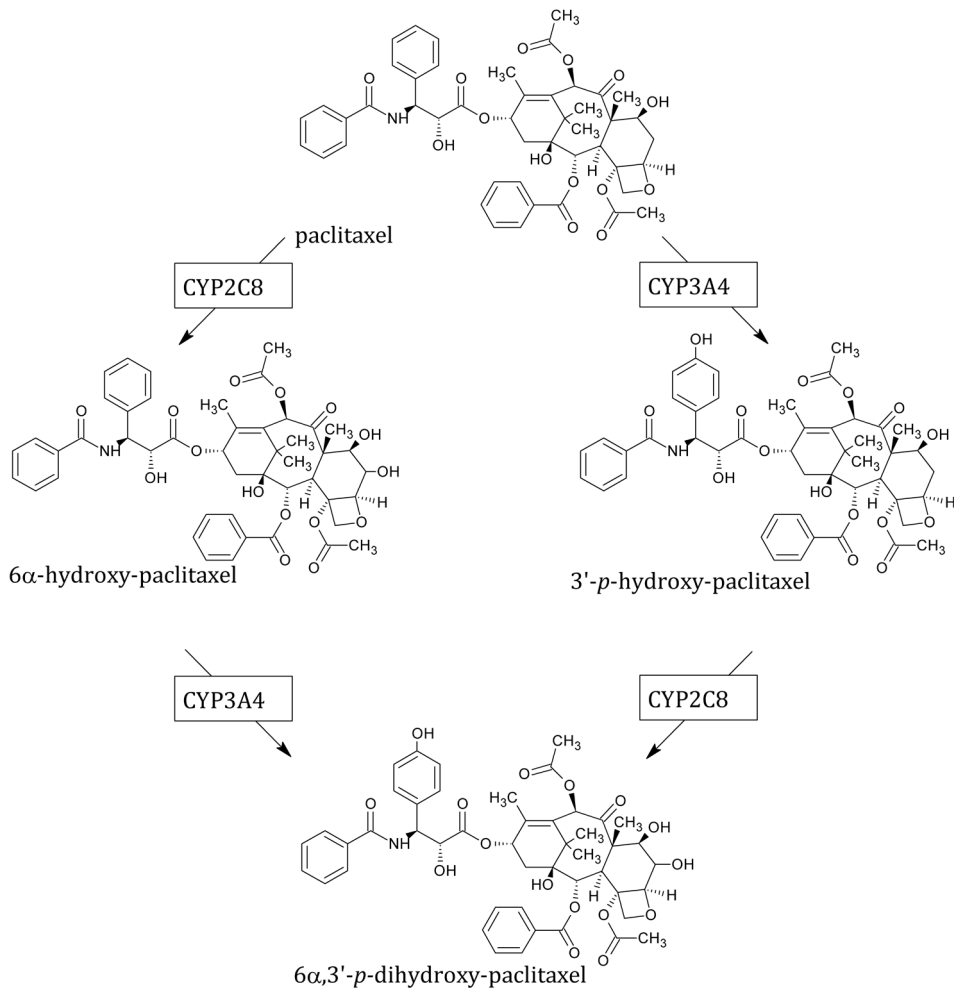
Hendriks JJMA, Beijnen JH, Schellens JHM. *Methylnaltrexon bij darmfunctiestoornissen door opioïdengebruik*. PW Wetenschappelijk Platform **2009**; 3 (11): 192-8.

Abstracts

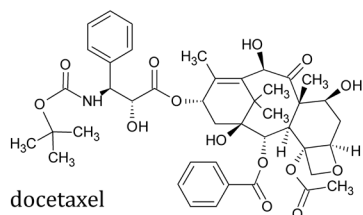
Hendriks JJMA, Koolen SLW, Stuurman FE, Rosing H, Schinkel AH, Marchetti S, Beijnen JH, Schellens JHM. *Plasma levels of docetaxel metabolites in humans after oral administration of docetaxel with and without ritonavir*. FIGON Dutch Medicine Days 2013.

Marchetti S, Stuurman FE, Koolen SLW, Moes JJ, **Hendriks JJMA**, Thijssen B, Huitema ADR, Nuijen B, Rosing H, Keessen M, Voest EE, Mergui-Roelvink M, Beijnen JHM, Schellens JH. *Phase I study of weekly oral docetaxel (ModraDoc001) plus ritonavir in patients with advanced solid tumors*. ASCO Meeting Abstracts **2012**; 30 (15_suppl): 2550.

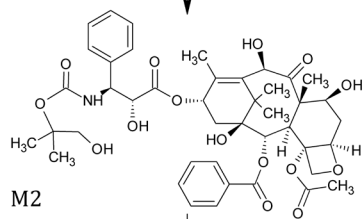
Paclitaxel and metabolites



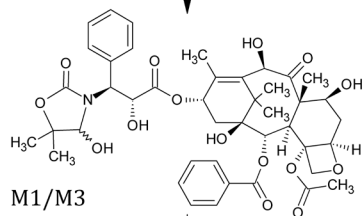
Docetaxel and metabolites



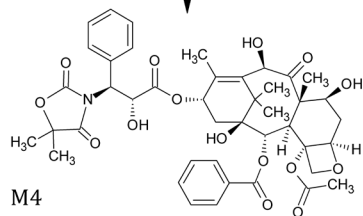
CYP3A4



CYP3A4



CYP3A4



Boosters

